Technical Report

BOUNDARY LAYER DEVELOPMENT OVER EQUALLY SPACED FENCES

by

R. J. Kung

and

E. J. Plate

U.S. Department of Interior
Office of Water Resources Research
Contract No. 14-01-0001

Fluid Dynamics and Diffusion Laboratory
College of Engineering
Colorado State University
Fort Collins, Colorado

June 1970 CER69-70RJK-EJP-33

From a dissertation submitted to the Graduate Faculty of Colorado State University in partial fulfillment of the requirements for the degree of Doctor of Philosophy

ABSTRACT

Experimental studies on a series of fences immerged in a smooth wall turbulent boundary layer are discussed in this report. Fences are placed at equal spacing and they are of equal height. The basic variables are the spacings of the fences and the ambient velocity. Six different experiments were performed by combining two ambient velocities with three fence spacings.

The flow field is subdivided into three regions. They are: the "smooth" region upstream from the leading fence; the "rough" region far downstream from the leading fence; and the "transition" region between the smooth region and rough region. Emphasis of this work is placed on the rough region. The flow in the rough region represents the overall effects of all upstream fences, in it the effect of each individual fence on the boundary layer can no longer be identified. Mean velocity profiles, static pressure profiles, turbulence, and form drag of fences are measured. Comparison between the measured results and existing theories are made. The flow in the smooth region can be correlated by the wall law and the defect law of a smooth wall turbulent boundary layer. Flow in the rough region is found to depend on fence height, fence spacing and their ratio. The universal velocity defect law breaks down in the rough region of the present study, however, an empirical expression for the velocity defect law is found. A model law is proposed for modeling the problem of multiple wind breaks. Also discussed is how an optimum wind break can be determined.

TABLE OF CONTENTS

TABLE OF CONTENTS - Continued

LIST OF TABLES

LIST OF FIGURES

LIST OF FIGURES - Continued

LIST OF FIGURES - Continued

LIST OF SYMBOLS

Symbol	Definition	Dimension
A,B,c	Constants	
c_f	Local shear coefficient	
C_f	Total drag coefficient	
D	Total drag force	MLT^{-2}
d	Diameter of hot wire	L
E	Mean voltage output of hot wire anemometer	V
e'	Fluctuating voltage	V
$\sqrt{\overline{e'^2}}$	Root mean square of voltage fluctuating	V
fgh	Velocity function	
H	Form factor	
h	Fence height	L
H_s	Static head	L
H_t	Total head	L
K	Roughness parameter	
k	Roughness height	L
L	Fence spacing	L
L_x	Integral scale of turbulence	L
ℓ	A length scale or wire length	L
ℓ_o	Thickness of internal boundary layer	L
p_r	Reference pressure	$ML^{-1}T^{-2}$
p_s	Static pressure	$ML^{-1}T^{-2}$
p_t	Total pressure	$ML^{-1}T^{-2}$

LIST OF SYMBOLS - Continued

Symbol	Definition	Dimension
R	Radius of pipe	L
R_L	Reynolds number based on fence spacing and ambient velocity	
R_x	Reynolds number based on distance x and ambient velocity	
R_θ	Reynolds number based on momentum thickness and ambient velocity	
S	Number of fences in a given area	
S	Sensitivity of hot wire	VTL^{-1}
S_α	Sensitivity of yawed wire	VTL^{-1}
T	Temperature	
t	Time	T
U_A	Approximate ambient velocity	LT^{-1}
$\overline{U}$	Magnitude of total velocity	LT^{-1}
u_a	Ambient velocity	LT^{-1}
u,v	Local mean velocity in x,y direction	LT^{-1}
u_o	Mean velocity at upstream	LT^{-1}
u_τ	Shear velocity obtained by direct measurement of wall shear stress	LT^{-1}
$u*$	Shear velocity obtained by indirect measurement of wall shear stress	LT^{-1}
$\sqrt{\overline{u'^2}}, \sqrt{\overline{v'^2}}$	Root square of velocity fluctuations	LT^{-1}
$\overline{u'v'}$	Turbulent shear stress per unit mass	L^2T^{-2}
x	Distance downstream from leading fence	L
y	Distance normal to surface measured from the wall	L

Symbol	Definition	Dimension
z_o	Distance normal to x and y measured from center tunnel	L
y_t	Vertical distance measured from the crest of roughness	L
α	Yaw angle of hot wire	
γ_m	Specific weight of mercury	$ML^{-2}T^{-2}$
Δ	Clauser's length scale	L
δ	Boundary layer thickness	L
δ^*	Displacement thickness	L
ε	Error in origin measured downward from the crest of the roughness	L
θ	Momentum thickness	L
κ	Von Karman constant	
λ	Density of roughness	
μ	Absolute viscosity	$ML^{-1}T^{-1}$
ν	Kinematic viscosity	L^2T^{-1}
π	Coles' pressure gradient parameter	
ρ	Mass density	ML^{-3}
σ	Standard deviation normal distributed probability function	
τ	Shear stress	$ML^{-1}T^{-2}$
τ_o	Wall shear stress	$ML^{-1}T^{-2}$
ψ	Normalized stream function	
ω	Wake function of Coles	

Chapter I

INTRODUCTION

Surface barriers are some of the earliest devices that man has used to change climatic conditions in order to protect crops and land from the ravages of wind. Systematic research on the effect of these wind breaks or barriers has been conducted in the United States since the Shelter Belt Program was begun on the high plains in the 1930's. The amount of material published on the subject of wind breaks is voluminous. Much of the research behind this material has been conducted through field investigations, which have studied the cultural effects of wind breaks on crop species, planting, management, and care of plants. Also some of the aerodynamic problems related to wind breaks have been studied, both in the field and in wind tunnels.

The goal of a wind break study is often to find the optimum arrangement between the cost of a wind break and the protection it provides for crops and land over a maximum region. Necessary or optimum protection can mean a number of things. It can mean reduction of wind speed below the dangerous level for a particular kind of crop, or it can mean the reduction of evaporation of water, or the reduction of heat transfer from air-water and air-soil interface, or the retention of carbon dioxide in the soil, or the reduction of wind erosion on small surface particles, such as seeds, surface soils, and fertilizers. Because of the many ramifications on designing the optimum arrangement of wind breaks, climatic, soil, crop, tillage, irrigation, meteorology, and economic data are important. Even though these data are important, some of the most important information needed for wind break design is the aerodynamics of wind flow about wind breaks.

Field research in the past on wind break dynamics has led to conflicting results. This is because of the difficulty of controlling the variables encountered. Also, a detailed field investigation can be extremely costly, both in time and money. Therefore, many of the basic problems of the aerodynamics of shelter belts are studied in wind tunnels.

Much research in wind tunnels, related to wind breaks, has dealt with single obstacle geometry. The results of this research are useful for designing single wind breaks, as well as providing understanding for some problems of fluid mechanics.

1.1 Scope of the Dissertation

In this dissertation the effects of a series of fences immerged in a smooth wall wind tunnel turbulent boundary layer are studied as an extension of the single fence problem. The fences were placed at equal spacings with the basic variables consisting of fence spacings and mean velocity. The emphasis of this work is placed on the region far downstream from the leading fence. The effects of each single fence on the boundary layer are not discussed in this dissertation, rather the overall characteristics of the turbulent boundary layers, which have been influenced by all the fences, are considered. Two ambient velocities and three fence spacings were chosen to give six different flow conditions. Streamwise pressure gradients at free stream are adjusted to nearly zero. Mean velocity profiles, static pressure profiles, and turbulence are measured. Comparison between present data and previous results on smooth wall and rough wall turbulent boundary layers are made. And finally, recommendations for applying the results to multiple wind breaks are made.

1.2 The Regions of the Air Flow Over Multiple Fences

When a series of equally spaced sharp-edged fences are immerged into a two-dimensional turbulent boundary layer, the influence of these fences is found to be different in different regions of the flow field. Those regions shall be discussed in this section.

A Cartesian coordinate system (x,y,z) is used to specify the physical spaces where x is the longitudinal downstream direction, y is the vertical direction measured upwards normal from the floor, and z is the lateral direction. The velocity components correspondent to the coordinate system (x,y,z) are (U,V,W). For two-dimensional turbulent flow $U = u + u'$, $V = v + v'$, and $W = w'$ where u and v denote the mean motion and u', v', and w' are the fluctuating quantities.

Fences are fixed on the floor perpendicular to the mean stream. The floor for $x < 0$ is considered to be aerodynamically smooth. The first fence is located at $x = 0$ and all fences are equally spaced downstream with a constant spacing L. Each fence has the same height h and the same width W.

As shown in Figure 1, three regions describe the entire flow field. Flow characteristics in each region obey a different law. A general description of the flow in each region will be given in the following few paragraphs.

Region I. The smooth region $(x < 0)$.

Since the distance from the leading edge of the smooth plate to the first fence is long (40 ft), the existence of velocity distributions that have a similarity shape is expected in this region $(x < 0)$. A boundary layer, in which similar velocity distributions exist, is usually called an equilibrium boundary layer. Results for the equilibrium boundary layer over the "smooth wall" can fully describe the flow in this region. A tremendous amount of theoretical and empirical knowledge on this kind of problem has accumulated in the last few decades. Prandtl and Karman provided the pioneer work, (see Schlichting, 1968). Millikan (1938), Ludwieg and Tillmann (1950), Hama (1954), and others provided experimental contributions; Coles (1955, 1956) and Clauser (1954, 1956) made important theoretical contributions to our understanding of the flow over smooth wall.

Region II. The transition region $(0 < x < x_1)$

When the boundary layer flow of Region I encounters an abrupt change in surface roughness (a series of fences in the present study represents the roughness), the new surface will cause a change of the flow from its equilibrium condition. The flow changes are confined, initially, to a thin layer adjacent to the surface. If the flow within the thin layer represents the statistical properties of the adjacent surface, and the flow outside this layer is not affected by the surface condition, such a layer is known as an internal boundary layer.

Elliott (1958), Panofsky and Townsend (1964), Townsend (1965a,b), and Blom and Wartena (1969) proposed theoretical approaches to calculate the flow disturbance caused by an abrupt change in surface roughness. Their general assumptions are:

(a) The total boundary layer thickness is much larger than the thickness of the internal boundary layer $(\delta >> \ell_o)$,

(b) The flow properties outside the layer are not disturbed. This assumption implies that the logarithmic velocity profile, which describes the flow in Region I, can also be used to describe the flow outside the internal boundary layer in Region II, and

(c) Inside the internal layer, the logarithmic velocity profile is assumed, with a new velocity scale and a new length.

Elliott (1958) made a theoretical study on this flow model by assuming that both velocity and length scale in

Region II are constants, where the length scale represents the statistical roughness height and the constant velocity scale indicates a constant shear stress over the internal boundary layer. In Elliott's model, the shear stress at the edge of the internal boundary layer is discontinuous. Panofsky and Townsend (1964) assumed a continuous shear stress connecting the inner and outer layers. Townsend (1965a,b) tried to summarize the internal boundary layer problem by assuming that the deviation of the flow properties from the upstream distributions is self-preserving in form. Both length scale and velocity scale used by Townsend are assumed to be functions of x only.

When compared with the results of Elliott (1958), Panofsky and Townsend (1964), and Townsend (1965a), the development of the internal boundary layer are found to be similar. However, the velocity distribution and the shear stress deviate considerably from one another. This can be found in Figure 2 of Townsend (1965a).

Plate and Hidy (1967) modified Townsend's theory by introducing a pressure gradient and a nonuniform surface stress. They found that the modified model could apply to a wind-tunnel flume boundary layer, where the boundary layer thickness and the thickness of internal boundary layer were of the same order. A detailed experimental study for the internal boundary layer flow model is presently being prepared by F. F. Yeh at Colorado State University as part of his Ph.D. dissertation.

Region III. The rough region $(x > x_1)$

Since the internal boundary layer will grow in depth downwind, it is possible to assume that at a point x_1 the influence of surface roughness has covered the whole boundary layer. From this point downstream the thickness of the boundary layer and the internal boundary layer will coincide. This region $(x > x_1)$ is named as "rough region." An analogy between the flow in this region and previous work on "rough wall" is expected. A review of the rough wall problem will be dealt with in the next chapter.

1.3 Purpose of the Dissertation

The problem of air flows over a rough surface has long been recognized as an important topic in fluid mechanics, and many experimental results on the problem have been published. However, most previous experiments do not include a boundary layer history, or in other words, the flow at $x = 0$ is essentially uniform. Furthermore, most previous work on the rough surface problem does not have a direct measurement on surface stress, which is found to be the most important quantity in turbulent boundary layer studies.

The present study will concentrate on the rough region (Region III, in Figure 1), with a nearly zero free stream pressure gradient. The main purposes of this study are:

(1) to compare the flow properties of a rough wall boundary layer flow between the sharp-edged fences and other roughness geometries,

(2) to compare the existing laws on a rough wall flow model after the surface stress is accurately measured,

(3) to correlate the form drag of fences to the free stream mean velocity and the spacing between fences, and

(4) to find the optimum arrangement for multiple wind breaks, and the modeling laws for multiple wind break problems.

Chapter II

LITERATURE REVIEW

When the spacing between the fences is not too large, one can easily see that the flow characteristics at a large distance downwind from the leading fence will represent the overall effects from each fence upstream. In other words, the effects of each individual fence to the boundary layer will not be significant. The boundary layers in this region, which are far downstream from the leading fence, can be classified as a rough wall turbulent boundary layer.

In working with the turbulent boundary layer over rough surface, it is advantageous to do a parallel study of turbulent boundary layer over a smooth surface because many valuable results from the latter problem can also apply to the former, with only slight modification. Furthermore, if there does exist any "universal" law, the results from a simpler flow condition (smooth-surface) can apply directly to a more complicated one (rough-surface).

Some previous work on turbulent boundary layers over both smooth and rough surfaces and research in the area of wind breaks will be reviewed in this chapter.

2.1 Turbulent Flow Over Smooth Surface

Since the fundamental equation of motion cannot yet be solved for a turbulent boundary layer flow, experimental and empirical investigations are important in understanding the general behavior of such a flow.

A considerable amount of experimental results on smooth wall turbulent boundary layer has been accumulated in the past by Schultz-Grunow (1940), Hama (1947, 1954), Ludwieg and Tillmann (1950), Baines (1950, 1951), and Klebanoff and Diehl (1951). In addition, semi-empirical analyses by Rotta (1950, 1955, 1962), Hama (1953a,b), Landweber (1952), Clauser (1954, 1955), Coles (1953, 1954, 1955, 1956), and Townsend (1956a,b) have helped clarify the smooth wall problem.

2.1.1 The wall law and defect law - Previous investigations of the turbulent boundary layer over smooth surface have indicated the existence of two universal laws, namely the "wall law" and the "defect law." The wall law, which was first introduced by Prandtl (1934) on the basis of his mixing length theory, states that the dimensionless velocity u/u_τ is a unique function of the dimensionless distance from the wall yu_τ/ν in the immediate wall vicinity. The functional relation reads

$$\frac{u}{u_\tau} = f\left[\frac{yu_\tau}{\nu}\right] \quad , \tag{2-1}$$

where ν is the kinematic viscosity $(\nu = \mu/\rho)$, and u_τ is the shearing velocity defined as

$$u_\tau = \sqrt{\tau_o/\rho} \quad ,$$

and τ_o is the surface shear stress. The square brackets in Equation 2-1 represent a functional dependence and will be used throughout this dissertation.

Coles (1954) proved theoretically through dimensional reasoning that the wall law (Eq. 2-1) must hold if a universal relation between u and y is to exist near a smooth wall.

On the other hand, Karman showed that a universal relation exists between the dimensionless velocity defect $(u_a-u)/u_\tau$ and y/h where h is the half width of a channel. This relation was derived through a similarity argument. (See page 553, Equation 19.21 of Schlichting, 1968). In a boundary layer flow Schultz-Grunow (1940) showed that the universal relation also exists if the distance y is normalized by the boundary layer thickness δ. Since the velocity profile near δ is nearly flat, the true value of δ is difficult to determine. Rotta (1950, 1955) found that the only possible well defined thickness is $\delta^* u_a/u_\tau$ and the dimensionless distance from wall does exist a universal relation. Where δ^* is the displacement thickness defined as

$$\delta^* = \int_0^\delta \left(1 - \frac{u}{u_a}\right) dy \tag{2-2}$$

Clauser (1954) found that the integration of $(u_a-u)/u_\tau$ with respect to y/δ, from 0 to δ, yields a constant value for a given pressure gradient. He proposed a thickness Δ defined as

$$\Delta = \int_0^\delta \frac{u_a-u}{u_\tau} dy = \delta \int_0^\delta \frac{u_a-u}{u_\tau} \, d\left(\frac{y}{\delta}\right) . \tag{2-3}$$

If one compares Equation 2-3 to Equation 2-2, $\Delta = \delta^* u_a / u_\tau$.

The general defect law has the form

$$\frac{u_a - u}{u_\tau} = g\left[\frac{y}{\ell}\right] \quad , \tag{2-4}$$

where ℓ is a thickness scale and

$$\ell = \begin{cases} \delta & - \quad \text{Schultz-Grunow (1940)} \\ \\ \Delta & - \quad \text{Rotta (1950, 1955) and} \\ & \quad\;\; \text{Clauser (1954).} \end{cases}$$

2.1.2 The logarithmic distribution near wall - The well known logarithmic profile was obtained originally by Prandtl through the mixing length theory (see Schlichting, 1968, pp. 554-555). Since this theory was based on an unrealistic assumption of the turbulent mechanism, which assumed the conservations of momentum of a "lump" of fluid in turbulent flow, the mixing length theory and similar theories are no longer considered generally useful in analyzing turbulent flow.

On the other hand, Millikan (1938) derived the logarithmic law on the assumption that the wall law and the defect law "overlap" in a region for pipe and channel flow. Clauser (1954) showed the same to be true for turbulent boundary layer flow.

If we rewrite Equation 2-4 and adopt Clauser's thickness scale, we arrive at

$$\frac{u}{u_\tau} = \frac{u_a}{u_\tau} - g\left[\frac{y}{\Delta}\right] \quad . \tag{2-5}$$

Also, we can write Equation 3-1 as

$$\frac{u}{u_\tau} = f\left[\frac{u_\tau \Delta}{\nu} \quad \frac{y}{\Delta}\right] \quad . \tag{2-6}$$

According to experimental evidence, there is a common region near the wall where these two quite different results will simultaneously correlate the velocity profiles. As we can see, the f function of Equation 2-6 contains the factor $u_\tau \Delta/\nu$ as a multiplier of y/Δ inside the function f, and Equation 2-5 contains u/u_τ as an additive term outside the g function. In fact, the only mathematical function where two product factors inside a function are equal to two additive functions containing each factor, is the logarithmic function. This implies that both g and f must be logarithmic in form. After examining many previous experimental data, Clauser arrived at the wall law for a smooth surface as

$$\frac{u}{u_\tau} = \frac{1}{\kappa} \ln\left(\frac{yu_\tau}{\nu}\right) + A \quad , \tag{2-7}$$

and the defect law as

$$\frac{u_a - u}{u_\tau} = -\frac{1}{\kappa} \ln\left(\frac{yu_\tau}{\delta^* u_a}\right) - B + \frac{\Delta u_1}{u_\tau} \quad , \tag{2-8}$$

where $\kappa = 0.41$. $A = 4.9$, $B = 0.6$ proposed by Clauser and $\Delta u_1/u_\tau$ depends on the pressure gradient. For zero pressure gradient $\Delta u_1/u_\tau = 0$, for a given non-zero pressure gradient $\Delta u_1/u_\tau$ results in a constant shift of the linear plot of Equation 2-8 from a constant pressure profile (refer to Figure 18, p. 102 of Clauser, 1954). And both relations 2-7 and 2-8 are found to apply within 10%-20% of the total boundary thickness. Moreover, Ludwieg and Tillmann (1950) found that the wall law, Equation 2-7, is a universal function for all pressure gradient near a smooth surface.

2.1.3 <u>Velocity profile at the outer portion</u> - Since the wall law (Eq. 2-1) was derived near the surface, and experimental results showed that Equation 2-7 can only apply to 10% to 20% of a boundary layer, it is necessary to add some function to Equation 2-1, in order to describe the flow of the entire boundary layer. Consider the flow beyond a thin laminar sublayer up to $y = \delta$ expressed as

$$\frac{u}{u_\tau} = f\left[\frac{yu_\tau}{\nu}\right] + h[x,y] \qquad (2\text{-}9)$$

where h is an arbitrary function except h is negligibly small in some finite region near wall, say about $y/\delta < 0.1$. Millikan (1938) proposed that h is a function of y/δ to describe the velocity profile which departs from the logarithmic law. After carefully examining many experimental data, Coles (1956) introduced the "law of wake," i.e.,

$$h = h\left[\pi, \frac{y}{\delta}\right] = \frac{\pi}{\kappa}\,\omega\left[\frac{y}{\delta}\right] \quad , \qquad (2\text{-}10)$$

where π is dependent on pressure gradient and turbulence intensity near the edge of boundary layer, and $\omega[y/\delta]$ is the wake function, thus, $\omega[1] = 2$, $\omega[0] = 0$ $\int_0^2 \frac{y}{\delta}\, d\omega = 1$. The relation between ω and y/δ is shown in Figure 2.

Substituting Equation 2-10 into Equation 2-9, the velocity distribution of the entire boundary layer beyond a thin sublayer becomes

$$\frac{u}{u_\tau} = \frac{1}{\kappa} \ln\left(\frac{yu_\tau}{\nu}\right) + c + \frac{\pi}{\kappa}\, \omega\left[\frac{y}{\delta}\right] \quad . \tag{2-11}$$

Coles (1956) had collected previous experimental data, and good correlations between those data and Equation 2-11 were found.

Hama (1954) arrived at another empirical relation for zero pressure gradient boundary layer flow, which has the form

$$\frac{u_a - u}{u_\tau} = 9.6\left(1 - \frac{y}{\delta}\right)^2 , \tag{2-12}$$

where $y/\delta > 0.15$.

Ross (1953) also ended up with empirical relation similar to Equation 2-12, but with a power of 3/2 instead of 2.

2.1.4 <u>The drag coefficient</u> - For a two-dimensional equilibrium boundary layer, the equation of motion has the form

$$\rho u \frac{\partial u}{\partial x} + \rho v \frac{\partial u}{\partial y} = - \frac{\partial p}{\partial x} + \frac{\partial \tau}{\partial y} \quad , \tag{2-13}$$

and the continuity equation reads

$$\frac{\partial u}{\partial x} + \frac{\partial v}{\partial y} = 0 \quad . \tag{2-14}$$

If Equation 2-13 is integrated from $y = 0$ to $y = \delta$ and Equation 2-14 is also introduced, Karman's momentum integral equation is then obtained as

$$c_f = 2\frac{d\theta}{dx} - \frac{\delta^* + 2\theta}{\frac{1}{2}\rho\, u_a^2}\frac{dp}{dx} \quad , \tag{2-15}$$

where c_f is the drag coefficient defined as $c_f = \tau_o/\frac{1}{2}\rho u_a^2$ and θ is the momentum thickness

$$\theta = \int_o^\delta \frac{u}{u_a}\left(1 - \frac{u}{u_a}\right) dy \quad . \tag{2-16}$$

Total force acting on a flat plate per unit width from x_1 to x_2 is

$$D = \int_{x_1}^{x_2} \tau_o[x]dx \quad . \tag{2-17}$$

The total drag coefficient is defined as

$$C_f = \frac{1}{x_2 - x_1}\int_{x_1}^{x_2} \frac{\tau_o}{\frac{1}{2}\rho u_a^2} dx = \frac{1}{x_2 - x_1}\int_{x_1}^{x_2} c_f\, dx \quad . \tag{2-18}$$

The usual way to calculate c_f and C_f is to assume a velocity profile with the help of some empirical relation between x and δ. Some early results on C_f are shown in Table 1.

It is difficult to decide which of the results in Table 1 is best for predicting the drag of a smooth plate. Each depends on the author's measurement and no one seems to have any better theoretical background than the others.

Furthermore, if a pressure gradient appears, none of the results in Table 1 are applicable. The drag coefficient must be a function of some parameter, which indicates the appearance of the pressure gradient, as well as a function of the Reynolds number R_x .

Ludwieg and Tillmann (1950) used a direct shear stress measurement method, developed by Ludwieg (1950), to measure the surface shear stress for a boundary layer with pressure gradient. The empirical relation found was

$$c_f = 0.246 \times 10^{-0.678H} \times R_\theta^{-0.268} \qquad (2\text{-}19)$$

where $H = \delta^*/\theta$, and $R_\theta = u_a\theta/\nu$.

If one substitutes Equation 2-7 into Equation 2-8,

$$\frac{u_a}{u_\tau} = \frac{1}{\kappa} \ln \left(\frac{u_\tau \Delta}{\nu} \right) + A - B + \frac{\Delta u_1}{u_\tau} \quad .$$

Since $\Delta = \delta^* u_a/u_\tau$ and $u_a/u_\tau = \sqrt{2/c_f}$,

$$\sqrt{2/c_f} = \frac{1}{\kappa} \ln \left(\frac{u_a \delta^*}{\nu} \right) + A - B + \frac{\Delta u_1}{u_\tau} \quad . \qquad (2\text{-}20)$$

Equation 2-20 was formulated by Clauser (1954) as the "universal skin friction law" of a smooth wall with equilibrium pressure gradients. As proposed by Clauser, $\kappa = 0.41$, $A = 4.9$, $B = 0.6$, and for zero pressure gradient $\Delta u_1/u_\tau = 0$. Equation 2-20 reduces to

$$\sqrt{2/c_f} = 5.6 \log \left(\frac{u_a \delta^*}{\nu}\right) + 4.3 \quad . \qquad (2\text{-}21)$$

Hama (1954) found that

$$\sqrt{2/c_f} = 5.45 \log \left(\frac{u_a \theta}{\nu}\right) + 5.55 \qquad (2\text{-}22)$$

is also an excellent approximation to Equation 2-21. Other investigators also found results similar to Equation 2-22, but with different numerical values compared to 5.45 and 5.55 of Equation 2-22. Typical are the values of 5.89 and 3.58 given by Squire and Young (1937), 5.85 and 4.1 by Landweber (1952), and 5.6 and 5.8 by Coles (1954, 1953).

2.2 Turbulent Flow Over Rough Surface

The earliest studies on roughness effects were conducted in pipe and flume flows, because the flow resistance can be calculated from the easily measurable head losses or water surface slopes. Nikuradse (1933) conducted a systematic series of experiments in sand roughened pipes. His result showed that the flow is dependent only on the roughness height for a rough pipe flow with high Reynolds number. Morris (1955, 1961) found that the roughness density is the only significant factor in determining the roughness effects of a channel flow.

Early experimental works on rough wall turbulent boundary layer flow are those of Tillmann (1945) and Baines (1950). However, the first extensive study on velocity distribution in the boundary layer over a rough plate was made by Moore (1951). The roughness used by Moore was two-dimensional traverse bars with controlled spacing to height ratio. Later, this kind of roughness, traverse bars, has been widely used in rough wall turbulent boundary layer studies by Hama (1954), Perry and Joubert (1963), Bhaduri (1966), Bettermann (1965), Liu *et al*. (1966), and Perry *et al*. (1969). The experimental results of all these investigators showed that Nikuradse's result on pipe, when flow is dependent on roughness height, is valid in rough wall boundary layer flow. Similar to the result found by Morris (1955, 1961) in channel flow, Sayre and Albertson (1961), Bettermann (1965) and Liu *et al*. (1966) found that both the roughness density and roughness height are important factors in rough wall turbulent boundary layer flow.

2.2.1 *Extrapolation of rough pipe results* - The framework of todays rough wall turbulent boundary analysis was introduced by Nikuradse (1933), who conducted experiments on circular pipe, roughened by sand with a definite grain size. By choosing pipes of varying diameters and by changing the size of grain, Nikuradse made a systematic study on R/k ratio from 15 to 500, where R is the radius of pipe and k denotes the grain size. Two important conclusions obtained were:

(1) Flow behavior depends on the Reynolds number and the relative roughness height k/R . However, at a higher Reynolds number, the flow becomes independent of viscosity (Reynolds number) and is a function of k/R only. This result can be found on page 580, Figure 20.18 of Schlichting (1968); and

(2) the smooth-wall defect law, Equation 2-8, is a universal relation for both smooth-wall and rough-wall.

Based on an assumption that the roughness effect is universal and independent of outside flow, Prandtl and Schlichting (1934) was able to transpose Nikuradse's rough pipe chart into roughened boundary layer flow. Experimental works by Moore (1951), Baines (1950), and Hama (1954) confirmed the first result found by Nikuradse in pipe flow; that is, at high Reynolds number, flow in a boundary layer over rough plate is independent on viscosity and is dependent on the geometry of the solid boundary.

Moore (1951) found that the universality of the defect law, which is the second result mentioned above found by Nikuradse (1933) in pipe flow, is also valid in rough wall turbulent boundary layer flow. This means that the defect law is independent of the surface condition. In addition, Moore (1951) provided an empirical relation to describe the flow in the region of $0.45 < y/\delta < 1$ was given as

$$\frac{u}{u_a} = 0.52\ (y/\theta)^{0.35} \quad . \tag{2-23}$$

The same result (Eq. 2-23) was found by Bhaduri (1966).

The empirical relation (Eq. 2-12) proposed by Hama (1954) can also apply to the rough surface boundary layer flow. Recently, Perry, Schofield, and Joubert (1969) found that relation 2-12 is applicable to the "d" type roughness as well as the "k" type roughness. The definitions of "d" and "k" roughness denote the significance length scale involved.

2.2.2 The wall law and the roughness function - Unlike the universality of the defect law (Eq. 2-8), the wall law for smooth surface (Eq. 2-7) cannot apply to rough surface flow directly. Prandtl (1934) has shown that when the wall is rough, the semilogarithmic part of Equation 2-7 is displaced downward, parallel to itself by an amount $\Delta u/u_\tau$, which depends on the roughness Reynolds number ku_τ/ν. A "universal" wall law for both smooth and rough flow was formulated by Clauser (1954), and is

$$\frac{u}{u_\tau} = \frac{1}{\kappa} \ln\left(\frac{yu_\tau}{\nu}\right) - \frac{\Delta u}{u_\tau}\left[\frac{ku_\tau}{\nu}\right] + A \; . \tag{2-24}$$

When ku_τ/ν is greater than 100, the asymptotic form of the roughness functions becomes

$$\frac{\Delta u}{u_\tau} = \frac{1}{\kappa} \ln\left(\frac{u_\tau k}{\nu}\right) + c \quad , \tag{2-25}$$

where c is a constant dependent on the roughness geometries.

Hama (1954) proposed a method to obtain the roughness function by knowing the local drag coefficient and the displacement thickness. Considered for a zero pressure rough surface flow, the defect law has the form

$$\frac{u_a - u}{u_\tau} = - \left(5.6 \log \frac{y u_\tau}{\delta^* u_a} + 0.6 \right) \quad . \qquad (2\text{-}26)$$

Substituting Equation 2-24 into Equation 2-26 and using the definition of c_f we will have:

$$\sqrt{2/c_f} = \left(5.6 \log \frac{u_a \delta^*}{\nu} + 4.3 \right) - \frac{\Delta u}{u_\tau} \quad ;$$

if c_f and δ^* can be measured

$$\frac{\Delta u}{u_\tau} = 5.6 \log \frac{u_a \delta^*}{\nu} + 4.3 - \sqrt{\frac{2}{c_f}} \quad . \qquad (2\text{-}27)$$

Perry et al. (1969) assumed a slightly different velocity distribution as

$$\frac{u}{u_\tau} = \frac{1}{\kappa} \ln \frac{(y_\tau + \varepsilon) u_\tau}{\nu} + A - \frac{\Delta u}{u_\tau} \qquad (2\text{-}28)$$

where y_τ is the measurement from the crest of transverse bars. The parameter ε is a distance below the crest, which will be referred to as the error in origin, and defines an origin for the profiles that will give the logarithmic distribution of velocity near the wall. The numerical value of ε was determined from a measured velocity profile through a graphical manner proposed by Perry and Joubert (1963).

Their experiments indicated that the roughness function is a function of ε rather than a function of k for a "d" type roughness. This property was previously found by Streeter and Chu (1949), and Ambrose (1956), where the friction factor to Reynolds number characteristics are insensitive to k/R for special kind of roughness geometries with a series of depression of grooves on smooth surface pipes.

The results found by Perry et al. (1969) are:

(a) for a "d" type roughness,

$$\frac{\Delta u}{u_\tau} = \frac{1}{\kappa} \ln \frac{\varepsilon u_\tau}{\nu} + c \quad , \tag{2-29}$$

where c depends on the roughness geometries, which resembles Streeter and Chu's (1949) and Ambroses' (1956) kinds of roughness, and

(b) for the conventional type of roughness or termed as the "k" type roughness, Equation 2-25 gives the relation of the roughness functions.

Bettermann (1965) using two-dimensional transverse bars of varying spacing, has been able to show that c (Eq. 2-25) is a function of the density of the roughness elements; and that at a certain density the value c reaches maximum. If λ is the ratio of total surface area to roughness elements, Bettermann found that for $1 \leqq \lambda \leqq 5$

$$\frac{\Delta u}{u_\tau} = 5.6 \log \frac{u_\tau k}{\nu} + 17.35\ (1.625 \log \lambda - 1), \tag{2-30}$$

and when $\lambda > 5$

$$\frac{\Delta u}{u_\tau} = 5.6 \log \frac{u_\tau k}{\nu} - 5.95 \; (1.103 \log\lambda - 1) \quad . \qquad (2\text{-}31)$$

2.3 Wind Breaks

Most of the previous works related to wind breaks have dealt with single breaks which are at variance to the scope of this study. However, information about single breaks has generated a great deal of interest in wind break research and has also provided valuable knowledge on design and use of single wind breaks.

A number of field investigations, which have increased knowledge about wind breaks in general, have been conducted to find answers on some of the aerodynamics problems related to wind breaks. Bates (1930, 1945, 1945a) conducted investigations on the influences of wind breaks to agronomic condition. DenUyl (1936) conducted field tests of five actual wind breaks over a period of five years. His data included records of temperature, humidity, and wind velocity. Others who have provided information from field investigations include Cheyney (1941), Hood (1938), and Clark (1934).

Woodruff and Zingg (1952) performed a wind tunnel study on wind breaks. They chose four different barriers, namely, a sharp-edged fence, a cylinder, a 45° triangular shape, and a model tree wind break. Their results showed that the sharp-edged fence and the triangular shape provided a longer protected region at a higher rate of wind reduction, say, for a 50% wind reduction, both the fence and the triangular shape provided a protected distance of 15.5 h downwind; for the model tree wind break a distance of 13 h was found. However, at a moderate rate of wind reduction the model tree wind break gives a longer distance of protected coverage than any of the solid breaks. At 25% of reduction the covered region of a model tree wind break is 27 h, while the covered region of a sharp-edged fence is 21.5 h, and the covered region of a triangular shape is 20.5 h. The same result, that a porous wind break will give a larger protected distance, were found by Nageli (1941) and Blenk and Trienes (1956).

Other wind tunnel studies of isolated solid obstacles have been investigated by Arie and Rouse (1956), Nagabhushanaiah (1961), Plate (1964), Chang (1966), and Good and Joubert (1968).

Arie and Rouse conducted an experiment holding a two-dimensional fence in a uniform flow. Good correlations between their experimental results and the theoretical model, which they had derived from the potential flow theory were found. Nagabhushanaiah provided experimental data on the measurement of two-dimensional fences immerged in a turbulent boundary layer with different heights. Experimental work by Chang showed that the velocity distribution along the separation region behind a two-dimensional wedge shaped model hill can be correlated to a theoretical model which was derived through the half-jet mixing flow theory. Plate found that the drag coefficient of an isolated two-dimensional fence, immerged in a thick boundary layer, can be fully specified by the separation pressure behind the solid fence. An empirical relation found by Plate, between the drag coefficient of the fence, C_D , and the h/δ ratio was also described in the same paper. Based on dimensional reasons Good and Joubert proposed that the only important velocity scale, when $h/\delta < 0.5$, is the shear velocity u_τ . And the drag coefficient C_τ based on u_τ was found by them to be

$$C_\tau = \frac{D}{h \frac{1}{2} \rho u_\tau^2} = f\left(\frac{u_\tau h}{\nu}\right) \quad , \qquad (2\text{-}32)$$

where D is the form drag of a two-dimensional fence, immerged in a smooth wall turbulent boundary layer.

Recently, Plate (1970) summarized the aerodynamics of shelter belts. He indicated that the drag coefficient, C_τ , of an isolated solid fence, immerged in a rough wall turbulent boundary layer, should be a function of h/z_o only; i.e.,

$$C_\tau = \frac{D}{\frac{1}{2} \rho u_\tau^2} = f\left(\frac{h}{z_o}\right) \quad , \qquad (2\text{-}33)$$

where z_o represents the roughness height of the boundary. Furthermore, for porous breaks, the drag coefficient should be defined by using u_b as a reference velocity:

$$C_b = \frac{D}{\frac{1}{2} \rho u_b^2 h} \quad , \qquad (2\text{-}34)$$

where u_b is the velocity behind a porous break. A modeling law was also proposed by Plate in the same paper:

$$\frac{h_m}{h_p} = \frac{z_{om}}{z_{op}} \quad , \tag{2-35}$$

where the subscripts m and p represent the quantities in the model and in the prototype, respectively.

Chapter III

INSTRUMENTATION AND EXPERIMENTAL PROCEDURE

Experiments were conducted in the large U. S. Army Meteorological wind tunnel, located in the Fluid Dynamics and Diffusion Laboratory at Colorado State University.

This chapter discusses the equipment used, measurement procedures, data reduction techniques, and the nature of experimental errors.

3.1 Wind Tunnel

All experiments were performed in the thick turbulent boundary layer of the wind tunnel mentioned above (Figure 3). This facility is described by Plate and Cermak (1963).

The tunnel is a recirculating type with velocities ranging from 0 to 120 ft/sec. The boundary layer is developed over an 80 ft long test section with a normal cross section 6 x 6 ft. The first 40 ft of the floor is plywood and the rest is a 40 ft long aluminum plate, which may be thermally controlled. The ambient air temperature in the wind tunnel can be controlled by a system of heating or cooling coils installed in the return section through which the circulating air passes. The ceiling of the wind tunnel can be set to adjust the pressure gradient of free stream.

In the present studies, the temperature control of the aluminum floor was not used, only the air was cooled to hold the ambient temperature constant. In addition, the free stream pressure gradients were adjusted nearly zero.

The turbulent intensity at free stream is low due to the damping screens and a 9:1 entrance contraction. Detailed measurement of the free stream turbulent intensity of this tunnel can be found in Tieleman (1967) and Zoric (1968).

A carriage system is also built inside the wind tunnel. The carriage moves along the wind tunnel on rails, which are fixed to the vertical walls of the tunnel. The carriage boom, which is intended for the mounting of probes, has independent movements vertically and horizontally. The carriage movement is provided with a remote control, and the position of the carriage boom is determined from the output of potentiometers through a digital volt meter (Hewlett-Packard 3440 model). The accuracy of the positional measurements can reach $\pm 0.0025''$ with 10 volts input of the potentiometer.

3.2 Fence Assembly

Fence elements were made from commercial aluminum angle beams, measuring $1'' \times 1'' \times 1/8$. One side of the angle beam was machine sharpened to 45° and the sharp edged side stood vertically as a fence, the other side served as the foot of the fence (refer to Figure 4). All fences were cut 6 ft long; conner fillets were used to insure all fences extended to the full tunnel width. The front edge of the first fence was located at x=0 , which indicates the leading edge of the aluminum floor or 40 ft from the wind tunnel entrance. From the first fence downstream, all fences were fixed on a 1/2 in. thick plywood floor. The spacing between each fence was chosen at a constant value L for each run. The plywood floor was made to cover the total test section. Double stick scotch tape was inserted between the fence foot and the plywood floor and 3/8 in. wood screws were used to fasten fences on the floor. Half inch wooden strips were glued to the bottom of the plywood to elevate it one inch above the original aluminum floor. In order to measure the stagnation pressure at the foot of each fence, three 1/16 in. ID pressure taps were drilled in front of each fence through the plywood floor. One pressure tap was drilled at the wind tunnel center line, the other two were drilled 12 in. to the right and to the left of the center line. Plastic tubes were connected to the pressure taps and let outside to the tunnel through the space between the plywood floor and the aluminum floor.

The 1 in. high plywood floor was extended 16 ft downstream from x=0 and 10 ft upstream. In addition, an 8 ft transition extended farther upstream to elevate the original floor to a 1 in. height. A sketch of the floor assembly is shown in Figure 4.

Pressure tapped fences, which were used to measure the form drag of fences, have the same shape and dimensions as the other fences except some pressure holes were drilled. Two tapped fences were made one for measuring the stagnation pressure on the front surface of a fence and another used to measure the separation pressure on the rear surface of a fence. Seven pressure holes were drilled on the first fence, with each hole spaced 1/8 in. in the vertical direction. And since the separation pressure was constant over the height of the fence (see Plate, 1964, and Nagabhushanaiah, 1961), only three pressure holes were drilled on the second fence (Figure 4). Three sets of such pressure holes were drilled on both tapped fences, one set was at the center line and the other two were located 12 in. right and left from the center line.

3.3 Log of Experiments

As mentioned previously the spacing between fences L and the ambient velocity u_a are the basic variables in this study. Six runs were performed by associating two mean velocities and three fence spacings. The flow condition of each run is shown as follows.

Run No.	I	II	III	IV	V	VI
U_A (fps)	30	30	45	45	45	30
L (inches)	12	6	6	12	18	18
X (ft)	16	16	15	15	15	15

where U_A represents the approximated ambient velocity, and X is the fence covered region downstream from $x = 0$.

Static pressure, mean velocities, and form drag of fences were measured for all six runs. Turbulence quantities were only measured for Run I and Run II. Data were collected from $x=0$ to $x=12'$, also the velocity profiles at $x = -4$, which is the station 4 ft upstream from the leading fence, were measured for all six runs. When the form drag was measured all other measurements were conducted right above each fence. For Run I and Run II measurements were also made between fences. Run Ia indicates the measurements between $x = 11$ ft and $x = 13$ ft of Run I. Run IIa represents the measurements between $x = 10$ ft and $x = 11$ ft of Run II.

Measurements of Runs I, Ia, II, IIa and VI were performed along an axis 12 in. aside from the tunnel center line. For Runs III, IV, and V, data were taken along the center line. The reason for doing this was to ensure that all measurements were conducted inside two-dimensional boundary layers. The results of two dimensionality of the boundary layers can be found in Chapter IV.

Table II shows the summary of the data collection program. While experiments were performed, all sensor probes were held on the carriage boom. A sketch of the relative positions of each sensor probe is shown in Figure 5.

3.4 Measurements of Mean Velocity and Static Pressure

Mean velocity profiles were measured by pitot tubes for all runs, and for Runs Ia and IIa, hot wire was also applied for measuring the mean velocities in the separation region and to cross check the values obtained by the pitot tubes.

3.4.1 Hot wire for mean velocity - The hot wire measurement of mean velocity was made with a 2×10^{-4} in. diameter platinum coated tungsten wire, which was held parallel to the floor and perpendicular to the local mean velocity. The hot wire anemometer used was a DSA type 55A01 constant temperature anemometer. A Colorado State University made integrator (Figure 6) was applied to obtain the mean D.C. output of the Disa anemometer. The mean velocity can be correlated to the mean D.C. voltage through a calibration curve.

The integrator was calibrated by introducing a constant voltage from a power supply. Figure 7 is the calibration curves of the integrator used.

Prior to the hot wire calibration, the hot wire was subject to operating condition of no flow for no less than 24 hours. This process, which is termed a "curing" process, ensured that the hot wire reached its stable condition before any calibration or measurement was made. The hot wire was calibrated against a 1/8 in. diameter standard pitot-static tube at station $x = -4$ in free stream. This point will be termed the "calibration point." During the experiments the hot wire was calibrated every two hours. No detectable change on the calibration curve was found for a properly "cooked" wire. Figure 8 is a typical calibration curve of the hot wire during one day of operation.

3.4.2 Pitot tube for mean velocity and static pressure - By means of pitot tubes, total head and static head were obtained for calculating mean velocities. Two United Sensor type PAC-12FC 1/8 in. diameter standard pitot-static tubes were used for this purpose. The total head was obtained from the dynamic tap of one pitot tube, and the static tap of another pitot tube provided the measurements of static head. These two taps were held parallel to mean stream side by side with a small distance apart (1/2 inch) in order to avoid the interference between each other (see Figure 5).

As found from experimentation, in the neighborhood of the fences large pressure gradients exist both in x and y direction. However, the pressure gradient in z direction is zero for a two-dimensional flow. Due to these reasons, the velocity measured by a single pitot tube must have a correction on the pressure gradient between the dynamic tap and the static, which the latter is 1/2 in. downwind from the former, on a standard 1/8 in. pitot static tube. On the other hand, when total head and static head were measured separately and both taps were held along z axis (Figure 5), the pressure gradient between the two taps was zero; hence, the correction due to the pressure gradient was not needed.

The total head and static head were measured by connecting the dynamic tap and the static tap to the P_x terminal of a Transonic type 120B equibar pressure meter. The P_{ref} terminal of the pressure meter was connected to the reference tap, which was located on the ceiling at the $x = -4$ station. For this arrangement the measured total and static head indicated the relative total and static pressure between the measuring point and the point that the reference tap located.

The D.C. output of the pressure meter, which indicates the pressure difference in mm of mercury between the P_x and P_{ref} terminals, was connected to the ordinate of x-y recorder (Moseley Autograf Model 153C). The abscissa of the recorder can be either set in time base, to obtain the time integration for a point by point measurement, or can connect to the potentiometer of the carriage to obtain a continuous profile. At each station, point by point measurements as well as the continuous profile were made on total head and static head. The continuous traverses at one station were used to calculate the velocities in the upper part of the flow and also used to cross check the measurements made by the point by point method. Figures 9 and 10 show two typical continuous traverses of the total head and static head, respectively. The data points on those traverses were measured by the "point by point" method.

Consider at one point that the total head is H_t mm of Hg and the static head is H_s mm of Hg , where $\gamma_m H_t = p_t - p_r$ and $\gamma_m H_s = p_s - p_r$, with

γ_m = specific weight of mercury (lb/ft^2),

p_t = pressure at dynamic tap = total pressure,

p_s = pressure at static tap = static pressure, and

p_r = pressure at reference tap.

If the pressure gradient between the dynamic and static taps is negligibly small, the local mean velocity can be calculated by

$$\frac{1}{2} \rho u^2 + p_s = p_t \quad ,$$

where ρ is the density of air.

Or we can write

$$u = 2.361 \, c \sqrt{(H_t - H_s)/\rho} \tag{3-1}$$

where c is the correction factor of the Transonic meter. The value of c was found to be 0.998 by calibrating the Transonic meter against a standard micromanometer (Flow Corporation Model MM2). The equation used to calculate the local mean velocities was

$$u = 2.358 \sqrt{(H_t - H_s)/\rho} \quad . \tag{3-2}$$

While ρ is dependent on both temperature T and barometric pressure p_o, a chart of ρ against T and p_o is shown in Figure 11.

Since the static head H_s represents the static pressure difference between the reference tap and the measuring point, the relative static pressure at that point can be fully specified by the measured static head.

3.5 Measurement of Turbulence

3.5.1 Hot wire probes and the associated instrumentations - Two types of hot wire probes were used to measure the turbulent quantities in the present experiments. One was a normal wire to measure $\overline{u'^2}$. Another was a rotating wire to measure $\overline{v'^2}$ and $\overline{u'v'}$. The normal wire was the same wire used on mean velocity measurements. The rotating wire was a 2×10^{-4} in. diameter platinum coated tungsten wire with an approximate length 0.06 in.

The wire was soldered to steel needle supports protruding from the two holes of a 3/32 in. diameter 12 in. long double drilled ceramic rod. The ceramic rod was held by the sliding bearing of the probe holder. A pointer was attached to the ceramic probe at the end opposite the hot wire. A protractor was fixed on the probe holder parallel to the moving plane of the pointer. Since the pointer was attached directly on the ceramic probe, the relative angle between the wire and the position of the pointer was fixed. When the wire was rotated at an angle, a synchronizing movement of the pointer over the surface of the protractor would indicate that angle. A sketch of the rotating wire is shown in Figure 5.

Since the angle of yaw of the rotating wire has prime importance in calculating $\overline{v'^2}$ and $\overline{u'v'}$, an alignment of the wire was necessary before any measurement was made. The alignment was made by means of a pendulum consisting of fine nylon thread with a small weight attached. The pendulum was hung beside the wire and the wire was adjusted parallel to the fine thread by rotating the ceramic probe. A microscope was used in this alignment process for more precision. Since the thread was perpendicular to the floor, the wire was also 90° from the x-axis. For convenience the pointer was also set at 90°. From this point on, the yaw of the rotating wire could be read directly from the protractor.

In addition, a further check of the wire was made by holding the wire at a calibration point (referring to Section 3.3.1) where the mean stream was parallel to the x-axis. If the hot wire had the same angle sensitivity calibration curve for angles at α and $180° - \alpha$, it indicated that the wire was made perfect symmetrically (will refer to "symmetrical wire" from now on). This kind of wire was used through the entire experiment. Theoretically, $\overline{v'^2}$ and $\overline{u'v'}$ can be calculated through measurements made by a wire at any two known angles, and it is not necessary for the wire to be a symmetrical one as long as the correspondent calibration curves are obtained. However, if the wire is symmetrical and the yaw of angles is chosen to be 45° and 135°, the simplest process for calibration and calculation is ensured. The symmetrical wire can be made by soldering the wire on the tip of the steel needle supports. A typical calibration curve for symmetrical wire used during the experiments is shown in Figure 12.

The hot wire anemometer used for the yawed wire was designed at Colorado State University by Finn and Sandborn (1967). This anemometer is a constant temperature type with the frequency response over 50 kHz.

The rms values of the fluctuating electric signals were measured by a True RMS Meter (Disa type 55D35). The frequency response of the rms meter is flat within 1 - 400 kHz. Six selectable time constants, which range from 0.1 to 30 seconds, are available in this instrument.

In the present experiments three rms values were measured at each data point. There were $\overline{e_o'^2}$ for normal wire, $\overline{e_1'^2}$ for 45° yaw of the yawed wire, and $\overline{e_2'^2}$ for 135° yaw. These rms values were read from the rms meter directly by selecting the time constant at 10 sec for most measurements and at 30 sec for high turbulent flow.

3.5.2 Measurement principles - In most gases the heat transfer from a small cylinder to air stream was found to be a function of the Reynolds number and the Prandtl number; for example, see page 608 of Goldstein (1958). This important finding serves as the basic principle for today's hot wire technique.

In the practical application of hot wire measurement, Baldwin, Sandborn and Lawrence (1960) found that the heat loss from the hot wire is a function of velocity, temperature, fluid properties, and angle of attack. In the present studies, temperature and fluid properties were considered to be constants, and the hot wire anemometer was used to detect the heat loss from the hot wire. The wire is held in x-y plane at an angle α to the x-axis and if $\overline{U}$ represents the magnitude of the vector sum of all velocity components at one instance where

$$\bar{U} = \sqrt{(u+u')^2 + v'^2 + w'^2} \quad . \tag{3-3}$$

The output of a hot wire anemometer has a functional relation

$$E = E[\bar{U},\alpha] \quad . \tag{3-4}$$

The response equation for hot wire in a two-dimensional turbulent flow was derived by Sandborn (1967) and Tieleman (1969). That is

$$e' = \frac{\partial E}{\partial u} u' + \frac{1}{u} \frac{\partial E}{\partial \alpha} v' \tag{3-5}$$

where e' represents the fluctuation in anemometer output and $\partial E/\partial u$ and $\partial E/\partial \alpha$ are the sensitivities of hot wire to velocity and angle of attack, respectively.

If one assumed that the heat transfer of a hot wire is only affected by the velocity component, which is normal to the wire, the angular sensitivity and the velocity sensitivity in Equation 3-5 has the form

$$\frac{1}{u} \frac{\partial E}{\partial \alpha} = \frac{\partial E}{\partial u} \cot\alpha \quad . \tag{3-6}$$

However, Webster (1962), Sandborn (1967), and Champagne et al. (1967) showed that relation 3-6 is not exactly true except at $\alpha = 90°$, where both $\cot \alpha$ and $\partial E/\partial x$ are zero. When the heat transfer from a hot wire is considered to be affected by both normal and parallel velocity components, Arya (1968) found that the relation between $\partial E/\partial u$ and $\partial E/\partial \alpha$ should have the form

$$\frac{1}{u} \frac{\partial E}{\partial \alpha} = c \frac{\partial E}{\partial u} \cot\alpha \tag{3-7}$$

and

$$c = \frac{1 - a^2}{1 + a^2 \cot^2 \alpha} \tag{3-8}$$

where a is a parameter, proposed by Hinze (1959) and Webster (1962), to indicate the effective heat transfer from the parallel component of velocity. Arya (1968) used $a = 0.2$ and hence, $c = 0.923$, for $\alpha = 45°$.

Substituting Equation 3-8 into Equation 3-5, thus

$$e' = \frac{\partial E}{\partial u} (u' + c\, v' \cot\alpha) \quad . \tag{3-9}$$

The application of Equation 3-9 in calculating $\overline{u'^2}$, $\overline{v'^2}$, and $\overline{u'v'}$ will be discussed in the following section.

(a) Calculating $\overline{u'^2}$ from the normal hot wire

The longitudinal turbulence $\overline{u'^2}$ was obtained by measuring the rms value and the mean velocity calibration curve of the normal hot wire. For normal wire measurement $\alpha = 90°$, Equation 3-9 reduces to

$$e'_o = S(u') \tag{3-10}$$

where e'_o indicates the anemometer response of the fluctuating velocity of normal wire, and $S = \partial E/\partial u$. After squaring Equation 3-10 and taking a time average one obtains

$$\overline{u'^2} = \frac{1}{S^2} \left(\sqrt{\overline{e'^2_o}}\right)^2 \tag{3-11}$$

where $\sqrt{\overline{e'^2_o}}$ is the rms value; of course, the sensitivity, S , can be obtained by measuring the slope of the normal wire calibration curve from Figure 8. However, the graphical method is not only inaccurate but also tedious, the sensitivity S was obtained by adopting King's law in the present studies. If one plots the square of the voltage output E^2 against the square root of corresponding mean velocity $\sqrt{\bar{u}}$, the best fit curve can be obtained from the least square method

$$E^2 = b + m \sqrt{\bar{u}} \quad . \tag{3-12}$$

From Equation 3-12 the sensitivity S becomes

$$S = \frac{\partial E}{\partial u} = \frac{1}{4E} \frac{m}{\sqrt{\bar{u}}} \quad . \tag{3-13}$$

Substituting Equation 3-12 into Equation 3-13 to eliminate E , one obtains

$$S^2 = \frac{m^2}{16u(b+m\sqrt{u})} \qquad (3\text{-}14)$$

where m and b are constants for a calibration curve and u is the local mean velocity.

(b) Calculating $\overline{v'^2}$ and $\overline{u'v'}$ from the yawed wire

The vertical turbulence intensity $\overline{v'^2}$ and the turbulent shear stress $\overline{u'v'}$ were measured by means of the rotating wire at two yawed angles. For convenience, the angles were chosen to be 45° and 135°. As mentioned in Section 3.5.1 and indicated in Figure 12, the calibration curves for 45° and 135° are identical; the calibration curve with 45° angle of yaw was prepared for present measurements. Of course, the testing of a "symmetrical wire" was performed before any calibration or measurement was made (refer to Section 3.5.1).

Now, squaring Equation 3-9 and taking a time average one obtains

$$\overline{e'^2_\alpha} = S^2_\alpha\,(\overline{u'^2} + 2\,c\,\overline{u'v'}\cot\alpha + c^2\,\overline{v'^2}\cot^2\alpha) \qquad (3\text{-}15)$$

where $\overline{e'^2_\alpha}$ represents the rms response of the yawed wire at α degrees yaw, and S_α is the correspondent velocity sensitivity $S_\alpha = (\frac{\partial E}{\partial u})_\alpha$. Assuming $\alpha = 45°$ and 135°, then for a symmetrical wire, $S_{45} = S_{135}$. If one lets $\overline{e'^2_1} = \overline{e'^2_{45}}$,

$\overline{e_2'^2} = \overline{e_{135}'^2}$, and $S_1 = S_{45} = S_{135}$, two response functions, correspondent to $\alpha = 45°$ and $135°$, can be written as

$$\overline{e_1'^2} = S_1^2 \left(\overline{u'^2} + 2\,c\,\overline{u'v'} + c^2\,\overline{v'^2}\right) \tag{3-16}$$

for $\alpha = 45°$,

and

$$\overline{e_2'^2} = S_1^2 \left(\overline{u'^2} - 2\,c\,\overline{u'v'} + c^2\,\overline{v'^2}\right) \tag{3-17}$$

for $\alpha = 135°$.

By adding Equations 3-16 and 3-17,

$$\overline{v'^2} = \frac{1}{2c^2} \left\{ \frac{1}{S_1^2} \left(\overline{e_1'^2} + \overline{e_2'^2}\right) - 2\,\overline{u'^2} \right\} \; ; \tag{3-18}$$

and subtracting 3-17 from 3-16, one obtains

$$\overline{u'v'} = \frac{1}{4cS_1^2} \left(\overline{e_1'^2} - \overline{e_2'^2}\right) \tag{3-19}$$

where $\overline{e_1'^2}$ and $\overline{e_2'^2}$ are measured data, $c = 0.923$, as given by Arya (1968), $\overline{u'^2}$ is obtained from Equations 3-11 and 3-14, and S_1 can be calculated from Equation 3-14 by using different values of m and b . These values are obtained from the calibration curve at 45° yaw. A typical calibration curve for the yawed wire is also shown in Figure 13.

3.6 Measurement of Form Drag of Fences

The form drag of all the fences was measured by means of two tapped fences; one was the "stagnation fence" and another was the "separation fence" (Section 3.2). The stagnation pressure acting on the upwind surface of a fence was measured through seven pressure taps on the stagnation fence. The stagnation pressure at the lowest point of the fence was measured through the pressure tap drilled through the plywood flow (Section 3.2). Stagnation pressure measurements at $y = 7/8"$, $6/8"$, $5/8"$, $4/8"$, $3/8"$, $2/8"$, $1/8"$, and $y = 0$ were recorded. By substituting the separation fence for the stagnation fence, the separation pressure on the lee side of a fence was measured. Separation pressures were measured at $y = 2/8"$, $4/8"$, and $7/8"$. Constant separation pressure was found in the y direction which is in agreement with Plate (1964) and Nagbhushanaiah (1961).

The form drag D of a fence was obtained graphically:

$$D = \int_{o}^{h} (p_f - p_b)\, dy \qquad (3\text{-}20)$$

where

h = fence height = 1 inch,

p_f = pressure measured by the stagnation fence, and

p_b = pressure measured by the separation fence = constant for each fence.

3.7 Errors in Measurements

Two types of errors are involved in all measurements, systematic errors and the random errors. Systematic errors are introduced by the nature of flow field, the limitations of measuring techniques, and inadequate design of instrumentation. Those errors caused repeated readings in error to the same amount without apparent reason. If the reason for causing the systematic error is known a suitable correction will eliminate the error. Random errors, on the other hand, are caused by the process of measurement, inherent error of instruments, the read out technique, and personal errors. Those errors caused readings to differ repeatedly for unknown reasons. Unlike the systematic errors, there is almost no way to eliminate random errors. However, for most experiments random errors can be reduced to a very small percent, such that the errors will not be significant in the overall result.

In this section possible sources of uncorrected systematic error will be described for various types of measurements, and estimations of the random errors on various results will be given.

3.7.1 The systematic errors - These kinds of errors occur systematically in measurements without apparent reasons. If the reasons are known, a suitable correction will eliminate the errors. Corrections of systematic errors were applied to the calibration or data reduction process and will not be discussed here.

In this section a brief discussion on these uncorrected systematic errors will be described. Usually these uncorrected errors are either too small to affect the result or are without a reliable correction method.

(a) Total head measurement errors

Systematic errors in total head, introduced by viscous, shear, and wall proximity effects, are discussed by MacMillan (1954). These errors are important only when the total head tube is immerged in the region near the wall, say in the laminar sublayer.

Turbulence effects on total head measurement have been studied by Goldstein (1965), Carmody (1964), Landweber (1966), and Tieleman (1967). Their results give a direct correlation between the measured total head and the turbulence intensities.

The pressure equation given by Goldstein is

$$p_{mt} = p_s + \frac{1}{2} \rho u^2 + \frac{1}{2} \rho (\overline{u'^2} + \overline{v'^2} + \overline{w'^2}) \quad , \qquad (3\text{-}21)$$

where p_{mt} is the measured total pressure, and p_s is the local static pressure. Since p_s is measured at the point where turbulence influence is significant, Tieleman (1967) proposed that

$$p_{mt} = p_\infty + \frac{1}{2} \rho u^2 + \frac{1}{2} \rho (\overline{u'^2} - \overline{v'^2} + \overline{w'^2}) \qquad (3\text{-}22)$$

where p_∞ is the static pressure at free stream and the vertical turbulence intensity is negligible at the point that p_∞ is measured.

Hinze (1959) questions Goldstein's expression for the following reason: Equation 3-21 might be correct if the opening of the total head is a true point or in other words, the opening must be infinitely small in dimensions. For a total head probe with a finite size in opening, the effects of v'^2 and w'^2 on the total pressure measurement will be dependent on the scales of v'^2 and w'^2. However, no quantitative correlation was given.

Richardson (1964) proposed another pressure relation as

$$p_{mt} = p_\infty + \frac{1}{2}\rho f(r)\ (u^2 + \overline{u'^2} + \overline{v'^2} + \overline{w'^2}) \qquad (3\text{-}23)$$

where f is a function of r, which characterizes the total pressure tube response, $f(r)$ is close to unity at low turbulent flow, say, $\{(\overline{u'^2} + \overline{v'^2} + \overline{w'^2})/u^2\}^{\frac{1}{2}} < 0.1$. No value of $f(r)$ was given on high turbulent flow.

(b) Static head measurement errors

The correlations between the measured static pressure p_{ms} and the true static pressure p_s in a turbulent flow field was suggested by Goldstein (1965):

$$p_{ms} = p_s + c_1\rho\ (\overline{v'^2} + \overline{w'^2}) \qquad (3\text{-}24)$$

where c_1 is the coefficient which indicates the effect of the inpact pressure of the fluctuating velocities normal to the static head tap openings. For isotropic turbulence Goldstein found that $c = 0.25$ and c_1 can only be obtained experimentally in a boundary layer flow. However, Hinze (1959) concluded a completely different result. Since the normal flow around a cylinder gives a resultant negative pressure, the measured static pressure p_{ms} should be lower than p_s, or in other words, the coefficeint c_1 must be negative. No systematic study on this correlation has been published.

(c) Hot wire measurement errors

Various types of systematic errors are involved in hot wire measurements. A brief discussion of these errors follow:

(i) Turbulence effect on mean output of hot wire

When a hot wire is immerged into a turbulent flow the heat transfer from the wire will be affected by both the mean and fluctuating velocities. Ven Der Hegge Zijnen (1938) found the heat transfer from a cylinder is a function of turbulent intensity $\sqrt{\overline{u'^2}}/u$ and L_x/d ratio, where L_x is the integral scale of turbulence and d is the diameter of the cylinder. In Figure 14 one can see the influence of heat transfer due to the turbulence effect.

As indicated by Sandborn (1968), for most turbulent boundary layer measurements, when L_x/d is greater than 500 and $\sqrt{\overline{u'^2}}/u$ less than 0.25, turbulence will not affect the mean hot wire output.

In the present studies the turbulent intensity can easily exceed 0.5 inside or near to the separation region. For flow at such a high turbulent level no correlation on the turbulence effect to heat transfer has been published. Therefore, there exists a high uncertainty factor for all mean velocity measurements near the fences.

(ii) Proximity of solid boundary - When hot wire is placed very close to a solid boundary, i.e., tunnel floor, the heat transfer from the wire will be affected by the boundary. This effect on heat transfer is due to the existence of temperature difference between the wire and the tunnel floor.

As found by Tieleman (1967), the solid boundary effect becomes important only when the hot wire is held within a distance of 0.02 in. from the floor. In the present experiments all measuring points were at much higher distances.

(iii) Finite length of hot wire - An ideal hot wire should be infinitely small both in length and diameter, such that the measurement obtained by this probe can be considered a truly point measurement. However, due to physical limitation, it is impossible to make such an ideal wire.

Both normal and yawed wires, used in experiments, had a diameter of 0.0002 in. and an approximate length of 0.06 in. When the dominating eddies are the same size or smaller than the length of the wire, the velocity fluctuations on one part of the wire may not be the same as those on the other part.

The difference in velocity will cause the measured rms value to be less than the true value.

Corrections have been proposed by Dryden et al. (1937), Frenkiel (1954), and Uberoi and Kovasznay (1953) by means of the "space-resolution correction" for rms voltage:

$$\frac{\overline{e_\ell'^2}}{\overline{e'^2}} = \frac{2}{\ell^2} \int_0^\ell (\ell - z)\ R_z(z)dz \tag{3-25}$$

where $\overline{e_\ell'^2}$ is the measured mean square value, ℓ is the "effective" length of the wire, and $R_z(z)$ is the lateral correlation coefficient. Unfortunately, $R_z(z)$ can only be obtained through a direct measurement which also needs a correction. In addition, ℓ is mainly dependent on definition and there is no reliable method available to predict the true value of ℓ .

(iv) Gradients of velocity and turbulence - It is clear that the normal wire, which is held parallel to z-axis, does not experience the problem of velocity or turbulence gradients. However, the gradient effects on the measurement made by the yawed wire could be important, especially where the gradients are large and the yawed wire is placed near the fence. Currently, no adequate method is available for correcting the errors when the hot wire experiences velocity and turbulence gradients. The only way to "examine" the gradient effects is to apply a direct measurement check. The normal wire was utilized to examine the gradient effect. Two sets of $\overline{u'^2}$ were measured for the same section; $\overline{u_1'^2}$ were measured by holding the normal wire horizontally and $\overline{u_2'^2}$ were measured by holding the normal wire vertically. Since $\overline{u_1'^2}$ do not experience any gradient effect, the deviation of $\overline{u_2'^2}$ from $\overline{u_1'^2}$ will indicate the region in which the gradient effect is important. The measured results of $\overline{u_1'^2}$ and $\overline{u_2'^2}$ are shown in Figure 15; no systematic difference can be found.

3.7.2 Random errors - The random errors discussed here are the errors that are caused by a large number of small effects, such as small changes in environment, personal errors in operation, and errors inherent in instrumentation. If no systematic error or mistake is involved in measuring processes, and each of the effects is independent to the others, the probability density distribution of a measured result is usually considered to be normally distributed:

$$P(x) = \frac{1}{\sigma\sqrt{2\pi}} \exp\left\{\frac{(x-\overline{x})^2}{2\sigma}\right\} \tag{3-26}$$

where $x-\overline{x}$ is the error of a measured value, $P(x)$ is the probability of occurrence of x , σ is the standard deviation and $\overline{x}$ is the mean of the distribution function.

The error of measured result can be estimated through the statistical method by repeating the measurements numerous times. Experiments where errors are evaluated by such repetition are called multi-sample experiments. However, for most engineering experiments it is not practical to estimate error by repetition, if for no other reasons than the time and cost required would be too costly for large scale experiments. Single-sample experiments are usually used to describe these kind of experiments. The reliability, as well as the error of a measured result, can only be estimated from the reliabilities of all factors involved.

The standard method for estimating the errors in multi-sample experiments can be found from the manual published by the American Society of Testing Materials (1949). The method for calculating errors in single-sample experiments has been the subject of many publications, such as Kline and McClintock (1953), Scarborough (1955), and Doebelin (1966).

The present study is a typical single-sample experiment. The random errors (referred to as "errors" for convenience) of all results were estimated by adopting the principle proposed by Kline and McClintock (1953).

If a result R is a known function of n independent variables $u_1, u_2 \ldots u_n$, one can write R in this form

$$R = R(u_1, u_2 \ldots u_n) \tag{3-27}$$

where the variables u_i, $i=1,2, \ldots n$, are considered to be the measured quantities (instrument output), and are in error by $\pm\Delta u_1, \pm\Delta u_2 \ldots \pm\Delta u_n$, respectively. Kline and McClintock (1953) suggest that an odd number should be given for each of the Δus'. For example, $\pm\Delta u$ (99 to 1) means that 99 out of 100 measured errors should be within the region $\pm\Delta u$. In most cases statistical bounds such as $3\sigma_i$ limits are given for each Δu_i . Here σ_i is the standard deviation of the error distribution for a given variable u_i . When u_i has normally distributed errors (Equation 3-26), $\pm\Delta u_i$ in $3\sigma_i$ limits means that 99.7 percent errors of u_i should occur between $+\Delta u_i$ and $-\Delta u_i$. Since the $\pm 3\sigma_i$ limits on describing the error bounds are widely used in engineering and industry, from this point on unless otherwise indicated, Δu_i will automatically adopt $\pm 3\sigma_i$ limits.

Now going back to Equation 3-27, consider that the variation δu_i of u_i, i=1,2,u are small, the correspondent variation δR of R can be approximated by the Taylor series expansion in linear form:

$$\delta R = \frac{\partial R}{\partial u_1} \delta u_1 + \frac{\partial R}{\partial u_2} \delta u_2 + \ldots + \frac{\partial R}{\partial u_n} \delta u_n \quad . \qquad (3\text{-}28)$$

If the errors Δu_i of u_i , i=1,2,... n are small (in most cases true) by substituting Δu_i to δu_i in Equation 3-28, the correspondent error of R can be expressed in two common forms. One is called the "maximum error" with the form

$$E_R = \left|\frac{\partial R}{\partial u_1} \Delta u_1\right| + \left|\frac{\partial R}{\partial u_2} \Delta u_2\right| + \ldots + \left|\frac{\partial R}{\partial u_n} \Delta u_n\right| \qquad (3\text{-}29)$$

where E_R indicates the maximum possible error of R .

Another expression is called the root-sum square error (see page 429 of Scarborough, 1955), where

$$\Delta R = \left\{ \left(\frac{\partial R}{\partial u_1}\right)^2 (\Delta u_1)^2 + \left(\frac{\partial R}{\partial u_2}\right)^2 (\Delta u_2)^2 + \ldots + \left(\frac{\partial R}{\partial u_n}\right)^2 (\Delta u_n)^2 \right\}^{\frac{1}{2}} . \tag{3-30}$$

In Equation 3-29 since Δu_i represents a $\pm 3\sigma_i$ limit on u_i the statistical bounds of E_R must be in a higher σ_R limits of R . In general, the statistical bounds of E_R are not known, and the comparison between E_R and Δu_i becomes meaningless. On the other hand, when the error ΔR in Equation 3-30 is expressed by the root-sum square function the statistical bounds of ΔR is the same as Δu_is', i.e., as well as Δu_is', ΔR also represents a $\pm 3\sigma_R$ limit on R. It is easy to see that Equation 3-30 is a reasonable expression in error estimation, and hence will be used to estimate the errors in all calculated results.

If by dividing ΔR by R , the expression $\Delta R/R$ gives a relative relation between the error ΔR and the mean result R , this is known to be a relative error.

The estimated errors of all measured results based on Equation 3-30 are shown in the following. Calculations can be found in the Appendix.

(i) u measured by pitot tubes:

$\frac{\Delta u}{u} = \pm 1\%$ for the best cases

$\frac{\Delta u}{u} = \pm 3\%$ for the worst cases.

(ii) u measured by hot wire:

$$\frac{\Delta u}{u} = \pm 11.4\% \quad \text{at 5 fps}$$

$$\frac{\Delta u}{u} = \pm 6.7\% \quad \text{at 30 fps}$$

(iii) $\overline{u'^2}$:

$$\frac{\Delta \overline{u'^2}}{\overline{u'^2}} = \pm 12\% \quad \text{overall measurements.}$$

(iv) $\overline{v'^2}$:

The relative error of $\overline{v'^2}$ varies from ± 0.2 to ± 2.5 which is dependent on the local $\overline{u'^2}$, $\overline{e_1'^2}$, $\overline{e_2'^2}$ and $\overline{v'^2}$. The error of $\overline{v'^2}$ can only be calculated from the local measurements through Equation 3-30. Some examples on $\Delta\overline{v'^2}/\overline{v'^2}$ are shown in Table A.2. At Station I(-4), which is the smooth wall equilibrium turbulent boundary layer, when $y/\delta = 0.2$ $\Delta\overline{v'^2}/\overline{v'^2} \approx \pm 40\%$ and for $y/\delta > 0.3$ the relative error of $\overline{v'^2}$ remains $\pm 30\%$.

(v) $\overline{u'v'}$:

The error of $\overline{u'v'}$ depends on local measurements of $\overline{e_1'^2}$, $\overline{e_2'^2}$, and $\overline{u'v'}$ and should be calculated at each data point. Table A.2 gives the results of $\Delta\overline{u'v'}/\overline{u'v'}$ for Stations I(-4), I(0), I(2), and I(5). At Station I(-4) when $y/\delta = 0.1$ $\overline{u'v'}/\overline{u'v'} \approx \pm 20\%$ and for $y/\delta > 0.2$ $\Delta\overline{u'v'}/\overline{u'v'} \approx \pm 10\%$.

Chapter IV

RESULTS AND DISCUSSIONS

Presented in this chapter are the results of the measured mean velocity distributions, drag force, and turbulence of a distributed turbulent boundary layer. The roughness elements used are sharp-edged fences, equally spaced on a flat surface. Emphasis is given to the "rough region" (Figure 1), which is far downstream from the leading fence. Boundary layer characteristics of the smooth region (Figure 1) are also presented here to give a better understanding of the present study. The broad characteristics of the boundary layer in the "transition region" are presented, but without detailed analysis. A Karman constant, $\kappa = 0.4$, was used in this study.

4.1 General Properties of the Boundary Layer

Since the wind tunnel at Colorado State University is large, the test section extending 80 ft in length, with a cross section 6 ft by 6 ft, it has a distinct advantage in meteorological studies when a thick boundary layer is required. However, due to the thickness of the boundary layer (more than 1.5 ft at Region III), the secondary flow may become large and will affect the two dimensionality of the boundary layer. The two dimensionality of the wind tunnel was checked by taking horizontal traverses of the pitot tube reading across the wind tunnel at various heights and several distances from the leading fences. At 30 fps, the most uniform region of the lateral direction velocity profiles was found to be between 4 in. and 14 in. west of the centerline. The velocity distributions across the wind tunnel at x = - 4 ft, 2 ft and 6 ft in various heights are shown in Figure 16. The lowest velocity occurred about 4 in. east of the centerline (refer to Figure 3), and the maximum difference was about 1 fps. When the fence spacings were changed from 12 in. to 18 in., the region of uniform flow was found unchanged. This is shown in Figure 17. However, when the mean velocity was set at 45 fps, the region of uniform flow shifted to the center. This is shown in Figure 18.

In order to ensure that the experiments were conducted inside a two-dimensional boundary layer, measurements of each run were performed along an axis parallel to the center line and where the flow in the lateral direction was uniform. Data for Runs I, Ia, II, IIa, and VI were taken along an axis 12 in. west of the tunnel center line; Runs III, IV, and V were measured along the center line.

Pressure gradients over that part of the test section that was covered fences were adjusted to nearly zero. The free stream static pressure of all six runs are shown in Figure 19.

When the smooth wall boundary layer in Region I of Figure 1 (referred to as the initial boundary layer) encounters a series of fences, the form drag of the fences introduces an increase in wall shear stress. The increase in wall shear causes the boundary layer to change from its initial condition. The flow changes are, initially, in a thin layer near the fences. This layer then increases in depth as it moves downwind. At a certain distance downstream from the leading fence, the velocity profiles become similar and the boundary layer is termed an equilibrium boundary layer. Figure 20 is the nondimensional plot of the velocity profiles of Run I. The velocity change is shown clearly in this figure. From Station I(9) downstream all nondimensional velocity profiles collapse into a single curve, and from this point an equilibrium boundary layer exists for $x > 9$ ft.

The increase in wall shear stress causes a loss of momentum of the boundary layer and retards the fluid. Therefore, the boundary layer thickness, δ , the momentum thickness, θ , as well as the displacement thickness, δ^* , must be increased at a faster rate. Figures 21 through 26 are the plots of δ , δ^* , θ and the shape factor H for Runs I through VI, respectively, where δ is defined as $u_\delta = 0.99\, u_a$, δ^* is defined in Equation 2-2, θ is defined in Equation 2-16, and $H = \delta^*/\theta$. The numerical value of the boundary layer parameters are shown in Table 3.

4.2 Mean Velocity Profiles, Static Pressure Distributions, and Streamlines

Tables IV and V are a summary of the measured mean velocities and static heads. Figures 27 and 28 show the velocity profiles, static head profiles, and streamline patterns of Runs I and II, respectively.

The dimensionless stream function is defined as

$$\psi = \frac{1}{h} \int_{o}^{y} \frac{u}{u_a} dy \quad . \tag{4-1}$$

One has a streamline by connecting a constant ψ from station to station. The velocity profiles, static head profiles, and streamlines of Runs Ia and IIa are shown in Figures 29 and 30, respectively. As mentioned previously, the pitot tube cannot be used to measure a reverse flow and the hot wire can only detect the magnitude of a velocity vector. In addition, the hot wire experienced large errors when measurements were conducted inside the separation bubble. For these reasons, Equation 4-1 cannot be used to calculate ψ for Runs Ia and IIa.

Therefore, an alternate method was used to determine the streamlines, based on the following considerations: Since the nondimensional stream function ψ, above each fence, can be well defined through Equation 4-1, the streamlines between two adjacent fences can be obtained by integrating the mean velocity profile downward from an assumed reference streamline. If ψ_1 is chosen to be the reference streamline and the height of ψ_1 at the nth fence is y_n, then at the $n+1$ fence the height is y_{n+1}. Usually y_n and y_{n+1} are chosen to be greater than the boundary layer thickness δ; thus, it is possible to assume that the height of ψ_1 varies linearly from y_n to y_{n+1}. If y_1

is the assumed height of ψ_1 at a station with distance x from the nth fence, and L is the spacing of fence, then,

$$y_1 = \frac{x}{L}(y_{n+1} - y_n) + y_n \quad .$$

The dimensionless stream function at that station becomes

$$\psi = \psi_1 + \int_{y_1}^{y} u dy \quad . \tag{4-2}$$

The location of the separation streamline can be found by finding y_s, such that $\int_{y_1}^{y_s} u dy = - \psi_1$. Figures 29 and 30 show the separation streamlines and other streamlines of Runs Ia and IIa, respectively. Flow patterns inside the separation bubble, which are shown in Figures 29 and 30, are defined qualitatively by the fact that the net flow across a vertical section from $y = 0$ to $y = y_s$ is zero, or

$$\int_{o}^{y_s} u dy = 0 \quad . \tag{4-3}$$

4.3 Boundary Layer at $x = - 4$ ft

As mentioned in Section 1.2, a smooth wall equilibrium turbulent boundary layer is expected to be found at $x = -$ 4 ft. Comparisons of the previous results on smooth wall equilibrium boundary layers to the present measurements at $x = - 4$ ft are presented in this section.

4.3.1 Wall shear stress measurements - Numerous methods in predicting the drag coefficient, c_f, are shown in Section 2.1.4. In general, c_f are found through a function of local boundary layer parameters, for example, see Equations 2-19, 2-21, and 2-22. Clauser (1954), however, proposed a graphical method to obtain c_f. He assumed that

$$\frac{u}{u_*} = \frac{1}{\kappa} \ln \frac{yu_\tau}{\nu} + c \tag{4-4}$$

is a universal function for smooth wall turbulent boundary layer flow. The symbol u_* represents the shear velocity which is determined by some indirect method other than a direct wall shear stress measurement. Let

$$\frac{u_*}{u_a} = \sqrt{\frac{c_f'}{2}} \quad ,$$

then Equation 4-4 becomes

$$\frac{u}{u_a} = \frac{1}{\kappa} \sqrt{\frac{c_f'}{2}} \ln \frac{yu_a}{\nu} \sqrt{\frac{c_f'}{2}} + c \quad . \tag{4-5}$$

The plotting of u/u_a vs. yu_a/ν gives a universal family with c_f' as a parameter of the experimental data near the wall are plotted in a like manner; i.e., u/u_a vs. yu_a/ν, c_f' can be determined by selecting the appropriate member of the family fitting the data points.

The method used here to determine u_* is slightly modified from Clauser's graphical method. If one rewrites Equation 4-4 into the following form

$$\frac{u}{u_*} = \frac{1}{\kappa} \ln \frac{yu}{\nu} \frac{u_*}{u} + c \quad ,$$

or

$$\frac{u}{u_*} + \frac{1}{\kappa} \ln \frac{u}{u_*} = \frac{1}{\kappa} \ln \frac{yu}{\nu} + c \quad . \tag{4-6}$$

The value of u_*/u at each data point near the wall is thus seen to depend only on the terms on the right hand side of Equation 4-6. Figure 31 shows a plot of u_*/u vs. $u/u_* + 2.5 \ln(u/u_*)$.

With $\kappa = 0.4$ and $c = 5.1$, then the right hand side of Equation 4-6 can be calculated from the measured data, and, u_*/u at that point, can be obtained from Figure 31. Figure 32 shows the relationship between y and u_* at stations $x = -4$ ft.

Another graphical method used is to plot u vs. $\log y$. The slope of the semi-log plot indicates the quantity of u_*. Figure 33 is the semi-log plots; the average u_*'s, calculated from Equation 4-6, are shown in solid lines. Since this method needs a slope measurement, it will create an error larger than the method proposed previously.

4.3.2 <u>The universal velocity distributions</u> - The wall law plots and defect law plots of stations $x = -4$ are shown in Figure 34 and Figure 35. The wall law is found to be

$$\frac{u}{u_*} = 5.76 \log \frac{yu_*}{\nu} + 5.1 \tag{4-7}$$

and the defect law in the "overlap" region reads

$$\frac{u - u_a}{u_*} = 5.76 \log \left(\frac{yu_*}{\delta^* u_a} \right) + 0.8 \quad . \tag{4-8}$$

For a comparison, Mellor and Gibson's (1966) theoretical velocity profile at zero pressure gradient is also plotted in Figure 35. In the "overlap" region the small difference between Equation 4-8 and Mellor and Gibson's profile is due to the choice of the Karman constant. But data in the outer layer deviate from the theoretical profile systematically. The deviation of the present data from Mellor and Gibson's profile may be an indication that the outer part of the boundary layer at $x = -4$ is not in its equilibrium condition yet.

As mentioned in Section 3.2, an eight-foot transition was used to raise the original tunnel floor one inch, and the leading fence was located 10 ft downwind from the starting edge of the one-inch high plywood floor. It is clear that the distance from the edge of the one-inch high floor to station $x = -4$ ft is only 6 ft. Since the pressure gradients upstream from station $x = -4$ ft were not controlled, boundary layer over the transition might experience different pressure gradients in different wind velocities. The difference in pressure gradients resulted in a difference in the boundary layer development. When the flow reached the edge of the one-inch high floor, the pressure gradient became nearly zero, and the boundary layer adjusted gradually to a zero pressure gradient equilibrium boundary layer. As suggested by Clauser (1954), only a small distance is needed for the lower layer (wall law region) to reach an equilibrium condition, but a much larger fetch is needed for the outer layer to reach its equilibrium condition. At station $x = -4$, which is 6 ft from the starting edge of the one-inch high flow, it is possible that only the wall law region has reached its equilibrium condition. This phenomena can be seen from Figures 34 and 35. In these figures data in both the wall law regions and "overlap" regions nicely correlate the universal laws of a zero incidence smooth wall equilibrium boundary layer. But, data in the outer layer, in Figure 35, deviates considerably from the universal defect law.

4.4 The Form Drag of Fences and the Average Wall Shear Stress

Measurements of form drag of fences were discussed in Section 3.5, and Equation 3-20 was used to determine the form drag where

$$D = \int_{o}^{h} (p_f - p_b)dy \quad . \tag{3-20}$$

The form drag coefficient is defined as

$$c_D = \frac{D}{\frac{1}{2} h\rho u_a^2} \quad . \tag{4-9}$$

If the distance between fence L is not large, the shear stress acting on the floor between adjacent fences is negligible when compared to the form drag acting on the fences. It is possible to assume that the average wall shear stress can be expressed as

$$\tau_o = \frac{1}{L} D \tag{4-10}$$

and the average drag coefficient of wall shear stress is

$$c_f = \frac{\tau_o}{\frac{1}{2}\rho u_a^2} = \frac{h}{L} c_D \quad . \tag{4-11}$$

The shear velocity is defined as

$$u_\tau = \sqrt{\frac{\tau_o}{\rho}} = \sqrt{\frac{D}{L\rho}} = u_a \sqrt{\frac{c_f}{2}} \quad . \tag{4-12}$$

Values of measured c_D , c_f , and u_τ for all six runs are shown in Table VI. Also in Table III, both u_τ and u_* are listed where u_*'s are the shear velocities obtained from the slopes of the semi-log plots, described in Section 4.3.1. The graphical method used in determining u_* for the smooth wall boundary layer cannot be used here. This is because the constant c in Equation 4-6 is not known for a rough wall boundary layer.

As found by Nikuradse (1933) and Hama (1954), when Reynolds number R_x is high, $R_x = u_a x/\nu$, c_f is independent of R_x and is a function of κ or $R_\kappa = \kappa u_a/\nu$ (refer to page 580 of Schlichting, 1968). At a distance far downstream from the leading fence, the important length scale in the multiple fence flow model is L and h . Since h is held constant in the present study, the length scale must be L . The measured c_f for each run at the largest x is plotted in Figure 36, and the relation between c_f and R_L is found to be

$$c_f = 0.282\ R_L^{-0.258} \tag{4-13}$$

where $R_L = u_a L/\nu$. The application range of Equation 4-13 is suggested to have the L/h ratio between 5 and 20.

The form drag coefficients of the leading fence c_{Do} are compared to the empirical relation given by Plate (1965). Figure 37 shows good agreement between the present data and Plate's empirical relation

$$c_{Do} = 1.05 \left(\frac{h}{\delta}\right)^{2/7}$$

where c_{Do} is the form drag coefficient of the leading fence.

4.5 Boundary Layer Above Fences

4.5.1 The equilibrium boundary layer - It has been shown in Figure 20 that the boundary layer deviated from the initial profile (at station x = - 4 ft) when it encountered the fences. But for $x > 9$ ft all nondimensional velocity profiles collapsed to a single curve, once more. This means that the boundary layer reached its equilibrium condition for $x > 9$ ft. Figure 38 is the replot of Figure 20 in y/δ and $(u-u_a)/u_\tau$ coordinates. Again, all profiles for $x > 9$ ft can be correlated into a single curve. If the velocity profiles of Stations I(13), II(11), III(12), IV(12), and VI(12) are plotted in y/δ vs. $(u-u_a)/u_\tau$, a single curve can be found, as seen in Figure 39. According to Clauser (1954), the boundary layers at all six stations here are in their equilibrium conditions; furthermore, the pressure gradients of all six stations are similar.

4.5.2 The plots of defect law - It has been found by many investigators that the velocity defect law in the "overlap" region should have the form

$$\frac{u - u_a}{u_\tau} = \frac{1}{\kappa} \ln \frac{yu_\tau}{\delta^* u_a} + B \quad . \tag{4-14}$$

If $\kappa = 0.41$, then $B = 0.6$; if $\kappa = 0.4$, then $B = 0.8$, and B is considered to be independent of surface roughness but a function of free stream pressure gradients.

However, present data indicate that B may be affected by the roughness geometry as well as the free stream pressure gradient. Figure 40 is the universal plot of Stations I(13), II(11), III(12), IV(12), V(12), and VI(12) in the overlap region, which has the relation

$$\frac{u - u_a}{u_\tau} = \frac{1}{\kappa} \ln \frac{yu_\tau}{\delta^* u_a} + 1.46 \quad . \tag{4-15}$$

Figures 41 through 46 are the same plots for Runs I through VI, respectively. Good agreement is found between present data and Equation 4-15.

An empirical relation in describing the outer layer flow is established by slightly modifying Hama's (1954) empirical relation as:

$$\frac{u_a - u}{u_\tau} = 8.4 \left(1 - \frac{1}{0.32} \frac{yu_\tau}{\delta^* u_a}\right)^2 \quad . \tag{4-16}$$

Equation 4-16 and Equation 4-15 are connected smoothly at $y/\delta = 0.18$.

If the defect law is a universal function, for $\kappa = 0.4$, B must be 0.8 and the pressure parameter in Equation 2-8 must be such that $\Delta u_1/u_\tau = 1.46 - 0.8 = 0.66$. The corresponding pressure gradient can be estimated from Mellor and Gibson (1966). It was found that when $\Delta u_1/u_\tau = 0.66$, then

$$\frac{\delta^*}{\tau_o} \frac{dp}{dx} = - 0.27 \quad . \tag{4-16}$$

The corresponding pressure gradient in mm of Hg per ft for each run should be:

Run	I	II	III	IV	V	VI
$\frac{dH_s}{dx}$ (mm Hg/ft)	-0.099	-0.111	-0.170	-0.155	-0.15	-0.075

If one refers to Figure 19, one can see that it is impossible for such a large free stream pressure gradient to exist. Therefore, the pressure parameter $\Delta u_1/u_\tau$ must also be a function of roughness geometry.

4.5.3 <u>The wall law plots and the roughness function</u> - Figures 47 through 52 are the wall law plots of Runs I through VI, respectively. Figure 53 is a plot of all six runs in a larger scale. The roughness function of all six runs can be obtained from Figure 54. The six runs have the relation:

Run	I	II	III	IV	V	VI
$\frac{\Delta u}{u_\tau}$	18.86	20.2	21.0	19.6	18.8	18.10

In Section 2.2.2 the relation between the roughness function $\Delta u/u_\tau$ and the roughness height k was shown in Equation 2-25 as

$$\frac{\Delta u}{u_\tau} = \frac{1}{\kappa} \ln \frac{ku_\tau}{\nu} + c \qquad (2\text{-}25)$$

where c is a constant, dependent on the roughness geometry. Bettermann (1966) working on the two-dimensional traverse bars, found that c is a function of the roughness density (Section 2.2.2).

In the present studies, the density of the fence can be represented as $S = h/L$. Here, S gives the number of fences within one fence height distance. If the roughness function (Equation 2-25) is rewritten

$$K = \frac{\Delta u}{u_\tau} - 5.76 \log \frac{hu_\tau}{\nu} \qquad (4\text{-}17)$$

K must be a function of S . Figure 54 is a plot of S vs. K and it shows that

$$K = 3.87 \log S + 5.66 \quad . \qquad (4\text{-}17a)$$

Therefore, the roughness function (Equation 2-25) for the boundary layer over sharp-edged multiple fences reads

$$\frac{\Delta u}{u_\tau} = 5.76 \log \frac{hu_\tau}{\nu} + 3.87 \log S + 5.66 \quad . \qquad (4\text{-}18)$$

Substituting Equation 4-18 into Equation 2-24

$$\frac{u}{u_\tau} = 5.76 \log \frac{y}{h} - 3.87 \log S - 0.56 \quad . \qquad (4\text{-}19)$$

The shear velocity, u_τ , can be determined from Equations 4-12 and 4-13, i.e.,

$$u_\tau = 0.375\, u_a\, R_L^{-0.129} \quad . \qquad (4\text{-}19a)$$

These results clearly show that inside the "wall law" region the velocity distribution above fences can be fully specified by u_a , L , and h . In other words, flow in rough regions is independent of the boundary layer history.

4.6 The Turbulence

The turbulence distributions of Runs I, Ia, II, and IIa are shown in Figures 55, 56, 57 and 58, respectively, and also tabulated in Table VII. "Over shoot" are found to exist in all turbulence quantities. Both $\overline{v'^2}$ and $\overline{u'v'}$ increase immediately when flow encountered the fences. But one can see from Figures 55 and 56 that at station $x = 0$, $\overline{u'^2}$ almost retained its initial quantities and the increase of $\overline{u'^2}$ occurs later. At a certain distance downstream from the leading fence, the distribution of each turbulence component is similar. Again this is an indication of the existence of the equilibrium turbulent boundary layer.

The turbulence intensities $\overline{u'^2}$ and $\overline{v'^2}$ at $x = -4$ ft are plotted in Figure 59. For a comparison, Klebanoff's (1954) smooth wall measurements are also plotted in Figure 59.

The turbulent shear stress $\overline{u'v'}$ at $x = -4$ ft near the wall is plotted in Figure 60. The shear velocity u_* determined in Section 4.4.1, is also shown in Figure 60. There appears to be good agreement between u_*^2 and $-\overline{u'v'}$ within a $\pm$ 5% difference. A nearly uniform stress region is also found in the lower portion of a smooth wall turbulent boundary layer.

Unlike the smooth wall case, the turbulent shear stress $-\overline{u'v'}$ near a rough wall does not have a uniform region. This can be found in Figures 61 and 62, where Figure 61 is the plot of $-\overline{u'v'}$ vs. y for Stations I(11), I(9), and I(7) and Figure 62 is the same plot for Stations II(11), II(10.5), II(10), and II(8). The corresponding u_τ^2 for each station is also shown. Correlations between u_τ^2 and $-\overline{u'v'}$ still exist. The maximum value of $-\overline{u'v'}$ is comparable to u_τ^2 within the random error range (Section 3.7.2).

4.7 Energy Balance

The mean energy of a turbulent boundary layer can be obtained by multiplying the boundary layer momentum equation by the local mean velocity. If Equation 2-13 is multiplied by u/ρ, thus

$$u\left(u\frac{\partial u}{\partial x} + v\frac{\partial u}{\partial y}\right) = -\frac{u}{\rho}\frac{\partial p}{\partial x} + \frac{u}{\rho}\frac{\partial \tau}{\partial y} , \qquad (4\text{-}20)$$

where

$$\tau = -\rho\overline{u'v'} + \mu\frac{\partial u}{\partial y} \quad . \tag{4-21}$$

The term $-\rho\overline{u'v'}$ is the turbulent shear stress and $\mu\frac{\partial u}{\partial y}$ is the viscous shear stress. At a finite distance normal to the wall (outside the laminar sublayer), the viscous shear stress is negligible in comparison to the turbulent shear stress, and hence,

$$\frac{u}{\rho}\frac{\partial\tau}{\partial y} = -u\frac{\partial\overline{u'v'}}{\partial y} = -\frac{\partial(u\,\overline{u'v'})}{\partial y} + \overline{u'v'}\frac{\partial u}{\partial y} \quad . \tag{4-22}$$

Substituting Equation 4-22 into Equation 4-20,

$$\underbrace{\frac{1}{2}\left(u\frac{\partial u^2}{\partial x} + v\frac{\partial u^2}{\partial y}\right)}_{\mathrm{I}} + \underbrace{\frac{u}{\rho}\frac{\partial p}{\partial x}}_{\mathrm{II}} + \underbrace{\frac{\partial(u\,\overline{u'v'})}{\partial y}}_{\mathrm{III}} - \underbrace{\overline{u'v'}\frac{\partial u}{\partial y}}_{\mathrm{IV}} = 0 \quad . \tag{4-23}$$

In Equation 4-23 the meaning of the various terms are:

(I) = work done per unit mass per unit time by the inertia force,

(II) = work done per unit mass and time by the static pressure,

(III) = transfer of energy by the shear stress, and

(IV) = turbulence production term or the production of turbulent energy from the loss of energy of the mean motion.

On most flat plate equilibrium boundary layers the pressure distributions along vertical direction are similar;

hence, $\partial p/\partial x$ at a station are independent on y. Under this condition, the terms (I) and (II) of Equation 4-23 are usually discussed as a whole and are called the convective transport term which represents the convective transport of the total energy per unit time and mass, for example, see page 64 of Hizne (1959). In the present flow model, due to the separation, the pressure gradient $\partial p/\partial x$ is expected to be different from point to point. Therefore, it is necessary to discuss the inertia term and the pressure term individually.

The balance of Equation 4-23 at a station is difficult to obtain. The terms $\partial u/\partial x$ and $\partial p/\partial x$ can only be estimated from the profiles measured at adjacent stations. The distribution of the turbulent shear stress, $-\overline{u'v'}$, is subject to error (see Appendix). Therefore, both the production term $-\overline{u'v'}\,\frac{\partial u}{\partial y}$ and the energy transfer term $\frac{\partial (u\,\overline{u'v'})}{\partial y}$ become unreliable. Since there is no way to obtain a perfect energy balance of a boundary layer, each term of Equation 4-23 is only an estimation.

As shown in Table V, the measurements of u, p, $\overline{u'v'}$ of Runs Ia and IIa are made one inch apart. The estimation of mean energy balance of the boundary layers at Stations Ia(11,2), Ia(11,4), and Ia(11,6) are discussed in the following text. Station Ia(11,2) (refer to Table II) is located at 2 in. downwind from the $x = 11$ ft fence of Runs Ia, Ia(11,4) and Ia(11,6) are located at 4 in. and 6 in., respectively, downwind from the same fence. After $\partial u/\partial x$ at various heights for a station are estimated, the vertical component of the mean motion can be estimated through the continuity equation

$$v = - \int_{o}^{y} \frac{\partial u}{\partial x} \, dy \quad . \tag{4-24}$$

Since the value of u as well as $\partial u/\partial x$ inside the separation bubble are not known, the use of Equation 4-24 must be modified. Suppose at $y = y_o$ the value of v is v_o, and $\partial u/\partial x$ for $y > y_o$ are known. Equation 4-24 can be written as

$$v = v_o - \int_{y_o}^{y} \frac{\partial u}{\partial x} \, dy \quad . \tag{4-25}$$

A smooth curve of $C(y) = - \int_{y_o}^{y} \frac{\partial u}{\partial x} \, dy$ can be obtained for $y > y_o$. The difference between $v(y)$ and $C(y)$ is only a constant v_o. In the lower region of the boundary layer, when the slopes of the streamlines are steep, the quantities of v at various heights can be estimated from the streamline pattern (Figure 29). Figure 63 shows the plots of $C(y)$ and v for Station Ia(11,6); $C(y)$ is calculated from the preceding text and v is estimated from Figure 29. It was found that after adding the curve $C(y)$ of a constant -1.34 fps, the curve $-1.34 + C(y)$ correlated the estimated v's within an error of $\pm$ 0.32 fps. Therefore, at Station Ia(11,6) the values of v at Station Ia(11,6) were calculated from

$$v = -1.36 - \int_{y_o}^{y} \frac{\partial u}{\partial y}\, dy \qquad (4\text{-}26)$$

where $y_o = 0.8$ in.

Figures 64, 65, and 66 show the balance of the mean energy in dimensional form of Stations Ia(11,2), Ia(11,4) and Ia(11,6), respectively. Some phenomena of the boundary layer between two fences can be seen from these figures:

(1) The pressure term $u/\rho\,(\partial p/\partial x)$ and the inertia term $\frac{1}{2}(u\partial u^2/\partial x + v\ \partial u^2/\partial y)$ dominate the mean energy balance.

(2) Near the wall, the production of the turbulent energy by this term $-\overline{u'v'}\,\frac{\partial u}{\partial y}$ is partly converted from the convective transport term (I and II of Equation 4-23) and partly from the energy transfer term $\frac{\partial (u\,\overline{u'v'})}{\partial y}$. The energy transfer term represents the total work by the turbulent shear stress, and is a flux of energy toward the wall.

(3) All three figures (64, 65, and 66) show that in the upper half of the boundary layers a gain of mean kinetic energy is balanced by the loss of static pressure of free stream. However, the lower half of the boundary layer seems to be not affected by the free stream pressure gradient, and is dependent on the static pressure distribution after separation. This means that the pressure gradient $\partial p/\partial x$ in the lower half of the boundary layer is dependent on its position. Furthermore, there is no way to correlate $\partial p/\partial x$ at one point in the lower part of the boundary layer to the value of $\partial p/\partial x$ at the free stream.

This may be an indication of why the universality of the defect law breaks down in the present flow model. (See Section 4.5.1).

4.8 Wind Reduction Rate

The wind reduction rate is defined as

$$R = \left(1 - \frac{u[y]}{u_o[y]}\right) \times 100 \quad , \tag{4-27}$$

where $u[y]$ is the local wind speed measured after placing fences, and $u_o[y]$ represents the local wind speed measured in clear tunnel. The values of u_o used in this analysis are measured at $x = -4$ ft. Figures 67, 68 and 69 are plots of constant R's for L = 6 in., 12 in. and 18 in., respectively. The wind reduction pattern is not affected by the ambient velocity. Furthermore, all six runs show that a constant R is reached at a distance about 110 h downwind from the leading fence, and that this distance is independent of L . A summary of the asymptotic heights at various wind reduction rates, R , for all three L's are as follows:

	20%	30%	40%	50%	60%
L = 6 in.	6.8h	4.8h	3.1h	2.0h	1.4h
L = 12 in.	6.4h	4.2h	2.9h	1.6h	---
L = 18 in.	6.0h	3.4h	1.9h	1.1h	---

Figure 70 shows the wind reduction pattern between fences for Case II (u_a = 30 fps, L = 6 in.) and Figure 71 is a same plot of Case I (u_a = 30 fps, L = 12 in.). Since the wind reduction pattern found in this study is dependent on L only, and for a more general flow condition the flow in rough region is dependent on h as well, which is shown in Equation 4-19, a possible modeling law can be written as

$$\frac{h_p}{h_m} = \frac{L_p}{L_m} \; . \tag{4-28}$$

An obvious result can be found from Figures 67 through 71 that a smaller L can provide a higher rate of wind reduction at a given height. However, when applying this result to design the wind breaks, a smallest L may not be necessary. For example, if a 40% of wind reduction within a 3h height is needed, $L = 12h$ will be an optimum arrangement; but when the wind reduction $R > 70\%$ is needed for $y < h$, fences must be placed for L less than 6h.

Chapter V

CONCLUSION

Flow condition of this experiment was a series of fences equally spaced on an aerodynamically smooth flat plate. Air flowed from the smooth surface toward the fences. Six runs of experiments were performed where each run was a different combination of two wind velocities and three fence spacings. Free stream pressure gradients for all six runs were adjusted to be nearly zero.

Results on measurements have been discussed in the preceding chapter. Several conclusions can be drawn from these results and discussions.

(1) The wall law and the defect law of the smooth wall equilibrium turbulent boundary layers can be used to correlate the velocity distributions at 4 ft upstream from the leading fence. A graphical method is developed to estimate the wall shear stress for smooth wall turbulent boundary layer.

(2) On the form drag coefficients of the leading fences, good agreement between present measurements and Plate's (1965) empirical relation was found.

(3) At a large distance downstream from the leading fence, similar velocity distributions above fences were found. This meant that the boundary layers of this region were in their equilibrium condition. This region was defined as the rough region.

(4) The universality of the defect law broke down in the rough region of the present flow model.

The constant B of the "overlap" region (Equation 4-14) was found previously to be a function of free stream pressure gradient only. For a zero pressure gradient boundary layers, many investigators found that $B = 0.8$ on either rough wall or smooth wall. However, data of the present experiment showed that $B = 1.46$ for all six runs. This concluded that B must be a function of roughness geometry as well as the pressure gradient at free stream.

(5) The roughness parameter of the wall law plots in rough region was found to be a function of the density of fences, S , as well as the fence height.

The average wall drag coefficients of the rough region, which representing the average force exerted on fences by the air flow, was found to be a function of free stream velocity and the spacing between fences.

These results indicated that flow in rough region could be fully specified by u_a , h , and L . In other words, the upstream boundary layer history does not affect the flow in the region which is far downwind from the leading fence.

(6) The wind reduction rate R was found to depend on the fence spacing, L , and to be independent of the ambient velocity. In general, the smaller L was the higher R was found at a given height. However, it was not necessary to place the fences at the smallest spacing in order to obtain an optimum arrangement of wind breaks.

A modeling law was proposed. The only requirement on modeling the multiple wind break was the similarity of h/L ratio between the model and the prototype.

BIBLIOGRAPHY

BIBLIOGRAPHY

Arie, M. and H. Rouse, (1956), "Experiments on two-dimensional flow over a normal wall," J. Fluid Mech., Vol. 1, pp. 129-141.

Arya, S. P. S., (1968), "Structure of stably stratified turbulent boundary layer," Ph.D. dissertation, Colorado State University, also technical report, CER68-69SPSA10, Engineering Research Center, Colorado State University, Fort Collins, Colorado.

American Society for Testing Materials, (1949), "ASTM manual on the presentation of data," third printing, ASTM Manual.

Baines, W. D., (1950), "An exploratory investigation of boundary-layer development on smooth and rough surface," Ph.D. dissertation, State University of Iowa, Iowa City, Iowa.

Baines, W. D., (1951), "A literature survey of boundary-layer development on smooth and rough surface at zero pressure gradient," Project Report, Iowa Inst. Hydraulic Res., State University of Iowa, Iowa City, Iowa.

Baldwin, L. V., V. A. Sandborn and J. C. Lawrence, (1960), "Heat transfer from transverse and yawed cylinders in continuum, slip and free molecule flow," J. Heat Transfer, ASME Trans. Ser. C, Vol. 82, No. 2.

Bates, C. G., (1930), "The windbreaks as a farm asset," U.S. Dept. Agr., Forest Serv. Bull. 1405.

Bates, C. G., (1945), "Shelterbelt influences: Part I, general description of studies made," J. Forestry 43, pp. 88-92.

Bates, C. G., (1945a), "Shelterbelt influence: Part II, the value of shelterbelts in house heating," J. Forestry 43, pp. 176-196.

Bettermann, D., (1965), "Contribution a l'etude la couche limite turbulente le long de plaques ruueuses," Centre National de la Recherche Scientifique, Paris, Rapport 65-6.

Bhaduri, S., (1966), "Mass diffusion from a point source in a turbulent boundary layer over a rough surface," Ph.D. dissertation, Colorado State University, Fort Collins, Colorado.

Blom, J. and L. Wartena, (1969), "The influence of changes in surface roughness on the development of the turbulent boundary layer in the lower layer of the atmosphere," J. Atmos. Sci., Vol. 26, p. 255.

Carmody, T., (1964), "Establishment of the wake behind a disk," J. Basic Engineering, Transaction of the ASME, December 1964, p. 869.

Champagne, F. H., C. H. Sleicher and O. H. Wehrmann, (1967), "Turbulence measurements with inclined hot wire, Part I: Heat transfer experiments with inclined hot wire." J. Fluid Mech., Vol. 28, p. 153.

Chang, S. C., (1966), "Velocity distribution in the separated flow behind a wedge shaped model hill," Master thesis, Colorado State University, also Technical Report CER65SCC66, Engineering Research Center, Colorado State University.

Cheyney, E. G., (1941), "Establishment, growth, and influence of shelterbelts in the prairie region of Minnesota," Minn. Agr. Expt. Sta. Bull. 285.

Clark, E. A., (1934), "A preliminary report on the growth and effectiveness of windbreaks in the high plains area of Oklahoma," Panhandle Bull. 55, Goodwell, Okla.

Clauser, F. H., (1954), "Turbulent boundary layers in adverse pressure gradients," J. Aero. Sci., Vol. 21, p. 91.

Clauser, F. H., (1956), "The turbulent boundary layer," Adv. Appl. Mech., Vol. 4, Academic Press, New York, New York.

Coles, D., (1953), "Measurements in the boundary layer on a smooth flat plate in supersonic flow - I. The problem of turbulent boundary layer," JFL. CIT., Rep. No. 20-69.

Coles, D., (1954), "The problem of the turbulent boundary layer," Zeitschrift fur angewandte Mathematik und Physik, Vol. 5, p. 181.

Coles, D., (1955), "The law of the wall in turbulent shear flow," Fiftieth Jahre Grenzschicht - forschung, p. 153.

Coles, S., (1956), "The law of the wake in the turbulent boundary layer," J. Fluid Mech., Vol. 1, p. 191.

Den Uyl, D., (1936), "The zone of effective windbreak influence," J. Forestry 34, p. 689.

Doebelin, E. O., (1966), "Measurement systems: application and design," McGraw-Hill Book Co., New York.

Dryden, H. L., G. B. Schubauer, W. C. Mock, Jr., and H. K. Skramstad, (1957), "Measurements of intensity and scale of wind tunnel turbulence and their relation to the critical Reynolds number of spheres," NACA T.R. 581.

Elliott, W. P., (1958), "The growth of the atmospheric internal boundary layer," Trans. Amer. Geophys. Union, Vol. 39, No. 6, p. 1048.

Finn, C. L. and V. A. Sandborn, (1967), "The design of a constant temperature hot wire anemometer," Technical Report CER66-67CLF36, Colorado State University, Fort Collins, Colorado.

Frenkiel, F. N., (1954), "Effects of wire length in turbulence investigations with hot wire anemometer," Aeronautical Quarterly 5, p. 1.

Furuya, Y. and H. Fujita, (1967), "Effect of surface roughness on the velocity defect law," The Physics of Fluid Supplement, p. S155.

Goldstein, S., (1965), "Modern developments in fluid dynamics," Dover Publication Inc., Vol. I and II, New York.

Good, M. C. and P. C. Joubert, (1968), "The form drag of two-dimensional bluff-plates immersed in turbulent boundary layers," J. Fluid Mech., Vol. 31, pp. 547-582.

Hama, H., (1947), "Turbulent boundary layer along a flat plate," Rept. Inst. Sci. Tech., University of Tokyo, Vol. 1, p. 13.

Hama, F. R., (1953a), "On the velocity distribution in the laminar sublayer and transition region in turbulent shear flow," J. Aero. Sci., Vol. 20, p. 648.

Hama, F. R., (1953b), "Discussion of L. Landweber (1952)".

Hama, F. R., (1954), "Boundary layer characteristics for smooth and rough surface," Annual meeting of the Soc. of Naval Architects and Marine Engrs., p. 333.

Hizne, J. O., (1959), "Turbulence: An introduction to its mechanism and theory," McGraw-Hill Book Company Inc., New York.

Hood, G. W., (1938), "Windbreaks help control erosion in Great Plains," Soil Conserv. III.

Klebanoff, P. S. and T. W. Diehl, (1951), "Some features of artificially thickened fully developed turbulent boundary layers with zero pressure gradient," NACA TM 2475.

Klebanoff, P. S., (1954), "Characteristics of turbulence in a boundary layer with zero pressure gradient," NACA TN 3178.

Kline, S. J. and F. A. McClintock, (1953), "Describing uncertainties in single-sample experiments," Mech. Eng., Vol. 75, p. 3.

Landweber, L., (1952), "Der reibungswiderstand der langsangestromten ebenen platte," Juhrbuch Schiffbautech. Ges., Vol. 46, p. 137.

Landweber, L., (1966), "Reanalysis of flat-plate boundary-layer data," Proceedings of Ninth International Towing Tank Conference, Paris, September 1966.

Liu, C. K., S. J. Kline and J. P. Johnston, (1966), "An experimental study of turbulent boundary layer on rough walls," Report MD-15, Thermosciences Division, Dept. of Mechanical Engineering, Stanford University, Stanford, California.

Ludwieg, H., (1950), "Instrument for measuring the wall shearing stress of turbulent boundary layer," NACA TM 1284.

Ludwieg, H. and W. Tillmann, (1950), "Investigations of the wall shearing stress in turbulent boundary layer," NACA TM 1285.

MacMillan, F. A., (1954), "Viscous effects on flattened point tubes at low speed," J. Roy. Aero. Soc., 58: 837-839.

Mellor, G. L. and D. M. Gibson, (1966), "Equilibrium turbulent boundary layers," J. Fluid Mech., Vol. 24, Part 2, p. 225.

Millikan, C. B., (1938), "A critical discussion of turbulent flows in channels and cirular tubes," Proceedings Fifth International Congress of Applied Mechanics, p. 386.

Moore, W. L., (1951), "An experimental investigation of the boundary layer development along a rough surface," Ph.D. dissertation, State University of Iowa, Iowa City, Iowa.

Morris, H. M., Jr., (1955), "Flow in rough conduits," Trans. ASCE, Vol. 120, p. 373.

Morris, H. M., Jr., (1961), "Design methods for flow in rough conduits," Trans. ASCE, Vol. 126.

Nagabhushanaiah, H. S., (1961), "Separation flow downstream of a plate set normal to a plane boundary," Ph.D. dissertation, Colorado State University, Fort Collins, Colorado.

Nageli, W., (1941), "Untersuchungen uber die windverhaltnisse in Bereich von windschutzstreifen," Mitteilungen der schweiz. Anstalt f.d. forstliche verschswesen, Vol. 23, pp. 221-276.

Nikuradse, J., (1933), "Stromungsgesetze in rauhen rohren," Forsch. Arb. Ing.-Wes., No. 361, also NACA TM 1292 (1950).

Nikuradse, J., (1942), "Turbulente reibungschichten an der platte," Report of ZWB, Berlin.

O'Loughlin, E. M. and E. G. MacDonald, (1964), "Some roughness concentration effects on boundary resistance," La Houille Blanche, 1 No. 7.

Panofsky, H. A. and A. A. Townsend, (1964), "Change of terrain roughness and the wind profile," Quart. J. Roy. Met. Soc., Vol. 90, p. 147.

Perry, A. E. and P. N. Joubert, (1963), "Rough-wall boundary layers in adverse pressure gradients," J. Fluid Mech., Vol. 17, Part 2, p. 195.

Perry, A. E., W. H. Schofield and P. N. Joubert, (1969), "Rough wall turbulent boundary layers," J. Fluid Mech., Vol. 37, Part 2, p. 383.

Plate, E. J. and J. E. Cermak, (1963), "Micrometeorological wind tunnel facility, description and characteristics," Technical Report, CER63EJP-JEC9, Engineering Research Center, Colorado State University, Fort Collins, Colorado.

Plate, E. J., (1965), "The drag on a smooth flat plate with a fence immersed in its turbulent boundary layer," ASME, Paper No. 64-FE-17.

Plate, E. J. and G. M. Hidy, (1967), "Laboratory study of air flowing over a smooth surface onto small water waves," J. Geophys. Res., Vol. 72, No. 18, p. 4627.

Plate, E. J., (1970), "The aerodynamics of shelter belts," Unpublished paper, Radiological Physics Division, Argonne National Laboratory, Argonne, Illinois.

Prandtl, L., (1934), "The mechanics of viscous fluids," Aerodynamic theory Vol. 3, edited by W. F. Durand.

Prandtl, L. and H. Schlichting, (1934), "Des Widerstands-gesetz rauher platten," Werft, Reederci, Hafen, p. 1.

Richardson, P. D., (1964), "Discussion of Carmody (1964)," J. Basic Engineering, Transactions of the ASME, December 1964, p. 880.

Ross, D., (1953), "A study of incompressible turbulent boundary layer," Ph.D. dissertation, Harvard University, TM NR 062-139-1, Pennsylvania State College.

Rotta, J. C., (1950), "Uber die theorie des turbulenten genezschichten," NACA TM 1344.

Rotta, J. C., (1955), "Similar solution of turbulent boundary-layer," J. Aero Sci., Vol. 22, p. 215.

Rotta, J. C., (1962), "Turbulent boundary layer in incom-pressible flow," Progress in Aero. Sci., Vol. 2, p. 1.

Sandborn, V. A., (1966), "Meteorology of fluid mechanics," Report CER66-67VAS32, College of Engineering, Colorado State University, Fort Collins, Colorado.

Sandborn, V. A., (1967), "Hot wire anemometer measurement in large scale boundary layers," Report CER66-67VAS32, Colorado State University, Fort Collins, Colorado.

Sandborn, V. A., (1968), Class notes of "The experimental method in fluid mechanics," CE-605, Civil Eng. Dept., Colorado State University, Fort Collins, Colorado.

Sayre, W. W. and M. L. Albertson, (1961), "Roughness spacing in rigid open channel," Technical Report CER59WS-MLA31, Engineering Research Center, Colorado State University, Fort Collins, Colorado. Also J. of the Hydraulic Division, Proceedings ASCE, p. 2823.

Scarborough, J. B., (1955), "Numerical mathematical analysis," Third Edition, The Johns Hopkins Press, Baltimore.

Schlichting, H., (1949), "Lecture series 'Boundary layer theory' Part I - Laminar flow," NACA TM 1217.

Schlichting, H., (1968), "Boundary layer theory," Sixth Edition, McGraw-Hill Book Co., New York.

Schoenherr, K. E., (1932), "Resistance of flat surface moving through a fluid," Trans. Soc. Nav. Arch. and Marine Engrs., Vol. 40.

Schultz-Grunow, F., (1940), "Neues reibungswiderstandsgesetz fur glatte platten," Luftfahrtforschung, also NACA TM 986, (1941).

Squire, H. B. and A. D. Young, (1937), "The calculation of the profile drag of aerofoils," ARCR & M 1838.

Streeter, V. L. and H. Chu, (1949), "Fluid and heat transfer in artificially roughened pipe," Final report Project 4918, Armour. Res. Foundation, Illinois Inst. of Tech.

Tieleman, H. W., (1967), "Viscous region of turbulent boundary layer," Ph.D. dissertation, Colorado State University, also Technical Report CER67-68HWT21, Engineering Research Center, Colorado State University, Fort Collins, Colorado.

Tillmann, W., (1945), "Investigation of some particularities of turbulent boundary layer on plates," Joint Intelligence Objective Agency, Washington, D. C.

Townsend, A. A., (1956a), "The properties of equilibrium boundary layer," J. Fluid Mech., Vol. 1, p. 561.

Townsend, A. A., (1956b), "The structure of turbulent shear flow," Cambridge University Press.

Townsend, A. A., (1965a), "Self-preserving flow inside a turbulent boundary layer," J. Fluid Mech., Vol. 22, Part 4, p. 773.

Townsend, A. A., (1965b), "The response of a turbulent boundary layer to abrupt changes in surface condition," J. Fluid Mech., Vol. 22, Part 4, p. 799.

Uberoi, M. S. and L. S. G. Kovasznay, (1953), "On mapping and measurement of random fields," Quarterly of Applied Mathematics, p. 375.

Ven Der Hegge Zijnen, B. G., (1958), "Heat transfer from horizontal cylinders in a turbulent airflow," Appl. Sci. Res., Vol. VII, Ser. A.

Wester, C. A. G., (1962), "An experimental study of turbulence in a density-stratified shear flow," J. Fluid Mech., Vol. 19, p. 221.

Woodruff, N. P. and A. W. Zingg, (1952), "Wind tunnel studies of windbreaks," Soil Conservation Service, U.S. Dept. of Agr. Paper No. SCS-RP-112

Zoric, D. L., (1968), "Approach of turbulent boundary layer of similarity," Ph.D. dissertation, Colorado State University, also Tech. Rept., CER68-69DLZ9, Engr. Res. Center, Colorado State University, Fort Collins, Colo.

APPENDIX

APPENDIX

The application of Equation 3-31 to estimate the errors for all measured results will be discussed here.

A.1 Error Estimation in Mean Velocity Measurement by Pitot Tubes

The mean velocity u was calculated from Equation 3-2 where

$$u = 2.358 \sqrt{\frac{H}{\rho}} \quad . \tag{A-1}$$

Thus,

$$\Delta u = \frac{2.358}{2} \left\{ \frac{(\Delta H)^2}{\rho H} + \frac{H}{\rho^3} (\Delta \rho)^2 \right\}^{\frac{1}{2}} \quad , \tag{A-2}$$

and

$$\frac{\Delta u}{u} = \frac{1}{2} \left\{ \frac{(\Delta H)^2}{H^2} + \frac{(\Delta \rho)^2}{\rho^2} \right\}^{\frac{1}{2}} \quad . \tag{A-3}$$

Since $H = H_t - H_s$, thus

$$\Delta H = \left\{ (\Delta H_t)^2 + (\Delta H_s)^2 \right\}^{\frac{1}{2}} \quad . \tag{A-4}$$

As mentioned in Section 3.4.2, both H_t and H_s were measured by means of a Transonic type 120B pressure meter. As given by the manufacturer, the relative errors of the Transonic meter is $\pm 2\%$ based on the full scale reading. In present measurements H_t were measured between 0.003 mm to 0.7 mm Hg in five meter ranges, and H_s were measured from -0.3 mm Hg to 0 mm Hg in four meter ranges. For a $\pm 2\%$ relative error of the full scale reading, the error in each meter range is:

H_t	=	0.01	0.03	0.1	0.3	1.0
$\pm\Delta H_t$	=	0.0002	0.0006	0.002	0.006	0.02
H_s	=	-0.01	-0.03	-0.1	-0.3	
$\pm\Delta H_s$	=	0.0002	0.0006	0.002	0.006	

Table A.1 gives an example on ΔH and $\Delta H/H$ for station V(12). The results show no systematic trend on relative error distribution. However, for the best case $\frac{\Delta H}{H} \approx 1.8\%$ and for the worst case $\frac{\Delta H}{H} \approx 6\%$.

The air density ρ was estimated from Figure 11 by measuring temperature T and barometric pressure p_o . The temperature was measured from a mercury in glass thermometer with accuracy within $\pm.5°F$, and p_o was measured by a mercury barometer (Ideal Aerosmith Inc.) with accuracy of ± 0.005 in. of Hg. During measurements were performed air temperature was held to near 80°F, a $\pm 0.5°F$ error provided a relative error of $\pm 0.6\%$, and the relative error in the barometric pressure reading was $\pm 0.02\%$ when p_o was near 25 in. of Hg.

Now, let us consider that $\Delta\rho/\rho = \pm 1\%$. This assumed error was introduced due to errors in T and p_o measurements and the estimation of ρ through a graphical manner. For the worst case where $\frac{\Delta H}{H} = \pm 0.06$

$$\frac{\Delta u}{u} = \frac{1}{2}\left\{(0.06)^2 + (0.01)^2\right\}^{\frac{1}{2}} \approx 0.03 \quad .$$

For the best case where $\frac{\Delta H}{H} = \pm 0.018$

$$\frac{\Delta u}{u} = \frac{1}{2}\left\{(0.018)^2 + (0.01)^2\right\}^{\frac{1}{2}} \simeq 0.01 \quad .$$

A.2 Error Estimation in Mean Velocity Measurements by Hot Wire

If Equation 3-12 is applied to calculate the mean velocity from the mean D.C. output E of the hot wire anemometer, the mean velocity can be expressed as

$$u = \left(\frac{E^2-b}{m}\right)^2 \quad . \qquad \text{(A-5)}$$

The partial derivatives of u with respect to b , m and E are

$$\frac{\partial u}{\partial b} = \frac{2(E^2-b)}{m^2}(-1)\,, \quad \frac{\partial u}{\partial E} = \frac{2(E^2-b)}{m^2}(2E)\,, \text{ and } \quad \frac{\partial u}{\partial m} = -\,\frac{2(E^2-b)^2}{m^3} \quad .$$

Substituting $\partial u/\partial b$, $\partial u/\partial E$, and $\partial u/\partial m$ into Equation 3-30 one has

$$\Delta u = \frac{2(E^2-b)}{m^2}\left\{(\Delta b)^2 + \Delta E^2 \;\; (\Delta E)^2 + \frac{(E^2-b)^2}{m^2}(\Delta m)^2\right\}^{\frac{1}{2}} \qquad \text{(A-6)}$$

Dividing Equation A-6 by Equation A-5

$$\frac{\Delta u}{u} = 2\left\{\frac{(\Delta b)^2}{(E^2-b)^2} + \frac{4E^2(\Delta E)^2}{(E^2-b)^2} + \frac{(\Delta m)^2}{m^2}\right\}^{\frac{1}{2}} \quad , \qquad \text{(A-7)}$$

or one can write

$$\frac{\Delta u}{u} = 2 \left\{ \frac{(\Delta b)^2}{m^2 u} + \frac{4(b+m\sqrt{u})^2}{m^2 u} \; \frac{(\Delta E)^2}{E^2} + \frac{(\Delta m)^2}{m^2} \right\}^{\frac{1}{2}} . \qquad \text{(A-8)}$$

As mentioned in Section 3.5.2, m and b are determined by the method of least square. In Equation A-8, Δm and Δb represent the error of m and b, respectively. These errors are introduced by the scattering of the calibration data points. If one considers that the error distribution functions along the mean calibration curve (Equation 3-12) are everywhere the same. The variance of the error distribution function σ^2 can be obtained from calibration data points where

$$\sigma^2 = \frac{1}{n} \sum_{i=1}^{n} (m\sqrt{u_i} + b - E_i^2)^2 \qquad \text{(A-9)}$$

n is the number of data points. And the variance of m and b can be written as

$$\sigma_m^2 = \frac{n\sigma^2}{\Delta} \qquad \text{(A-10)}$$

and

$$\sigma_m^2 = \frac{\sigma^2 \sum_{i=1}^{n} (\sqrt{u_i})^2}{\Delta} \qquad \text{(A-11)}$$

where

$$\Delta = n \sum_{i=1}^{n} (\sqrt{u_i})^2 - \left(\sum_{i=1}^{n} \sqrt{u_i} \right)^2 . \qquad \text{(A-12)}$$

Equations A-10 and A-11 can be found in many statistics books. For example, see page 121 of Young (1962).

If the normal hot wire calibration curve of Figure 13 is used in calculating the mean velocity u, it was found that by appling the least square method $b = 18.03$ and $m = 5.34$. And from Equation A-11, $\sigma_b = 0.189$, from Equation A-10, $\sigma_m = 0.052$. As mentioned in Section 3.6.2, all errors discussed here are in $\pm 3\sigma$ limits. Thus $\Delta b = \pm 3\sigma_b = \pm 0.567$ and $\Delta m = \pm 3\sigma_m = \pm 0.156$.

The error in measuring E was introduced by the integrating process. The time of integration was counted by a stop watch. After repeating test, the error in integrating a constant 6 volt D.C. through one minute was found to be $\Delta E = \pm 0.0148$ volt. If the relative error in measuring E is considered to be a constant for all measurements $\frac{\Delta E}{E} = \frac{\pm 0.0148}{6} = \pm 0.0025 =$ constant, and since b, m, Δb, and Δm are constants, the relative error $\Delta u/u$ in Equation A-8 is a function of u. The relation between $\Delta u/u$ and u is shown in Figure A.1. When $u = 5$ fps, which indicates the lower limit that King's law is valid, $\Delta u/u = \pm 11.4\%$, and when $u = 30$ fps, $\Delta u/u = \pm 6.7\%$. This concludes that the mean velocity measured by hot wire experiences a much higher error than that measured by pitot tubes.

A.3 Error Estimation in $\overline{u'^2}$

Refer to Equation 3-11 that

$$\overline{u'^2} = \frac{1}{S^2} \overline{e_o'^2} \; ; \tag{3-11}$$

thus

$$\overline{\Delta u'^2} = \left\{ \frac{1}{(S^2)^2} (\Delta \overline{e_o'^2}) + \frac{(\overline{e_o'^2})^2}{(S^2)^4} (\Delta S^2)^2 \right\}^{\frac{1}{2}}$$

and

$$\frac{\overline{\Delta u'^2}}{\overline{u'^2}} = \left\{ \frac{(\Delta \overline{e_o'^2})^2}{(\overline{e'^2})^2} + \frac{(\Delta S^2)^2}{(S^2)^2} \right\}^{\frac{1}{2}} . \qquad \text{(A-13)}$$

Since

$$S^2 = \left(\frac{dE}{du} \right)^2 = \frac{m^2}{16\ E^2 u} \qquad \text{(A-14)}$$

and

$$\frac{\partial S^2}{\partial m} = \frac{2m}{16\ E^2 u} , \quad \frac{\partial S^2}{\partial E} = - \frac{2m^2}{16\ E^2 u}$$

and

$$\frac{\partial S^2}{\partial u} = - \frac{m^2}{16\ E^2 u} ,$$

then

$$\frac{\Delta S^2}{S^2} = \left\{ 4 \frac{(\Delta m)^2}{m^2} + 4 \frac{(\Delta E)^2}{E^2} + \frac{(\Delta u)^2}{u^2} \right\}^{\frac{1}{2}} . \qquad \text{(A-15)}$$

If the normal wire calibration curve in Figure 13 is also used here $\frac{\Delta m}{m} = \pm \frac{0.156}{5.34} = \pm 0.0292$ and $\frac{\Delta E}{E} = \pm 0.0025$. Consider the mean velocities were measured by pitot tubes, for the worst case $\Delta u/u = \pm 0.03$. Substituting all numerical values into Equation A-15,

$$\frac{\Delta S^2}{S^2} = \left\{4 \times (0.0292)^2 + 4(0.0025)^2 + (0.03)^2\right\}^{\frac{1}{2}}$$

$$= 0.0658 \quad . \tag{A-16}$$

The instrument used to measure $\overline{e'^2}$ was a DSA type 55D35 True RMS meter. The relative error in measuring the mean square quantity $\overline{e_o'^2}$ is ±10% which is provided by the manufacturer. Substituting Equation A-16 and

$\frac{\Delta\overline{e_o'^2}}{\overline{e_o'^2}} = \pm 0.1$ into Equation A-13

$$\frac{\Delta\overline{u'^2}}{\overline{u'^2}} = \left\{(0.1)^2 + (0.0658)^2\right\}^{\frac{1}{2}} = 0.120 \quad , \tag{A-17}$$

or

$$\frac{\Delta\overline{u'^2}}{\overline{u'^2}} = \pm 12\% \quad . \tag{A-18}$$

A.4 <u>Error Estimation in $\overline{v'^2}$ and $\overline{u'v'}$</u>

Refer to Equation 3-18

$$\overline{v'^2} = \frac{1}{2c^2}\left(\frac{\overline{e_1'^2}}{S_1^{\ 2}} + \frac{\overline{e_2'^2}}{S_1^{\ 2}} - 2\overline{u'^2}\right) \tag{4-18}$$

and

$$\overline{v'^2} = \frac{1}{2c^2}\left\{(\Delta W_1)^2 + (\Delta W_2)^2 + 4(\Delta\overline{u'^2})^2\right\}^{\frac{1}{2}} \tag{A-19}$$

where

$$\Delta W_1 = \Delta\left(\frac{\overline{e_1'^2}}{S_1^{\;2}}\right) \quad \text{and} \quad \Delta W_2 = \Delta\left(\frac{\overline{e_2'^2}}{S_1^{\;2}}\right) .$$

Since

$$\Delta W_1 = \left\{\frac{1}{(S_1^{\;2})^2}\,(\Delta\overline{e_1'^2})^2 + \frac{(\overline{e_1'^2})^2}{(S^2)^4}\,(\Delta S_1^{\;2})^2\right\}^{\frac{1}{2}}$$

$$= \frac{\overline{e_1'^2}}{S_1^{\;2}}\left\{\frac{(\Delta\overline{e_1'^2})^2}{(\overline{e_1'^2})^2} + \frac{(\Delta S_1^{\;2})^2}{(S_1^{\;2})^2}\right\}^{\frac{1}{2}} \qquad \text{(A-20)}$$

where $\frac{\Delta S_1^{\;2}}{S_1^{\;2}}$ has the same form as $\frac{\Delta S^2}{S^2}$ in Equation A-15. And Equation A-20 can be written as

$$\Delta W_1 = W_1\gamma \qquad \text{(A-21)}$$

where

$$\gamma = \left\{\frac{(\Delta\overline{e_1'^2})}{(\overline{e_1'^2})^2} + \frac{(\Delta S_1^{\;2})^2}{(S_1^{\;2})^2}\right\}^{\frac{1}{2}}$$

$$= \left\{\frac{(\Delta\overline{e_1'^2})^2}{(\overline{e_1'^2})^2} + 4\,\frac{(\Delta m_1)^2}{(m_1)^2} + 4\,\frac{(\Delta E)^2}{E^2} + \frac{(\Delta u)^2}{u^2}\right\}^{\frac{1}{2}} . \qquad \text{(A-22)}$$

From the calibration curve of the yawed wire in Figure 13, it was found that $m_1 = 0.231$, $\Delta m_1 = \pm 0.00716$, and $\frac{\Delta m_1}{m_1} = \frac{\pm 0.0716}{0.231} \approx \pm 0.031$. Again, if one considers that

$$\frac{\Delta\overline{e_1'^2}}{\overline{e_1'^2}} = \frac{\Delta\overline{e_2'^2}}{\overline{e_1{}^2}} = \pm 0.1 \quad , \quad \frac{\Delta E}{E} = \pm 0.0025 \quad \text{and} \quad \frac{\Delta u}{u} = \pm 0.03 \text{ , thus}$$

$$\gamma = \left\{(0.1)^2 + 4(0.031)^2 + 4(0.0025)^2 + (0.03)^2\right\}^{\frac{1}{2}}$$

$$= 0.1215 \quad , \tag{A-23}$$

and similarly, $\Delta W_2 = W_2\gamma$. Dividing Equation A-19 by $\overline{v'^2}$ and letting $\dfrac{\Delta\overline{u'^2}}{\overline{u'^2}} = t$, one has

$$\frac{\Delta\overline{v'^2}}{\overline{v'^2}} = \frac{1}{2\overline{v'^2}c^2}\left\{(W_1^2 + W_2^2)\gamma^2 + 4(\overline{u'^2})^2\ t^2\right\}^{\frac{1}{2}} \quad . \tag{A-24}$$

The relative error of $\overline{u'v'}$ can be found in a similar way such that

$$\frac{\Delta\overline{u'v'}}{\overline{u'v'}} = \frac{1}{4c\overline{u'v'}}\left\{(W_1^2 + W_2^2)\gamma^2\right\}^{\frac{1}{2}} \quad . \tag{A-25}$$

As one can see from Equations A-24 and A-25, the relative error on $\overline{v'^2}$ and $\overline{u'v'}$ are dependent on how W_1 , W_2 , $\overline{v'^2}$, $\overline{u'v'}$, and $\overline{u'^2}$ are related. Table A.2 gives an example on estimating $\Delta\overline{v'^2}/\overline{v'^2}$ and $\Delta\overline{u'v'}/\overline{u'v'}$ for Station I(-4), I(0), I(2) and I(5). The calibration curves used on calculating the turbulent quantities are shown in Figure 13, and the numerical constants used in Equations A-24 and A-25 are: $c = 0.923$, $\gamma = \pm 0.1215$, and $t = \pm 0.120$.

The results in Table 13 show that the measurements of $\overline{v'^2}$ are very inaccurate. At Station I(-4) when measurements were conducted near the wall $\frac{\Delta\overline{v'^2}}{\overline{v'^2}} = \pm 2.53$. At y/δ near 0.1 $\Delta\overline{v'^2}/\overline{v'^2} \simeq \pm 40\%$ and at best the relative error of $\overline{v'^2}$ are more than $\pm 20\%$. At the same station the relative error of $\overline{u'v'}$ are found between $\pm 10\%$ to $\pm 20\%$ which depend on the local W_1, W_2 and $\overline{u'v'}$.

TABLES

TABLE I EARLY RESULTS OF TOTAL DRAG COEFFICIENT FOR SMOOTH SURFACE BOUNDARY LAYER FLOW WITH ZERO PRESSURE GRADIENT

Author	Velocity Profile	Result
Schlichting (1949)	$\frac{u}{u_a} = \left(\frac{y}{\delta}\right)^{1/7}$	$C_f = - .074 R_x^{-1/5}$
Schlichting (1949)	$\frac{u}{u_\tau} = 2.495 \ln\left(1 + 8.93 \frac{u_\tau y}{\nu}\right)$	$C_f = 0.455(\ln R_x)^{-2.53}$
Schoenherr (1932)	$\frac{u}{u_\tau} = \frac{1}{x}\left\{\ln\left(\frac{u_\tau y}{\nu}\right) + F\left[\frac{y}{\delta}\right]\right\}$	$C_f^{-1/2} = 4.13 \ln (R_x C_f)$
Schultz-Grunow (1940)	$\frac{u}{u_\tau} = a + b \ln\left(\frac{y u_\tau}{\nu}\right)$	$C_f = 0.425(-0.407 + \ln R_x)^{-2.64}$
Nikuradse (1942)	$\frac{u}{u_a} = f\left[\frac{y}{\delta^*}\right]$	$C_f = 0.0267 R_x^{-0.139}$

$$R_x = \frac{u_a x}{\nu} \quad , \quad C_f = \frac{2\theta}{x}$$

TABLE II DATA COLLECTION PROGRAM

Run	U_A (fps)	L (inches)	Measurements Made: Vel.*	Pre.**	Turb.†	Drag††	x , Data at Longitudinal Distance (ft)
I	30	12	√	√	√	√	-4, 0, 1, 2, 3, 5, 7, 9, 11, 12, 13
Ia	30		√	√	√		11'-1", 2", 3", 4", 6", 8", 10", 12'-1", 2", 3", 4", 6", 8", 10"
II	30	6	√	√	√	√	-4, 0, 0.5, 1, 1.5, 2, 2.5, 3, 4, 6, 8, 10, 10.5, 11
IIa	30		√	√	√		10'-1", 2", 3", 4", 5", 7", 8", 9", 10", 11"
III	45	6	√	√		√	-4, 0, 1, 2, 4, 6, 10, 12
IV	45	12	√	√		√	-4, 0, 1, 2, 4, 6, 8, 10, 12
V	45	18	√	√		√	-4, 0, 1.5, 3, 6, 9, 12
VI	30	18	√	√		√	-4, 0, 1, 5, 3, 6, 9, 12

*Vel. mean velocity profile
**Pre. static pressure profile
†Turb. turbulence measurements
††Drag form drag on fences

TABLE III BOUNDARY LAYER PARAMETERS

Station	Run	X	u_a (fps)	$\times 10^3$ (slugs/ft^3)	$\times 10^4$ (ft^2/sec)	(inches)	(inches)	(inches)	u (ft/sec)	u_* (ft/sec)
I(-4) II(-4)	I II	-4'	30.11	1.861	2.035	12.20	1.070	1.305	---	1.050
III(-4) IV(-4) V(-4)	III IV V	-4'	44.28	1.881	2.015	15.96	2.012	1.640	---	1.460
VI(-4)	VI	-4'	30.07	1.882	2.013	14.49	1.89	1.486	---	1.017
I(0)	I	0'	29.98	1.861	2.035	12.88	2.508	2.241	4.360	3.196
I(1)	I	1'	30.20	1.861	2.035	13.62	2.950	2.244	1.256	3.246
I(2)	I	2'	30.28	1.861	2.035	14.15	3.255	2.520	3.073	3.374
I(3)	I	3'	30.13	1.861	2.035	14.55	3.479	2.624	2.916	3.491
I(5)	I	5'	30.38	1.861	2.035	15.26	3.873	2.829	2.768	2.328
I(7)	I	7'	30.45	1.861	2.035	15.88	4.226	2.990	2.612	2.550
I(9)	I	9'	30.60	1.861	2.035	16.50	4.588	3.171	2.543	2.493
I(11)	I	11'	30.88	1.861	2.035	17.11	4.801	3.277	2.531	2.469
I(12)	I	12'	30.97	1.861	2.035	17.39	4.884	3.307	2.517	2.464
I(13)	I	13'	31.16	1.861	2.035	17.48	4.893	3.335	2.526	2.456
II(0)	II	0'	30.38	1.875	2.021	12.89	2.502	2.057	6.180	---
II(0.5)	II	0.5'	30.61	1.875	2.021	14.08	2.663	1.937	---	---
II(1)	II	1'	30.30	1.875	2.021	14.22	2.895	2.038	2.252	3.804
II(1.5)	II	1.5'	30.66	1.875	2.021	14.57	3.067	2.340	2.958	4.950
II(2)	II	2'	30.57	1.875	2.021	14.82	3.189	2.431	2.900	4.429
II(2.5)	II	2.5'	30.77	1.875	2.021	15.07	3.432	2.528	2.959	4.140
II(3)	II	3'	30.59	1.875	2.021	15.27	3.553	2.598	2.942	4.012
II(4)	II	4'	30.56	1.875	2.021	15.63	3.681	2.646	2.834	3.631
II(5)	II	5'	30.82	1.875	2.021	15.94	3.902	2.750	2.799	3.231
II(6)	II	6'	30.44	1.875	2.021	16.16	4.142	2.817	2.740	2.676
II(8)	II	8'	30.61	1.875	2.021	16.71	4.477	2.995	2.723	2.663
II(10)	II	10'	30.95	1.875	2.021	17.25	4.878	3.155	2.743	2.682
II(10.5)	II	10.5'	30.97	1.875	2.021	17.32	4.883	3.170	2.744	2.685
II(11)	II	11'	31.11	1.875	2.021	17.37	4.898	3.218	2.756	2.695
III(0)	III	0'	44.43	1.848	2.050	17.30	3.130	2.689	8.836	---
III(1)	III	1'	44.60	1.848	2.050	17.76	3.660	2.806	2.377	8.339
III(2)	III	2'	44.77	1.848	2.050	18.34	4.115	3.008	3.660	6.228
III(4)	III	4'	45.27	1.848	2.050	19.06	4.662	3.267	4.199	4.881
III(6)	III	6'	44.77	1.848	2.050	19.49	5.109	3.403	3.979	3.904
III(10)	III	10'	44.43	1.848	2.050	20.55	5.726	3.678	3.741	3.667
III(12)	III	12'	44.67	1.848	2.050	21.06	5.968	3.860	3.757	3.663
IV(0)	IV	0'	44.90	1.835	2.065	17.90	3.168	2.699	6.221	---
IV(1)	IV	1'	45.10	1.835	2.065	18.60	3.542	2.715	2.289	7.921
IV(2)	IV	2'	44.81	1.835	2.065	19.10	3.815	2.996	4.291	5.243
IV(4)	IV	4'	45.24	1.835	2.065	19.53	4.350	3.253	4.088	5.385
IV(6)	IV	6'	45.70	1.835	2.065	20.11	4.734	3.460	3.889	3.492
IV(8)	IV	8'	44.88	1.835	2.065	21.51	5.089	3.576	3.593	3.391
IV(10)	IV	10'	44.73	1.835	2.065	21.17	5.488	3.715	3.459	3.365
IV(12)	IV	12'	45.17	1.835	2.065	21.32	5.699	3.837	3.474	3.377
V(0)	V	0'	45.06	1.889	2.006	17.42	3.118	2.689	5.183	---
V(1.5)	V	1.5'	45.37	1.889	2.006	18.13	3.606	2.798	3.248	---
V(3)	V	3'	45.52	1.889	2.006	19.48	3.965	3.117	4.130	---
V(6)	V	6'	45.15	1.889	2.006	20.24	4.686	3.437	3.644	3.205
V(9)	V	9'	44.94	1.889	2.006	20.86	5.091	3.649	3.340	3.165
V(12)	V	12'	45.01	1.889	2.006	21.43	5.508	3.846	3.309	3.170
VI(0)	VI	0'	29.51	1.882	2.013	16.32	2.999	2.556	3.326	---
VI(1.5)	VI	1.5'	29.97	1.882	2.013	17.42	3.433	2.876	2.151	---
VI(3)	VI	3'	29.94	1.882	2.013	18.06	2.815	2.971	2.720	---
VI(6)	VI	6'	29.67	1.882	2.013	18.84	4.352	3.320	2.392	2.319
VI(9)	VI	9'	29.78	1.882	2.013	19.19	4.930	3.354	2.309	2.250
VI(12)	VI	12'	29.89	1.882	2.013	19.86	5.289	3.627	2.293	2.243
Ia(11,1)	Ia	11' "	30.92	1.861	2.035	17.26	4.842	3.282		
Ia(11,2)	Ia	11'2"	30.89	1.861	2.035	17.26	4.842	3.282		
Ia(11,3)	Ia	11'3"	30.75	1.861	2.035	17.26	4.842	3.282		
Ia(11,4)	Ia	11'4"	30.80	1.861	2.035	17.26	4.842	3.282		
Ia(11,6)	Ia	11'6"	30.90	1.861	2.035	17.26	4.842	3.282		
Ia(11,8)	Ia	11'8"	30.90	1.861	2.035	17.26	4.842	3.282		
Ia(11,10)	Ia	11'10"	30.93	1.861	2.035	17.26	4.842	3.282		
Ia(12,1)	Ia	12'1"	30.70	1.861	2.035	17.44	4.889	3.321		
Ia(12,2)	Ia	12'2"	30.70	1.861	2.035	17.44	4.889	3.321		
Ia(12,3)	Ia	12'3"	30.68	1.861	2.035	17.44	4.889	3.321		
Ia(12,4)	Ia	12'4"	30.80	1.861	2.035	17.44	4.889	3.321		
Ia(12,6)	Ia	12'6"	30.90	1.861	2.035	17.44	4.889	3.321		
Ia(12,8)	Ia	12'8"	30.91	1.861	2.035	17.44	4.889	3.321		
Ia(12,10)	Ia	12'10"	30.95	1.861	2.035	17.44	4.889	3.321		
IIa(10,1)	IIa	10'1"	31.17	1.861	2.035	17.28	4.881	3.163		
IIa(10,2)	IIa	10'2"	31.16	1.861	2.035	17.28	4.881	3.163		
IIa(10,3)	IIa	10'3"	31.18	1.861	2.035	17.28	4.881	3.163		
IIa(10,4)	IIa	10'4"	31.22	1.861	2.035	17.28	4.881	3.163		
IIa(10,5)	IIa	10'5"	31.23	1.861	2.035	17.28	4.881	3.163		
IIa(10,7)	IIa	10'7"	31.22	1.861	2.035	17.33	4.890	3.194		
IIa(10,8)	IIa	10'8"	31.26	1.861	2.035	17.33	4.890	3.194		
IIa(10,9)	IIa	10'9"	31.37	1.861	2.035	17.33	4.890	3.194		
IIa(10,10)	IIa	10'10"	31.21	1.861	2.035	17.33	4.890	3.194		
IIa(10,11)	IIa	10'11"	31.24	1.861	2.035	17.33	4.890	3.194		

Notes: u = shear velocity calculated from the form drag of fence.

u_* = shear velocity measured from velocity profile.

TABLE IV VELOCITY DISTRIBUTIONS OF STATIONS AT x = - 4 ft

Stations I(-4) and II(-4)		Stations III(-4), IV(-4) and VI(-4)		Station VI(-4)	
y (inches)	u (fps)	y (inches)	u (fps)	y (inches)	u (fps)
0.104	15.239	0.0942	22.091	0.0662	14.083
0.144	15.788	0.141	23.79	0.0989	14.488
0.190	16.522	0.320	26.410	0.136	15.692
0.267	17.533	0.441	27.807	0.204	16.486
0.374	18.183	0.642	28.990	0.291	17.315
0.458	18.671	0.796	30.084	0.416	18.415
0.621	19.608	1.235	31.719	0.536	18.996
0.838	20.418	1.815	33.159	0.723	19.721
1.236	21.246	2.186	33.831	1.134	20.878
1.617	21.934	2.610	34.380	1.654	21.891
2.050	22.690	3.075	35.235	2.189	22.707
2.960	23.709	4.077	36.301	3.136	23.529
3.801	24.84	4.922	37.224	4.098	24.417
4.424	25.423	5.772	37.943	4.358	24.655
5.121	26.080	6.804	38.670	4.833	25.071
6.051	26.802	8.145	39.613	5.606	25.776
6.862	27.188	9.541	40.508	6.376	26.409
7.693	27.689	11.690	41.720	8.633	27.508
9.062	28.423	13.270	42.463	9.921	28.127
10.532	29.091	14.505	43.205	11.441	28.961
12.226	29.697	15.801	43.802	12.065	29.044
13.458	29.888	17.032	44.193	13.761	29.454
15.042	30.006	18.528	44.428	14.657	29.783
16.321	30.108	20.130	44.428	15.965	29.864
17.705	30.110	22.976	44.428	17.474	30.060
18.564	30.110			18.618	30.068
19.571	30.108			19.658	30.068
21.577	30.111			21.426	30.068
23.861	30.110			23.875	30.068

TABLE V VELOCITY DISTRIBUTIONS AND STATIC HEAD DISTRIBUTIONS FOR $x \geq 0$ ft

Station I(0)			Station I(1)			Station I(2)			Station I(3)			Station I(5)		
y (inches)	u (fps)	H_s (mm Hg)	y (inches)	u (fps)	H_s (mm Hg)	y (inches)	u (fps)	H_s (mm Hg)	y (inches)	u (fps)	H_s (mm Hg)	y (inches)	u (fps)	H_s (mm Hg)
1.08	16.27	-0.0532	1.08	7.74	-0.0200	1.08	9.63	-0.0210	1.08	8.73	-0.0125	1.08	10.77	-0.0155
1.12	16.53	-0.0485	1.25	8.65	-0.0220	1.25	11.96	-0.0178	1.25	10.84	-0.0123	1.25	11.47	-0.0150
1.50	18.27	-0.0404	1.50	10.84	-0.0243	1.50	13.73	-0.0160	1.50	12.85	-0.0122	1.50	12.20	-0.0166
2.05	21.37	-0.0176	1.75	13.00	-0.0265	1.75	14.73	-0.0145	1.75	14.36	-0.0119	1.75	13.06	-0.0150
2.50	22.92	-0.0075	2.00	14.78	-0.0280	2.00	16.09	-0.0135	2.00	15.62	-0.0115	2.00	13.83	-0.0139
3.00	23.53	-0.0050	2.25	16.68	-0.0280	2.50	17.89	-0.0110	2.50	17.28	-0.0108	2.50	15.48	-0.0131
4.00	24.63	-0.0028	2.50	18.53	-0.0268	3.00	19.90	-0.0094	3.00	18.71	-0.0100	3.00	17.25	-0.0125
5.00	25.45	-0.0025	3.00	22.42	-0.0230	4.00	22.88	-0.0050	4.00	21.45	-0.0078	4.00	19.32	-0.0107
7.00	26.88	-0.0015	3.50	24.02	-0.0198	6.00	25.68	-0.0014	5.00	23.62	-0.0045	5.00	21.80	-0.0088
10.00	28.50	0.0015	4.00	24.86	-0.0176	8.00	27.27	-0.0005	7.00	26.32	-0.0015	7.00	25.29	-0.0047
13.00	29.65	0.0032	5.00	25.86	-0.0155	10.00	28.39	0.0005	9.00	27.74	-0.0002	9.00	27.34	-0.0019
16.00	29.96	0.005	7.00	27.35	-0.0120	13.00	29.61	0.0010	11.00	28.82	0.0004	11.00	28.54	-0.0005
19.00	29.96	0.006	9.00	28.48	-0.0090	16.00	30.22	0.0018	13.00	29.61	0.0012	13.00	29.29	0.0007
23.00	29.98	0.006	12.00	29.53	-0.0045	19.00	30.26	0.0030	16.00	30.29	0.0025	16.00	30.14	0.0024
			15.00	30.16	-0.0010	23.00	30.28	0.0035	19.00	30.40	0.0031	19.00	30.38	0.0035
			18.00	30.20	0.0012				23.00	30.39	0.0040	23.00	30.53	0.0050
			21.00	30.17	0.0030									
			23.00	30.13	0.0040									

Station I(7)			Station I(9)			Station I(11)			Station I(12)			Station I(13)		
y (inches)	u (fps)	H_s (mm Hg)	y (inches)	u (fps)	H_s (mm Hg)	y (inches)	u (fps)	H_s (mm Hg)	y (inches)	u (fps)	H_s (mm Hg)	y (inches)	u (fps)	H_s (mm Hg)
1.08	9.15	-0.0132	1.08	8.72	-0.0137	1.08	9.04	-0.0173	1.08	9.47	-0.0200	1.08	9.65	-0.0255
1.25	10.42	-0.0129	1.25	9.71	-0.0135	1.25	9.58	-0.0167	1.25	10.03	-0.0196	1.25	10.65	-0.0251
1.50	11.74	-0.0122	1.50	10.87	-0.0132	1.50	10.51	-0.0159	1.50	11.21	-0.0190	1.50	11.67	-0.0245
1.75	12.30	-0.0116	1.75	11.82	-0.0129	1.75	11.32	-0.0153	1.75	12.28	-0.0184	1.75	12.30	-0.0240
2.0	13.19	-0.0112	2.00	12.53	-0.0125	2.00	12.21	-0.0148	2.00	13.04	-0.0178	2.00	13.45	-0.0235
2.50	14.96	-0.0108	2.50	13.84	-0.0120	2.50	13.38	-0.0138	2.50	14.26	-0.0170	2.50	14.75	-0.0227
3.00	16.12	-0.0108	3.00	15.21	-0.0113	3.00	14.43	-0.0136	3.00	15.60	-0.0163	3.00	15.90	-0.0220
4.00	18.15	-0.0101	4.00	17.99	-0.0162	4.00	16.44	-0.0133	4.00	17.71	-0.0147	4.00	17.78	-0.0207
5.00	20.23	-0.0088	6.00	21.27	-0.0087	5.00	18.30	-0.0129	5.00	19.78	-0.0130	6.00	21.23	-0.0187
7.00	23.94	-0.0056	8.00	24.43	-0.0064	7.00	21.59	-0.0108	7.00	22.69	-0.0116	8.00	24.11	-0.0167
9.00	26.55	-0.0026	10.00	26.71	-0.0035	9.00	24.81	-0.0087	9.00	25.17	-0.0107	10.00	26.50	-0.0137
11.00	28.42	0.000	13.00	29.05	0.0000	11.00	27.36	-0.0067	11.00	27.19	-0.0083	13.00	29.17	-0.0093
14.00	29.74	0.0023	16.00	30.15	0.0022	13.00	28.87	-0.0036	13.00	28.97	-0.0054	16.00	30.33	-0.0054
.00	30.36	0.0039	19.00	30.60	0.0040	16.00	30.21	-0.0010	16.00	30.39	-0.0026	19.00	31.09	-0.0030
20.00	30.45	0.0052	23.00	30.60	0.0050	19.00	30.71	0.0007	19.00	30.92	-0.0005	23.00	31.16	-0.0005
23.00	30.45	0.0052				23.00	30.88	0.0024	23.00	30.97	0.0015			

Station II(0)			Station II(0.5)			Station II(1)			Station II(1.5)			Station II(2)		
y (inches)	u (fps)	H_s (mm Hg)	y (inches)	u (fps)	H_s (mm Hg)	y (inches)	u (fps)	H_s (mm Hg)	y (inches)	u (fps)	H_s (mm Hg)	y (inches)	u (fps)	H_s (mm Hg)
1.09	19.35	-.0660	1.09	17.18	-.0372	1.06	16.26	-.0600	1.07	8.27	0.00	1.11	9.75	-.0050
1.24	17.23	-.0500	1.14	12.57	-.0356	1.31	18.24	-.0740	1.30	11.43	-.0060	1.32	11.45	-.0081
1.49	20.25	-.0320	1.36	13.79	-.0360	1.54	19.73	-.0750	1.54	13.11	-.0069	1.62	13.01	-.0100
1.62	21.25	-.0250	1.67	18.09	-.0371	2.04	22.47	-.0740	1.95	16.10	-.0063	2.04	15.53	-.0092
1.87	22.34	-.0180	1.98	22.08	-.0371	2.76	24.19	-.0470	2.34	18.29	-.0046	2.87	19.86	-.0078
2.32	23.25	-.0100	2.37	25.28	-.0341	3.50	25.45	-.0240	3.31	22.90	-.0026	4.05	23.94	-.0050
2.84	24.56	-.0060	2.89	27.03	-.0305	4.25	26.31	-.0240	4.52	25.44	-.0010	5.42	25.86	-.0022
3.69	25.46	-.0023	3.81	27.79	-.0260	5.24	27.09	-.0230	6.48	26.90	-.0006	6.80	26.88	-.0013
4.34	26.10	-.0004	4.81	28.16	-.0210	6.48	27.79	-.0220	8.70	28.32	0.00	8.73	28.07	-.0003
5.10	26.63	.0012	6.31	28.56	-.0141	7.95	29.04	-.0210	10.65	29.31	.0008	10.70	29.17	.0006
6.19	27.52	.0030	7.87	28.92	-.0090	9.69	29.55	-.0150	12.00	29.63	.0025	12.00	29.65	.0020
7.73	28.48	.0050	9.76	29.50	-.0025	11.00	29.75	-.0050	14.00	30.17	.0035	14.00	30.22	.0036
9.64	29.00	.0068	10.50	29.57	-.0017	13.00	29.85	.0080	16.00	30.59	.0045	16.00	30.55	.0048
11.00	29.60	.0070	12.00	29.88	.0015	15.00	30.20	.0100	18.00	30.66	.0055	18.00	30.55	.0057
13.00	30.05	.0090	14.00	30.49	.0040	17.00	30.30	.0110	20.00	30.66	.0065	20.00	30.57	.0063
15.00	30.37	.0095	15.00	30.59	.0050	19.00	30.27	.0115	21.50	30.61	.0075	21.50	30.57	.0063
17.00	30.38	.0102	16.00	30.61	.0058	21.50	30.26	.0118						
19.00	30.34	.0110	18.00	30.61	.0075									
21.50	30.34	.0110	20.00	30.54	.0088									
			21.50	30.46	.0105									

Station II(2.5)			Station II(3)			Station II(4)			Station II(5)			Station II(6)		
y (inches)	u (fps)	H_s (mm Hg)	y (inches)	u (fps)	H_s (mm Hg)	y (inches)	u (fps)	H_s (mm Hg)	y (inches)	u (fps)	H_s (mm Hg)	y (inches)	u (fps)	H_s (mm Hg)
1.11	9.66	-.0064	1.13	9.02	-.0074	1.12	8.01	-.0036	1.11	8.35	-.0085	1.18	8.94	--
1.36	11.47	-.0093	1.37	9.92	-.0091	1.35	10.61	-.0069	1.34	9.78	-.0102	1.29	9.58	--
1.58	12.66	-.0100	1.64	12.36	-.0094	1.71	11.78	-.0087	1.72	12.06	-.0110	1.43	10.49	--
2.00	14.51	-.0109	2.00	14.09	-.0098	2.13	14.47	-.0095	2.08	13.42	-.0116	1.66	11.26	--
2.48	17.11	-.0106	2.39	15.95	-.0096	2.99	17.29	-.0096	2.94	16.60	-.0118	2.04	12.61	--
2.84	18.65	-.0101	3.18	18.86	-.0088	4.09	20.85	-.0084	3.66	18.25	-.0111	2.51	14.04	-.0126
3.56	20.93	-.0085	4.07	21.61	-.0072	5.45	24.09	-.0054	4.78	21.75	-.0103	3.19	15.62	-.0121
4.29	23.08	-.0074	5.26	24.66	-.0047	7.14	26.59	-.0021	6.54	25.52	-.0073	4.09	18.21	-.0116
5.32	25.29	-.0053	6.82	26.37	-.0021	9.07	27.86	-.0004	8.21	27.38	-.0043	5.32	21.01	-.0106
6.61	26.30	-.0038	8.31	27.29	-.0008	11.38	29.16	.0018	10.04	28.43	-.0021	6.75	23.99	-.0055
8.45	27.71	-.0025	10.22	28.58	.0008	13.00	29.83	.0025	11.83	29.57	-.0004	8.57	26.91	-.0048
10.39	28.61	-.0015	12.00	29.46	.0019	15.00	30.27	.0036	13.00	29.82	.0007	10.54	28.53	-.0021
12.00	29.82	.0007	14.00	30.29	.0032	17.00	30.46	.0047	15.00	30.43	.0022	12.85	29.79	-.0005
14.00	30.43	.0012	16.00	30.53	.0042	19.00	30.56	.0055	17.00	30.70	.0037	15.25	30.31	.0008
16.00	30.71	.0024	18.00	30.59	.0050	21.50	30.47	.0075	19.00	30.82	.0043	14.00	29.93	.0004
18.00	30.76	.0035	20.00	30.55	.0058				21.50	30.78	.0050	17.00	30.39	.0020
20.00	30.77	.0043	21.50	30.54	.0060							19.00	30.44	.0030
21.50	30.76	.0045										21.00	30.44	.0040
												23.00	30.42	.0045

TABLE V VELOCITY DISTRIBUTIONS AND STATIC HEAD DISTRIBUTIONS FOR $x \geqq 0$ ft - Continued

Station II(8)			Station II(10)			Station II(10.5)			Station II(11)			Station III(0)		
y (inches)	u (fps)	H_s (mm Hg)	y (inches)	u (fps)	H_s (mm Hg)	y (inches)	u (fps)	H_s (mm Hg)	y (inches)	u (fps)	H_s (mm Hg)	y (inches)	u (fps)	H_s (mm Hg)
1.18	7.00	-.0075	1.13	7.90	-.0104	1.14	8.77	-.0149	1.13	8.57	-.0160	1.14	21.96	-0.1505
1.26	8.42	-.0084	1.18	8.23	-.0098	1.21	8.89	-.0146	1.19	8.70	-.0159	1.20	25.81	-0.1500
1.37	9.00	-.0093	1.25	8.58	-.0100	1.46	10.17	-.0144	1.32	9.56	-.0148	1.30	28.84	-0.1272
1.47	9.52	-.0095	1.31	8.75	-.0096	1.82	11.42	-.0150	1.61	10.86	-.0149	1.50	31.20	-0.1050
1.60	10.07	-.0103	1.39	9.31	-.0102	2.19	12.78	-.0155	1.90	11.46	-.0152	1.75	32.39	-0.0841
1.96	11.50	-.0105	1.52	9.36	-.0102	3.05	15.08	-.0158	2.32	13.11	-.0152	2.00	33.21	-0.0759
2.44	12.97	-.0105	1.60	10.08	-.0102	3.97	16.91	-.0154	2.81	13.43	-.0153	2.50	33.98	-0.0629
3.16	14.72	-.0109	1.74	10.74	-.0106	4.87	18.19	-.0154	3.52	16.01	-.0154	3.00	34.59	-0.0572
4.12	16.99	-.0112	2.09	11.82	-.0109	5.97	20.36	-.0145	4.27	17.15	-.0158	3.50	35.15	-0.0525
5.23	19.59	-.0112	2.45	12.94	-.0114	7.46	22.86	-.0129	5.22	18.76	-.0155	4.00	35.58	-0.0481
6.79	22.54	-.0091	3.06	14.27	-.0116	9.07	25.65	-.0105	6.33	20.57	-.0145	5.00	36.38	-0.0422
8.78	26.45	-.0056	3.86	15.99	-.0115	10.77	27.68	-.0080	7.81	23.37	-.0128	6.00	37.11	-0.0358
10.87	28.32	-.0025	4.75	17.70	-.0116	12.70	29.48	-.0056	9.62	26.44	-.0104	7.00	37.76	-0.0303
13.20	29.49	-.0003	6.25	20.85	-.0104	14.69	30.39	-.0040	11.40	28.31	-.0078	8.00	38.43	-0.0270
15.70	30.40	.0008	7.71	23.42	-.0096	16.69	30.97	-.0030	13.40	29.92	-.0054	10.00	39.82	-0.0213
17.00	30.60	.0013	9.78	26.50	-.0055	18.50	30.97	-.0010	15.14	30.59	-.0041	12.00	41.12	-0.0153
19.00	30.61	.0020	11.87	28.46	-.0027	21.00	30.97	-.0005	17.00	30.95	-.0035	14.00	42.35	-0.0151
21.00	30.59	.0025	13.92	29.67	-.0004	22.50	30.95	.0005	19.00	31.11	-.0028	16.00	43.40	-0.0150
23.25	30.56	.0030	15.98	30.30	.0009				21.00	31.11	-.0023	18.00	44.13	-0.0135
			18.00	30.73	.0010				22.50	31.09	-.0020	19.00	44.26	-0.0122
			20.00	30.93	.0020							20.00	44.36	-0.0120
			22.50	30.95	.0025							21.00	44.40	-0.0118
												22.00	44.43	-0.0115
												24.33	44.43	-0.0115

Station III(1)			Station III(2)			Station III(4)			Station III(6)			Station III(10)		
y (inches)	u (fps)	H_s (mm Hg)	y (inches)	u (fps)	H_s (mm Hg)	y (inches)	u (fps)	H_s (mm Hg)	y (inches)	u (fps)	H_s (mm Hg)	y (inches)	u (fps)	H_s (mm Hg)
1.00	--	-0.0430	1.10	11.90	-0.0483	1.06	10.12	-0.0432	1.04	9.67	-0.0462	1.24	11.89	-0.0442
1.07	10.70	-0.0473	1.24	13.34	-0.0505	1.22	12.30	-0.0452	1.26	10.84	-0.0475	1.53	13.83	-0.0505
1.20	12.28	-0.0581	1.51	16.38	-0.0521	1.55	15.54	-0.0505	1.58	13.02	-0.0446	1.78	15.03	-0.0515
1.50	17.10	-0.0648	1.78	18.62	-0.0552	2.11	18.94	-0.0571	1.94	15.49	-0.0520	2.14	16.92	-0.0542
2.00	23.10	-0.0590	2.03	20.91	-0.0564	2.61	21.33	-0.0585	2.64	18.54	-0.0535	2.71	18.78	-0.0561
2.50	27.99	-0.0523	2.43	23.99	-0.0548	3.23	23.99	-0.0589	3.31	21.61	-0.0562	3.19	20.25	-0.0569
3.00	31.35	-0.0469	2.99	27.23	-0.0515	3.98	27.40	-0.0574	3.95	24.24	-0.0560	3.89	22.50	-0.0580
3.50	33.39	-0.0452	3.72	30.81	-0.0475	4.86	30.67	-0.0545	4.88	27.23	-0.0551	4.85	25.22	-0.0575
4.00	34.46	-0.0429	4.75	34.11	-0.0442	5.93	33.62	-0.0483	6.03	30.12	-0.0522	5.88	27.78	-0.0562
5.00	35.79	-0.0424	5.80	35.49	-0.0413	7.11	35.96	-0.0425	7.11	32.99	-0.0490	7.12	30.57	-0.0535
6.00	36.83	-0.0423	6.92	36.71	-0.0385	8.36	37.68	-0.0385	8.23	35.41	-0.0449	8.21	32.99	-0.0503
7.00	37.68	-0.0421	8.11	37.72	-0.0365	9.92	39.23	-0.0361	9.92	38.19	-0.0405	9.81	35.92	-0.0446
8.00	38.59	-0.0420	9.55	38.82	-0.0343	10.86	40.01	-0.0355	10.88	39.17	-0.0381	10.99	37.64	-0.0411
10.00	40.04	-0.0402	10.78	39.73	-0.0324	12.00	40.79	-0.0350	12.00	40.16	-0.0369	12.30	39.13	-0.0382
12.00	41.34	-0.0383	12.00	40.68	-0.0308	14.00	42.06	-0.0342	14.00	41.77	-0.0352	13.60	40.23	-0.0359
14.00	42.63	-0.0337	14.00	41.93	-0.0274	16.00	43.23	-0.0315	16.00	42.91	-0.0326	15.00	41.38	-0.0342
16.00	43.47	-0.0282	16.00	43.09	-0.0265	18.00	44.23	-0.0303	18.00	43.92	-0.0305	17.00	42.42	-0.0320
18.00	44.26	-0.0260	18.00	44.02	-0.0253	20.00	44.90	-0.0270	20.00	44.50	-0.0276	19.00	43.23	-0.0304
19.00	44.43	-0.0253	20.00	44.60	-0.0242	21.00	45.10	-0.0262	21.00	44.67	-0.0260	21.00	43.95	-0.0256
20.00	44.53	-0.0235	21.00	44.74	-0.0237	22.00	45.21	-0.0250	22.00	44.74	-0.0245	22.00	44.26	-0.0269
21.00	44.60	-0.0224	22.00	44.77	-0.0235	23.00	45.27	-0.0245	23.00	44.77	-0.0243	23.00	44.43	-0.0265
22.00	44.60	-0.0220	23.00	44.77	-0.0235	24.40	45.27	-0.0245	24.40	44.77	-0.0243	24.50	44.43	-0.0265
24.40	44.60	-0.0220	24.00	44.77	-0.0235									

Station III(12)			Station IV(0)			Station IV(1)			Station IV(2)			Station IV(4)		
y (inches)	u (fps)	H_s (mm Hg)	y (inches)	u (fps)	H_s (mm Hg)	y (inches)	u (fps)	H_s (mm Hg)	y (inches)	u (fps)	H_s (mm Hg)	y (inches)	u (fps)	H_s (mm Hg)
1.06	9.82	-0.0562	1.08	21.73	-.1520	1.07	10.98	-.0537	1.09	15.44	-.0693	1.08	15.32	-.0883
1.19	11.12	-0.0591	1.23	25.43	-.1130	1.27	14.78	-.0720	1.21	17.71	-.0673	1.22	17.34	-.0800
1.35	12.52	-0.0610	1.39	28.42	-.1020	1.51	17.94	-.0770	1.49	20.47	-.0630	1.48	18.19	-.0700
1.62	13.92	-0.0625	1.66	30.83	-.0810	1.73	20.54	-.0770	1.83	22.19	-.0582	1.83	20.54	-.0590
1.95	15.05	-0.0740	1.98	32.50	-.0590	1.96	23.64	-.0760	2.34	25.61	-.0550	2.24	23.00	-.0553
2.38	16.94	-0.0654	2.44	33.92	-.0580	2.28	27.88	-.0740	2.92	28.74	-.0520	2.93	25.96	-.0500
2.82	18.62	-0.0660	3.02	34.45	-.0510	2.60	29.98	-.0720	3.40	31.10	-.0485	3.85	28.84	-.0400
3.32	20.17	-0.0671	3.78	35.41	-.0440	3.05	33.01	-.0670	4.13	33.56	-.0450	4.96	31.82	-.0315
3.89	21.54	-0.0667	4.63	36.09	-.0380	3.63	35.41	-.0600	4.78	35.33	-.0421	6.02	34.34	-.0275
4.76	23.87	-0.0642	5.49	36.55	-.0350	4.45	36.76	-.0570	5.40	36.14	-.0393	7.15	36.59	-.0260
5.92	26.50	-0.0581	6.52	37.69	-.0330	5.30	37.57	-.0550	6.25	36.91	-.0368	8.48	38.27	-.0255
7.22	29.51	-0.0535	7.85	38.57	-.0300	6.27	38.45	-.0540	7.22	37.68	-.0337	9.81	39.39	-.0250
8.85	32.94	-0.0492	8.99	39.39	-.0280	7.16	39.12	-.0530	8.33	38.45	-.0320	10.98	40.19	-.0250
10.38	35.49	-0.0441	10.71	40.26	-.0240	8.02	39.62	-.0520	9.81	39.57	-.0308	12.50	41.27	-.0250
12.00	37.96	-0.0404	12.00	41.16	-.0220	9.18	40.30	-.0500	10.99	40.22	-.0299	14.00	42.07	-.0249
1 .00	40.16	-0.0383	14.00	42.47	-.0190	10.38	40.95	-.0473	13.00	41.54	-.0283	16.00	43.20	-.0248
16.00	41.81	-0.0362	16.00	43.65	-.0160	12.00	42.05	-.0425	15.00	42.84	-.0266	18.00	44.10	-.0222
18.00	42.98	-0.0341	18.00	44.35	-.0140	14.00	43.24	-.0368	17.00	43.70	-.0240	20.00	44.93	-.0208
20.00	43.82	-0.0335	20.00	44.78	-.0135	16.00	43.96	-.0306	19.00	44.23	-.0225	21.00	45.10	-.0200
22.00	44.40	-0.0332	22.00	44.90	-.0130	18.00	44.49	-.0250	21.00	44.75	-.0215	22.00	45.20	-.0200
23.00	44.60	-0.0330	23.00	44.90	-.0130	20.00	44.95	-.0225	22.00	44.81	-.0215	23.00	45.24	-.0200
24.00	44.67	-0.0330	24.20	44.90	-.0130	21.00	45.10	-.0210	23.00	44.81	-.0215	24.20	45.24	-.0200
24.40	44.67	-0.0330				22.00	45.10	-.0200	24.20	44.81	-.0215			
						24.20	45.10	-.0200						

TABLE V VELOCITY DISTRIBUTIONS AND STATIC HEAD DISTRIBUTIONS FOR x $\geq$ 0 ft - Continued

Station IV(6)			Station IV(8)			Station IV(10)			Station IV(12)			Station V(0)		
y (inches)	u (fps)	H_s (mm Hg)	y (inches)	u (fps)	H_s (mm Hg)	y (inches)	u (fps)	H_s (mm Hg)	y (inches)	u (fps)	H_s (mm Hg)	y (inches)	u (fps)	H_s (mm Hg)
1.10	15.39	-.0670	1.10	13.95	-.0882	1.08	13.83	-.0710	1.08	13.35	-.0742	1.06	24.28	-.1830
1.33	16.44	-.0650	1.28	15.49	-.0792	1.18	14.47	-.0690	1.20	14.30	-.0721	1.19	25.53	-.1600
1.58	17.85	-.0640	1.49	16.73	-.0715	1.35	15.09	-.0650	1.48	16.30	-.0675	1.38	28.53	-.1270
1.96	19.79	-.0600	1.82	18.55	-.0642	1.58	16.47	-.0633	1.82	17.79	-.0633	1.62	29.99	-.0850
2.56	21.96	-.0568	2.28	20.28	-.0574	1.89	18.12	-.0615	2.35	20.14	-.0593	1.98	32.81	-.0710
3.13	24.25	-.0537	2.74	22.03	-.0538	2.33	20.00	-.0575	2.92	22.04	-.0567	2.41	33.43	-.0590
3.82	26.60	-.0510	3.32	23.73	-.0515	2.96	22.05	-.0543	3.73	23.89	-.0550	2.99	34.43	-.0510
4.66	29.03	-.0475	3.99	25.13	-.0480	3.78	24.44	-.0518	4.65	26.07	-.0538	3.73	35.69	-.0440
5.75	31.78	-.0437	4.87	27.31	-.0457	4.63	26.00	-.0487	5.58	28.03	-.0527	4.69	36.68	-.0414
6.91	34.23	-.0400	5.91	29.77	-.0430	5.71	28.15	-.0470	6.75	30.33	-.0520	5.77	37.72	-.0386
8.14	36.47	-.0370	7.05	32.22	-.0400	6.87	29.44	-.0455	7.87	32.22	-.0500	6.89	38.50	-.0346
9.35	38.37	-.0330	8.26	34.69	-.0363	7.96	32.57	-.0425	8.98	33.94	-.0475	8.12	39.44	-.0325
10.94	40.24	-.0303	9.55	36.69	-.0325	8.99	34.61	-.0396	10.38	36.09	-.0440	9.66	40.38	-.0300
11.50	40.66	-.0296	10.84	38.57	-.0300	10.22	36.55	-.0370	12.00	38.45	-.0410	11.32	41.43	-.0262
13.00	41.53	-.0280	12.50	40.03	-.0278	12.00	38.75	-.0337	14.00	40.61	-.0372	13.00	42.39	-.0233
15.00	42.75	-.0260	14.00	41.16	-.0260	14.00	40.52	-.0308	16.00	42.36	-.0340	15.00	43.44	-.0200
17.00	43.87	-.0240	16.00	42.64	-.0238	16.00	42.01	-.0283	18.00	43.60	-.0320	17.00	44.43	-.0175
19.00	44.71	-.0224	18.00	43.61	-.0225	18.00	43.06	-.0257	20.00	44.32	-.0300	19.00	44.98	-.0163
21.00	45.37	-.0200	20.00	44.59	-.0220	20.00	43.89	-.0235	22.00	44.91	-.0283	20.00	45.04	-.0150
22.00	45.57	-.0190	21.00	44.82	-.0218	22.00	44.55	-.0216	23.00	45.05	-.0266	21.00	45.06	-.0125
23.00	45.70	-.0178	22.00	44.88	-.0215	23.00	44.70	-.0200	24.40	45.17	-.0250	23.00	45.06	-.0125
24.50	45.70	-.0178	23.00	44.88	-.0215	24.25	44.73	-.0190				24.24	45.06	-.0125
			24.10	44.88	-.0215									

Station V(1.5)			Station V(3)			Station V(6)			Station V(9)			Station V(12)		
y (inches)	u (fps)	H_s (mm Hg)	y (inches)	u (fps)	H_s (mm Hg)	y (inches)	u (fps)	H_s (mm Hg)	y (inches)	u (fps)	H_s (mm Hg)	y (inches)	u (fps)	H_s (mm Hg)
1.09	23.01	-.1630	1.23	20.82	-.1320	1.10	16.89	-.1068	1.08	15.78	-.0844	1.09	15.17	-.0900
1.26	19.41	-.0918	1.45	24.71	-.1200	1.22	18.33	-.0870	1.22	16.98	-.0788	1.28	17.00	-.0790
1.58	21.65	-.0810	1.78	25.69	-.1038	1.48	19.82	-.0732	1.47	18.38	-.0666	1.56	18.79	-.0708
1.89	23.54	-.0750	2.13	26.39	-.0862	1.76	21.09	-.0668	1.74	19.53	-.0583	1.96	20.46	-.0650
2.36	27.01	-.0675	2.71	28.18	-.0743	2.22	22.72	-.0600	2.16	21.19	-.0533	2.51	22.45	-.0600
2.89	30.23	-.0610	3.38	30.38	-.0640	2.93	24.65	-.0550	2.68	22.90	-.0508	3.18	24.16	-.0570
3.52	33.16	-.0550	3.99	32.03	-.0550	3.89	27.72	-.0506	3.19	24.26	-.0482	3.98	25.81	-.0540
4.36	35.40	-.0490	4.88	34.29	-.0467	5.06	30.38	-.0460	3.87	25.88	-.0462	5.02	27.78	-.0518
5.22	36.79	-.0460	6.06	36.36	-.0375	6.16	33.03	-.0410	4.86	27.67	-.0437	6.16	29.71	-.0483
6.31	37.80	-.0425	7.20	37.70	-.0300	7.33	35.05	-.0357	5.96	29.83	-.0418	7.32	31.78	-.0465
7.58	39.12	-.0410	8.63	38.83	-.0275	8.58	36.74	-.0318	7.24	32.28	-.0384	8.58	33.58	-.0425
8.86	40.14	-.0394	10.50	40.01	-.0268	9.87	38.35	-.0287	8.56	34.81	-.0350	9.92	35.52	-.0390
10.23	41.05	-.0375	11.68	41.12	-.0245	11.37	39.72	-.0260	9.91	37.11	-.0320	10.58	36.61	-.0375
12.00	42.49	-.0353	13.00	42.03	-.0230	13.00	40.78	-.0240	11.33	39.04	-.0288	12.00	38.51	-.0340
14.00	43.64	-.0320	15.00	43.16	-.0218	15.00	42.17	-.0220	13.00	40.69	-.0264	14.00	40.45	-.0300
16.00	44.25	-.0280	17.00	44.15	-.0200	17.00	43.21	-.0213	15.00	42.01	-.0225	16.00	41.95	-.0268
18.00	44.91	-.0240	19.00	44.79	-.0184	19.00	44.27	-.0208	17.00	43.03	-.0190	18.00	43.03	-.0240
20.00	45.33	-.0210	21.00	45.41	-.0174	21.00	44.90	-.0188	19.00	43.90	-.0166	20.00	44.03	-.0225
21.00	45.37	-.0200	22.00	45.49	-.0168	22.00	45.13	-.0187	21.00	44.48	-.0140	22.00	44.65	-.0200
22.00	45.37	-.0200	23.00	45.52	-.0168	23.00	45.15	-.0175	22.00	44.68	-.0130	23.00	44.91	-.0190
24.24	45.37	-.0200	24.27	45.52	-.0168	24.22	45.15	-.0175	23.00	44.92	-.0125	24.24	45.01	-.0180
									24.23	44.94	-.0120			

Station VI(0)			Station VI(1.5)			Station VI(3)			Station VI(6)			Station VI(9)		
y (inches)	u (fps)	H_s (mm Hg)	y (inches)	u (fps)	H_s (mm Hg)	y (inches)	u (fps)	H_s (mm Hg)	y (inches)	u (fps)	H_s (mm Hg)	y (inches)	u (fps)	H_s (mm Hg)
1.08	14.16	-.0510	1.08	11.87	-.0450	1.06	11.28	-.0500	1.08	9.99	-.0375	1.08	10.32	-.0410
1.22	16.14	-.0430	1.26	12.59	-.0396	1.22	13.98	-.0440	1.24	10.78	-.0318	1.26	11.21	-.0337
1.38	17.23	-.0370	1.58	14.08	-.0340	1.48	14.95	-.0385	1.46	11.92	-.0290	1.51	12.20	-.0283
1.62	19.39	-.0300	1.92	15.95	-.0310	1.86	15.48	-.0270	1.69	12.87	-.0260	1.88	13.41	-.0225
2.15	21.07	-.0200	2.52	18.61	-.0270	2.37	16.94	-.0250	2.06	13.87	-.0230	2.38	14.68	-.0203
2.69	22.33	-.0175	3.18	20.97	-.0236	2.96	18.39	-.0233	2.54	15.00	-.0210	2.92	15.67	-.0190
3.27	22.96	-.0158	3.91	22.43	-.0200	3.69	20.09	-.0214	2.98	16.05	-.0200	3.70	17.07	-.0178
3.89	23.41	-.0142	4.98	23.96	-.0170	4.48	21.52	-.0190	3.63	17.39	-.0182	4.54	18.34	-.0170
4.66	24.02	-.0130	6.06	24.77	-.0148	5.32	22.98	-.0160	4.36	18.89	-.0167	5.47	19.67	-.0157
5.55	24.58	-.0126	7.18	25.52	-.0140	6.40	24.15	-.0120	5.04	19.82	-.0153	6.52	21.01	-.0142
6.54	25.16	-.0119	8.32	26.15	-.0136	7.67	25.24	-.0100	6.00	21.28	-.0140	7.72	22.34	-.0126
7.47	25.74	-.0118	9.70	26.87	-.0130	8.97	26.24	-.0086	7.18	22.87	-.0117	8.98	23.79	-.0110
8.87	26.48	-.0100	11.20	27.52	-.0128	10.36	26.95	-.0075	8.70	24.57	-.0100	10.36	25.01	-.0093
9.96	26.97	-.0097	12.50	27.95	-.0120	12.00	27.76	-.0064	9.99	25.46	-.0080	11.55	25.94	-.0083
10.45	27.65	-.0094	14.00	28.40	-.0100	14.00	28.57	-.0058	11.43	26.51	-.0075	13.00	26.82	-.0071
12.00	27.80	-.0082	16.00	28.99	-.0100	16.00	29.23	-.0046	13.00	27.31	-.0070	15.00	28.16	-.0059
14.00	28.55	-.0075	18.00	29.54	-.0088	18.00	29.75	-.0040	15.00	28.13	-.0053	17.00	28.79	-.0050
16.00	29.18	-.0065	20.00	29.92	-.0085	20.00	29.94	-.0040	17.00	28.81	-.0045	19.00	29.36	-.0042
18.00	29.50	-.0050	22.00	29.97	-.0085	22.00	29.94	-.0040	19.00	29.45	-.0040	20.00	29.58	-.0037
20.00	29.51	-.0042	24.29	29.97	-.0085	24.26	29.94	-.0040	20.00	29.60	-.0030	21.00	29.76	-.0033
22.00	29.48	-.0036							21.00	29.67	-.0025	22.00	29.78	-.0027
24.28	29.48	-.0036							22.00	29.67	-.0025	23.00	29.76	-.0022
									24.21	29.67	-.0025	24.22	29.76	-.0022

TABLE V VELOCITY DISTRIBUTIONS AND STATIC HEAD DISTRIBUTIONS FOR $x \geq 0$ ft - Continued

Station VI(12)		
y (inches)	u (fps)	H_s (mm Hg)
1.10	9.84	-.0327
1.31	11.11	-.0287
1.54	11.86	-.0266
1.88	12.97	-.0255
2.25	13.93	-.0223
2.72	14.94	-.0210
3.11	15.68	-.0205
3.70	16.57	-.0193
4.58	17.32	-.0185
5.57	19.12	-.0175
6.72	20.59	-.0163
7.88	21.97	-.0151
9.04	23.40	-.0140
10.42	24.62	-.0128
12.00	26.12	-.0115
14.00	27.51	-.0097
16.00	28.54	-.0083
18.00	29.24	-.0069
20.00	29.59	-.0058
21.00	29.74	-.0053
22.00	29.88	-.0047
23.00	29.89	-.0043
24.24	29.89	-.0040

Station Ia(11,1)			
y (inches)	u (fps)	u_h (fps)	H_s (mm Hg)
.25	---	3.68	-.0377
.59	---	3.88	-.0411
1.07	---	6.75	-.0420
1.28	---	10.21	-.0413
1.34	11.34	11.65	-.0401
1.90	14.86	14.02	-.0318
2.75	15.94	15.90	-.0241
3.83	17.47	17.52	-.0185
4.76	19.04	---	-.0161
5.54	20.21	---	-.0143
6.82	22.25	---	-.0125
8.10	24.22	---	-.0110
9.60	25.98	---	-.0072
11.00	27.51	---	-.0050
12.50	28.60	---	-.0033
13.95	29.41	---	-.0020
15.78	30.14	---	-.0007
17.50	30.43	---	.0015
20.40	30.92	---	.0020
23.00	30.92	---	.0025

Station Ia(11,2)			
y (inches)	u (fps)	u_h (fps)	H_s (mm Hg)
.10	---	4.11	-.0395
.35	---	5.43	-.0432
.77	---	4.50	-.0460
1.14	7.90	7.96	-.0459
1.31	10.27	10.83	-.0433
1.52	12.27	12.29	-.0393
1.79	14.88	14.68	-.0370
2.84	16.21	16.29	-.0275
3.92	17.71	17.08	-.0210
6.12	21.18	---	-.0149
7.19	22.88	---	-.0121
8.20	24.22	---	-.0111
9.40	25.87	---	-.0086
10.50	27.00	---	-.0067
11.88	28.03	---	-.0048
13.25	29.01	---	-.0033
14.92	29.86	---	-.0017
16.50	30.54	---	-.0007
18.00	30.68	---	.0007
19.80	30.88	---	.0014
23.00	30.89	---	.0030

Station Ia(11,3)			
y (inches)	u (fps)	u_h (fps)	H_s (mm Hg)
.10	---	3.51	-.0298
.27	---	4.64	-.0346
.69	---	4.52	-.0372
1.10	---	8.28	-.0376
1.25	10.31	10.78	-.0371
1.40	11.12	11.35	-.0364
1.70	13.86	13.68	-.0345
2.71	16.13	16.05	-.0261
4.10	17.94	---	-.0203
5.71	20.43	---	-.0160
7.04	22.45	---	-.0134
8.28	24.22	---	-.0106
9.50	25.97	---	-.0080
10.85	27.34	---	-.0068
12.50	28.54	---	-.0043
14.17	29.43	---	-.0025
16.08	30.11	---	-.0011
17.94	30.50	---	---
20.50	30.75	---	.0010
23.00	30.72	---	.0020

Station Ia(11,4)			
y (inches)	u (fps)	u_h (fps)	H_s (mm Hg)
.10	---	3.73	-.0173
.35	---	4.12	-.0215
.80	---	5.96	-.0256
1.07	---	8.38	-.0263
1.33	10.36	10.40	-.0271
1.60	12.37	12.33	-.0261
1.92	14.11	14.15	-.0244
2.59	15.42	15.44	-.0220
3.18	16.58	16.36	-.0200
4.00	17.73	---	-.0176
4.78	19.09	---	-.0168
6.07	21.23	---	-.0131
7.30	23.01	---	-.0122
8.50	24.58	---	-.0102
9.55	25.88	---	-.0089
11.00	27.56	---	-.0064
12.55	28.80	---	-.0042
14.42	29.70	---	-.0024
16.00	30.18	---	-.0015
17.75	30.56	---	-.0011
19.80	30.77	---	.0010
21.40	30.77	---	.0018
23.00	30.80	---	.0020

Station Ia(11,6)			
y (inches)	u (fps)	u_h (fps)	H_s (mm Hg)
.90	---	3.02	-.0001
.31	---	1.08	-.0036
.55	---	6.33	-.0062
.92	---	8.92	-.0090
1.58	11.41	11.84	-.0109
2.68	14.92	14.68	-.0122
4.12	17.83	17.77	-.0128
5.49	20.16	---	-.0127
6.90	22.56	---	-.0121
8.50	24.87	---	-.0098
10.30	27.08	---	-.0075
13.00	29.10	---	-.0041
14.78	29.99	---	-.0025
16.25	30.48	---	-.0014
18.80	30.78	---	.0003
21.00	30.88	---	.0012
23.00	30.89	---	.0020

Station Ia(11,8)			
y (inches)	u (fps)	u_h (fps)	H_s (mm Hg)
.10	4.80	5.35	.0084
.37	6.07	6.42	.0044
.73	7.68	7.70	.0013
1.40	10.36	10.26	-.0012
2.06	11.92	11.83	-.0034
2.50	13.77	13.82	-.0046
3.25	14.98	14.80	-.0066
3.85	16.95	16.90	-.0077
5.05	18.31	---	-.0098
6.10	20.92	---	-.0107
7.79	22.88	---	-.0099
9.33	25.63	---	-.0085
10.89	27.08	---	-.0068
12.75	29.44	---	-.0047
15.93	30.26	---	-.0021
19.14	30.80	---	-.000
23.00	30.90	---	.0018

Station Ia(11,10)			
y (inches)	u (fps)	u_h (fps)	H_s (mm Hg)
.10	4.51	5.25	.0138
.37	6.33	6.42	.0109
.78	7.91	8.03	.0072
1.44	10.04	10.24	.0035
2.10	12.33	12.30	-.0008
2.86	14.71	14.68	-.0047
4.92	19.18	19.22	-.0098
5.96	20.78	---	-.0110
7.00	22.47	---	-.0115
9.43	25.46	---	-.0092
10.90	27.05	---	-.0070
12.50	28.53	---	-.0050
14.50	29.72	---	-.0028
16.40	30.40	---	-.0015
17.20	30.74	---	-.0008
19.90	30.86	---	.0007
23.00	30.93	---	.0022

Station Ia(12,1)			
y (inches)	u (fps)	u_h (fps)	H_s (mm Hg)
.25	---	3.85	-.0422
.35	---	2.26	-.0426
.64	---	2.62	-.0454
1.15	6.56	7.08	-.0444
1.25	9.60	10.15	-.0428
1.34	9.51	12.37	-.0410
1.77	15.03	14.96	-.0370
2.63	15.88	15.78	-.0288
3.60	17.05	17.15	-.0214
4.84	19.15	---	-.0187
6.00	20.68	---	-.0154
7.38	22.93	---	-.0132
8.78	24.81	---	-.0116
10.74	26.82	---	-.0094
12.40	28.16	---	-.0060
14.35	29.47	---	-.0032
16.48	30.17	---	-.0018
18.00	30.35	---	-.0003
19.45	30.53	---	-.000
21.00	30.66	---	.0008
23.00	30.70	---	.0020

TABLE V VELOCITY DISTRIBUTIONS AND STATIC HEAD DISTRIBUTIONS FOR $x \geq 0$ ft - Continued

Station Ia(12,2)

y (inches)	u (fps)	u_h (fps)	H_s (mm Hg)
.08	---	3.96	-.0446
.37	---	4.38	-.0481
1.00	6.04	7.42	-.0520
1.21	8.82	9.33	-.0494
1.25	9.4	10.24	-.0496
1.43	11.82	11.68	-.0467
1.62	13.75	13.85	-.0442
2.00	15.81	15.76	-.0385
2.69	16.43	---	-.0325
4.40	18.38	---	-.0235
5.50	19.99	---	-.0200
6.56	21.55	---	-.0180
8.13	23.84	---	-.0150
9.73	25.80	---	-.0124
11.60	27.59	---	-.0094
12.80	28.51	---	-.0077
14.52	29.49	---	-.0056
16.15	30.09	---	-.0040
17.90	30.40	---	-.0023
19.30	30.63	---	-.0015
23.00	30.70	---	---

Station Ia(12,3)

y (inches)	u (fps)	u_h (fps)	H_s (mm Hg)
.08	---	3.67	-.0353
.37	---	4.42	-.0408
.98	6.33	7.88	-.0444
1.18	8.25	8.42	-.0445
1.29	9.86	10.66	-.0444
1.65	12.57	12.58	-.0408
1.88	14.76	14.69	-.0390
2.94	16.76	16.70	-.0314
4.32	18.69	---	-.0243
5.54	20.27	---	-.0217
7.25	22.49	---	-.0165
8.56	24.38	---	-.0156
10.20	26.38	---	-.0125
11.80	27.99	---	-.0098
14.00	29.49	---	-.0066
15.66	29.96	---	-.0050
17.60	30.43	---	-.0030
19.20	30.60	---	-.0020
21.00	30.68	---	-.0012
23.00	30.65	---	---

Station Ia(12,4)

y (inches)	u (fps)	u_h (fps)	H_s (mm Hg)
.07	---	2.21	-.0222
.35	---	3.75	-.0266
.85	5.36	7.32	-.0311
1.1	9.22	9.23	-.0313
1.23	10.65	11.54	-.0316
1.80	13.65	14.08	-.0301
2.69	15.87	15.07	-.0262
3.40	17.22	17.08	-.0241
4.41	18.77	18.78	-.0222
5.72	20.48	---	-.0192
6.94	22.27	---	-.0178
8.30	24.01	---	-.0152
9.32	25.35	---	-.0137
10.82	27.13	---	-.0110
12.20	28.42	---	-.0090
14.06	29.54	---	-.0066
15.65	30.11	---	-.0050
17.58	30.49	---	-.0033
19.25	30.70	---	-.0020
21.00	30.75	---	-.0010
23.00	30.80	---	---

Station Ia(12,6)

y (inches)	u (fps)	u_h (fps)	H_s (mm Hg)
.07	---	2.89	-.0044
.42	---	2.21	-.0056
.62	6.8	7.66	-.0112
.84	7.28	8.52	-.0129
1.24	9.49	10.55	-.0147
2.00	13.14	13.05	-.0155
3.32	16.36	16.38	-.0167
4.18	18.35	---	-.0174
5.46	20.42	---	-.0173
6.95	22.22	---	-.0163
8.42	24.12	---	-.0145
9.55	25.42	---	-.0129
10.94	26.90	---	-.0109
12.23	28.12	---	-.0092
13.75	29.22	---	-.0075
15.55	30.09	---	-.0057
17.30	30.53	---	-.0040
19.40	30.82	---	-.0024
21.00	30.90	---	-.0016
23.00	30.82	---	-.0005

Station Ia(12,8)

y (inches)	u (fps)	u_h (fps)	H_s (mm Hg)
.09	4.06	5.76	.0041
.49	5.87	6.30	-.0016
1.10	8.61	9.08	-.0048
1.62	10.82	10.06	-.0070
2.60	14.08	13.87	-.0090
3.58	16.55	16.23	-.0120
4.92	19.04	---	-.0149
6.10	19.53	---	-.0158
7.00	22.25	---	-.0155
8.63	23.53	---	-.0141
9.88	26.04	---	-.0131
11.80	27.35	---	-.0104
13.55	29.22	---	-.0084
15.75	29.96	---	-.0058
17.75	30.71	---	-.0041
19.20	30.70	---	-.0029
21.00	30.91	---	-.0018
23.00	30.90	---	-.0006

Station Ia(12,10)

y (inches)	u (fps)	u_h (fps)	H_s (mm Hg)
.09	3.67	5.35	.0111
.55	6.09	7.02	.0064
1.10	8.79	9.13	.0024
1.90	11.71	11.96	-.0032
2.40	13.15	13.00	-.0052
2.85	14.64	14.52	-.0081
3.50	16.11	16.20	-.0117
4.01	17.39	---	-.0141
5.17	19.42	---	-.0161
6.08	20.77	---	-.0166
7.33	22.69	---	-.0160
8.48	24.19	---	-.0156
9.90	26.09	---	-.0135
11.35	27.77	---	-.0116
13.25	29.19	---	-.0078
15.20	30.16	---	-.0065
17.23	30.73	---	-.0047
19.20	30.95	---	-.0032
21.00	30.94	---	-.0020
23.00	30.94	---	-.0010

Station IIa(10,1)

y (inches)	u (fps)	u_h (fps)	H_s (mm Hg)
.29	---	3.02	-.0196
.35	---	4.13	-.0203
.49	---	4.99	-.0211
.68	---	4.67	-.0226
.84	---	7.35	-.0229
1.03	5.19	8.03	-.0230
1.19	7.7	9.12	-.0215
1.37	9.35	10.87	-.0202
1.68	11.85	12.02	-.0179
1.99	12.41	12.88	-.0165
2.32	13.24	13.56	-.0156
2.89	14.84	14.67	-.0146
3.45	16.16	16.23	-.0143
4.25	17.43	17.40	-.0135
5.11	18.96	---	-.0122
6.31	21.52	---	-.0118
7.80	23.69	---	-.0096
9.55	26.57	---	-.0069
11.36	28.69	---	-.0041
13.17	29.87	---	-.0021
14.93	30.64	---	-.0008
16.00	30.86	---	-.0007
18.00	31.05	---	-.0003
20.00	31.17	---	.0002
22.50	31.15	---	.0007

Station IIa(10,2)

y (inches)	u (fps)	u_h (fps)	H_s (mm Hg)
.12	---	3.15	-.0160
.22	---	4.33	-.0156
.36	---	4.88	-.0175
.58	---	4.62	-.0193
.91	4.1	6.78	-.0197
1.13	6.8	8.02	-.0194
1.22	7.45	9.35	-.0185
1.42	8.8	10.06	-.0179
1.87	11.2	11.92	-.0168
2.51	13.2	12.89	-.0160
3.35	14.9	14.50	-.0152
4.31	16.73	16.92	-.0145
5.49	19.11	---	-.0141
6.63	21.09	---	-.0127
7.85	23.55	---	-.0113
9.25	25.50	---	-.0093
10.78	27.58	---	-.0062
12.53	29.18	---	-.0045
14.65	30.20	---	-.0028
16.00	30.62	---	-.0014
18.00	31.05	---	-.0002
20.00	31.16	---	.0005

Station IIa(10,3)

y (inches)	u (fps)	u_h (fps)	H_s (mm Hg)
.12	---	2.96	-.0080
.22	---	3.67	-.0102
.36	---	4.18	-.0111
.55	---	3.98	-.0118
.72	4.35	5.72	-.0126
.89	5.5	7.46	-.0133
1.13	7.2	8.09	-.0138
1.41	8.7	9.32	-.0138
1.87	10.6	11.32	-.0131
2.51	12.65	12.96	-.0140
3.35	14.8	14.60	-.0143
4.34	16.9	16.72	-.0146
5.48	19.20	---	-.0142
6.66	21.43	---	-.0125
7.79	23.63	---	-.0116
9.27	25.72	---	-.0091
10.81	27.45	---	-.0069
12.52	29.14	---	-.0047
14.64	30.10	---	-.0029
16.00	30.80	---	-.0021
18.00	31.09	---	-.0010
20.00	31.18	---	---
22.50	31.16	---	.0005

Station IIa(10,4)

y (inches)	u (fps)	u_h (fps)	H_s (mm Hg)
.12	---	3.26	-.0007
.28	---	4.38	-.0011
.50	---	4.20	-.0040
.62	---	3.02	-.0052
.79	5.5	6.68	-.0060
1.13	7.1	8.98	-.0074
1.49	10.02	11.22	-.0082
1.89	12.45	12.98	-.0096
2.65	14.9	14.67	-.0113
3.42	15.39	15.20	-.0132
4.53	17.79	17.82	-.0138
5.76	20.08	---	-.0137
7.50	23.27	---	-.0120
9.31	26.06	---	-.0100
11.20	28.20	---	-.0067
13.26	29.91	---	-.0040
15.54	30.71	---	-.0022
17.00	31.01	---	-.0013
19.00	31.21	---	-.0005
21.00	31.22	---	.0002
22.50	31.22	---	.0003

Station IIa(10,5)

y (inches)	u (fps)	u_h (fps)	H_s (mm Hg)
.58	4.21	---	---
1.08	7.64	---	-.0055
1.50	8.94	---	-.0077
2.00	11.01	---	-.0100
2.50	12.69	---	-.0118
3.00	14.28	14.30	-.0132
3.50	15.57	---	-.0145
4.00	16.79	---	-.0152
5.00	18.74	---	-.0154
6.00	20.59	---	-.0147
7.00	22.45	---	-.0135
8.00	24.33	---	-.0118
9.00	25.78	---	-.0101
10.00	27.27	---	-.0086
11.50	28.77	---	-.0066
13.00	29.80	---	-.0048
14.50	30.39	---	-.0036
16.00	30.84	---	-.0028
18.00	31.17	---	-.0018
20.00	31.23	---	-.0010
22.50	31.21	---	-.0005

Station IIa(10,7)

y (inches)	u (fps)	u_h (fps)	H_s (mm Hg)
.13	---	2.88	-.0198
.25	---	3.75	-.0227
.43	---	4.22	-.0239
.70	---	4.08	-.0238
1.02	4.7	6.88	-.0211
1.19	8.04	9.28	-.0206
1.23	8.8	9.99	-.0196
1.66	11.	10.98	-.0188
2.24	13.1	12.73	-.0169
2.89	14.7	14.30	-.0160
3.74	16.15	16.36	-.0152
4.71	18.38	---	-.0144
6.15	20.87	---	-.0135
7.80	23.95	---	-.0117
9.56	26.64	---	-.0091
11.54	28.70	---	-.0062
13.83	30.27	---	-.0042
15.00	30.56	---	-.0032
17.00	30.93	---	-.0023
19.00	31.21	---	-.0015
21.00	31.22	---	-.0008
22.50	31.22	---	-.0007

TABLE V VELOCITY DISTRIBUTIONS AND STATIC HEAD DISTRIBUTIONS FOR $x \geq 0$ ft - Continued

Station IIa(10,8)

y (inches)	u (fps)	u_h (fps)	H_s (mm Hg)
.16	---	3.22	-.0166
.34	---	3.35	-.0190
.58	---	3.75	-.0202
.91	3.8	4.83	-.0213
1.17	7.25	7.99	-.0203
1.33	8.6	9.20	-.0198
1.92	11.4	11.00	-.0178
2.66	13.4	13.55	-.0165
3.46	15.1	15.02	-.0161
4.56	16.93	16.78	-.0153
6.10	19.96	---	-.0142
7.90	23.28	---	-.0121
9.73	26.05	---	-.0094
11.75	28.15	---	-.0068
12.50	28.84	---	-.0059
14.02	30.06	---	-.0049
16.00	30.67	---	-.0033
18.00	31.15	---	-.0024
20.00	31.26	---	-.0016
22.50	31.25	---	-.0013

Station IIa(10,9)

y (inches)	u (fps)	u_h (fps)	H_s (mm Hg)
.16	--	2.98	-.0082
.36	--	3.32	-.0111
.57	--	4.67	-.0119
.76	4.83	5.75	-.0127
.86	5.4	6.68	-.0138
1.25	7.8	8.24	-.0150
1.59	9.5	9.89	-.0141
2.10	11.5	10.96	-.0150
2.78	13.4	13.52	-.0159
3.69	15.	15.21	-.0160
4.86	17.1	16.89	-.0159
6.36	20.71	--	-.0143
8.13	23.65	--	-.0130
9.92	26.34	--	-.0099
12.06	28.73	--	-.0073
14.34	30.12	--	-.0052
16.00	30.64	--	-.0037
18.00	30.92	--	-.0025
20.00	31.04	--	-.0020
21.50	31.14	--	-.0015
22.50	31.37	--	-.0013

Station IIa(10,10)

y (inches)	u (fps)	u_h (fps)	H_s (mm Hg)
.16	--	3.17	-.0015
.31	--	3.78	-.0038
.46	--	3.65	-.0046
.59	--	5.23	-.0052
.71	4.9	7.02	-.0059
1.16	7.3	8.33	-.0083
1.48	10.1	10.96	-.0093
1.93	12.5	11.89	-.0111
2.63	14.7	14.87	-.0126
3.38	17.7	17.60	-.0150
4.55	18.49	--	-.0163
6.15	20.76	--	-.0150
7.84	23.54	--	-.0132
9.40	25.70	--	-.0112
10.84	27.74	--	-.0091
12.34	28.99	--	-.0069
14.02	30.10	--	-.0054
15.28	30.77	--	-.0044
17.00	31.01	--	-.0033
19.00	31.15	--	-.0024
21.00	31.21	--	-.0016
22.50	31.21	--	-.0013

Station IIa(10,11)

y (inches)	u (fps)	u_h (fps)	H_s (mm Hg)
.59	3.98	--	--
1.10	7.03	--	-.0065
1.50	8.60	--	-.0097
2.00	10.89	--	-.0116
2.50	12.35	--	-.0130
3.00	14.05	--	-.0140
3.50	15.16	--	-.0148
4.00	16.27	--	-.0153
4.50	17.45	--	-.0158
5.00	18.47	--	-.0160
6.00	20.28	--	-.0153
7.00	21.76	--	-.0142
8.00	23.18	--	-.0126
9.00	24.72	--	-.0113
10.00	20.26	--	-.0089
14.50	30.20	--	-.0049
16.00	30.74	--	-.0039
17.50	31.03	--	-.0033
19.00	31.17	--	-.0027
20.50	31.24	--	-.0022
22.50	31.23	--	-.0020

TABLE VI DRAG COEFFICIENT OF FENCES AND AVERAGE SHEAR VELOCITIES OF WALL

Station	U_a (fps)	c_D	c_f	U_τ (fps)
I(0)	29.98	.508	.0423	4.36
I(1)	30.20	.0415	.0035	1.256
I(2)	30.28	.247	.0206	3.073
I(3)	30.40	.221	.0184	2.916
I(5)	30.38	.199	.0166	2.768
I(7)	30.46	.176	.0147	2.612
I(9)	30.60	.167	.0138	2.543
I(11)	30.88	.161	.0134	2.531
I(12)	30.97	.159	.0132	2.517
I(13)	31.16	.158	.0131	2.526
II(0)	30.38	.505	.0842	6.232
II(0.5)	30.61	—	—	—
II(1)	30.30	.0663	.0110	2.252
II(1.5)	30.66	.112	.0186	2.958
II(2)	30.57	.108	.0180	2.900
II(2.5)	30.77	.111	.0185	2.959
II(3)	30.59	.111	.0185	2.942
II(4)	30.56	.103	.0172	2.834
II(5)	30.82	.099	.0165	2.799
II(6)	30.44	.0972	.0162	2.740
II(8)	30.61	.0950	.0158	2.723
II(10)	30.95	.0943	.0157	2.743
II(10.5)	30.97	.0942	.0157	2.744
II(11)	31.11	.0942	.0157	2.756
III(0)	44.43	.475	.0791	8.836
III(1)	44.60	.0825	.0138	3.699
III(2)	44.77	.0802	.0134	3.661
III(4)	45.27	.103	.0172	4.200
III(6)	44.77	.0948	.0158	3.979
III(10)	44.43	.0151	.0142	3.741
III(12)	44.67	.0849	.0141	3.757

Station	U_a (fps)	c_D	c_f	U_τ (fps)
IV(0)	44.90	.478	.0398	6.337
IV(1)	45.10	.0620	.0052	2.289
IV(2)	44.81	.220	.0183	4.291
IV(4)	45.24	.196	.0163	4. 88
IV(6)	45.70	.174	.0145	3.889
IV(8)	44.88	.154	.0128	3.593
IV(10)	44.73	.144	.0120	3.459
IV(12)	45.17	.142	.0118	3.474
V(0)	45.06	.476	.0265	5.183
V(1.5)	45.37	.185	.0103	3.248
V(3)	45.52	.172	.0095	3.130
V(6)	45.15	.235	.0130	3.644
V(9)	44.94	.199	.0110	3.340
V(12)	45.01	.195	.0108	3.309
VI(0)	29.51	.487	.0271	3.432
VI(1.5)	29.97	.185	.0103	2.151
VI(3)	29.94	.297	.0165	2.720
VI(6)	29.67	.234	.0180	2.392
VI(9)	29.78	.216	.0120	2.309
VI(12)	29.89	.212	.0118	2.293

TABLE VII TURBULENCE DISTRIBUTIONS FOR RUNS I, II, Ia, AND IIa

Station I(-4) and II(-4)
u_a = 30.11 (fps)

y (in.)	u $\left(\frac{ft}{sec}\right)$	$\overline{u'^2}$ $\left(\frac{ft^2}{sec^2}\right)$	$\overline{v'^2}$ $\left(\frac{ft^2}{sec^2}\right)$	$\overline{u'v'}$ $\left(\frac{ft^2}{sec^2}\right)$
0.12	14.86	7.15	0.34	-1.09
0.23	17.03	8.09	0.69	-1.03
0.50	19.01	6.99	1.33	-1.02
0.85	20.36	6.39	1.58	-1.02
1.18	21.06	5.75	1.63	-1.01
1.89	22.13	5.00	1.96	-1.05
2.82	23.78	4.54	1.83	-0.97
4.28	25.29	4.05	1.62	-1.02
5.77	26.56	3.33	1.26	-0.78
7.67	27.73	2.67	1.20	-0.73
9.68	28.82	1.57	0.94	-0.49
11.04	29.40	0.94	0.53	-0.23
13.01	29.89	0.36	0.18	-0.06
15.27	30.08	0.14	0.06	-0.01

Station I(0).
u_a = 29.98 (fps)

y (in.)	u $\frac{ft}{sec}$	$\overline{u'^2}$ $\left(\frac{ft^2}{sec^2}\right)$	$\overline{v'^2}$ $\left(\frac{ft^2}{sec^2}\right)$	$\overline{u'v'}$ $\left(\frac{ft^2}{sec^2}\right)$
1.12	16.83	2.91	12.21	-5.89
1.30	19.01	4.15	12.34	-6.26
1.44	20.22	5.17	12.14	-6.39
1.94	21.83	5.37	8.45	-4.68
2.17	22.26	5.30	6.99	-4.08
2.65	23.06	4.58	4.85	-2.87
3.30	23.96	4.29	3.44	-2.23
4.13	24.85	3.97	3.00	-1.89
5.34	25.90	3.39	2.25	-1.52
6.88	26.82	2.93	1.74	-1.15
8.49	27.70	2.55	1.24	-0.81
10.07	28.5	1.94	0.89	-0.59
11.92	29.35	1.08	0.55	-0.33
13.78	29.80	0.45	0.37	-0.14

Station I(1)
u_a = 30.20 (fps)

y (in.)	u $\frac{ft}{sec}$	$\overline{u'^2}$ $\left(\frac{ft^2}{sec^2}\right)$	$\overline{v'^2}$ $\left(\frac{ft^2}{sec^2}\right)$	$\overline{u'v'}$ $\left(\frac{ft^2}{sec^2}\right)$
1.10	8.02	18 62	3.41	-0.59
1.21	8.93	21 85	2.85	-0.50
1.39	9.82	25 74	1.40	-2.05
1.65	11.92	32.43	2.22	-4.01
2.01	14.85	35 67	4.17	-5.62
2.63	19.53	25.06	5.68	-4.80
3.40	23.82	9.55	3.79	-2.23
4.48	25.42	4.85	1.14	-0.98
5.46	26.31	4.17	1.06	-0.78
6.72	27.25	3.62	0.78	-0.70
8.12	28.05	2.96	0.93	-0.64
9.70	28.80	2.34	0.96	-0.49
11.52	29.42	1.61	0.51	-0.35
13.64	29.90	0.72	0.39	-0.24
15.67	30.16	0.23	0.21	-0.08

Station I(2)
u_a = 30.28 (fps)

y (in.)	u $\frac{ft}{sec}$	$\overline{u'^2}$ $\left(\frac{ft^2}{sec^2}\right)$	$\overline{v'^2}$ $\left(\frac{ft^2}{sec^2}\right)$	$\overline{u'v'}$ $\left(\frac{ft^2}{sec^2}\right)$
1.1	10.42	6.81	7.92	-2.73
1.21	11.83	8.16	9.69	-3.65
1.39	13.11	10.68	11.65	-5.01
1.64	14.28	12.80	14.31	-6.70
2.01	16.06	17.82	15.74	-8.52
2.61	18.62	24.20	14.58	-9.89
3.39	21.35	22.57	10.79	-8.24
4.46	23.78	10.96	5.12	-3.97
5.38	25.02	5.79	2.62	-1.69
6.62	26.24	4.05	1.10	-0.91
8.07	27.28	2.94	1.25	-0.78
9.70	28.16	2.43	0.92	-0.65
11.50	29.03	1.79	0.60	-0.43
13.66	29.88	0.83	0.36	-0.20
15.65	30.01	0.30	0.26	-0.10

Station I(3)
u_a = 30.40 (fps)

y (in.)	u $\frac{ft}{sec}$	$\overline{u'^2}$ $\left(\frac{ft^2}{sec^2}\right)$	$\overline{v'^2}$ $\left(\frac{ft^2}{sec^2}\right)$	$\overline{u'v'}$ $\left(\frac{ft^2}{sec^2}\right)$
1.1	9.62	7.69	12.03	-0.39
1.20	10.73	8.20	8.08	-2.71
1.38	11.82	9.48	9.69	-3.88
1.62	13.50	14.76	11.91	-6.13
1.95	15.42	19.51	13.85	-8.20
2.61	17.73	24.09	14.73	-9.78
3.37	19.85	24.76	10.83	-8.20
4.48	22.52	16.78	9.21	-5.38
5.38	24.21	[illegible]	4.66	-2.98
6.61	25.90	5.81	2.53	-1.63
8.09	27.18	3.31	1.31	-0.81
9.69	28.22	2.84	1.06	-0.75
11.48	29.11	[illegible]	0.69	-0.46
13.66	29.90	0.99	0.46	-0.26
15.61	30.03	0.39	0.28	-0.12

Station I(5)
u_a = 30.38 (fps)

y (in.)	u $\frac{ft}{sec}$	$\overline{u'^2}$ $\left(\frac{ft^2}{sec^2}\right)$	$\overline{v'^2}$ $\left(\frac{ft^2}{sec^2}\right)$	$\overline{u'v'}$ $\left(\frac{ft^2}{sec^2}\right)$
1.10	10.02	6.78	6.74	-1.78
1.20	11.22	8.77	8.05	-2.83
1.38	12.11	10.78	8.60	-3.27
1.61	12.93	12.61	10.85	-4.62
1.96	14.05	17.00	12.01	-6.65
2.61	15.83	21.53	11.09	-7.59
3.34	17.75	23.38	9.01	-7.02
4.48	20.62	21.98	8.49	-6.41
5.38	22.55	19.22	7.82	-5.20
6.61	24.72	12.74	4.22	-3.18
8.07	26.55	6.53	2.95	-1.71
9.69	27.83	3.21	1.49	-0.76
11.47	28.75	1.96	0.98	-0.53
13.39	29.40	1.24	0.37	-0.21
15.74	30.01	0.51	0.32	-0.11

Station I(7)
u_a = 30.45 (fps)

y (in.)	u $\left(\frac{ft}{sec}\right)$	$\overline{u'^2}$ $\left(\frac{ft^2}{sec^2}\right)$	$\overline{v'^2}$ $\left(\frac{ft^2}{sec^2}\right)$	$\overline{u'v'}$ $\left(\frac{ft^2}{sec^2}\right)$
1.08	8.62	6.78	9.40	-0.07
1.20	9.75	7.48	7.08	-2.15
1.46	11.22	10.46	8.67	-3.59
1.88	12.95	15.02	10.62	-5.36
2.48	14.70	19.81	11.19	-6.96
3.23	16.63	21.88	8.61	-6.16
4.26	18.70	22.34	7.92	-6.03
5.35	20.95	20.46	7.88	-5.67
6.48	23.02	15.12	8.05	-4.03
7.82	25.05	11.21	4.12	-2.40
9.11	26.62	7.32	2.38	-1.53
10.46	27.95	4.17	1.92	-0.92
12.27	29.10	2.20	0.89	-0.41
14.18	29.80	0.99	0.67	-0.47

Station I(9)
u_a = 30.60 (fps)

y (in.)	u $\left(\frac{ft}{sec}\right)$	$\overline{u'^2}$ $\left(\frac{ft^2}{sec^2}\right)$	$\overline{v'^2}$ $\left(\frac{ft^2}{sec^2}\right)$	$\overline{u'v'}$ $\left(\frac{ft^2}{sec^2}\right)$
1.08	9.22	6.66	9.35	-0.28
1.20	10.13	7.55	6.87	-2.06
1.34	10.85	9.32	7.24	-2.53
1.56	11.50	11.33	8.30	-3.36
1.94	12.70	14.79	10.09	-5.31
2.39	13.83	18.44	9.67	-6.16
2.97	15.25	20.34	9.70	-6.51
3.74	16.92	21.41	8.07	-5.47
4.41	18.28	19.84	8.51	-5.75
5.38	20.12	18.60	8.08	-4.82
6.44	22.03	17.62	7.42	-4.92
7.77	24.05	13.69	5.72	-3.38
9.22	25.93	10.50	3.95	-2.69
10.71	27.42	6.12	2.40	-1.50
12.94	29.01	2.36	1.22	-0.59
14.37	29.51	1.16	0.59	-0.25

Station I(11)
u_a = 30 88 (fps)

y (in.)	u $\left(\frac{ft}{sec}\right)$	$\overline{u'^2}$ $\left(\frac{ft^2}{sec^2}\right)$	$\overline{v'^2}$ $\left(\frac{ft^2}{sec^2}\right)$	$\overline{u'v'}$ $\left(\frac{ft^2}{sec^2}\right)$
1.09	8.43	5.52	10.09	-0.39
1.23	9.62	7.46	6.48	-2.34
1.47	10.55	9.00	8.30	-3.21
1.75	11.52	11.54	9.19	-4.05
2.19	12.71	15.94	9.60	-5.48
2.61	13.73	17.88	9.68	-5.76
3.29	15.23	19.51	8.75	-5.95
4.04	16.75	18.55	7.82	-5.75
5.13	18.63	17.53	7.41	-5.31
6.20	20.41	15.62	7.96	-4.72
7.67	22.75	14.18	6.68	-3.66
9.48	25.42	11.07	4.12	-2.65
11.38	27.68	6.76	2.04	-1.44
13.43	30.10	3.14	1.06	-0.56

Station II(0)
u_a = 30.38 (fps)

y (in.)	u $\left(\frac{ft}{sec}\right)$	$\overline{u'^2}$ $\left(\frac{ft^2}{sec^2}\right)$	$\overline{v'^2}$ $\left(\frac{ft^2}{sec^2}\right)$	$\overline{u'v'}$ $\left(\frac{ft^2}{sec^2}\right)$
1.09	19.35	4.11	16.19	-6.23
1.24	17.23	4.14	14.95	-6.60
1.49	20.25	5.28	13.51	-7.15
1.62	21.25	5.43	12.28	-6.61
1.87	22.34	5.36	10.96	-6.13
2.32	23.25	4.88	7.54	-3.31
2.84	24.56	4.36	6.32	-1.53
3.69	25.46	4.25	4.94	-0.93
4.34	26.10	4.23	3.34	-1.14
5.10	26.65	3.62	2.25	-1.01
6.19	27.52	3.24	1.62	-0.88
7.73	28.48	2.73	1.34	-0.77
9.64	29.00	1.55	0.93	-0.58

Station II(1)
u_a = 30.30 (fps)

y (in.)	u $\left(\frac{ft}{sec}\right)$	$\overline{u'^2}$ $\left(\frac{ft^2}{sec^2}\right)$	$\overline{v'^2}$ $\left(\frac{ft^2}{sec^2}\right)$	$\overline{u'v'}$ $\left(\frac{ft^2}{sec^2}\right)$
1.06	16.26	36.46	11.34	- 2.10
1.31	18.24	42.79	14.90	- 8.20
1.54	19.73	47.19	15.55	-11.57
2.04	22.47	45.04	11.13	-11.80
2.76	24.19	20.59	6.85	- 4.62
3.50	25.45	6.96	4.95	- 2.70
4.25	26.31	4.07	3.21	- 1.24
5.24	27.09	3.66	2.71	- 1.01
6.48	27.79	3.32	1.91	- 0.95
7.95	29.04	2.69	1.23	- 0.73
9.69	29.55	1.72	0.84	- 0.41

Station II(2)
u_a = 30.37 (fps)

y (in.)	u $\left(\frac{ft}{sec}\right)$	$\overline{u'^2}$ $\left(\frac{ft^2}{sec^2}\right)$	$\overline{v'^2}$ $\left(\frac{ft^2}{sec^2}\right)$	$\overline{u'v'}$ $\left(\frac{ft^2}{sec^2}\right)$
1.11	9.75	17.39	10.57	- 2.53
1.32	11.45	21.71	14.25	- 4.44
1.62	13.01	27.74	15.51	- 5.80
2.04	15.53	33.42	21.92	- 9.49
2.87	19.86	32.57	21.22	-10.29
4.05	23.94	13.93	9.17	- 4.98
5.42	25.86	5.05	4.82	- 1.79
6.80	26.88	3.01	3.05	- 0.88
8.73	28.07	2.09	1.51	- 0.74
10.70	29.17	1.18	0.84	- 0.35

Station II(3)
u_a = 30.55 (fps)

y (in.)	u $\left(\frac{ft}{sec}\right)$	$\overline{u'^2}$ $\left(\frac{ft^2}{sec^2}\right)$	$\overline{v'^2}$ $\left(\frac{ft^2}{sec^2}\right)$	$\overline{u'v'}$ $\left(\frac{ft^2}{sec^2}\right)$
1.13	9.02	14.66	11.34	- 0.86
1.37	9.92	17.83	13.99	- 3.30
1.64	12.36	24.00	15.04	- 7.25
2.00	14.09	27.37	20.60	- 8.44
2.39	15.95	29.20	21.05	- 9.52
3.18	18.86	25.99	21.65	- 9.13
4.07	21.61	18.63	16.60	- 6.07
5.26	24.66	10.52	10.28	- 3.41
6.82	26.37	3.71	5.03	- 1.08
8.31	27.29	2.52	3.74	- 0.74
10.22	28.38	1.31	1.39	- 0.46

TABLE VII TURBULENCE DISTRIBUTIONS FOR RUNS I, II, Ia, AND IIa - Continued

Station II(4)
u_a = 30.56 (fps)

y (in.)	u $\left(\frac{ft}{sec}\right)$	$\overline{u'^2}$ $\left(\frac{ft^2}{sec^2}\right)$	$\overline{v'^2}$ $\left(\frac{ft^2}{sec^2}\right)$	$\overline{u'v'}$ $\left(\frac{ft^2}{sec^2}\right)$
1.12	8.01	11.20	10.32	-1.76
1.35	10.61	15.28	11.89	-2.49
1.71	11.78	22.02	14.36	-5.44
2.13	14.47	27.94	16.82	-6.44
2.99	17.29	27.33	18.57	-7.84
4.09	20.85	22.48	17.75	-7.36
5.45	24.09	13.39	12.69	-4.69
7.14	26.59	8.42	6.46	-1.86
9.07	27.86	3.69	2.99	-0.77
11.38	29.16	1.64	0.55	-0.34

Station II(6)
u_a = 30.44 (fps)

y (in.)	u $\left(\frac{ft}{sec}\right)$	$\overline{u'^2}$ $\left(\frac{ft^2}{sec^2}\right)$	$\overline{v'^2}$ $\left(\frac{ft^2}{sec^2}\right)$	$\overline{u'v'}$ $\left(\frac{ft^2}{sec^2}\right)$
1.18	8.94	14.07	11.23	-0.73
1.29	9.58	16.22	11.60	-1.47
1.43	10.49	19.30	12.98	-2.83
1.66	11.26	22.68	13.60	-4.26
2.04	12.61	25.66	15.52	-5.80
2.51	14.04	27.00	17.87	-6.80
3.19	15.62	26.71	18.79	-7.29
4.09	18.21	23.80	18.08	-7.62
5.32	21.01	19.94	14.84	-6.57
6.75	23.99	14.86	10.62	-3.73
8.57	26.91	7.07	6.21	-2.07
10.54	28.53	2.67	2.37	-0.81
12.85	29.79	1.63	1.00	-0.27
15.28	30.31	0.77	0.48	-0.25

Station II (8)
u_a = 30.61 (fps)

y (in.)	u $\left(\frac{ft}{sec}\right)$	$\overline{u'^2}$ $\left(\frac{ft^2}{sec^2}\right)$	$\overline{v'^2}$ $\left(\frac{ft^2}{sec^2}\right)$	$\overline{u'v'}$ $\left(\frac{ft^2}{sec^2}\right)$
1.18	7.00	9.63	9.05	-0.31
1.26	8.42	12.89	10.64	-1.00
1.37	9.00	14.29	11.89	-1.50
1.47	9.52	16.43	11.58	-1.97
1.60	10.07	18.85	12.41	-2.96
1.96	11.50	23.28	13.91	-4.37
2.44	12.97	25.47	15.79	-5.90
3.16	14.72	27.29	18.20	-6.96
4.12	16.99	23.92	17.33	-7.18
5.23	19.59	20.57	16.59	-7.08
6.79	22.54	16.34	12.70	-4.95
8.78	26.45	10.20	7.19	-2.67
10.87	28.32	3.97	4.08	-0.93
13.20	29.49	1.68	1.38	-0.42
15.70	30.40	0.73	0.63	-0.21

Station II(10)
u_a = 30.95 (fps)

y (in.)	u $\left(\frac{ft}{sec}\right)$	$\overline{u'^2}$ $\left(\frac{ft^2}{sec^2}\right)$	$\overline{v'^2}$ $\left(\frac{ft^2}{sec^2}\right)$	$\overline{u'v'}$ $\left(\frac{ft}{sec^2}\right)$
1.13	7.90	10.82	10.53	-0.36
1.18	8.23	12.08	10.20	-0.46
1.25	8.58	13.19	10.24	-0.94
1.31	8.75	14.00	10.70	-1.31
1.39	9.31	15.33	11.52	-1.70
1.52	9.36	16.09	12.53	-2.33
1.60	10.08	18.12	13.05	-2.74
1.74	10.74	20.00	14.51	-3.55
2.09	11.82	21.78	15.90	-5.03
2.45	12.94	25.65	16.84	-5.47
3.06	14.27	27.42	17.70	-6.06
3.86	15.99	25.64	17.29	-6.62
4.75	17.70	22.17	16.45	-6.96
6.25	20.85	18.54	15.82	-5.74
7.71	23.42	15.75	12.93	-4.31
9.78	26.50	10.05	7.31	-3.09
11.87	28.46	4.10	4.43	-1.42
13.92	29.67	1.78	1.88	-0.62
15.98	30.30	0.67	0.83	-0.31

Station II(10.5)
u_a = 30.97 (fps)

y (in.)	u $\left(\frac{ft}{sec}\right)$	$\overline{u'^2}$ $\left(\frac{ft^2}{sec^2}\right)$	$\overline{v'^2}$ $\left(\frac{ft^2}{sec^2}\right)$	$\overline{u'v'}$ $\left(\frac{ft^2}{sec^2}\right)$
1.14	8.77	12.96	10.81	-0.20
1.21	8.89	14.07	10.50	-0.67
1.46	10.17	17.58	12.82	-2.08
1.82	11.42	21.59	14.43	-4.30
2.19	12.78	24.34	15.29	-5.04
3.05	15.08	27.15	18.11	-6.06
3.97	16.91	25.37	17.57	-6.57
4.87	18.19	21.95	17.28	-7.35
5.97	20.36	19.55	16.93	-6.78
7.46	22.86	15.65	14.41	-4.88
9.07	25.65	11.69	10.14	-3.57
10.77	27.68	6.46	7.70	-2.49
12.70	29.48	3.08	3.66	-1.22
14.69	30.39	1.38	1.13	-0.26
16.69	30.97	0.59	0.50	-0.15

Station II(11)
u_a = 31.11 (fps)

(in.)	u $\left(\frac{ft}{sec}\right)$	$\overline{u'^2}$ $\left(\frac{ft^2}{sec^2}\right)$	$\overline{v'^2}$ $\left(\frac{ft^2}{sec^2}\right)$	$\overline{u'v'}$ $\left(\frac{ft^2}{sec^2}\right)$
1.13	8.57	12.49	11.06	-0.39
1.19	8.70	12.47	10.03	-0.65
1.32	9.56	15.95	12.73	-1.54
1.61	10.86	20.01	14.27	-3.24
1.90	11.46	21.68	14.64	-4.15
2.32	13.11	24.95	16.80	-5.32
2.81	13.43	26.81	17.95	-5.58
3.52	16.01	25.61	18.99	-6.55
4.27	17.15	23.80	17.65	-6.95
5.22	18.76	21.02	16.99	-6.23
6.33	20.57	17.57	16.39	-5.79
7.81	23.37	15.32	13.01	-4.43
9.62	26.44	10.36	8.94	-2.92
11.40	28.31	4.78	6.60	-2.11
13.40	29.92	2.28	2.28	-0.62
15.14	30.59	1.32	0.94	-0.36

Station Ia(11,1)
u_a = 30.92 (fps)

y (in.)	u $\left(\frac{ft}{sec}\right)$	u'^2 $\left(\frac{ft^2}{sec^2}\right)$	v'^2 $\left(\frac{ft^2}{sec^2}\right)$	$\overline{u'v'}$ $\left(\frac{ft^2}{sec^2}\right)$
1.16	7.68	20.18	2.23	-2.88
1.52	12.20	25.70	5.02	-3.13
1.95	14.35	16.12	9.80	-2.61
2.49	15.42	16.49	11.73	-5.42
3.12	16.45	18.68	9.37	-6.04
4.04	17.82	18.22	8.22	-5.33
4.68	18.78	16.85	8.84	-5.07
5.69	20.35	15.56	7.99	-4.89
6.98	22.40	15.18	5.86	-3.77
8.42	24.73	12.32	5.19	-3.04
9.79	26.44	8.34	3.71	-1.85
11.63	28.02	5.46	2.07	-0.87
13.26	29.06	2.53	1.22	-0.42

Station Ia(11,2)
u_a = 30.89 (fps)

y (in.)	u $\left(\frac{ft}{sec}\right)$	u'^2 $\left(\frac{ft^2}{sec^2}\right)$	v'^2 $\left(\frac{ft^2}{sec^2}\right)$	$\overline{u'v'}$ $\left(\frac{ft^2}{sec^2}\right)$
1.15	8.75	18.05	0.90	-1.94
1.41	11.62	28.81	4.56	-3.03
1.82	14.50	23.41	8.17	-2.47
2.25	15.45	17.79	9.08	-2.88
2.85	16.32	17.98	10.70	-5.02
3.96	17.91	18.72	7.19	-5.50
5.20	19.72	16.01	7.88	-4.84
6.92	22.20	14.24	6.48	-4.18
8.93	25.18	10.16	4.82	-2.71
10.63	27.21	7.65	3.80	-1.49
12.84	28.82	3.35	1.38	-0.52

Station Ia(11,3)
u_a = 30.75 (fps)

y (in.)	u $\left(\frac{ft}{sec}\right)$	u'^2 $\left(\frac{ft^2}{sec^2}\right)$	v'^2 $\left(\frac{ft^2}{sec^2}\right)$	$\overline{u'v'}$ $\left(\frac{ft^2}{sec^2}\right)$
0.99	6.03	16.03	2.28	-1.92
1.34	11.41	20.12	7.31	-2.54
1.70	13.40	24.83	8.95	-2.87
2.27	15.12	20.62	10.04	-2.18
2.93	16.40	19.79	9.66	-2.44
4.10	18.09	19.22	8.88	-4.51
5.42	20.02	16.52	8.39	-4.73
7.11	22.55	14.78	5.84	-3.51
8.82	25.04	10.93	4.73	-2.90
11.41	27.82	7.62	2.25	-1.46
14.02	29.31	2.21	1.52	-0.50

Station Ia(11,4)
u_a = 30.80 (fps)

y (in.)	u $\left(\frac{ft}{sec}\right)$	u'^2 $\left(\frac{ft^2}{sec^2}\right)$	v'^2 $\left(\frac{ft^2}{sec^2}\right)$	$\overline{u'v'}$ $\left(\frac{ft^2}{sec^2}\right)$
0.86	7.28	15.42	1.37	-2.18
0.96	8.76	17.61	2.20	-2.06
1.92	13.52	22.48	9.42	-3.03
2.75	15.74	20.42	10.24	-2.76
3.94	17.82	19.05	8.29	-3.60
5.28	19.88	16.72	8.19	-4.01
6.71	22.12	15.56	6.70	-3.74
8.35	24.43	12.63	5.35	-2.92
10.15	26.60	9.03	3.10	-1.95
12.50	28.72	4.74	1.67	-0.58

Station Ia(11,6)
u_a = 30.89 (fps)

y (in.)	u $\left(\frac{ft}{sec}\right)$	u'^2 $\left(\frac{ft^2}{sec^2}\right)$	v'^2 $\left(\frac{ft^2}{sec^2}\right)$	$\overline{u'v'}$ $\left(\frac{ft^2}{sec^2}\right)$
0.95	8.51	12.93	4.73	-3.03
1.06	9.62	14.03	5.19	-3.33
1.25	10.00	15.88	7.98	-3.76
1.95	12.76	21.06	9.59	-3.65
2.67	14.78	21.62	9.62	-3.33
3.86	17.02	18.35	8.95	-4.08
5.38	20.01	17.11	8.17	-4.89
6.92	22.66	14.72	6.51	-4.15
8.52	25.02	12.22	4.71	-3.18
10.38	27.12	9.13	3.45	-1.90
12.62	28.99	4.35	1.07	-0.74

Station Ia(11,8)
u_a = 30.90 (fps)

y (in.)	u $\left(\frac{ft}{sec}\right)$	$\overline{u'^2}$ $\left(\frac{ft^2}{sec^2}\right)$	$\overline{v'^2}$ $\left(\frac{ft^2}{sec^2}\right)$	$\overline{u'v'}$ $\left(\frac{ft^2}{sec^2}\right)$
0.28	5.78	5.32	3.70	-0.34
0.38	6.03	5.72	4.77	-1.08
0.54	6.98	6.78	6.17	-1.72
0.77	7.83	7.81	6.44	-2.33
1.12	9.21	12.42	9.20	-3.93
1.63	10.12	16.53	9.46	-3.59
2.24	13.24	17.89	9.93	-4.60
2.88	14.98	20.88	9.83	-4.63
3.78	16.75	19.80	8.94	-5.42
4.95	19.08	17.71	8.21	-5.12
6.47	20.17	15.88	6.75	-4.09
8.41	24.02	12.42	5.00	-3.28
10.29	26.89	8.40	3.07	-1.92
12.56	28.73	4.58	1.26	-0.99

Station Ia(11,10)
u_a = 30.93 (fps)

y (in.)	u $\left(\frac{ft}{sec}\right)$	u'^2 $\left(\frac{ft^2}{sec^2}\right)$	v'^2 $\left(\frac{ft^2}{sec^2}\right)$	$\overline{u'v'}$ $\left(\frac{ft^2}{sec^2}\right)$
0.17	4.86	4.59	1.89	-0.51
0.38	6.73	5.98	2.74	-0.56
0.74	8.36	10.18	6.64	-1.07
1.21	9.58	11.56	8.02	-2.58
1.74	11.13	15.62	9.16	-4.61
2.43	13.22	18.43	10.18	-5.62
3.12	15.23	19.76	9.29	-5.90
4.16	17.49	19.13	8.42	-5.46
5.36	19.83	17.22	7.47	-4.91
6.83	22.18	15.08	6.17	-4.03
8.48	24.32	12.44	4.95	-2.77
10.19	26.35	8.64	3.11	-1.94
12.30	28.38	4.92	1.38	-1.10
14.73	29.92	1.79	0.61	-0.28

Station Ia(12,1)
u_a = 30.70 (fps)

y (in.)	u $\left(\frac{ft}{sec}\right)$	$\overline{u'^2}$ $\left(\frac{ft^2}{sec^2}\right)$	$\overline{v'^2}$ $\left(\frac{ft^2}{sec^2}\right)$	$u'v'$ $\left(\frac{ft^2}{sec^2}\right)$
1.28	10.88	26.16	3.68	-3.48
1.45	12.98	25.57	5.37	-2.86
1.69	14.62	19.48	9.02	-2.42
1.95	15.38	15.83	10.25	-3.47
2.14	15.62	16.10	10.38	-4.04
2.96	16.42	18.18	9.40	-5.85
3.69	17.35	19.38	9.45	-5.67
4.57	18.52	18.02	8.37	-5.56
5.92	20.50	16.11	8.18	-4.50
7.35	22.62	14.37	5.87	-4.01
9.23	25.66	9.89	4.15	-2.56
10.38	27.03	8.60	3.24	-1.83
13.62	29.08	2.73	1.21	-0.45

TABLE VII TURBULENCE DISTRIBUTIONS FOR RUNS I, II, Ia, AND IIa - Continued

Station Ia(12,2)
u_a = 30.70 (fps)

y (in.)	u $\left(\frac{ft}{sec}\right)$	$\overline{u'^2}$ $\left(\frac{ft^2}{sec^2}\right)$	$\overline{v'^2}$ $\left(\frac{ft^2}{sec^2}\right)$	$\overline{u'v'}$ $\left(\frac{ft^2}{sec^2}\right)$
1.12	7.62	21.06	1.83	-2.53
1.15	8.01	26.95	6.51	-2.53
1.76	14.28	22.93	6.88	-2.69
2.61	16.48	17.64	9.99	-4.04
2.86	16.71	18.54	10.14	-5.05
3.87	17.88	18.90	9.63	-5.26
5.38	19.76	17.63	7.86	-4.52
7.64	22.85	13.60	6.18	-3.55
10.20	26.48	8.62	3.53	-2.02
12.74	28.62	4.41	1.21	-0.77

Station Ia(12,3)
u_a = 30.68 (fps)

y (in.)	u $\left(\frac{ft}{sec}\right)$	$\overline{u'^2}$ $\left(\frac{ft^2}{sec^2}\right)$	$\overline{v'^2}$ $\left(\frac{ft^2}{sec^2}\right)$	$\overline{u'v'}$ $\left(\frac{ft^2}{sec^2}\right)$
1.02	7.25	17.15	1.37	-2.14
1.21	10.03	21.42	2.48	-2.70
1.62	13.13	24.29	4.85	-2.76
2.15	15.52	22.84	8.20	-2.46
2.86	16.65	20.66	9.20	-3.95
4.19	18.42	18.17	8.15	-4.52
5.61	20.35	16.47	7.60	-4.70
7.62	23.08	14.60	5.76	-3.91
10.10	26.31	8.95	2.89	-2.02
12.72	28.73	4.45	0.95	-0.76

Station Ia(12,4)
u_a = 30.80 (fps)

y (in.)	u $\left(\frac{ft}{sec}\right)$	$\overline{u'^2}$ $\left(\frac{ft^2}{sec^2}\right)$	$\overline{v'^2}$ $\left(\frac{ft^2}{sec^2}\right)$	$\overline{u'v'}$ $\left(\frac{ft^2}{sec^2}\right)$
1.05	9.26	20.64	1.83	-2.23
1.78	13.50	23.27	6.02	-3.53
2.11	14.73	22.59	9.26	-1.32
2.85	16.12	20.02	9.39	-2.13
4.15	18.25	18.76	8.52	-3.96
5.55	20.32	17.01	7.49	-4.14
6.90	22.15	15.46	6.44	-4.19
8.52	24.33	12.19	4.73	-2.72
10.29	26.55	9.06	3.14	-2.06
12.45	28.62	4.68	1.37	-1.05

Station Ia(12,5)
u_a = 30.68 (fps)

y (in.)	u $\left(\frac{ft}{sec}\right)$	$\overline{u'^2}$ $\left(\frac{ft^2}{sec^2}\right)$	$\overline{v'^2}$ $\left(\frac{ft^2}{sec^2}\right)$	$\overline{u'v'}$ $\left(\frac{ft^2}{sec^2}\right)$
1.06	8.51	14.81	2.95	-2.87
1.42	10.48	17.13	8.27	-3.86
2.24	14.95	20.79	10.52	-3.09
2.84	16.08	20.87	9.44	-2.83
3.72	17.62	19.99	8.76	-4.04
4.85	19.32	18.02	7.67	-5.01
6.31	21.42	15.99	7.61	-4.23
8.08	23.75	13.13	4.83	-3.18
10.06	26.30	9.68	3.31	-1.84
12.48	28.65	5.49	1.73	-0.66

Station Ia(12,8)
u_a = 30.91 (fps)

y (in.)	u $\left(\frac{ft}{sec}\right)$	$\overline{u'^2}$ $\left(\frac{ft^2}{sec^2}\right)$	$\overline{v'^2}$ $\left(\frac{ft^2}{sec^2}\right)$	$\overline{u'v'}$ $\left(\frac{ft^2}{sec^2}\right)$
0.33	5.63	5.45	3.18	-0.82
0.57	6.58	8.03	6.15	-1.43
0.98	8.43	12.12	6.99	-2.88
1.58	10.89	16.99	8.63	-4.02
2.21	13.30	18.13	9.43	-4.10
3.26	15.82	20.40	9.98	-5.29
4.69	18.62	18.45	8.05	-4.96
6.32	21.11	15.53	7.34	-4.21
8.41	24.23	12.50	4.47	-2.91
10.56	26.89	8.21	2.12	-1.82

Station Ia(12,10)
u_a = 30.95 (fps)

y (in.)	u $\left(\frac{ft}{sec}\right)$	$\overline{u'^2}$ $\left(\frac{ft^2}{sec^2}\right)$	$\overline{v'^2}$ $\left(\frac{ft^2}{sec^2}\right)$	$\overline{u'v'}$ $\left(\frac{ft^2}{sec^2}\right)$
0.46	6.98	6.45	5.24	-1.05
0.72	7.89	8.93	6.74	-1.30
1.02	8.64	10.49	7.96	-2.61
1.45	10.24	14.57	8.83	-3.25
2.09	12.51	17.52	10.20	-5.72
2.83	14.88	19.36	9.73	-6.02
4.13	17.02	19.82	8.82	-5.70
6.11	20.85	16.44	7.11	-4.34
8.17	23.72	13.91	5.24	-3.10
10.30	26.71	9.81	2.78	-1.83

Station IIa(10,1)
u_a = 31.17 (fps)

y (in.)	u $\left(\frac{ft}{sec}\right)$	$\overline{u'^2}$ $\left(\frac{ft^2}{sec^2}\right)$	$\overline{v'^2}$ $\left(\frac{ft^2}{sec^2}\right)$	$\overline{u'v'}$ $\left(\frac{ft^2}{sec^2}\right)$
1.37	9.35	24.78	18.27	-5.20
1.68	11.85	29.52	14.98	-4.49
1.99	12.41	25.11	15.09	-4.50
2.32	13.24	24.17	15.88	-5.63
2.89	14.84	26.83	14.32	-6.15
3.45	16.16	26.83	15.75	-6.65
4.25	17.43	24.41	17.70	-7.36
5.11	18.96	21.18	17.40	-6.87
6.31	21.52	19.45	15.72	-6.01
7.80	23.69	14.82	13.56	-4.35
9.55	26.57	9.84	9.15	-3.26
11.36	28.69	5.24	4.61	-2.06
13.17	29.87	2.28	2.84	-0.98
14.93	30.64	1.17	1.75	-0.23

Station IIa(10,2)
u_a = 31.16 (fps)

y (in.)	u $\left(\frac{ft}{sec}\right)$	$\overline{u'^2}$ $\left(\frac{ft^2}{sec^2}\right)$	$\overline{v'^2}$ $\left(\frac{ft^2}{sec^2}\right)$	$\overline{u'v'}$ $\left(\frac{ft^2}{sec^2}\right)$
.91	4.1	7.44	8.66	-0.94
1.13	6.8	16.14	11.19	-1.58
1.42	8.8	25.49	16.89	-5.15
1.87	11.2	33.32	21.08	-6.41
2.51	13.2	25.82	15.66	-5.56
3.35	14.9	27.81	17.72	-6.66
4.31	16.73	23.16	17.55	-7.37
5.49	19.11	21.56	16.97	-6.73
6.53	21.09	19.37	14.35	-5.17
7.35	23.54	16.17	11.35	-4.24
9.25	25.50	11.91	9.49	-3.05
10.78	27.58	6.69	5.98	-2.33
12.53	29.18	3.63	3.38	-1.07
14.55	30.20	1.51	1.43	-0.29

Station IIa(10,3)
u_a = 31.16 (fps)

y (in.)	u $\left(\frac{ft}{sec}\right)$	$\overline{u'^2}$ $\left(\frac{ft^2}{sec^2}\right)$	$\overline{v'^2}$ $\left(\frac{ft^2}{sec^2}\right)$	$\overline{u'v'}$ $\left(\frac{ft^2}{sec^2}\right)$
1.13	7.2	22.06	10.30	-1.22
1.41	8.7	25.69	14.38	-2.85
1.87	1.6	29.74	18.61	-4.43
2.51	12.65	30.27	20.55	-5.76
3.35	14.8	26.48	17.77	-6.58
4.34	16.9	23.88	17.75	-6.21
5.48	19.20	20.94	16.16	-6.70
6.66	21.43	16.72	15.16	-5.52
7.79	23.63	15.54	12.30	-4.58
9.27	25.72	10.66	9.95	-3.56
10.81	27.45	5.49	6.19	-2.44
12.52	29.13	3.08	3.49	-0.87
14.64	30.10	1.40	1.55	-0.32

Station IIa(10,4)
u_a = 31.22 (fps)

y (in.)	u $\left(\frac{ft}{sec}\right)$	$\overline{u'^2}$ $\left(\frac{ft^2}{sec^2}\right)$	$\overline{v'^2}$ $\left(\frac{ft^2}{sec^2}\right)$	$\overline{u'v'}$ $\left(\frac{ft^2}{sec^2}\right)$
.79	5.5	16.36	7.40	-0.59
1.13	7.1	21.18	10.02	-1.59
1.49	1.0	22.42	12.85	-3.11
1.89	12.45	25.90	15.82	-4.57
2.65	14.9	28.71	19.12	-6.13
3.42	15.39	27.92	18.49	-5.65
4.53	17.79	22.74	16.71	-6.78
5.76	20.08	19.20	16.01	-6.32
7.50	23.27	15.86	13.97	-5.29
9.31	26.06	10.89	8.78	-3.06
11.20	28.20	6.17	5.99	-1.34
13.26	29.91	2.53	2.87	-0.37
15.54	30.71	1.27	0.36	-0.12

Station IIa(10,7)
u_a = 31.22 (fps)

y (in.)	u $\left(\frac{ft}{sec}\right)$	$\overline{u'^2}$ $\left(\frac{ft^2}{sec^2}\right)$	$\overline{v'^2}$ $\left(\frac{ft^2}{sec^2}\right)$	$\overline{u'v'}$ $\left(\frac{ft^2}{sec^2}\right)$
1.02	4.7	14.36	12.85	-2.26
1.19	8.04	20.67	16.65	-3.71
1.66	11.0	29.76	15.59	-5.00
2.24	13.1	23.52	15.95	-5.53
2.89	14.7	26.64	17.36	-5.99
3.74	16.15	25.93	17.45	-6.55
4.71	18.58	22.17	17.18	-7.08
6.15	20.87	17.86	15.95	-5.91
7.80	23.95	14.11	12.47	-4.92
9.56	26.64	9.31	9.08	-3.04
11.54	28.70	5.18	5.21	-1.63
13.83	30.27	1.88	1.80	-0.39

Station IIa(10,8)
u_a = 31.24 (fps)

y (in.)	u $\left(\frac{ft}{sec}\right)$	$\overline{u'^2}$ $\left(\frac{ft^2}{sec^2}\right)$	$\overline{v'^2}$ $\left(\frac{ft^2}{sec^2}\right)$	$\overline{u'v'}$ $\left(\frac{ft^2}{sec^2}\right)$
.91	3.8	10.47	6.85	-1.31
1.33	8.6	24.56	14.53	-2.03
1.92	11.4	32.50	21.71	-6.54
2.56	13.4	26.07	16.73	-6.06
3.46	15.1	26.51	18.02	-6.28
4.56	16.93	23.69	17.58	-6.95
6.10	19.96	19.38	16.10	-6.31
7.90	23.28	13.96	12.45	-4.57
9.73	26.03	8.88	8.58	-2.99
11.75	28.15	5.25	4.66	-2.03
14.02	30.06	1.03	1.61	-0.57

Station IIa(10,9)
u_a = 31.36 (fps)

y (in.)	u $\left(\frac{ft}{sec}\right)$	$\overline{u'^2}$ $\left(\frac{ft^2}{sec^2}\right)$	$\overline{v'^2}$ $\left(\frac{ft^2}{sec^2}\right)$	$\overline{u'v'}$ $\left(\frac{ft^2}{sec^2}\right)$
1.25	7.8	19.60	12.45	-1.80
1.59	9.5	25.39	13.98	-3.33
2.10	11.5	29.86	20.65	-5.78
2.78	13.4	29.29	19.19	-6.48
3.69	15.0	25.75	18.54	-6.47
4.86	17.1	21.79	16.72	-6.62
6.36	20.71	18.10	16.02	-5.78
8.13	23.65	14.24	12.52	-4.09
9.92	25.34	9.82	8.35	-3.26
12.06	28.73	4.41	4.07	-1.46
14.34	30.12	1.07	1.67	-0.34

Station IIa(10,10)
u_a = 31.21 (fps)

y (in.)	u $\left(\frac{ft}{sec}\right)$	$\overline{u'^2}$ $\left(\frac{ft^2}{sec^2}\right)$	$\overline{v'^2}$ $\left(\frac{ft^2}{sec^2}\right)$	$\overline{u'v'}$ $\left(\frac{ft^2}{sec^2}\right)$
1.16	7.33	19.09	10.42	-1.22
1.48	10.12	21.50	12.98	-2.87
1.93	12.50	24.00	15.21	-4.56
2.63	14.73	27.25	18.14	-6.19
3.38	17.74	28.17	19.19	-5.93
4.55	18.49	22.92	17.94	-7.02
6.15	20.76	18.08	15.83	-6.09
7.84	23.54	15.66	12.31	-4.27
9.40	25.70	11.16	8.14	-3.22
10.84	27.74	6.19	6.85	-2.43
12.34	28.99	4.58	3.64	-1.27
14.02	30.10	1.20	1.75	-0.40
15.28	30.77	0.47	0.88	-0.19

TABLE A.1 ERRORS IN TOTAL HEAD AND STATIC HEAD MEASUREMENTS FOR STATION V(12)

H_t (mm Hg)	ΔH_t (mm Hg)	H_s (mm Hg)	ΔH_s (mm Hg)	H (mm Hg)	ΔH (mm Hg)	$\frac{\Delta H}{H}$ (mm Hg)
.006	.0006	-.09	.002	.084	.00209	.0249
.019	11	-.079	.002	.098	.00209	.0213
.044	.002	-.0708	.002	.1144	.00283	.0247
.077	.002	-.0651	.002	.1421	.00283	.0199
.111	.006	-.0602	.002	.1712	.00632	.0369
.141	.006	-.0571	.002	.1981	.00632	.0319
.172	.006	-.0589	.002	.2259	.00632	.0280
.21	.006	-.0518	.002	.2618	.00632	.0241
.251	.006	-.0483	.002	.2993	.00632	.0211
.296	.006	-.0465	.002	.3425	.00632	.0185
.340	.02	-.0390	.002	.3790	.0201	.0530
.389	.02	-.0375	.002	.4265	.0201	.0471
.417	.02	-.0342	.002	.4512	.0201	.0445
.469	.02	-.0298	.0006	.4988	.0200	.0403
.525	.02	-.0268	.0006	.5518	.0200	.0362
.570	.02	-.0240	.0006	.5940	.0200	.0337
.604	.02	-.0225	.0006	.6265	.0200	.0319
.638	.02	-.0200	.0006	.6580	.0200	.0304
.665	.02	-.0190	.0006	.6840	.0200	.0293
.665	.02	-.0190	.0006	.6840	.0200	.0293

TABLE A.2 ERRORS IN TURBULENCE FOR STATIONS I(-4), I(0), I(2), AND I(5)

Station I(-4) Run I x = - 4 ft.

y (inches)	u (fps)	$\sqrt{\overline{e_o'^2}}$ (volts)	$\sqrt{\overline{e_1'^2}}$ (volts)	$\sqrt{\overline{e_2'^2}}$ (volts)	$\overline{u'^2}$ $(\frac{ft^2}{sec^2})$	$\overline{v'^2}$ $(\frac{ft^2}{sec^2})$	$\overline{u'v'}$ $(\frac{ft^2}{sec^2})$	$\frac{\Delta\overline{v'^2}}{\overline{v'^2}}$	$\frac{\Delta\overline{u'v'}}{\overline{u'v'}}$
0.12	14.86	.149	.0337	.0255	7.15	0.34	-1.09	2.53	.159
0.23	17.03	.145	.0328	.0262	8.09	0.69	-1.03	1.41	.188
0.50	19.01	.126	.0297	.0235	6.99	1.33	-1.02	.636	.174
0.83	20.36	.115	.0279	.0218	6.39	1.58	-1.02	.492	.163
1.18	21.06	.107	.0265	.0202	5.75	1.63	-1.01	.431	.152
1.89	22.13	.101	.0258	.0195	5.50	1.96	-1.05	.345	.145
2.82	23.78	.087	.0203	.0197	4.54	1.83	-0.97	.303	.124
4.28	25.29	.080	.0212	.0148	4.05	1.02	-1.02	.308	.111
5.77	26.56	.070	.0184	.0131	3.33	1.26	-0.78	.324	.116
7.67	27.73	.061	.0166	.0113	2.67	1.20	-0.73	.275	.103
9.68	28.82	.046	.0131	.0088	1.57	0.94	-0.49	.211	.100
11.04	29.40	.035	.0096	.0070	0.94	0.52	-0.23	.225	.119
13.01	29.89	.021	.0056	.0045	0.36	0.18	-0.06	.246	.166
15.27	30.08	.013	.0032	.0029	0.14	0.06	-0.01	.283	.357

Station I(0) Run I x = 0 ft.

y (inches)	u (fps)	$\sqrt{\overline{e_o'^2}}$ (volts)	$\sqrt{\overline{e_1'^2}}$ (volts)	$\sqrt{\overline{e_2'^2}}$ (volts)	$\overline{u'^2}$ $(\frac{ft^2}{sec^2})$	$\overline{v'^2}$ $(\frac{ft^2}{sec^2})$	$\overline{u'v'}$ $(\frac{ft^2}{sec^2})$	$\frac{\Delta\overline{v'^2}}{\overline{v'^2}}$	$\frac{\Delta\overline{u'v'}}{\overline{u'v'}}$
1.12	16.83	.087	.0503	.0162	2.91	12.21	-5.89	.068	.065
1.30	19.01	.097	.0481	.0166	4.15	12.34	-6.26	.074	.063
1.44	20.22	.104	.0473	.0174	5.17	12.14	-6.39	.082	.064
1.94	21.83	.101	.0397	.0171	5.37	8.45	-4.67	.102	.067
2.17	22.26	.099	.0369	.0164	5.30	6.99	-4.08	.115	.068
2.65	23.06	.090	.0312	.0154	4.58	4.85	-2.87	.134	.072
3.30	23.96	.085	.0274	.0143	4.29	3.44	-2.23	.168	.075
4.13	24.85	.079	.0251	.0138	3.97	2.99	-1.89	.176	.077
5.34	25.90	.072	.0220	.0122	3.39	2.25	-1.52	.196	.077
6.88	26.82	.065	.0193	.0114	2.93	1.74	-1.15	.215	.082
8.49	27.70	.060	.0167	.0108	2.55	1.24	-0.81	.257	.093
10.07	28.50	.051	.0142	.0092	1.94	0.89	-0.59	.271	.095
11.92	29.35	.037	.0078	.0074	1.08	0.55	-0.33	.229	.065
13.78	29.8	.024	.0072	.0050	0.45	0.37	-0.14	.157	.110

Station I(2) Run I x = 2 ft.

y (inches)	u (fps)	$\sqrt{\overline{e_o'^2}}$ (volts)	$\sqrt{\overline{e_1'^2}}$ (volts)	$\sqrt{\overline{e_2'^2}}$ (volts)	$\overline{u'^2}$ $(\frac{ft^2}{sec^2})$	$\overline{v'^2}$ $(\frac{ft^2}{sec^2})$	$\overline{u'v'}$ $(\frac{ft^2}{sec^2})$	$\frac{\Delta\overline{v'^2}}{\overline{v'^2}}$	$\frac{\Delta\overline{u'v'}}{\overline{u'v'}}$
1.10	10.42	.182	.059	.040	6.81	7.92	-2.73	.131	.131
1.21	11.83	.184	.057	.034	8.16	6.69	-3.65	.173	.100
1.39	13.11	.197	.065	.040	10.68	11.65	-5.01	.136	.106
1.64	14.28	.204	.069	.040	12.80	14.31	-6.70	.133	.096
2.01	16.06	.224	.072	.041	17.82	15.74	-8.50	.159	.092
2.61	18.62	.237	.0705	.0408	24.20	14.58	-9.89	.218	.088
3.39	21.35	.210	.0599	.0356	22.57	10.79	-8.24	.267	.088
4.46	23.78	.136	.0389	.0231	10.96	5.12	-3.97	.271	.086
5.38	25.02	.096	.0264	.0175	5.79	2.62	-1.69	.276	.100
6.62	26.24	.078	.0198	.0140	4.05	1.10	-0.91	.446	.113
8.07	27.28	.065	.0175	.0120	2.94	1.25	-0.78	.291	.106
9.70	28.16	.058	.0154	.0104	2.43	0.92	-0.65	.323	.101
11.50	29.03	.048	.0127	.0088	1.79	0.60	-0.43	.363	.108
13.66	29.88	.032	.0087	.0062	0.83	0.36	-0.20	.283	.114
15.65	30.01	.019	.0058	.0042	0.30	0.26	-0.09	.149	.113

Station I(5) Run I x = 5 ft.

y (inches)	u (fps)	$\sqrt{\overline{e_o'^2}}$ (volts)	$\sqrt{\overline{e_1'^2}}$ (volts)	$\sqrt{\overline{e_2'^2}}$ (volts)	$\overline{u'^2}$ $(\frac{ft^2}{sec^2})$	$\overline{v'^2}$ $(\frac{ft^2}{sec^2})$	$\overline{u'v'}$ $(\frac{ft^2}{sec^2})$	$\frac{\Delta\overline{v'^2}}{\overline{v'^2}}$	$\frac{\Delta\overline{u'v'}}{\overline{u'v'}}$
1.10	10.02	.184	.0549	.0420	6.78	6.74	-1.78	.145	.176
1.20	11.22	.197	.0595	.0420	8.77	8.05	-2.83	.155	.140
1.38	12.11	.208	.0611	.0432	10.78	8.60	-3.27	.173	.138
1.61	12.93	.216	.0658	.0436	12.61	10.85	-4.62	.163	.118
1.96	14.05	.238	.0713	.0459	17.00	12.01	-6.65	.193	.103
2.61	15.83	.248	.0707	.0434	21.53	11.09	-7.59	.253	.100
2.34	17.75	.241	.0651	.0417	23.38	9.01	-7.02	.328	.103
4.48	20.62	.212	.0572	.0372	21.98	8.42	-6.41	.327	.102
5.38	22.55	.187	.0503	.0341	19.22	7.82	-5.20	.306	.108
6.61	24.72	.144	.0375	.0258	12.74	4.22	-3.18	.370	.108
8.08	26.55	.098	.0266	.0185	6.53	2.95	-1.71	.274	.109
9.69	27.83	.067	.0179	.0130	3.21	1.49	-0.76	.266	.119
11.47	28.75	.051	.0141	.0098	1.96	0.98	-0.53	.249	.107
13.39	29.40	.040	.0099	.0077	1.24	0.37	-0.21	.403	.144
15.74	30.01	.025	.0070	.0054	0.51	0.32	-0.11	.20	.140

FIGURES

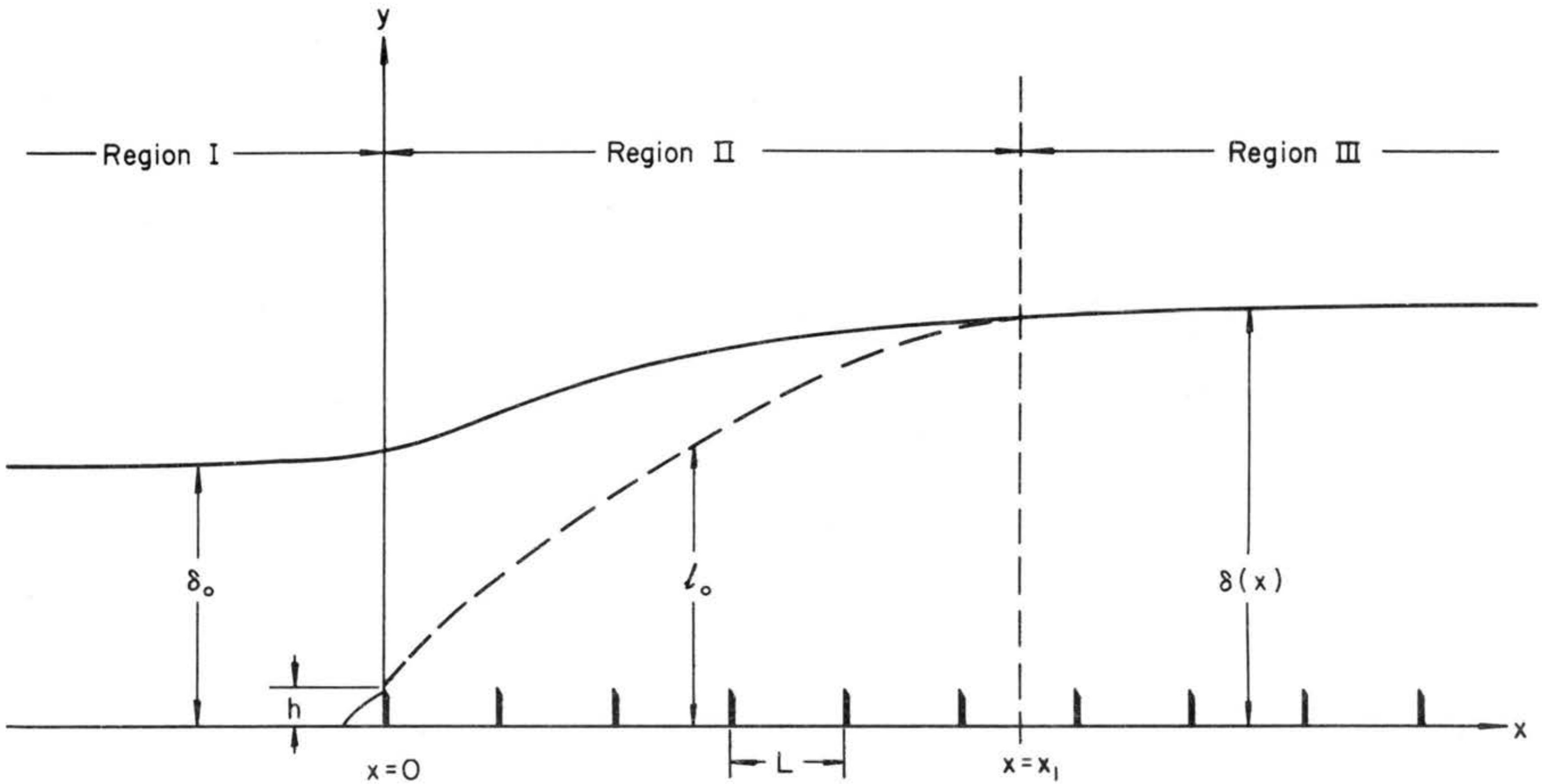

Figure 1 Sketch of the flow condition

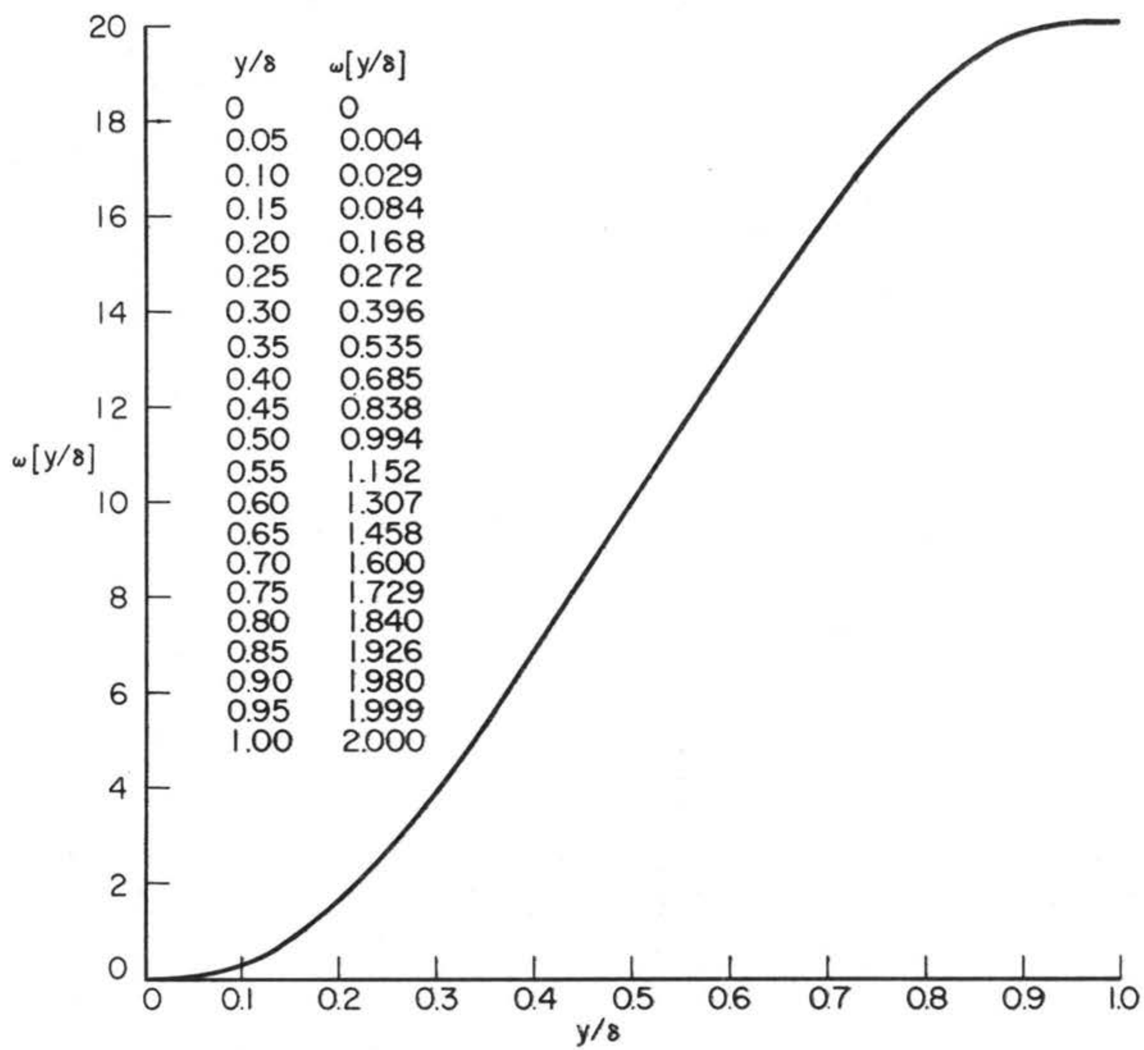

y/δ	ω[y/δ]
0	0
0.05	0.004
0.10	0.029
0.15	0.084
0.20	0.168
0.25	0.272
0.30	0.396
0.35	0.535
0.40	0.685
0.45	0.838
0.50	0.994
0.55	1.152
0.60	1.307
0.65	1.458
0.70	1.600
0.75	1.729
0.80	1.840
0.85	1.926
0.90	1.980
0.95	1.999
1.00	2.000

Figure 2 Cole's wake function

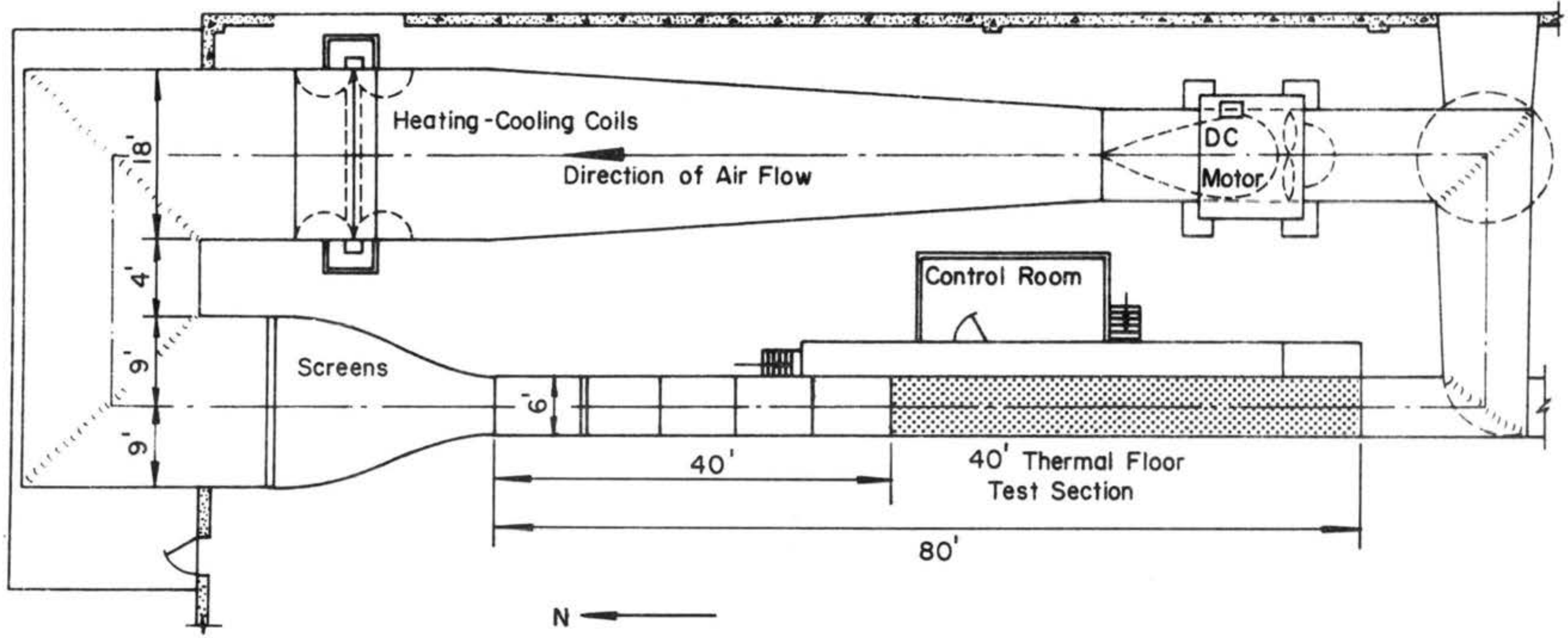

Figure 3 Plane view of the wind tunnel

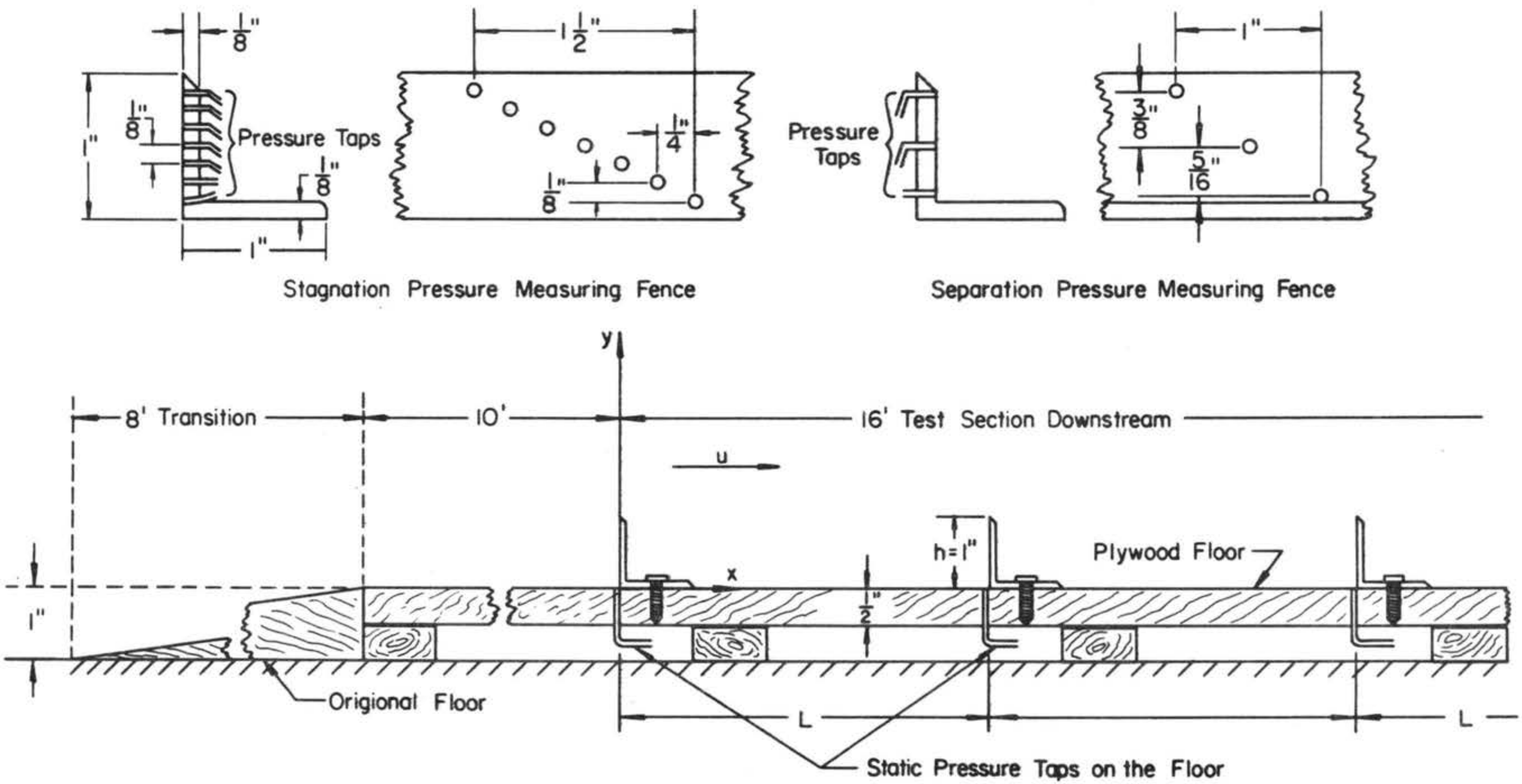

Figure 4 Sketch of floor and fence assembly

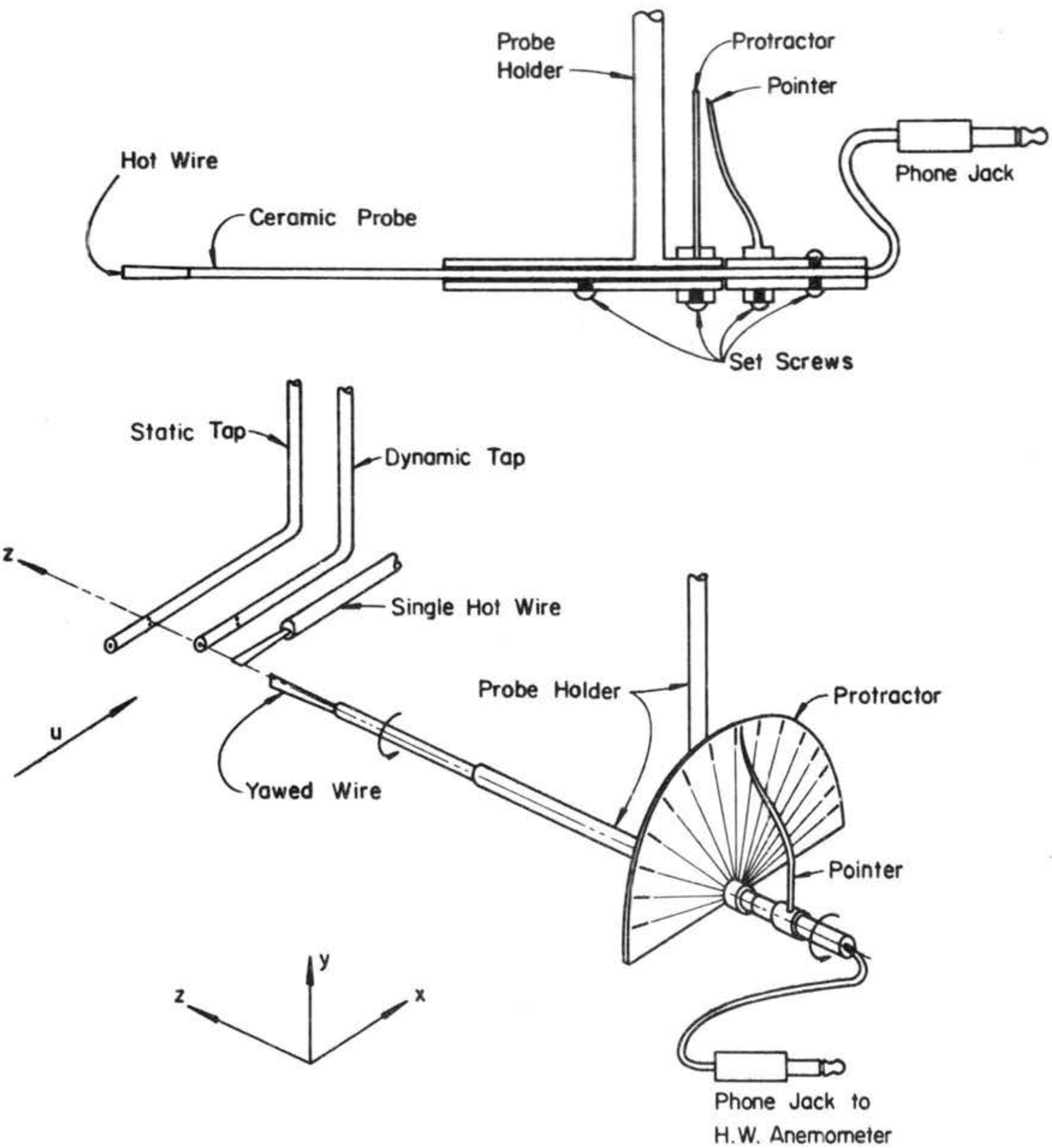

Figure 5 Rotating hot wire probe and the relative position of other sensor probes

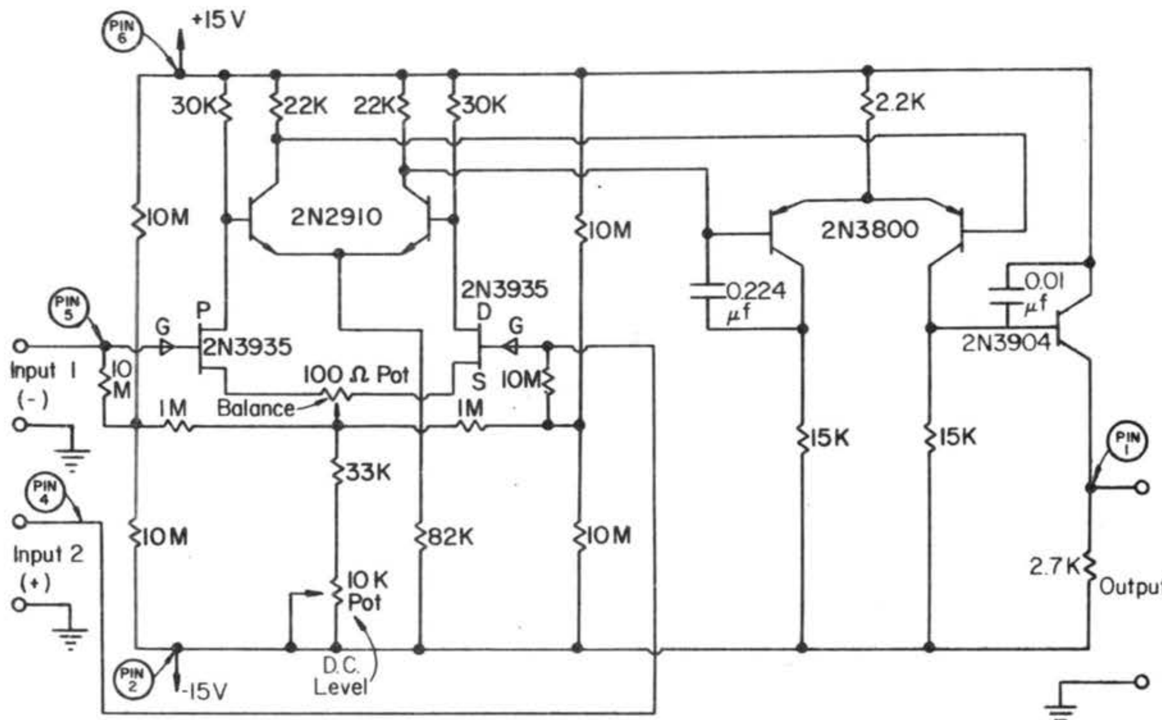

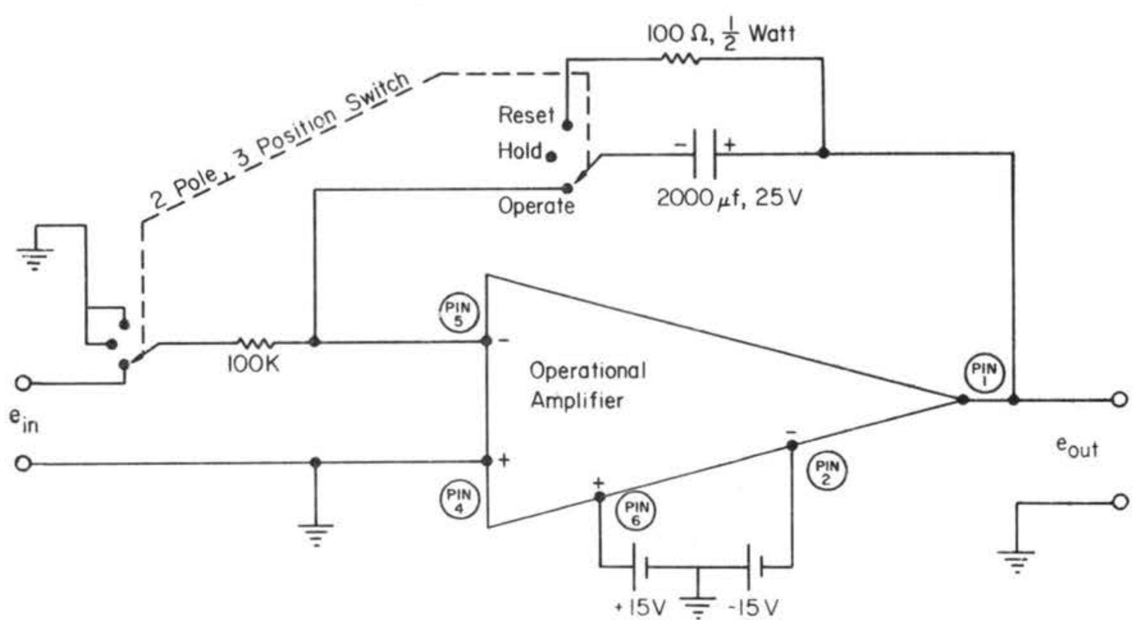

Figure 6 The integrator

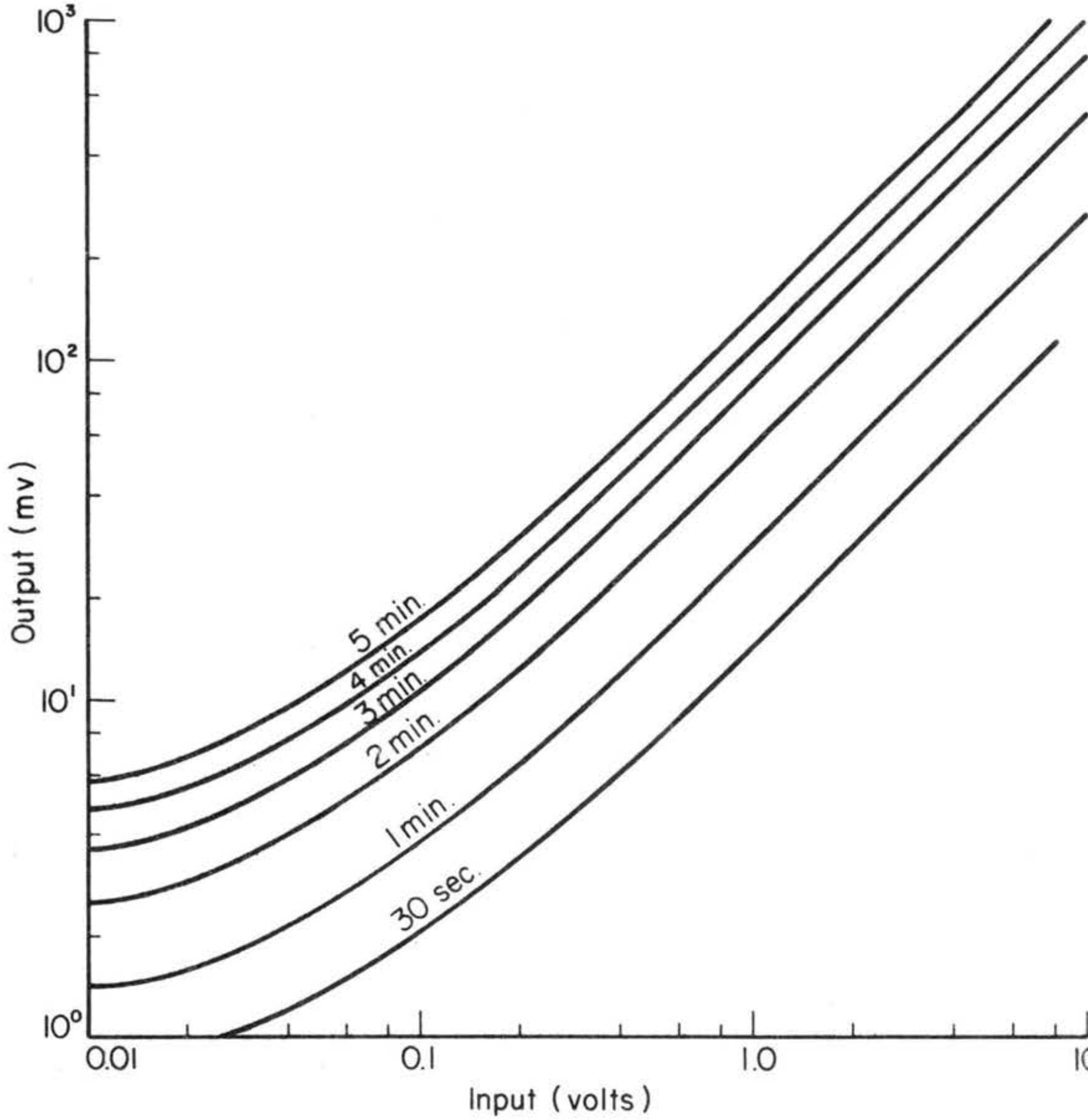

Figure 7 Calibration curves of the integrator

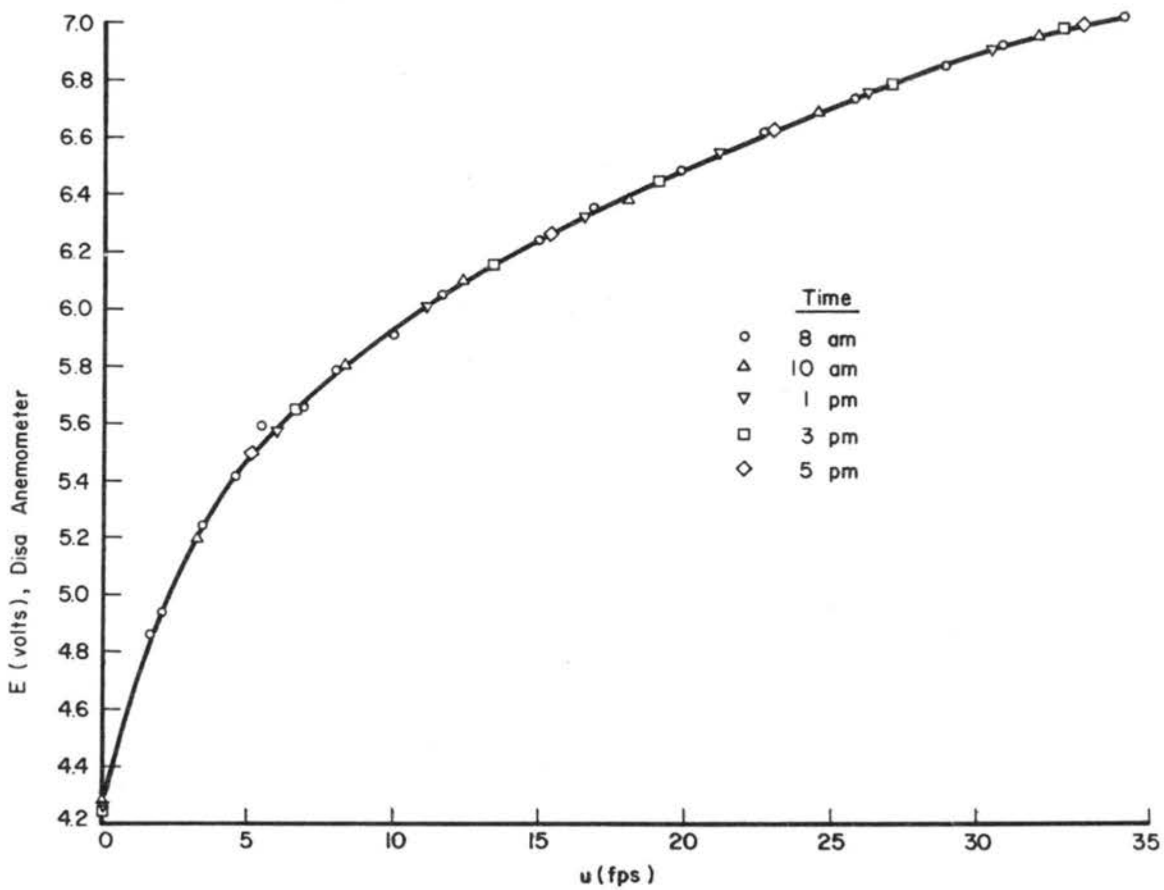

Figure 8 Typical calibration curve of the normal hot wire during one day of operation

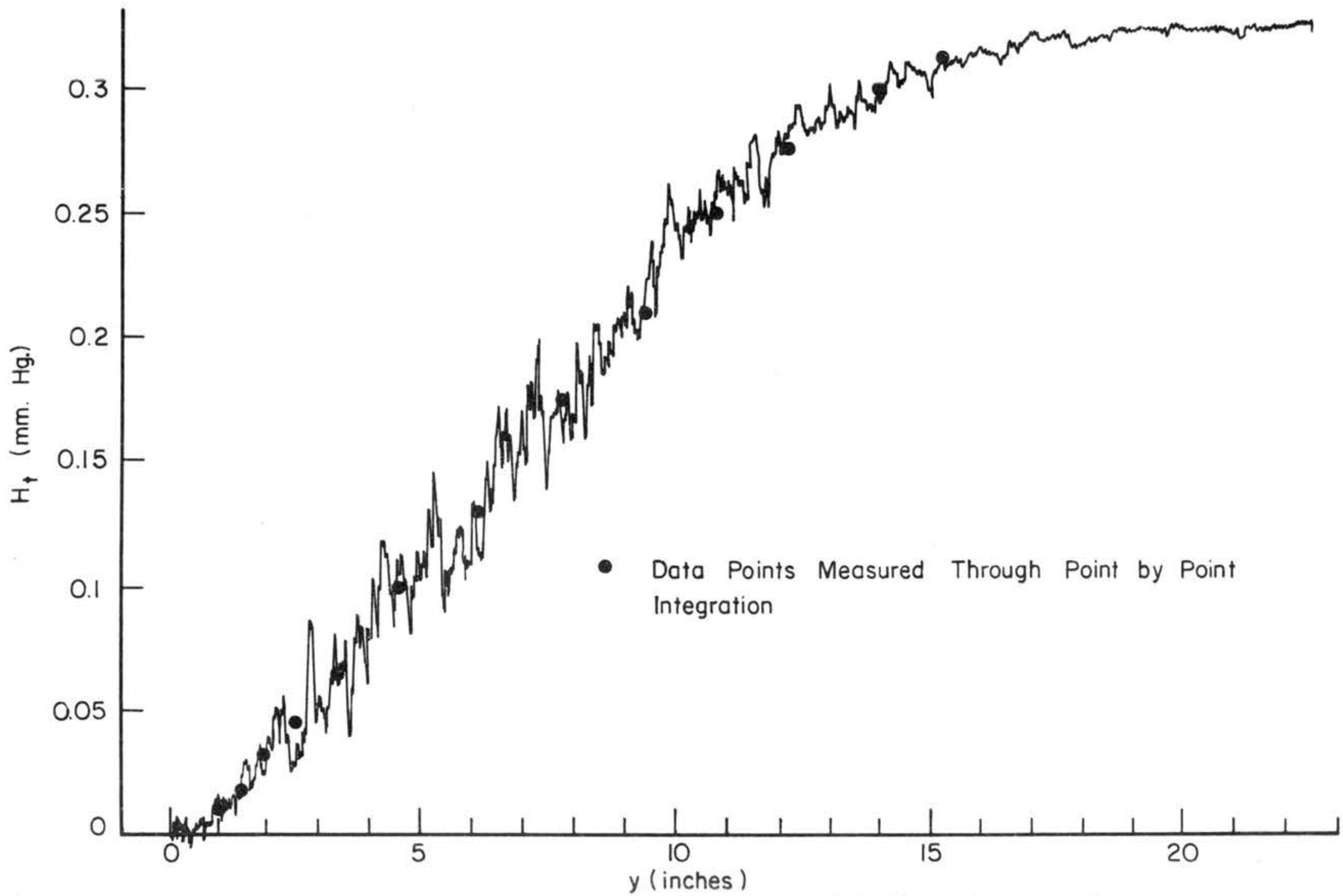

Figure 9 Typical continuous traverses and point by point data for total head measurement

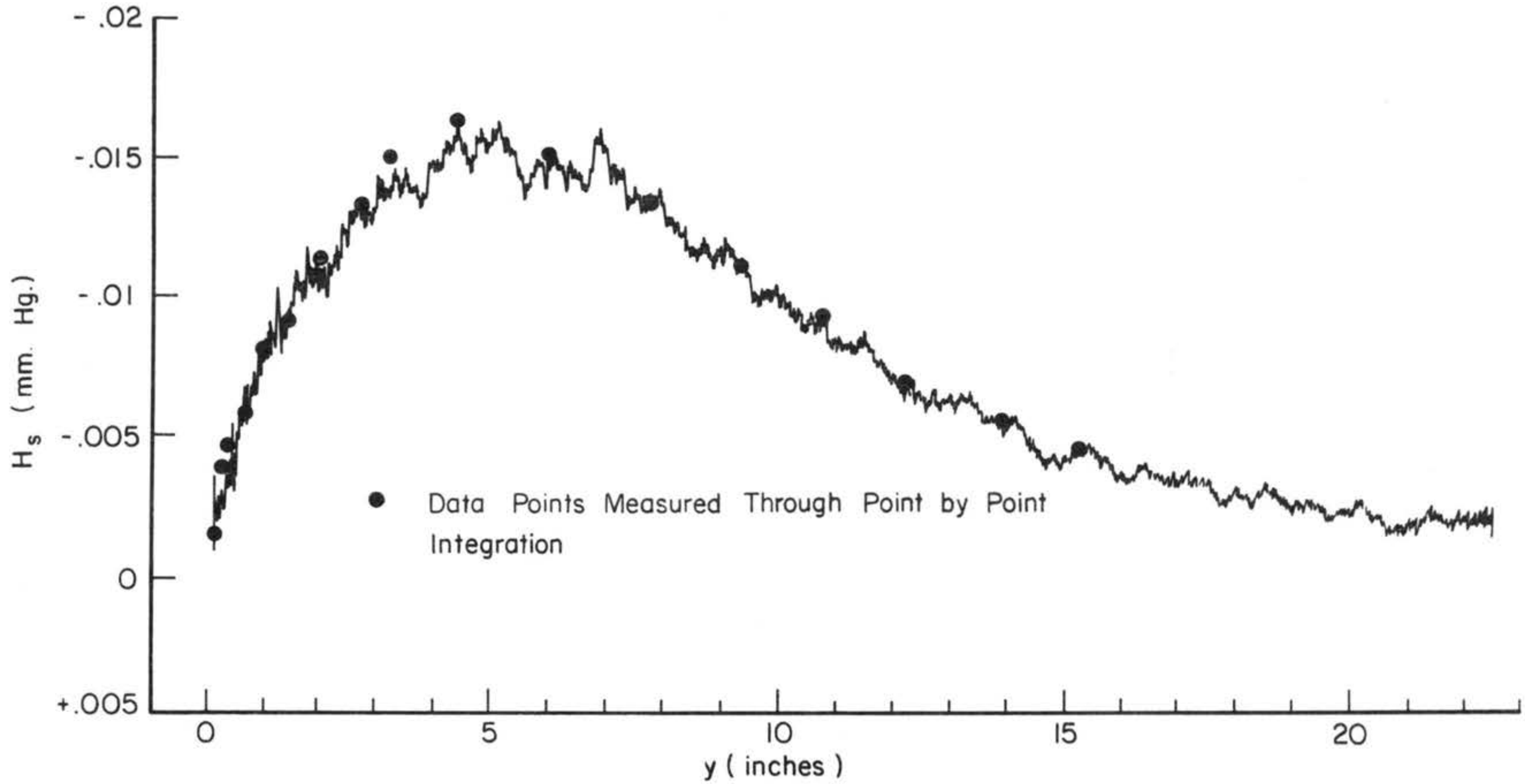

Figure 10 Typical continuous traverses and point by point data for static head measurement

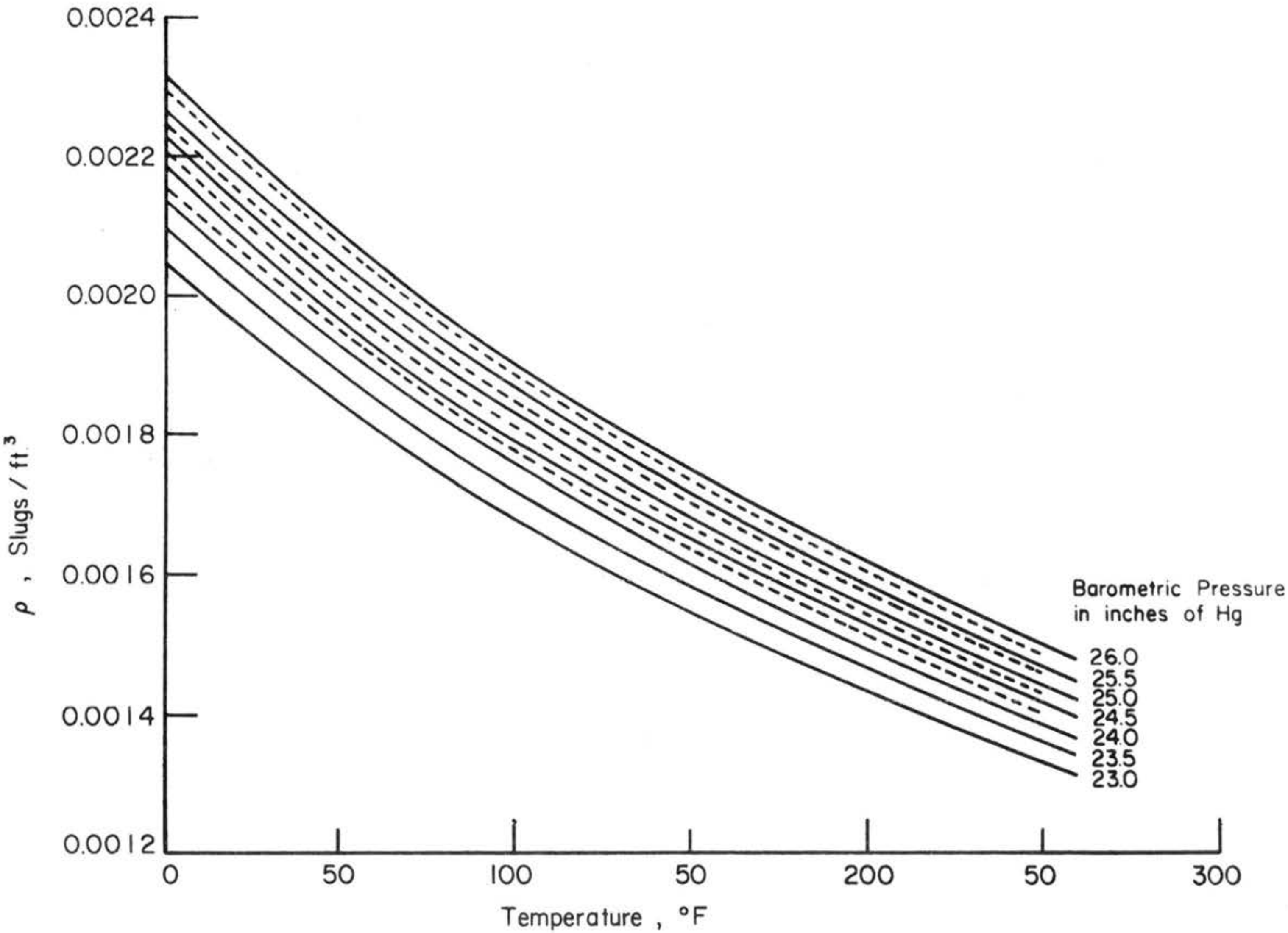

Figure 11 Air density ρ as a function of temperature and pressure

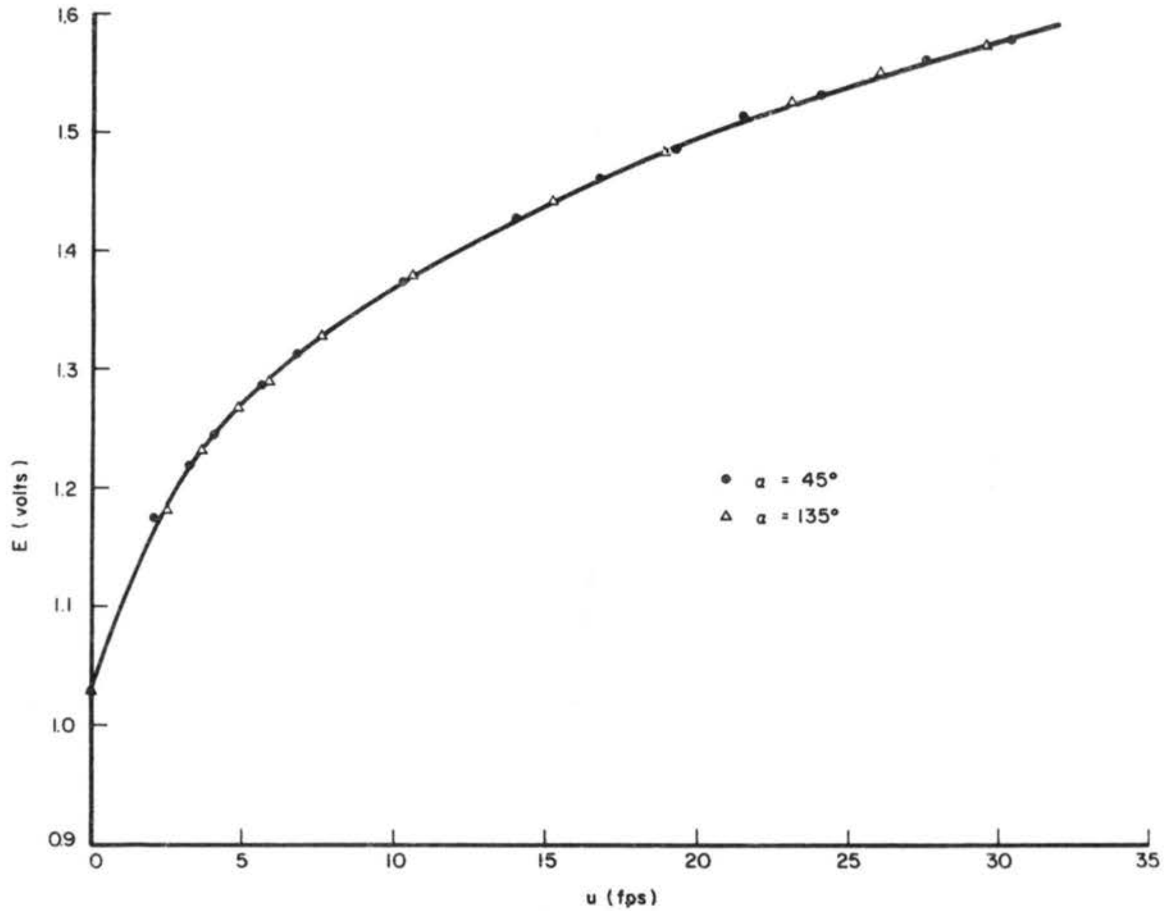

Figure 12 Typical calibration curve of a yawed wire at 45° and 135°

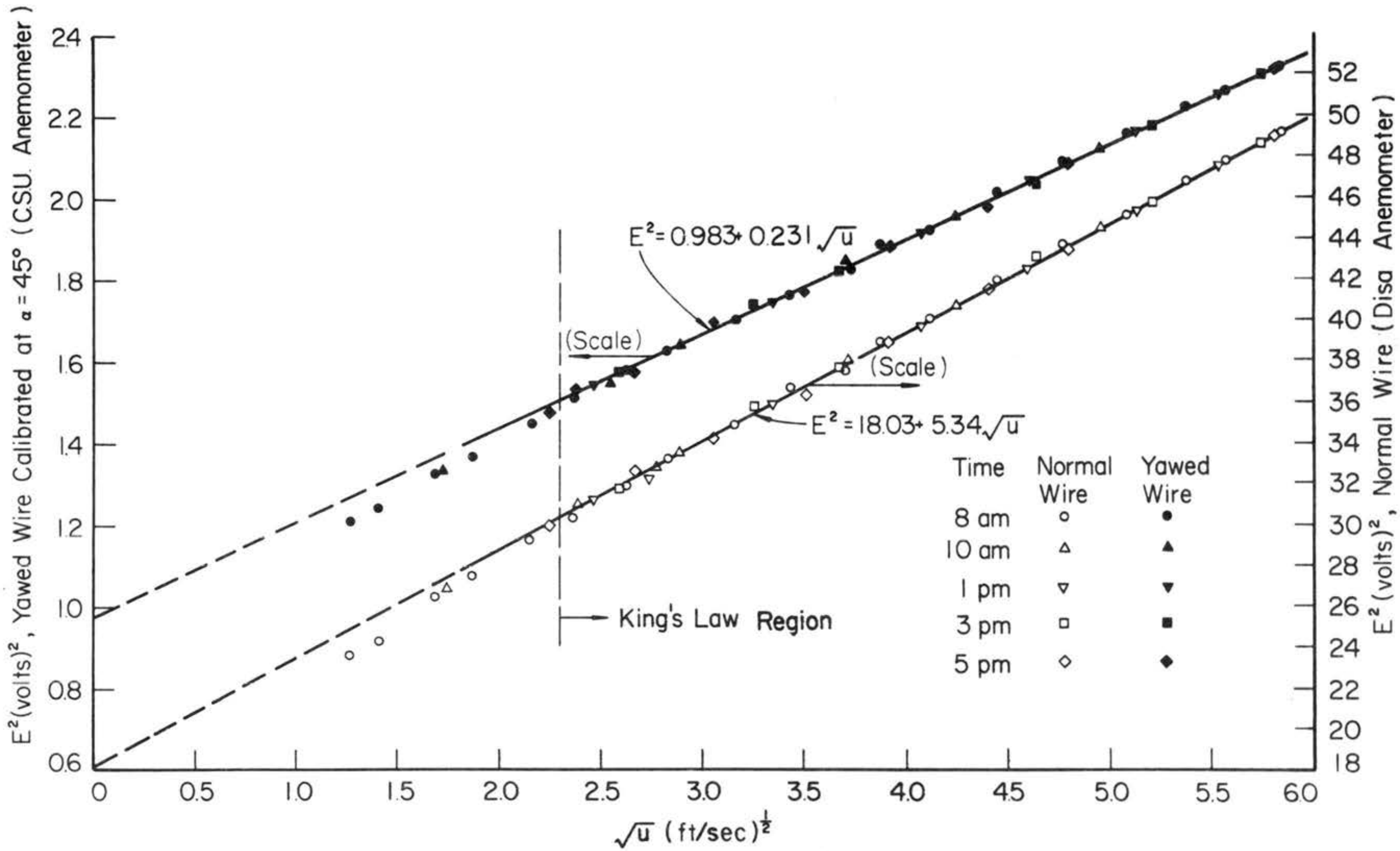

Figure 13 Typical calibration curves of the normal wire and the yawed wire

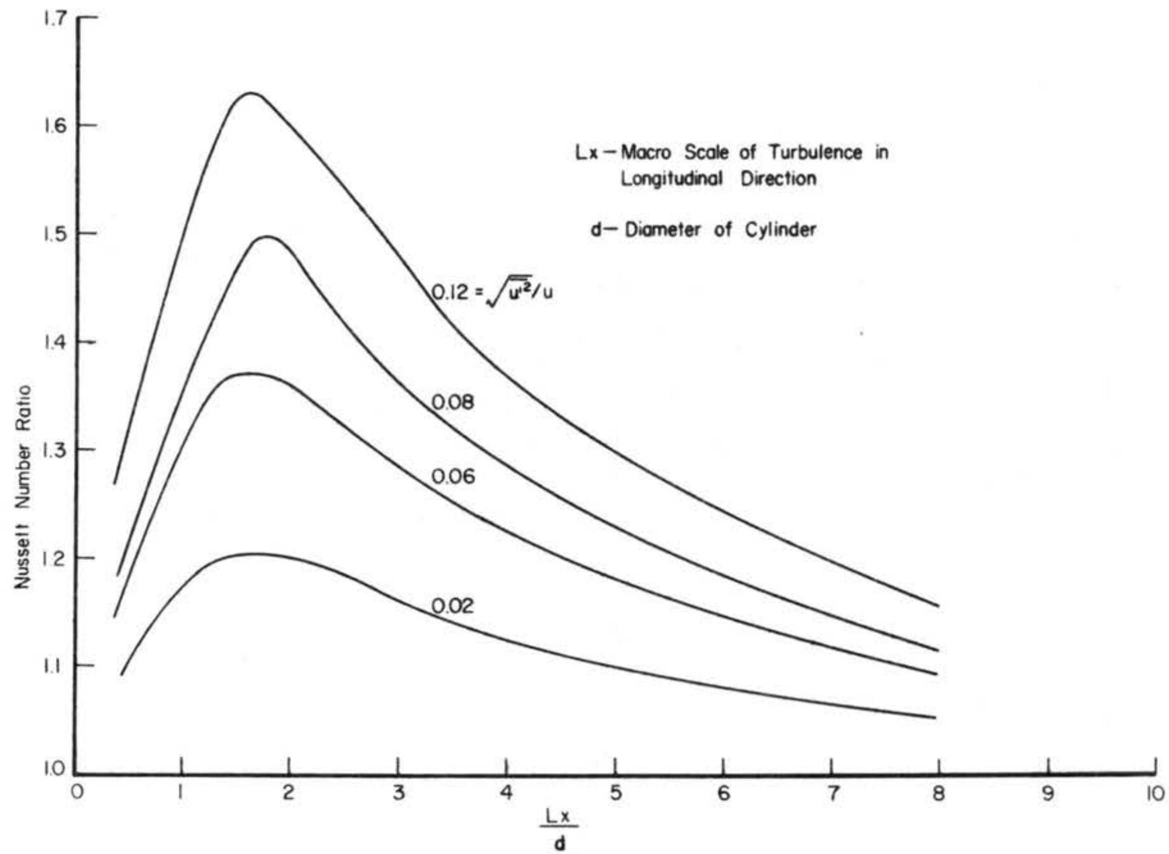

Figure 14 Increase in heat transfer from a cylinder due to turbulence

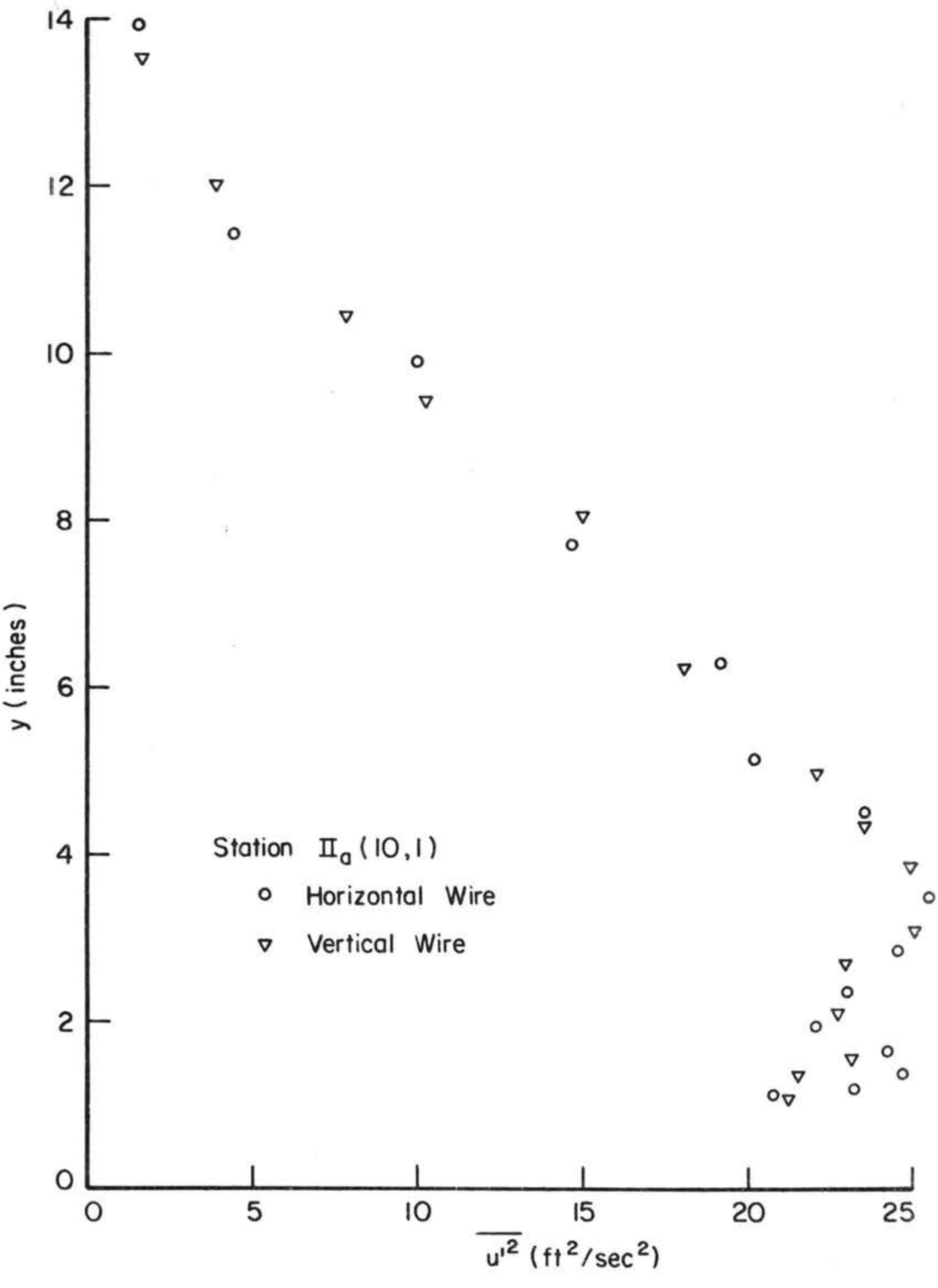

Figure 15 Examination of the effects on $\overline{u'^2}$ measurements due to the gradients of velocity and turbulence

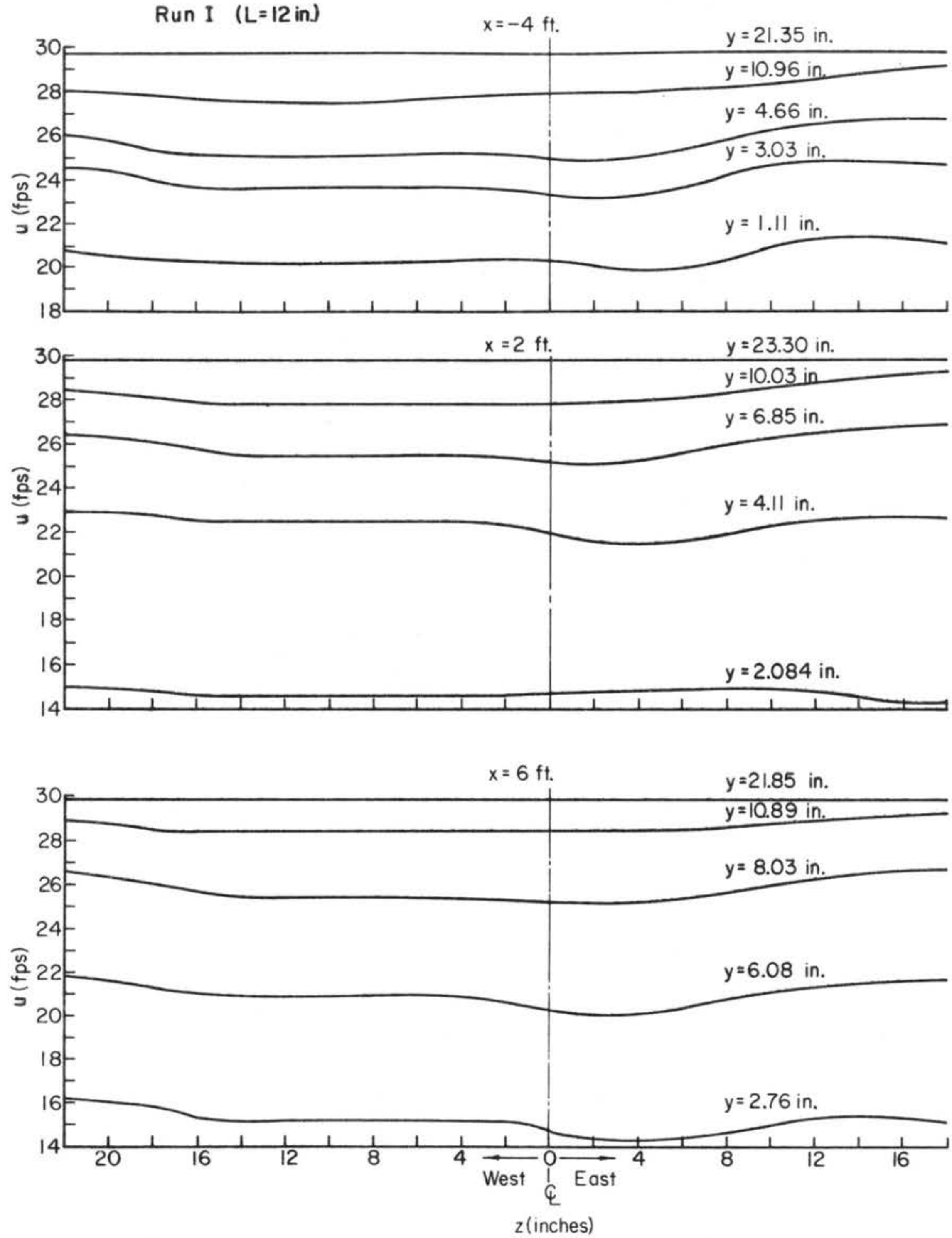

Figure 16 Two-dimensionality test of the boundary layer at u = 30 fps, L = 6 in.

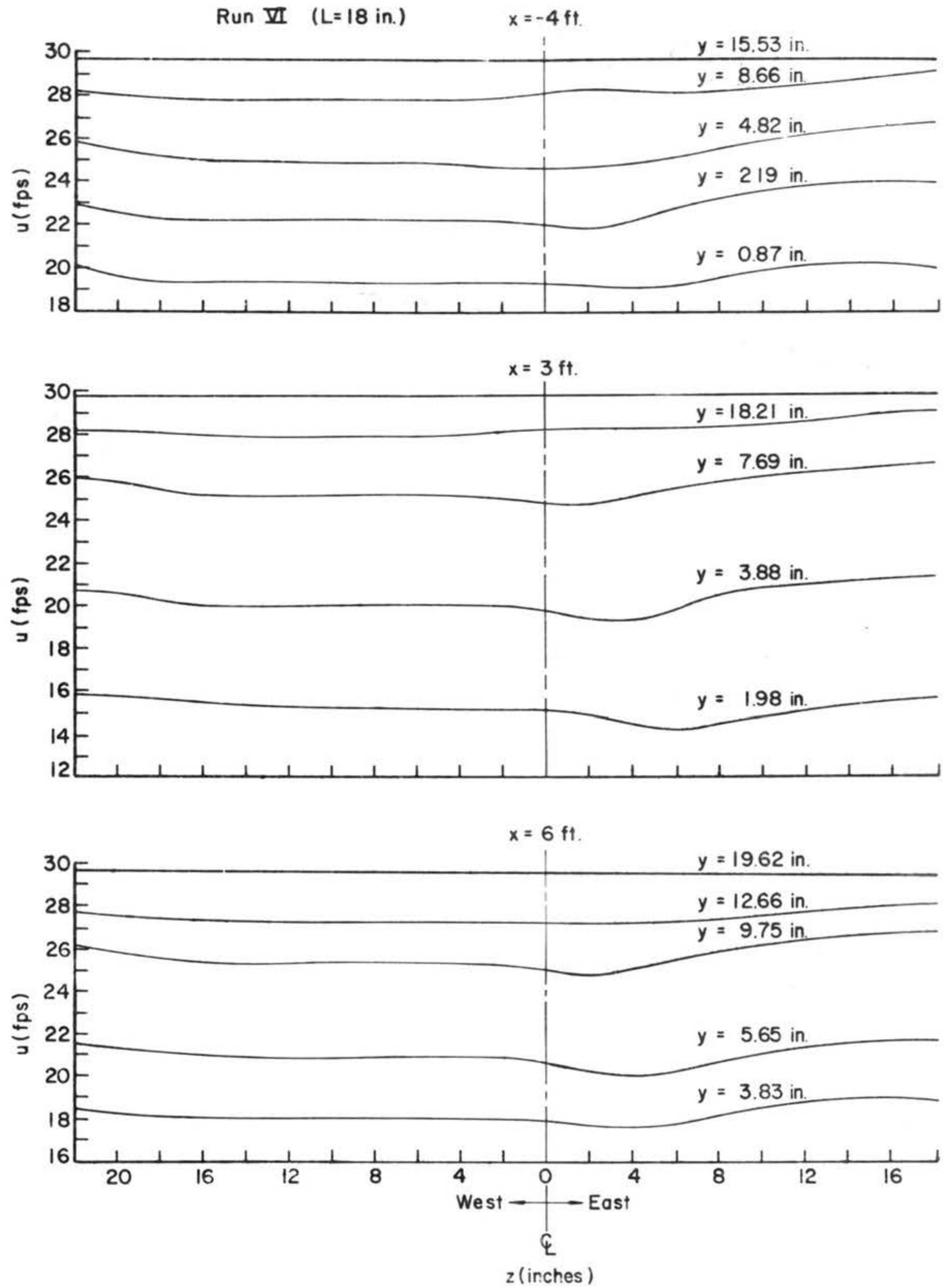

Figure 17 Two-dimensionality test of the boundary layer at u = 30 fps, L = 18 in.

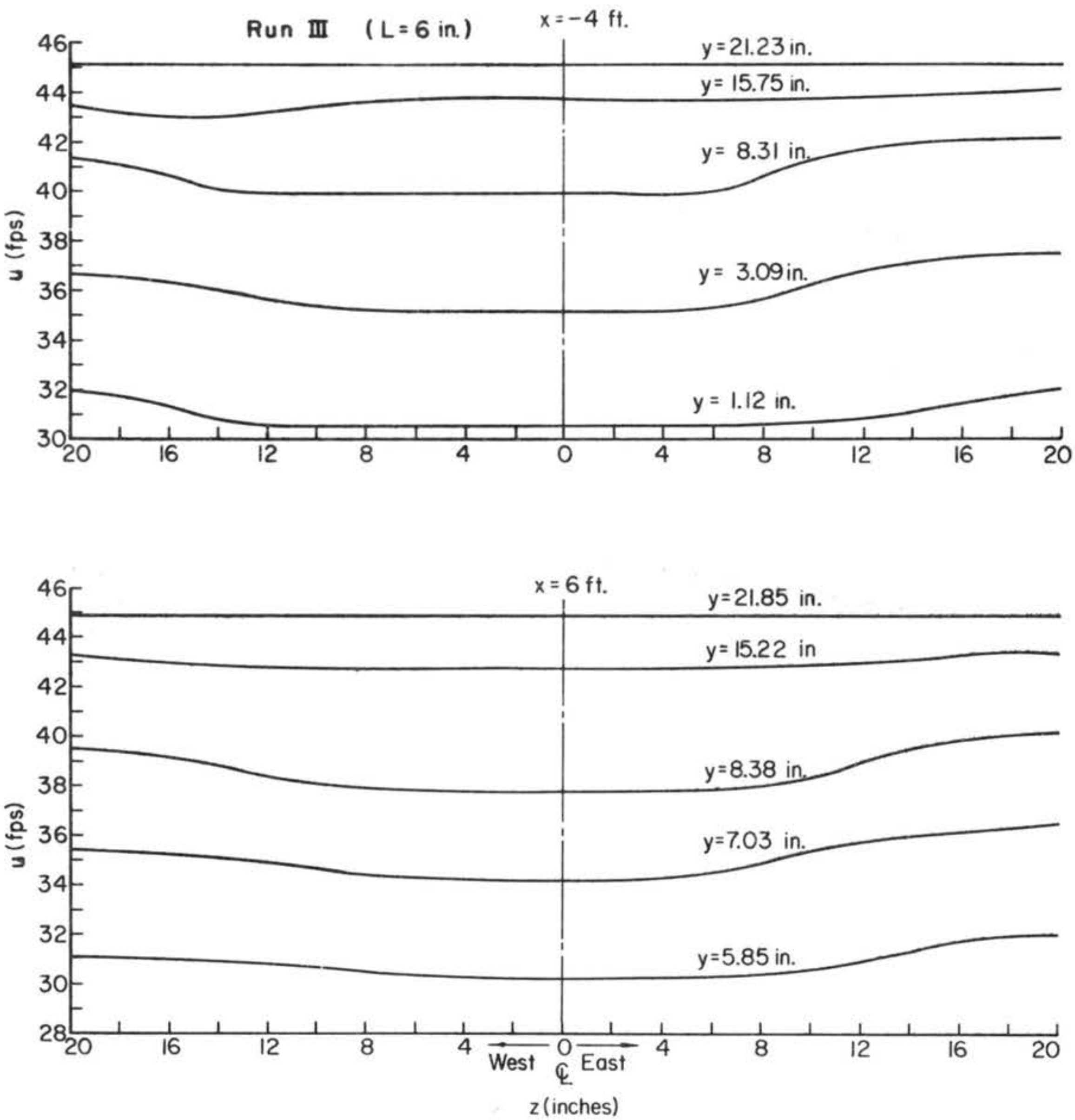

Figure 18 Two-dimensionality test of the boundary layer at u = 45 fps, L = 12 in.

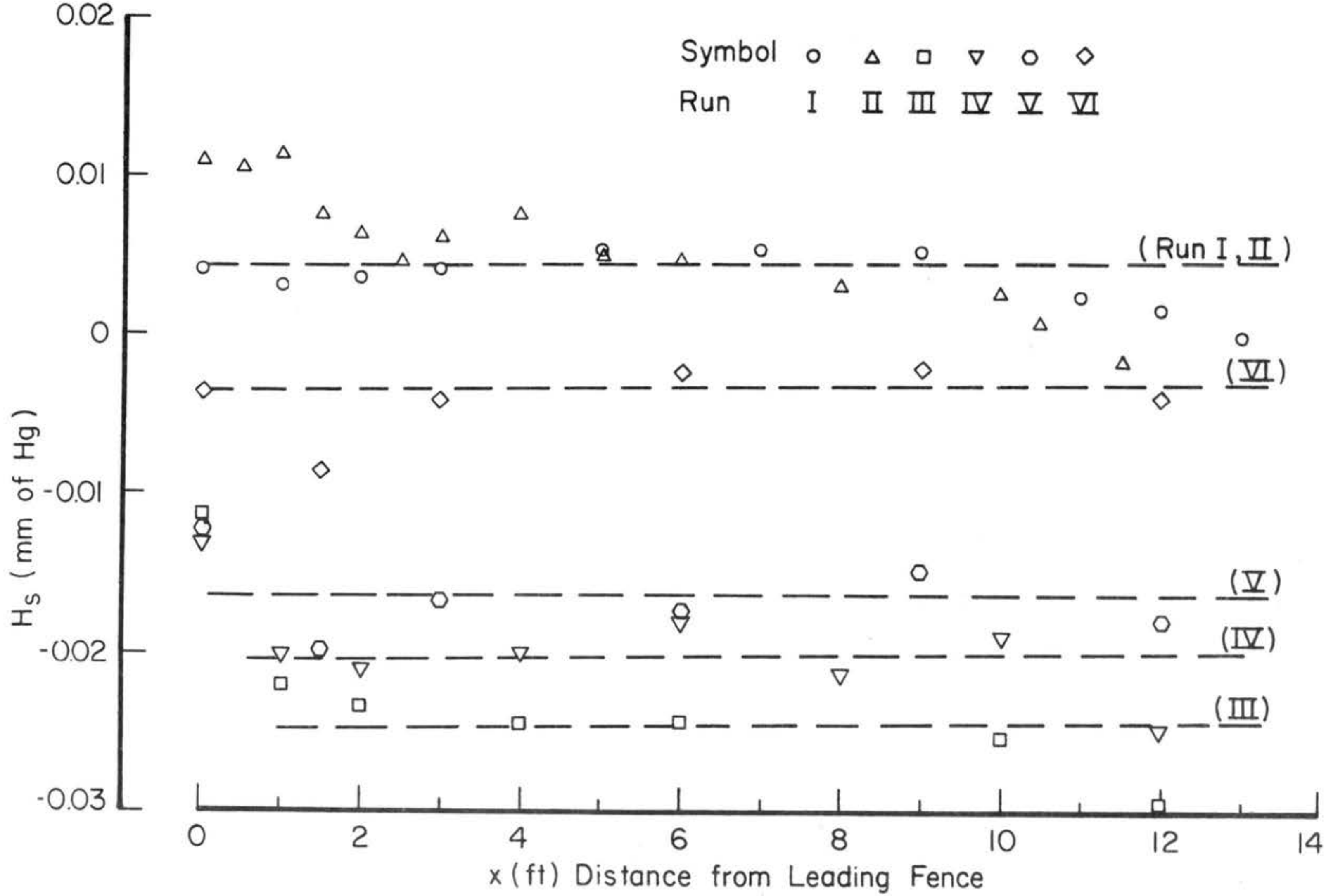

Figure 19 Free stream static head distributions

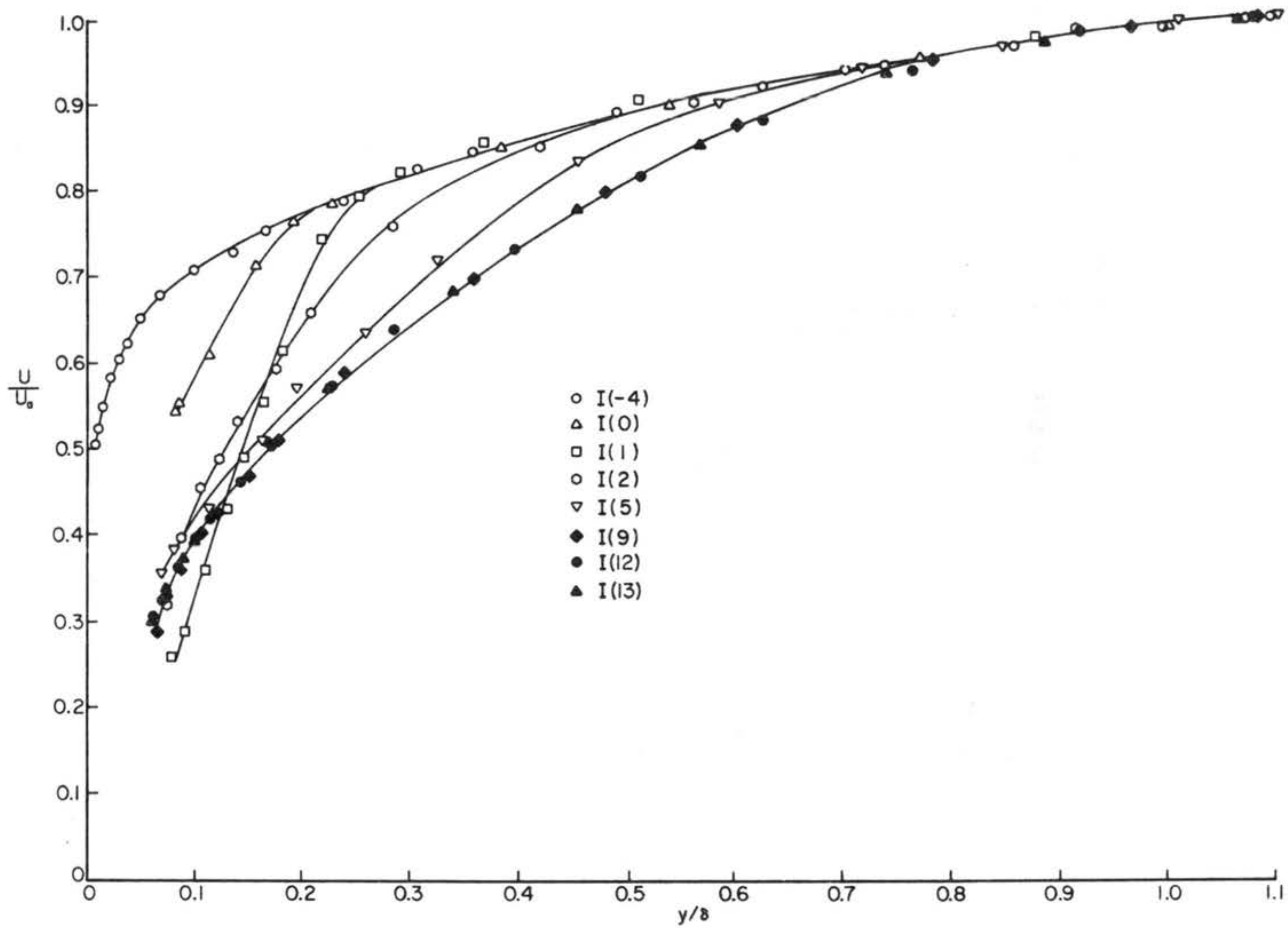

Figure 20 Dimensionless plot of the boundary layer for Run I

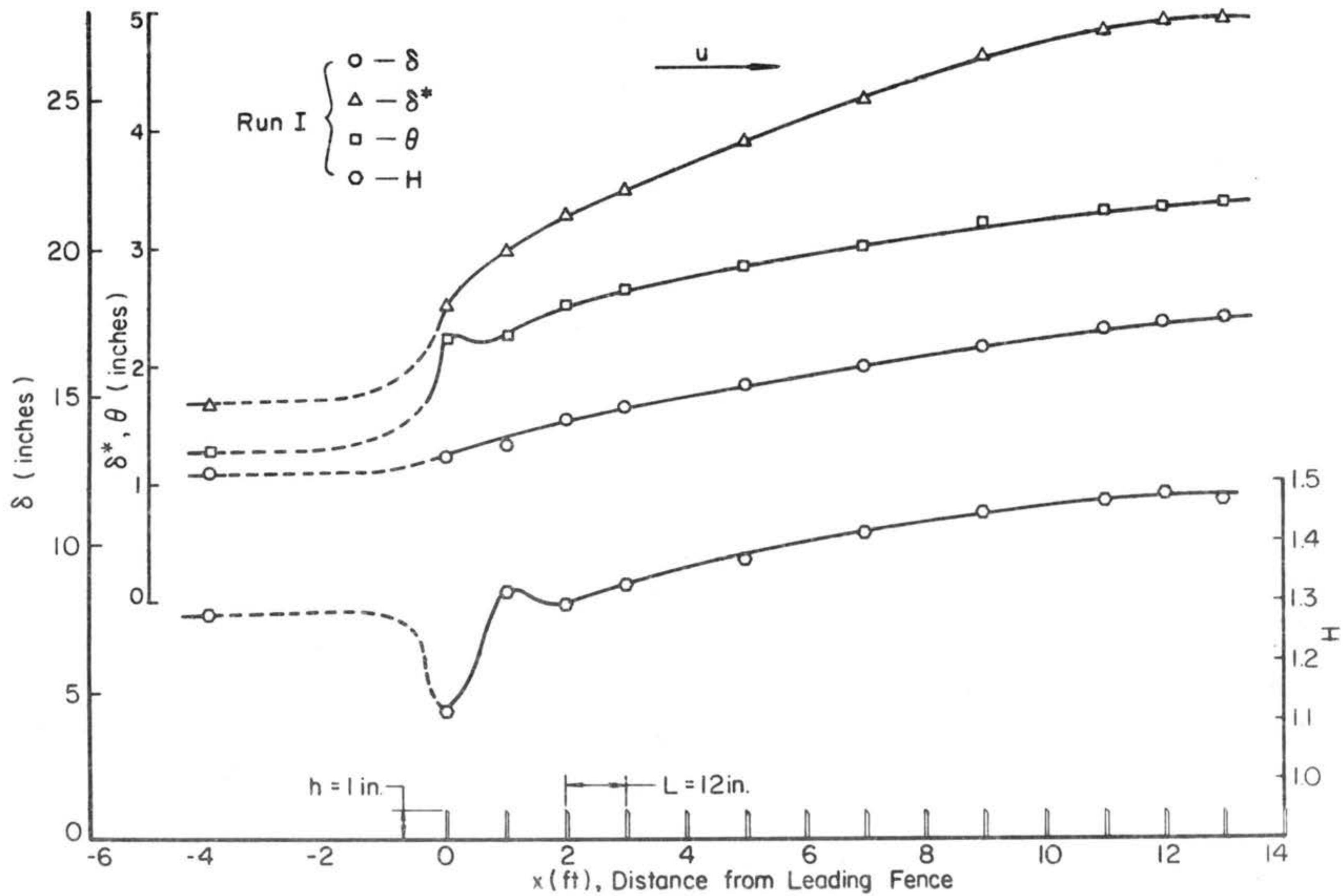

Figure 21 Flow parameters δ, δ*, θ and H of Run I

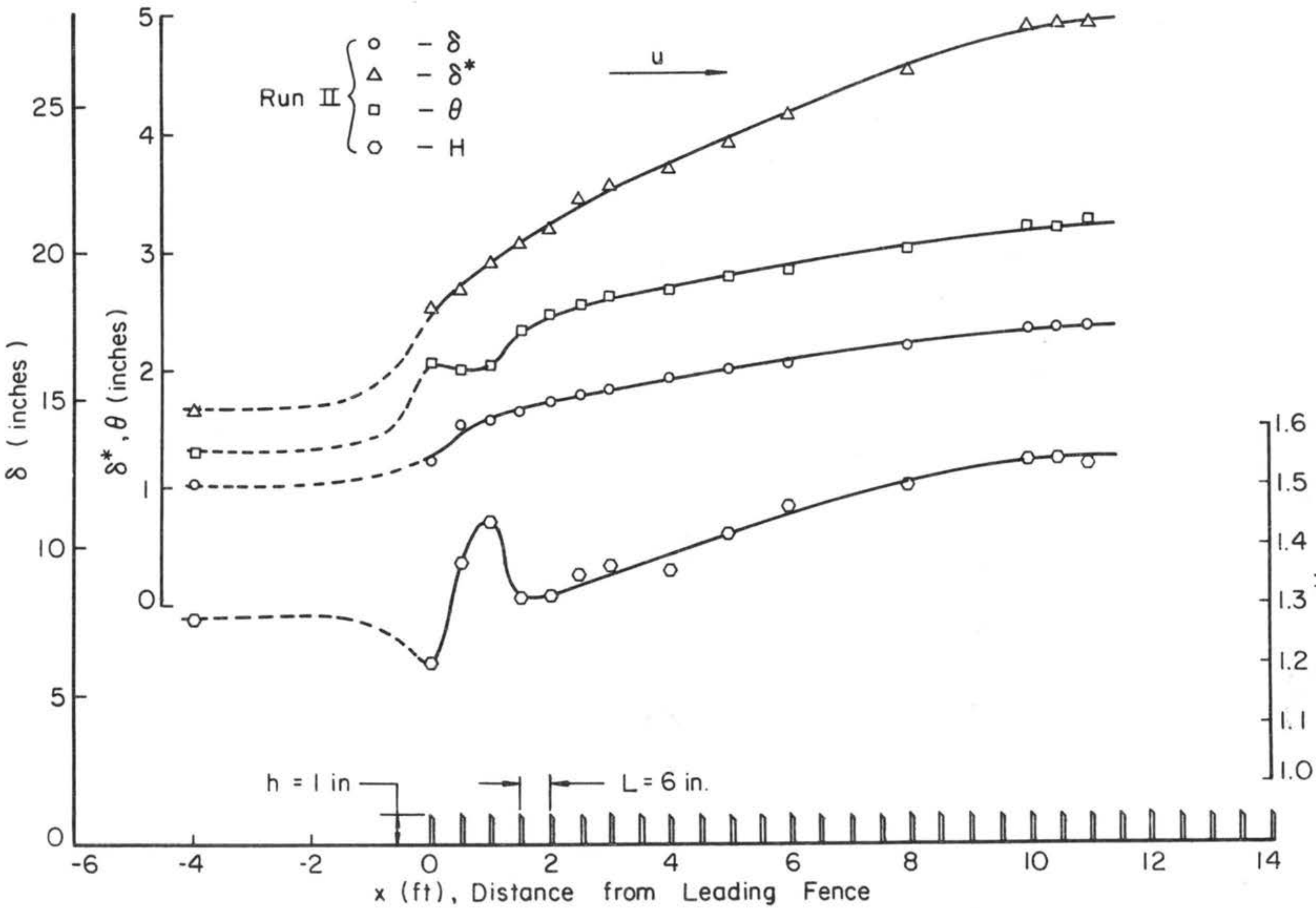

Figure 22 Flow parameters δ , δ* , θ and H of Run II

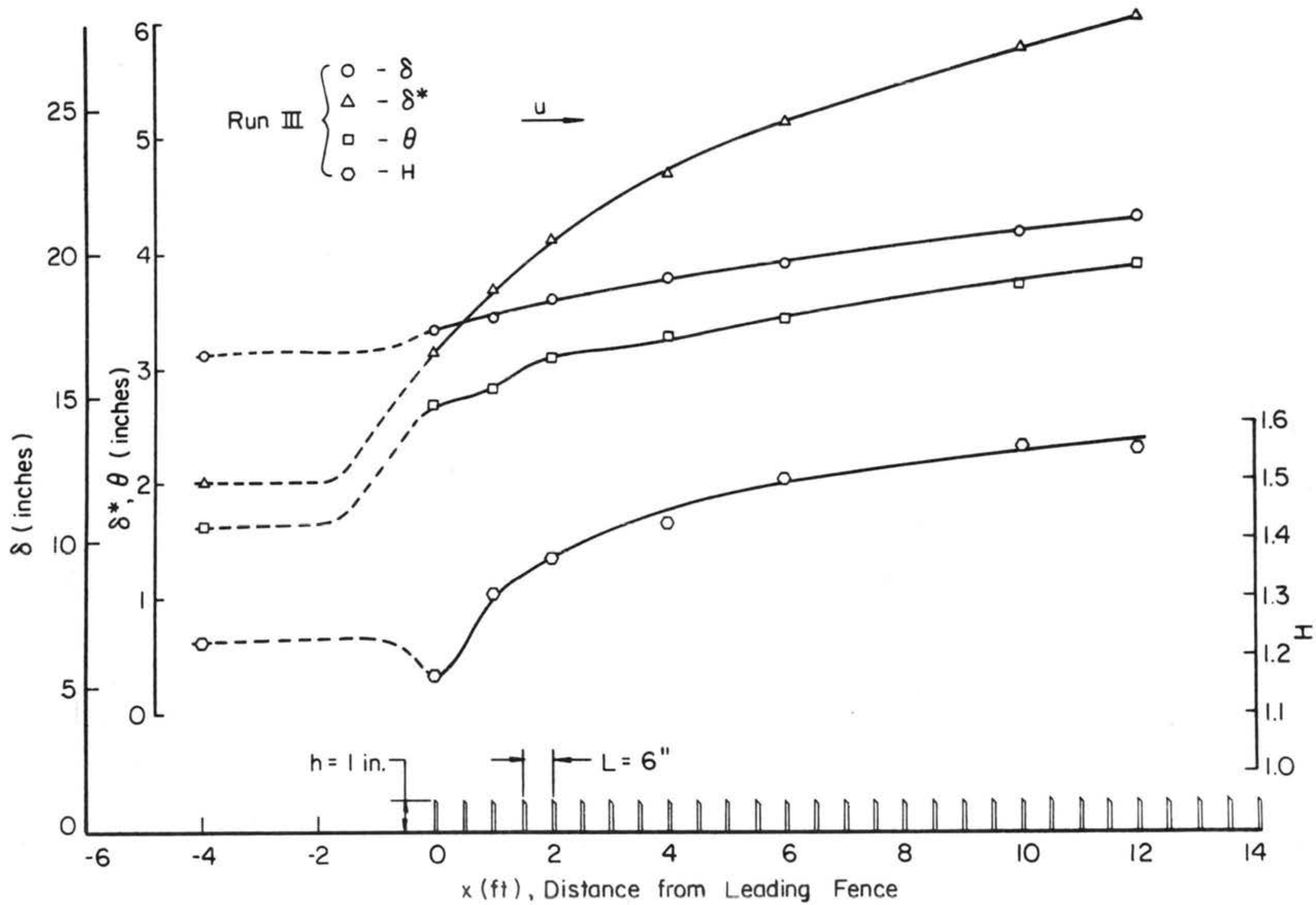

Figure 23 Flow parameters δ , δ* , θ and H of Run III

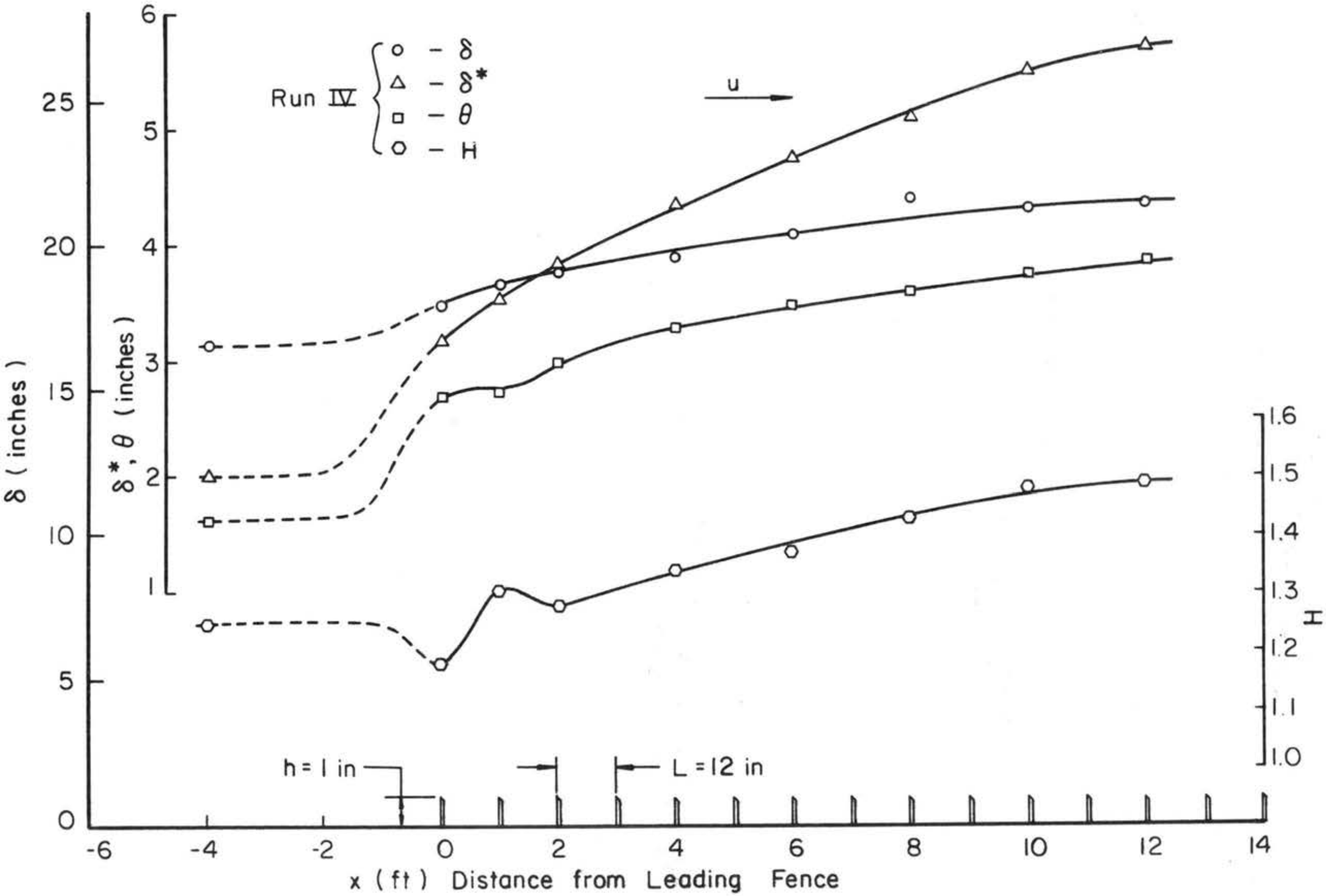

Figure 24 Flow parameters δ , δ^* , θ and H of Run IV

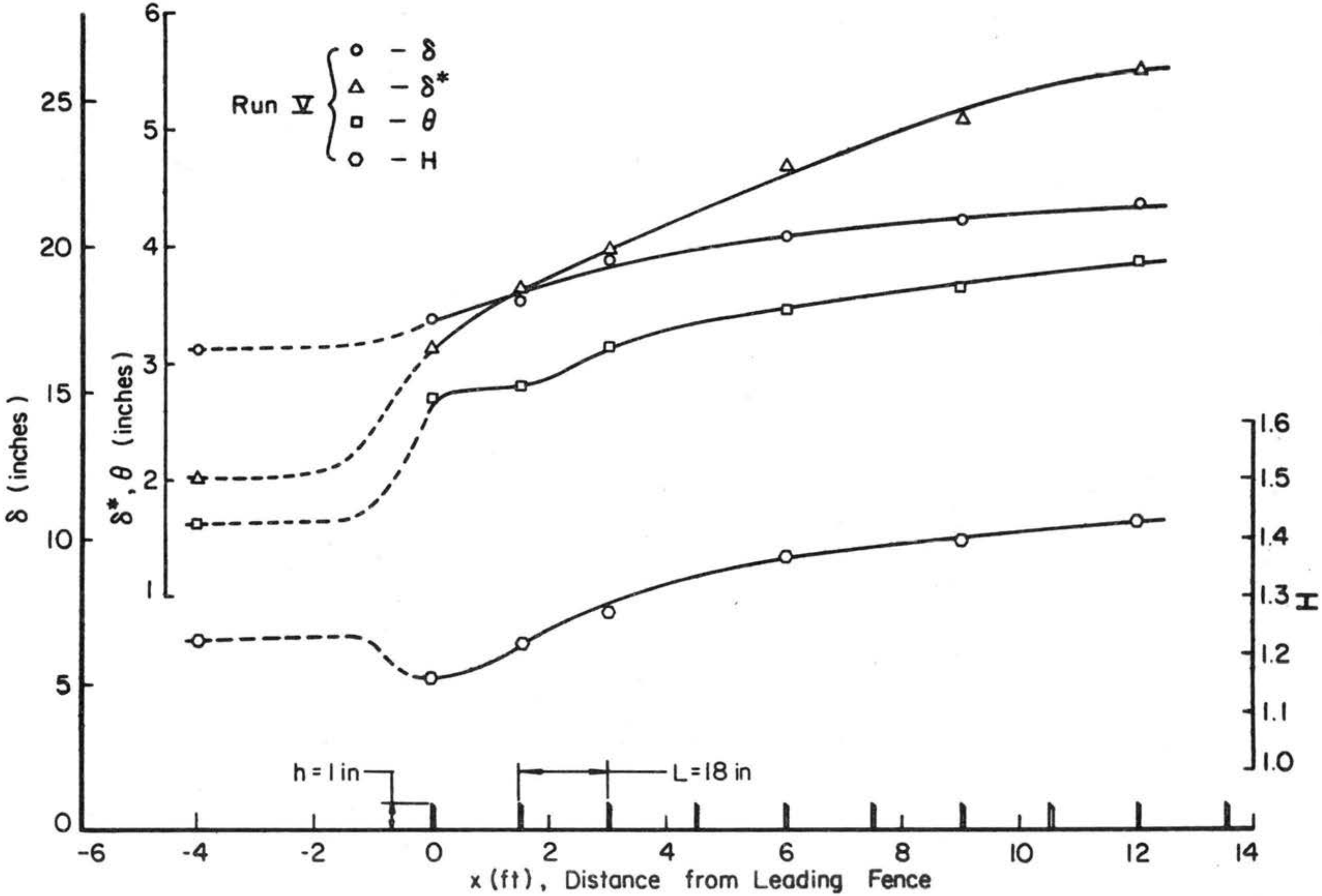

Figure 25 Flow parameters δ , δ* , θ and H of Run V

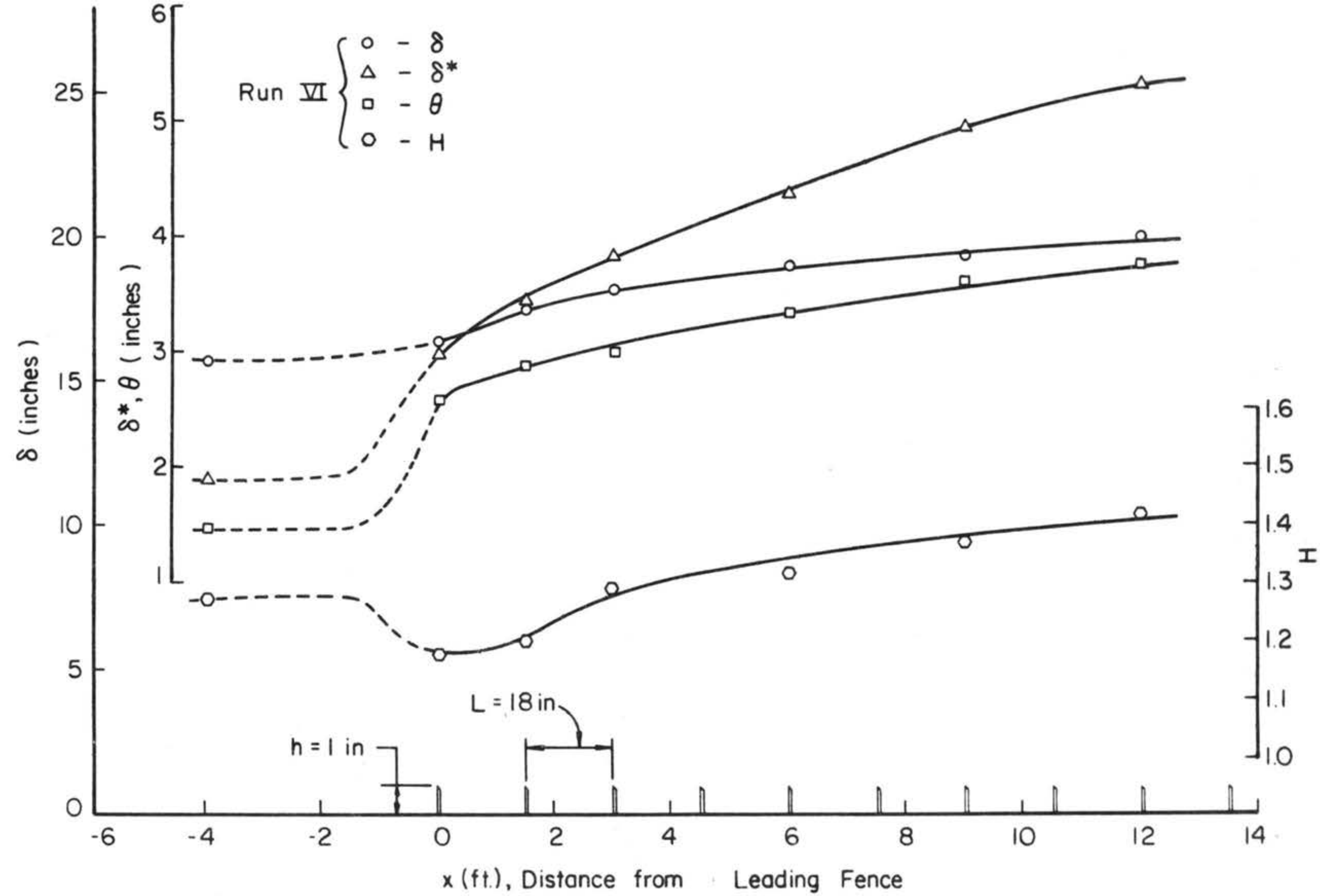

Figure 26 Flow parameters δ , δ^* , θ and H of Run VI

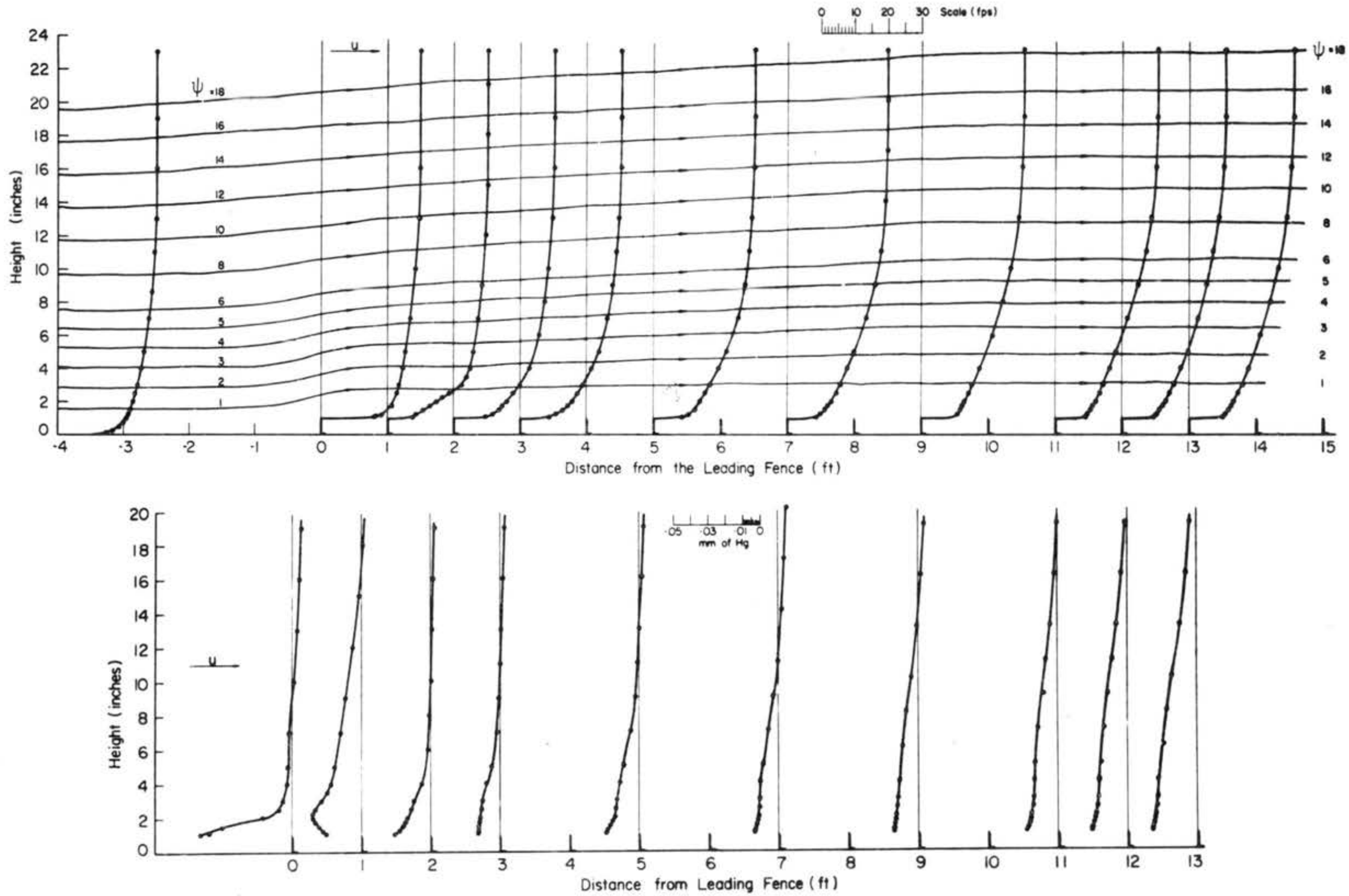

Figure 27 Velocity profiles, stream lines and static head distributions of Run I

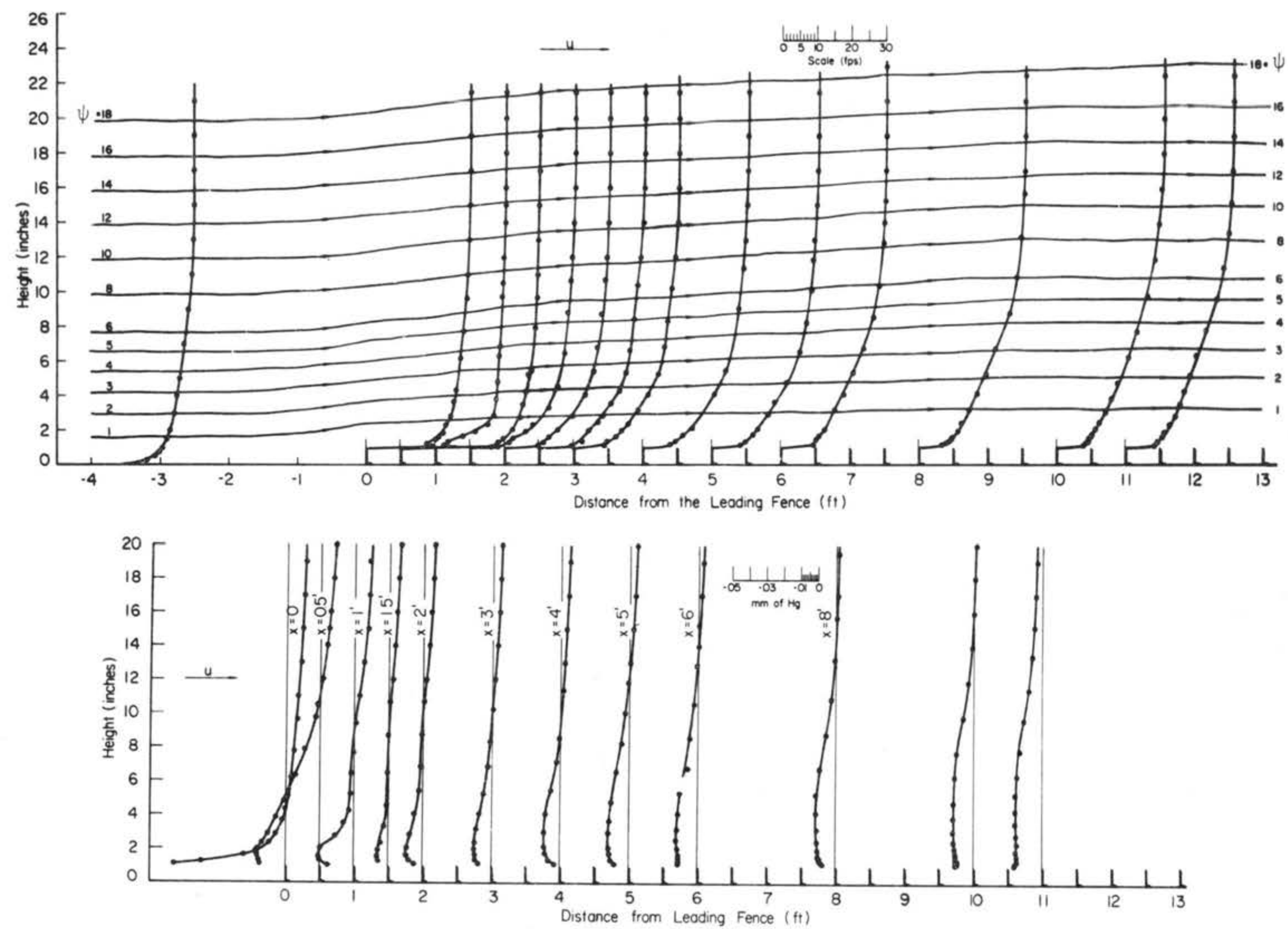

Figure 28 Velocity profiles, stream lines and static head distributions of Run II

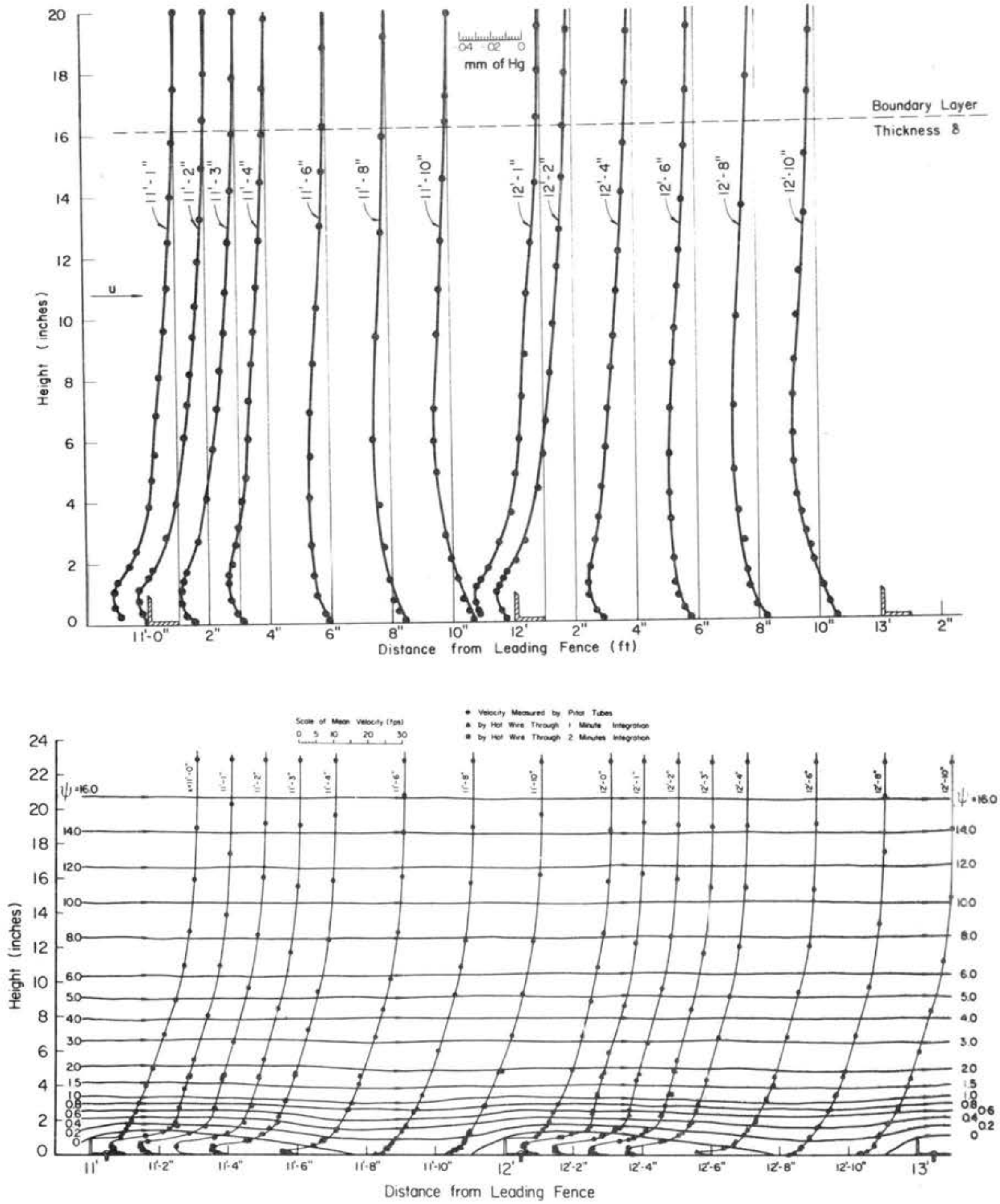

Figure 29 Velocity profiles, stream lines and static head distributions of Run Ia

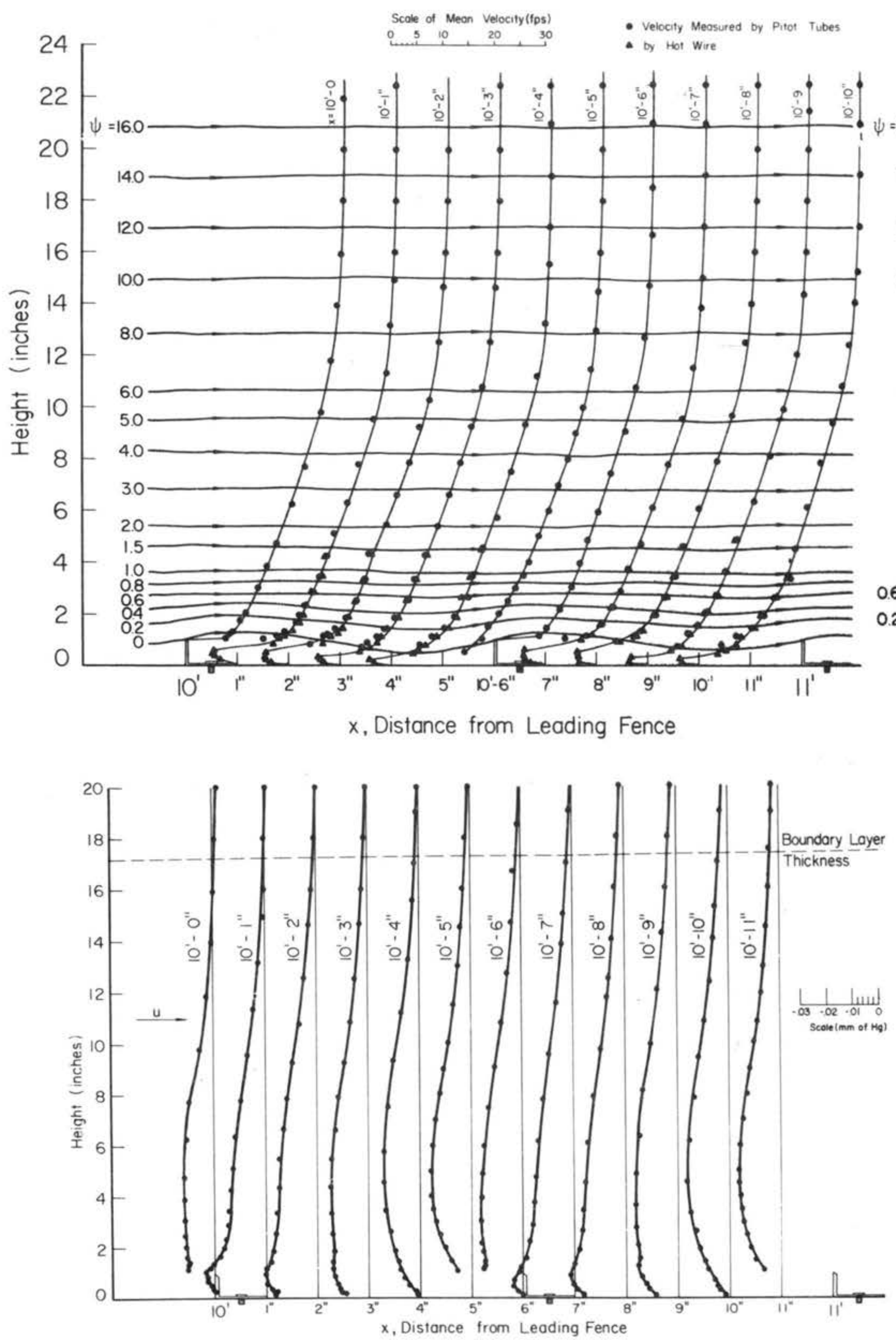

Figure 30 Velocity profiles, stream lines and static head distributions of Run IIa

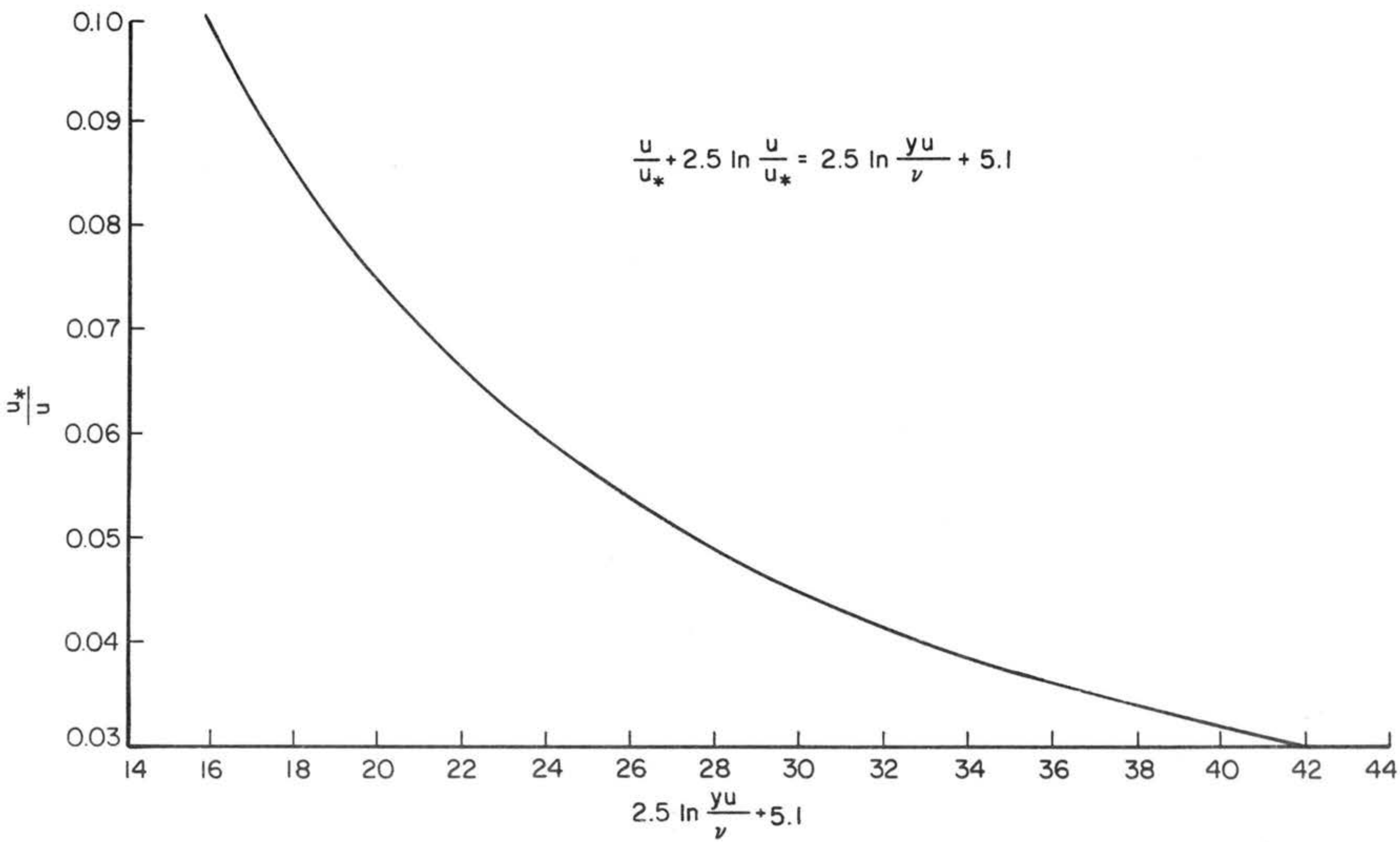

Figure 31 Determining u*/u from local measured data of a smooth wall turbulent boundary layer

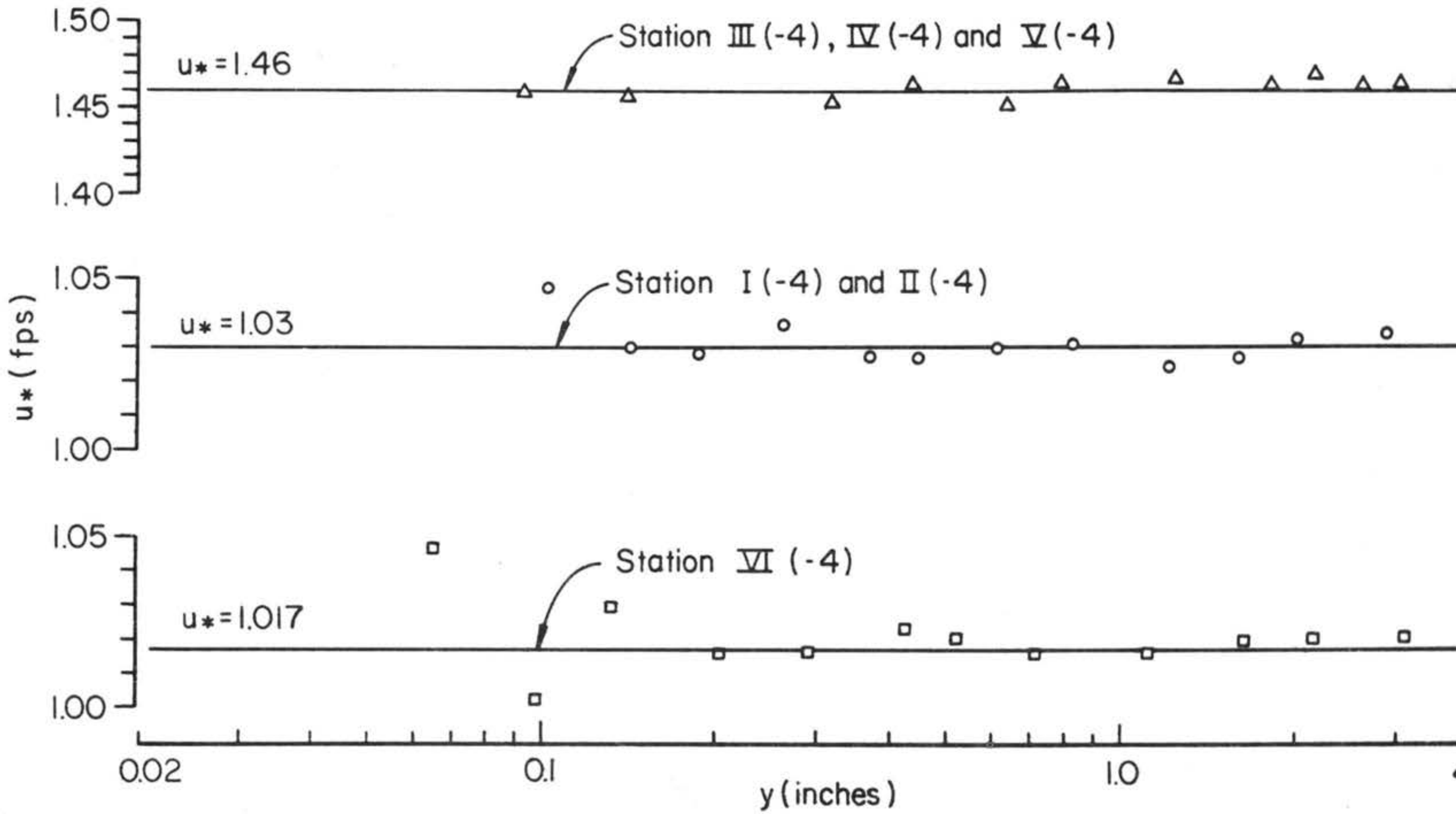

Figure 32 u* as a function of height for stations at x = - 4 ft

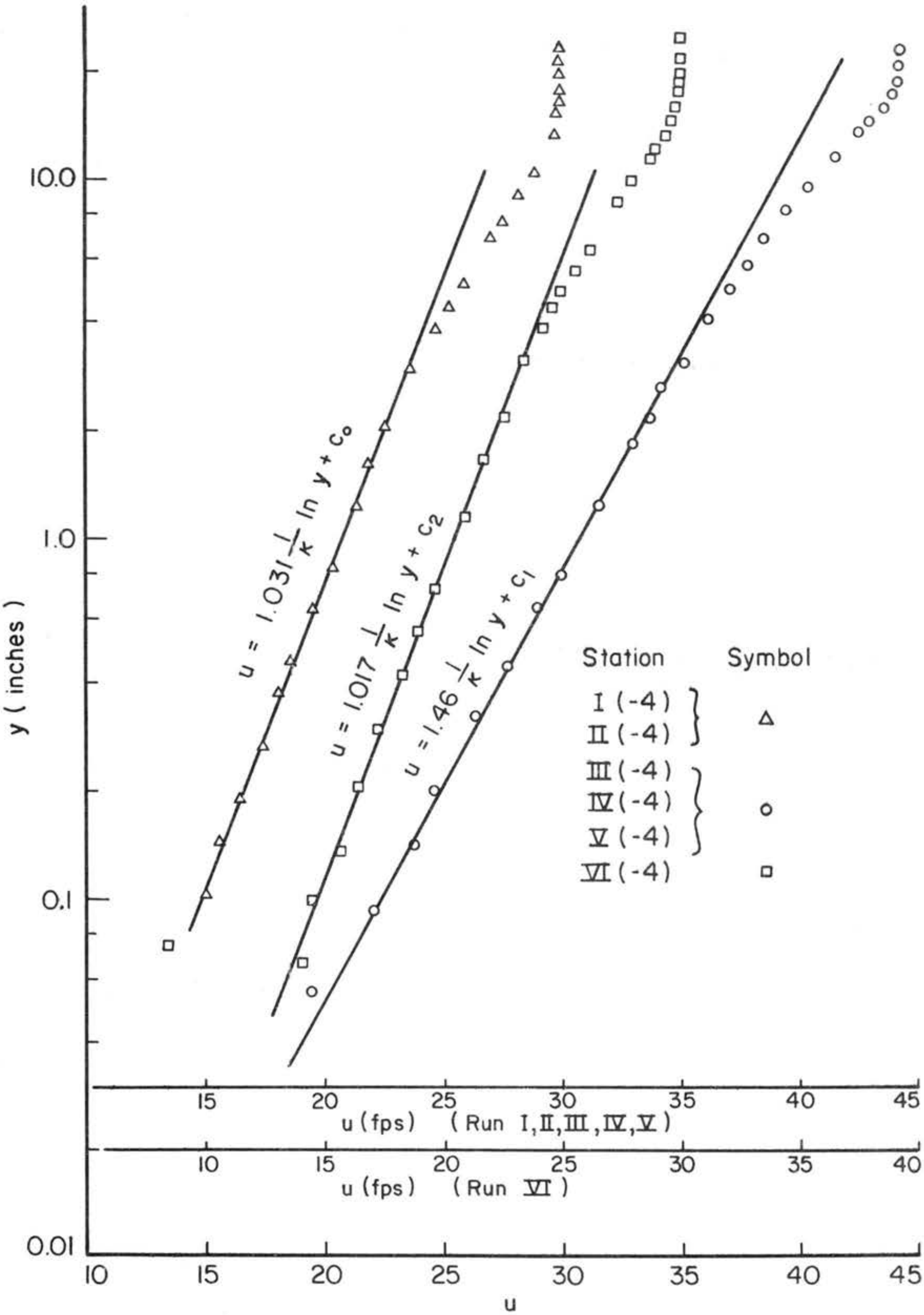

Figure 33 Semi-log plot of the velocity profiles at stations x = - 4 ft

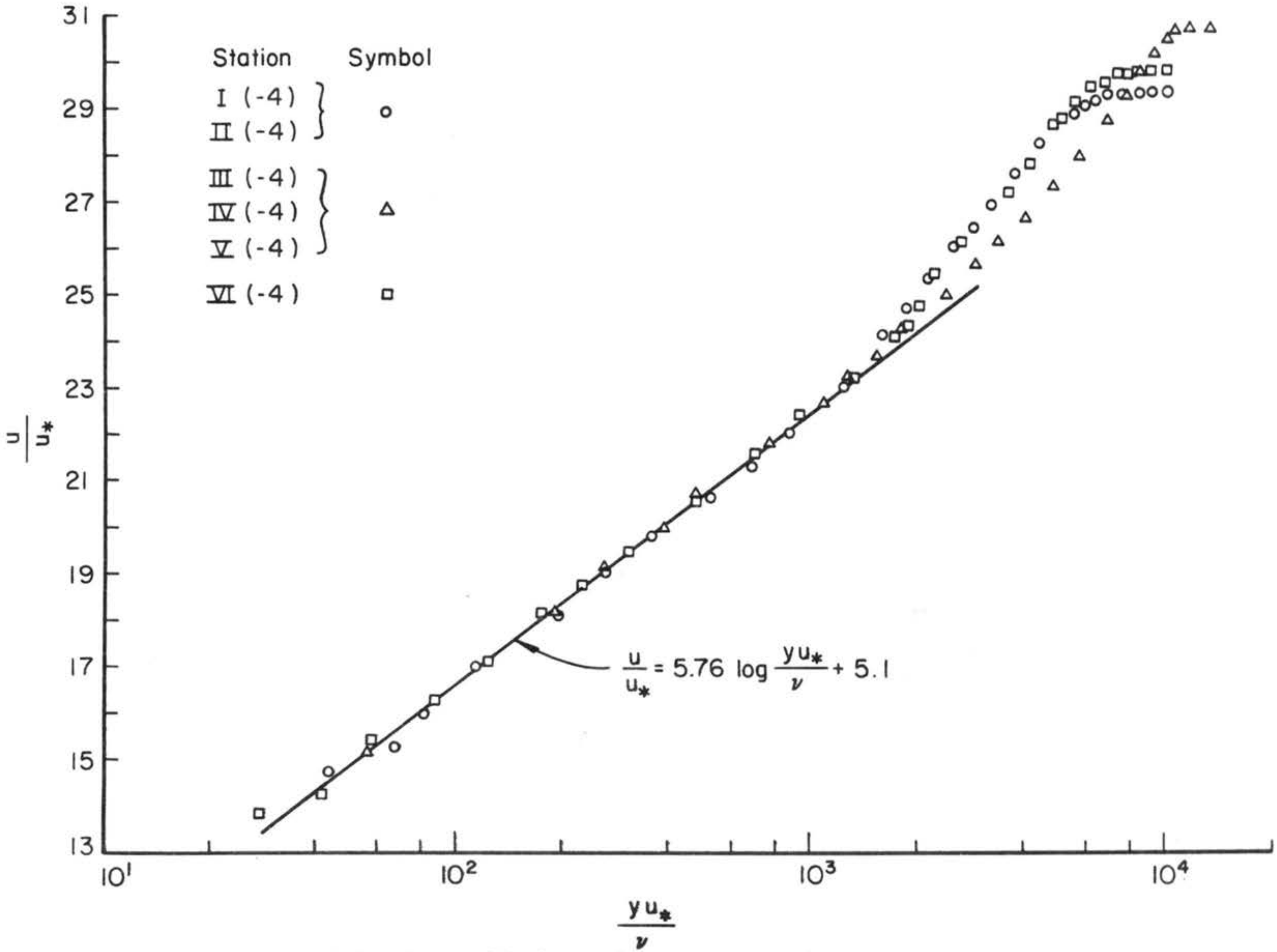

Figure 34 The wall law plots at stations x = - 4 ft

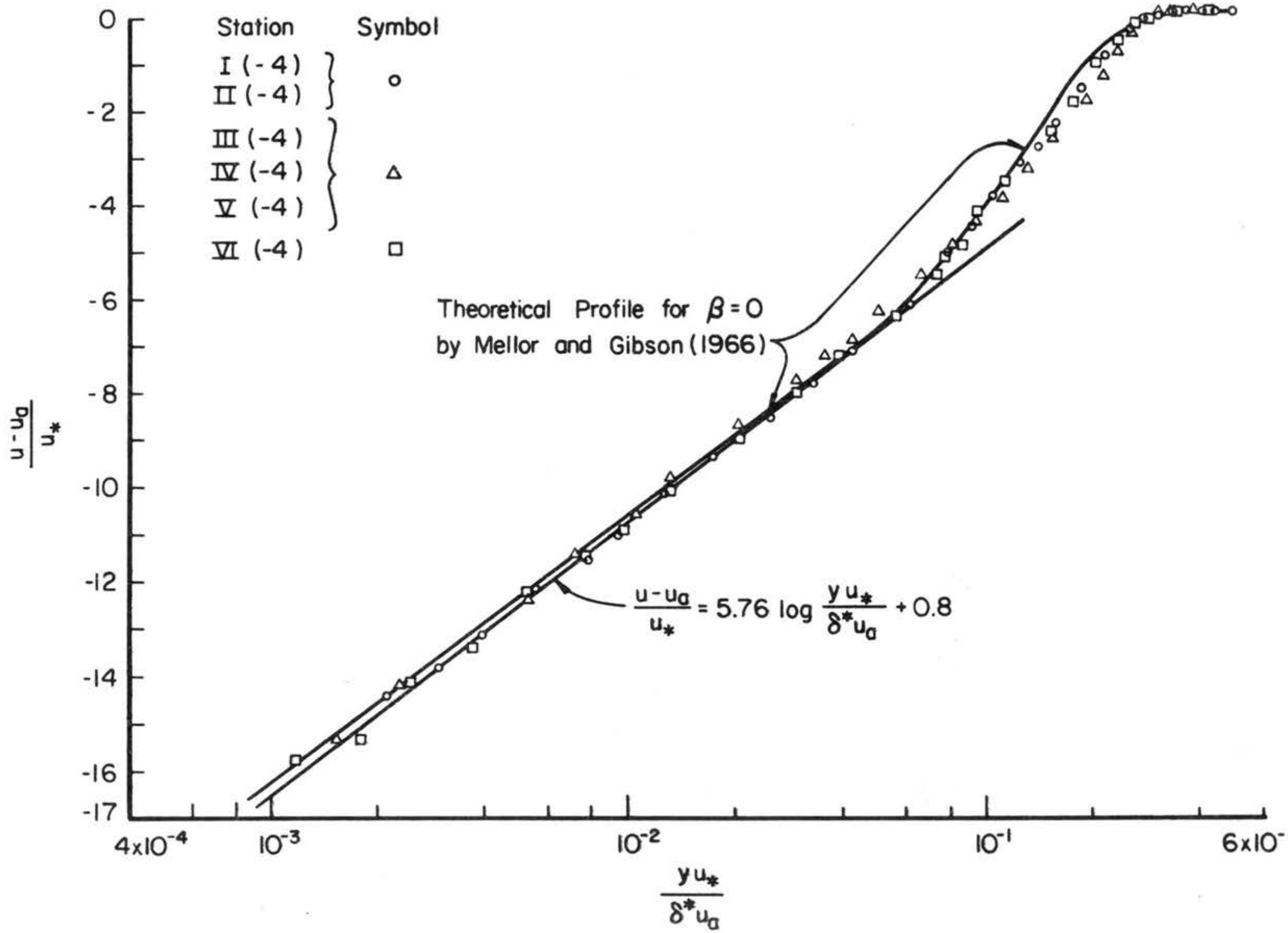

Figure 35 The defect law plots at stations x = - 4 ft

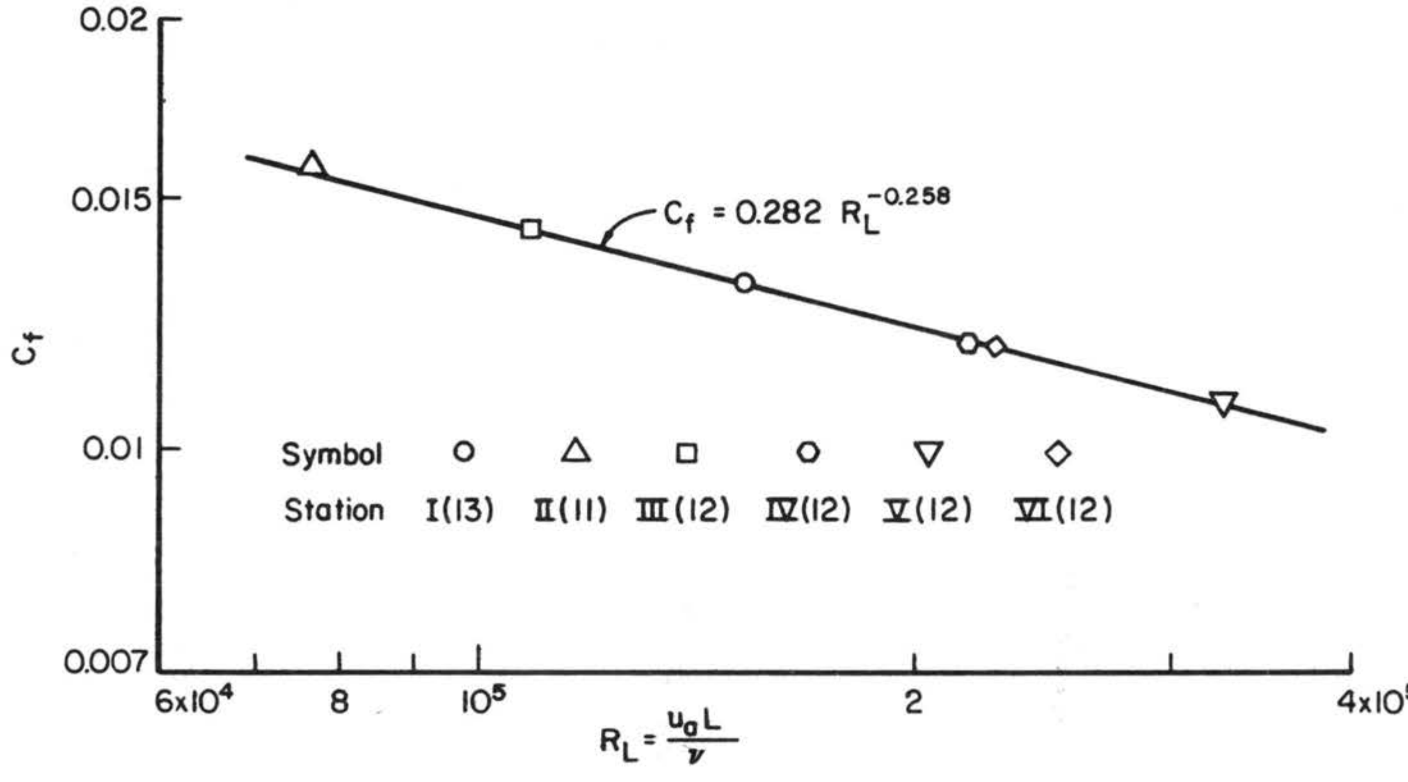

Figure 36 c_f as a function of R_L

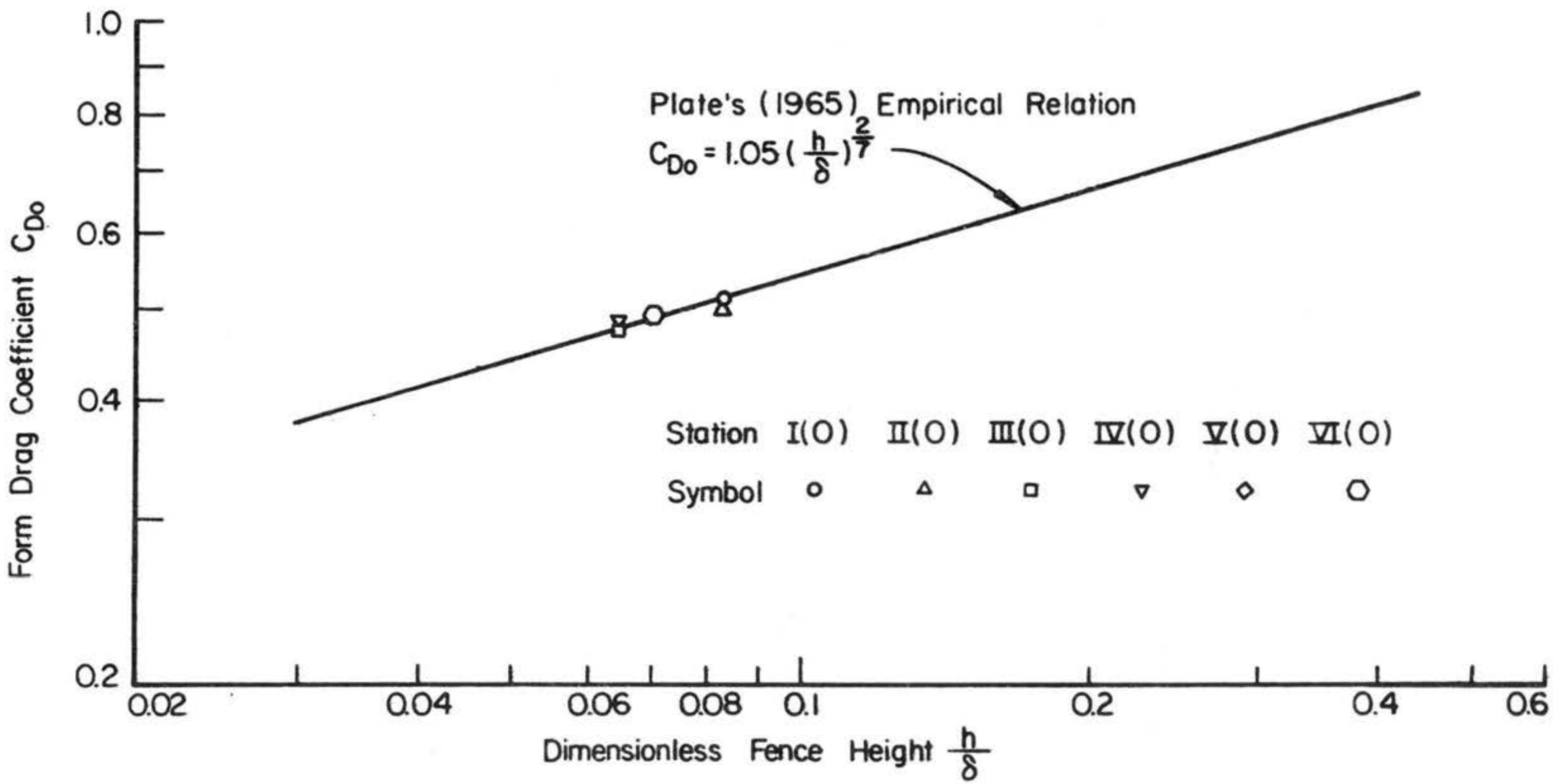

Figure 37 Comparing c_{Do} to Plate's empirical relation

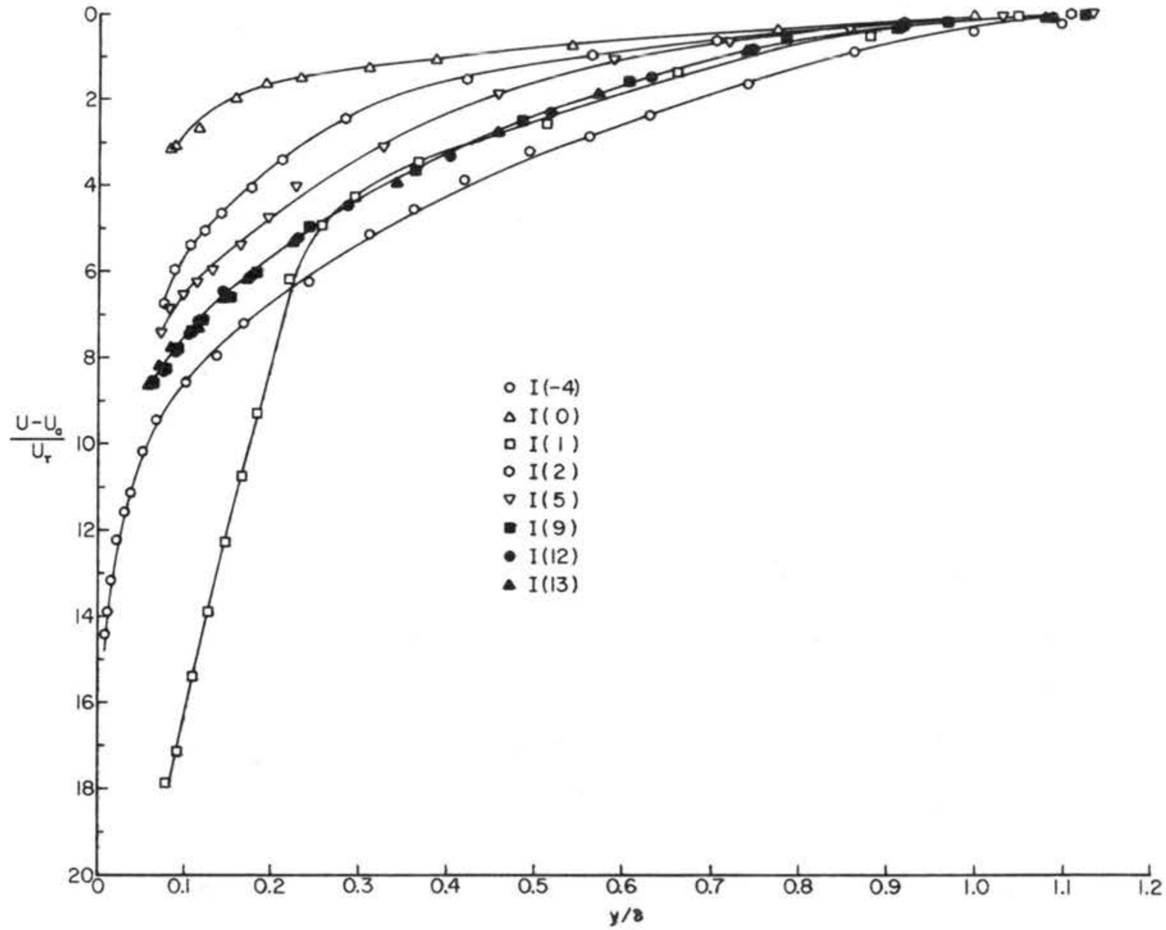

Figure 38 Universal plot of the velocity profiles of Run I

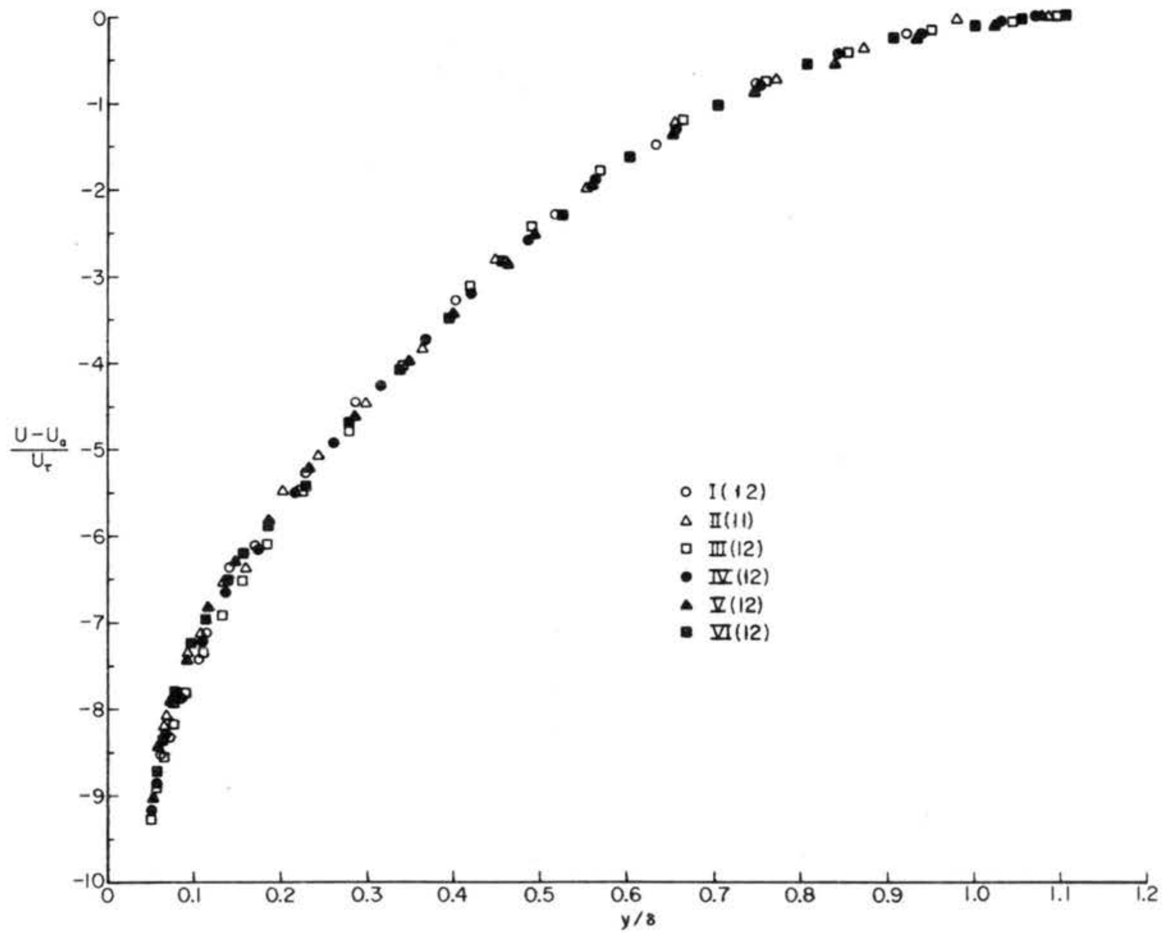

Figure 39 Universal plot of the velocity profiles of all six runs

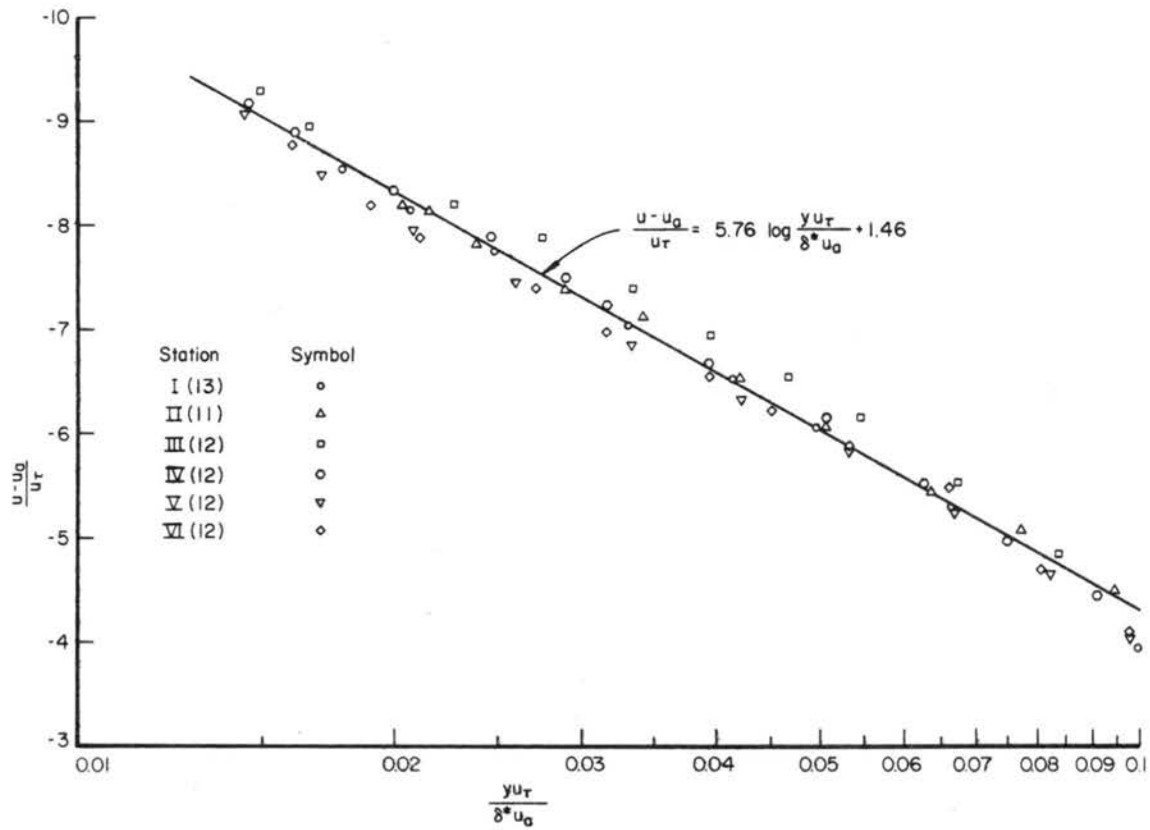

Figure 40 Universal plots of the overlap region at Stations I(13), II(11), III(12), IV(12), V(12) and VI(12)

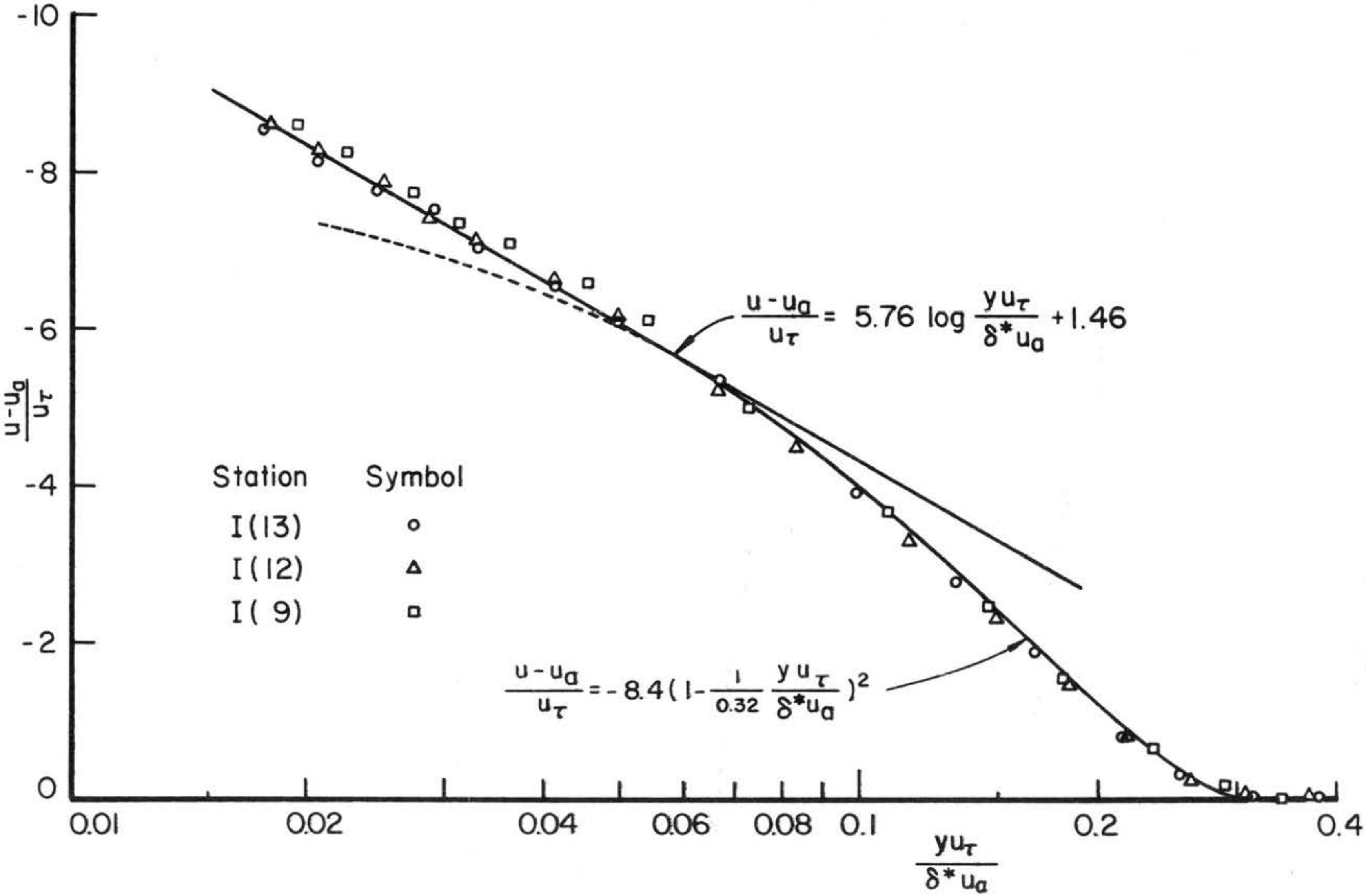

Figure 41 The defect law plot of Run I

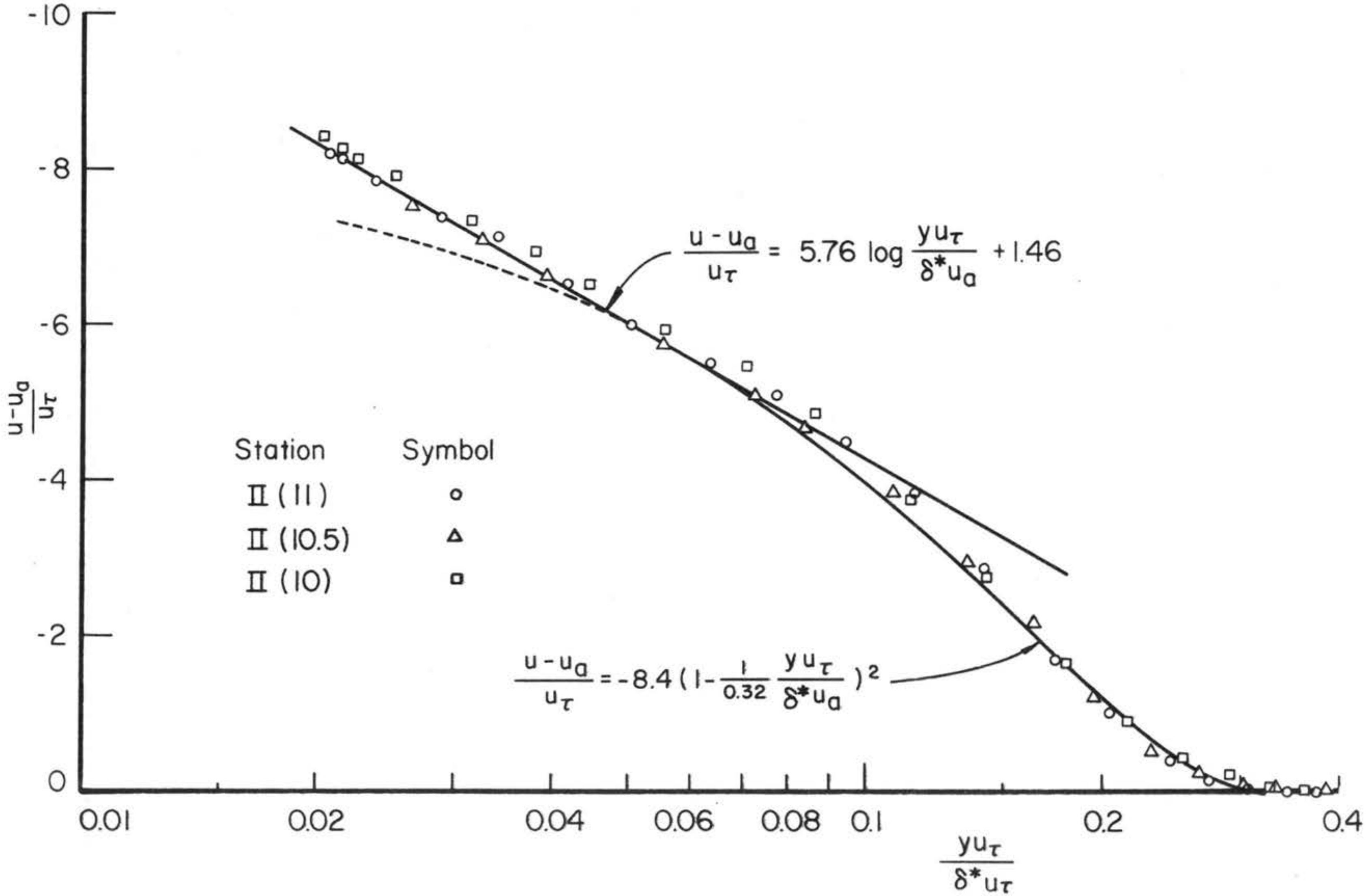

Figure 42 Defect law plot of Run II

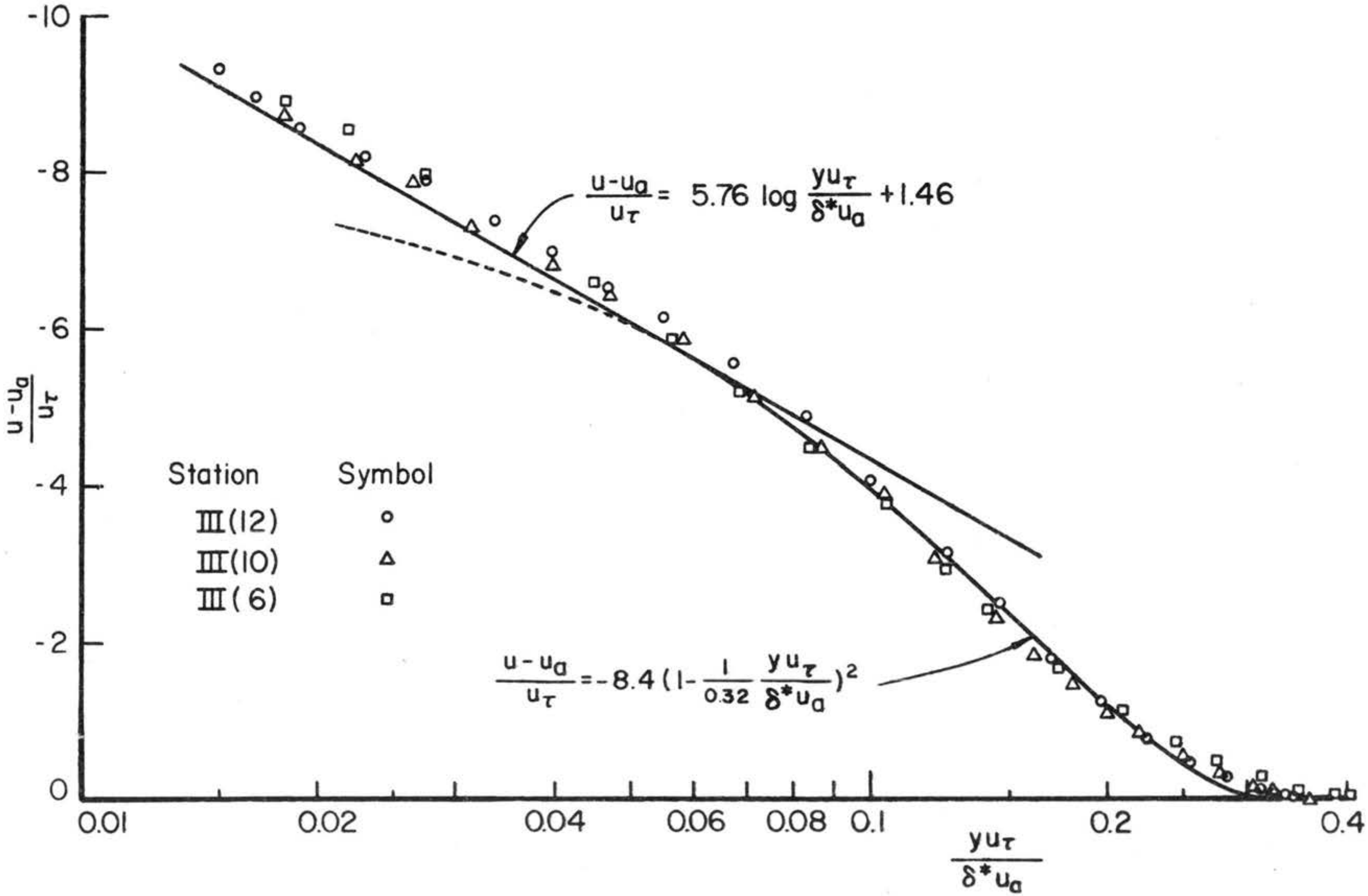

Figure 43 Defect law plot of Run III

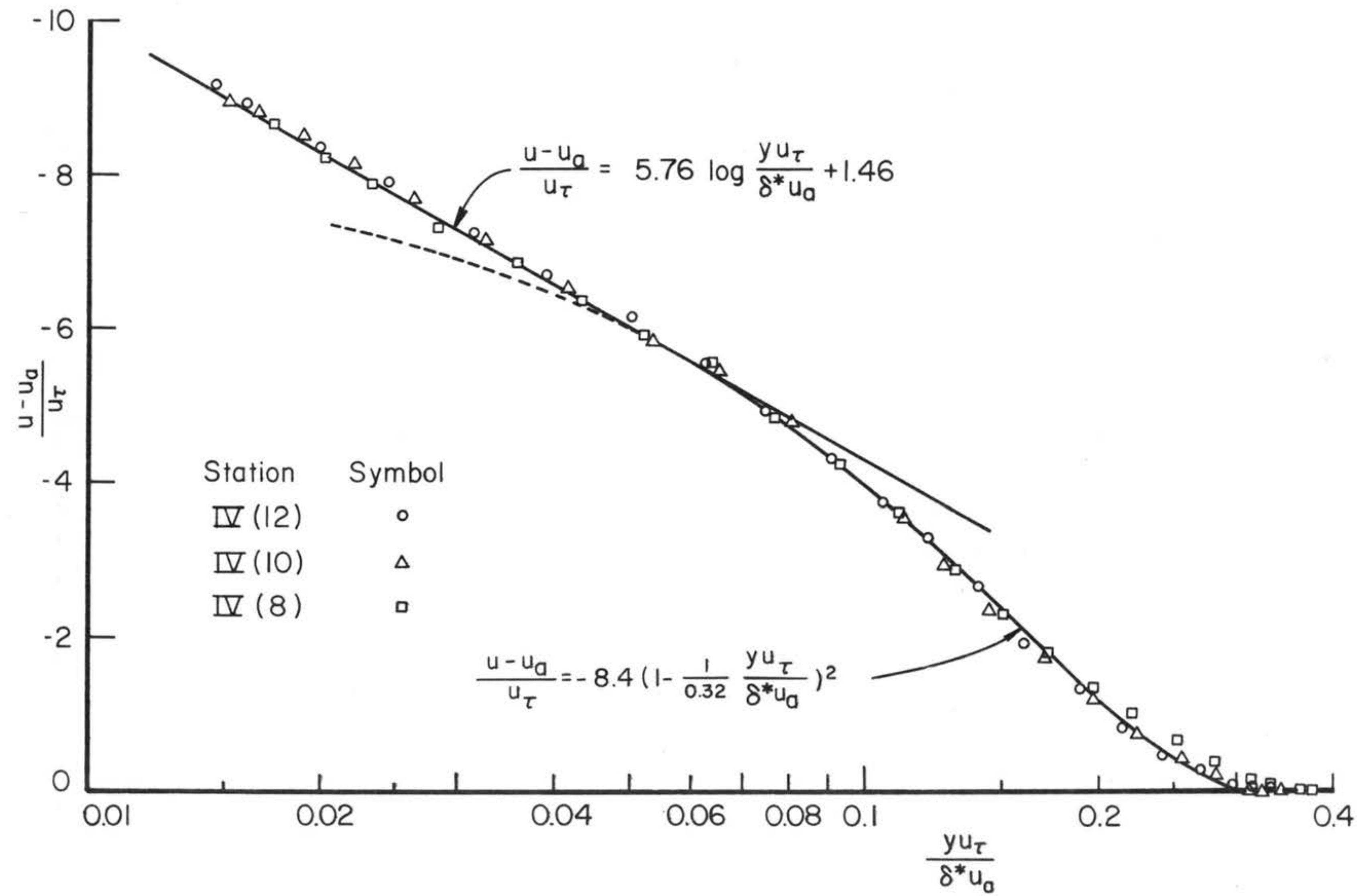

Figure 44 Defect law plot of Run IV

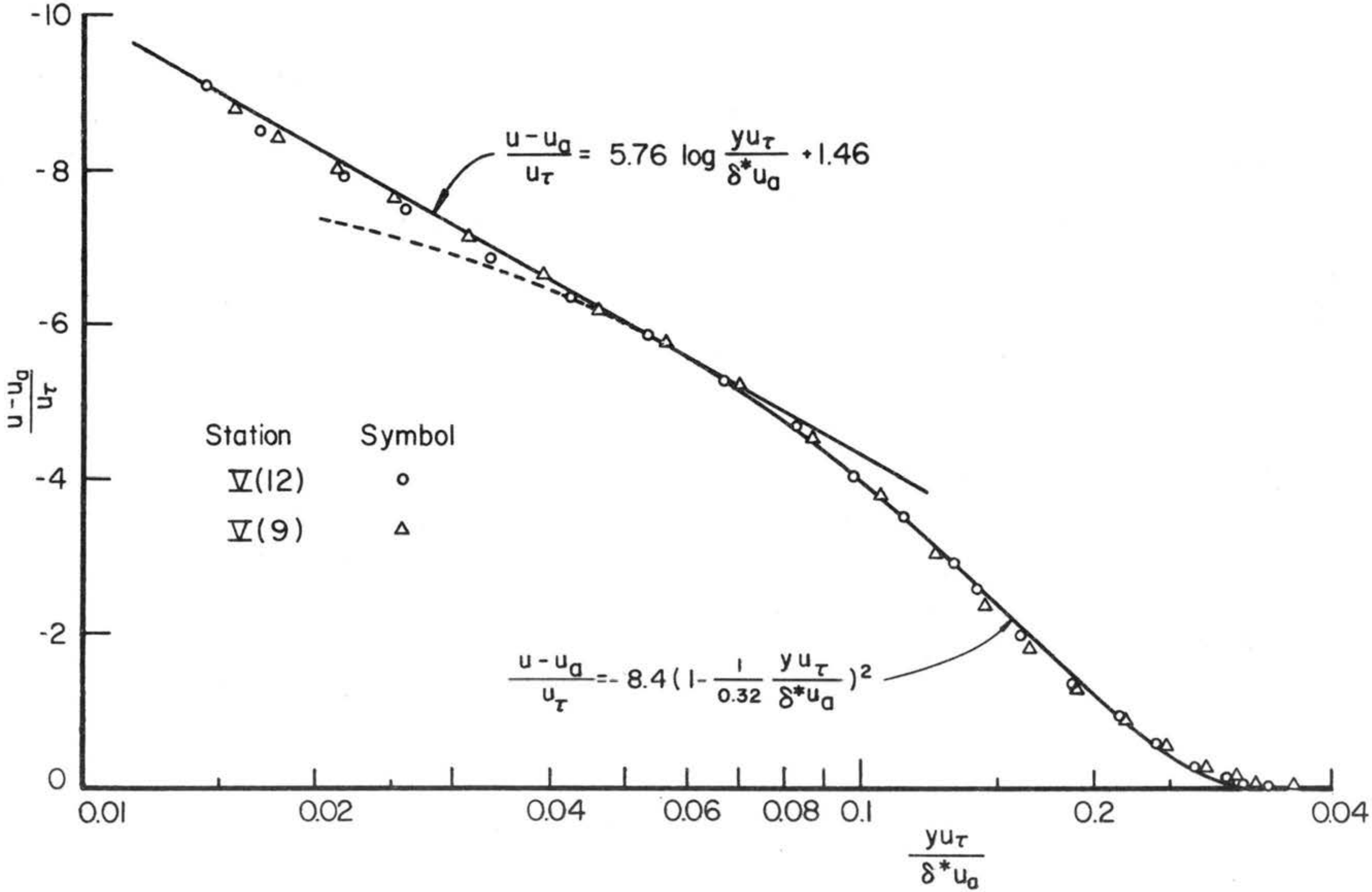

Figure 45 Defect law plot of Run V

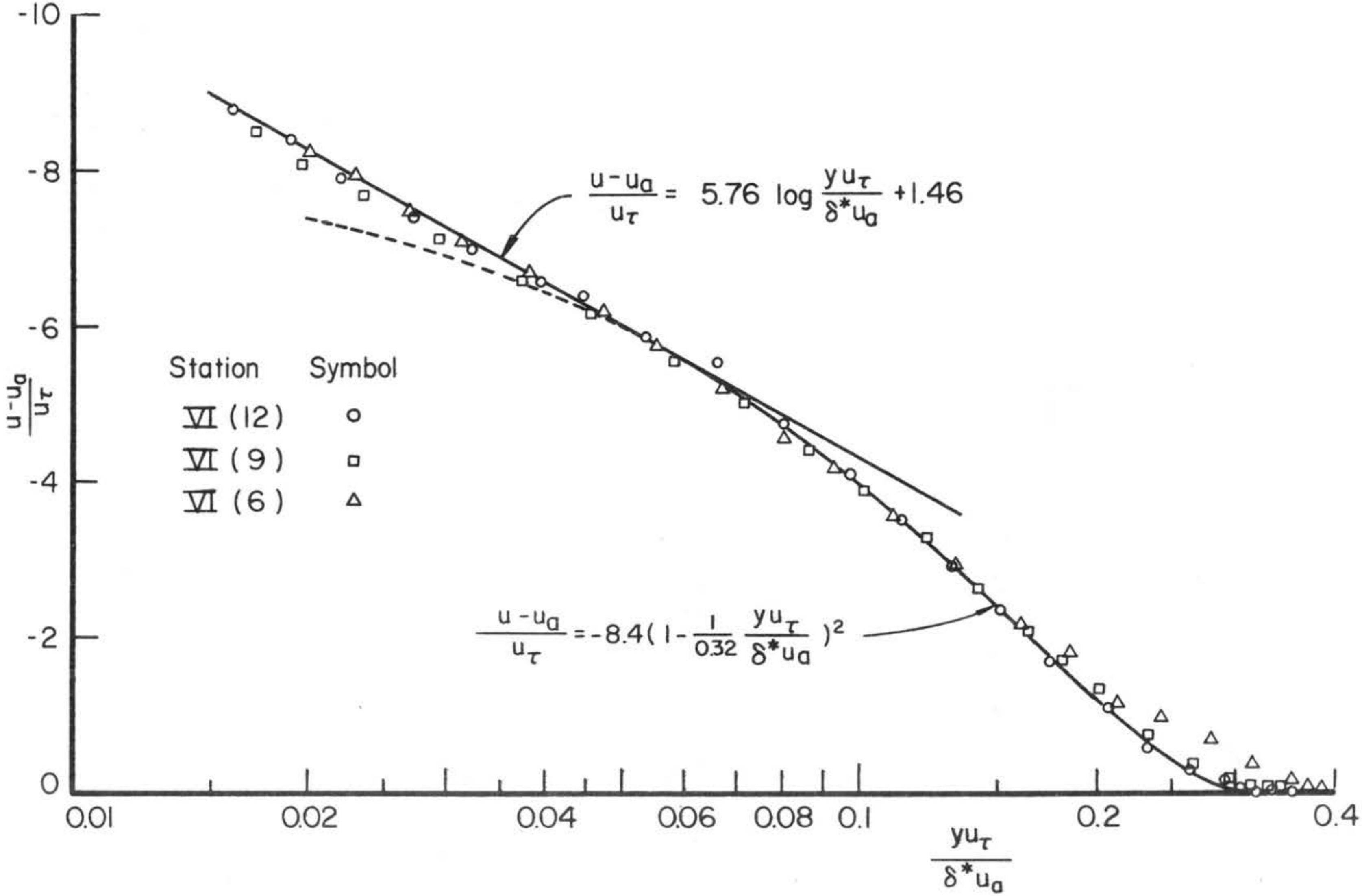

Figure 46 Defect law plot of Run VI

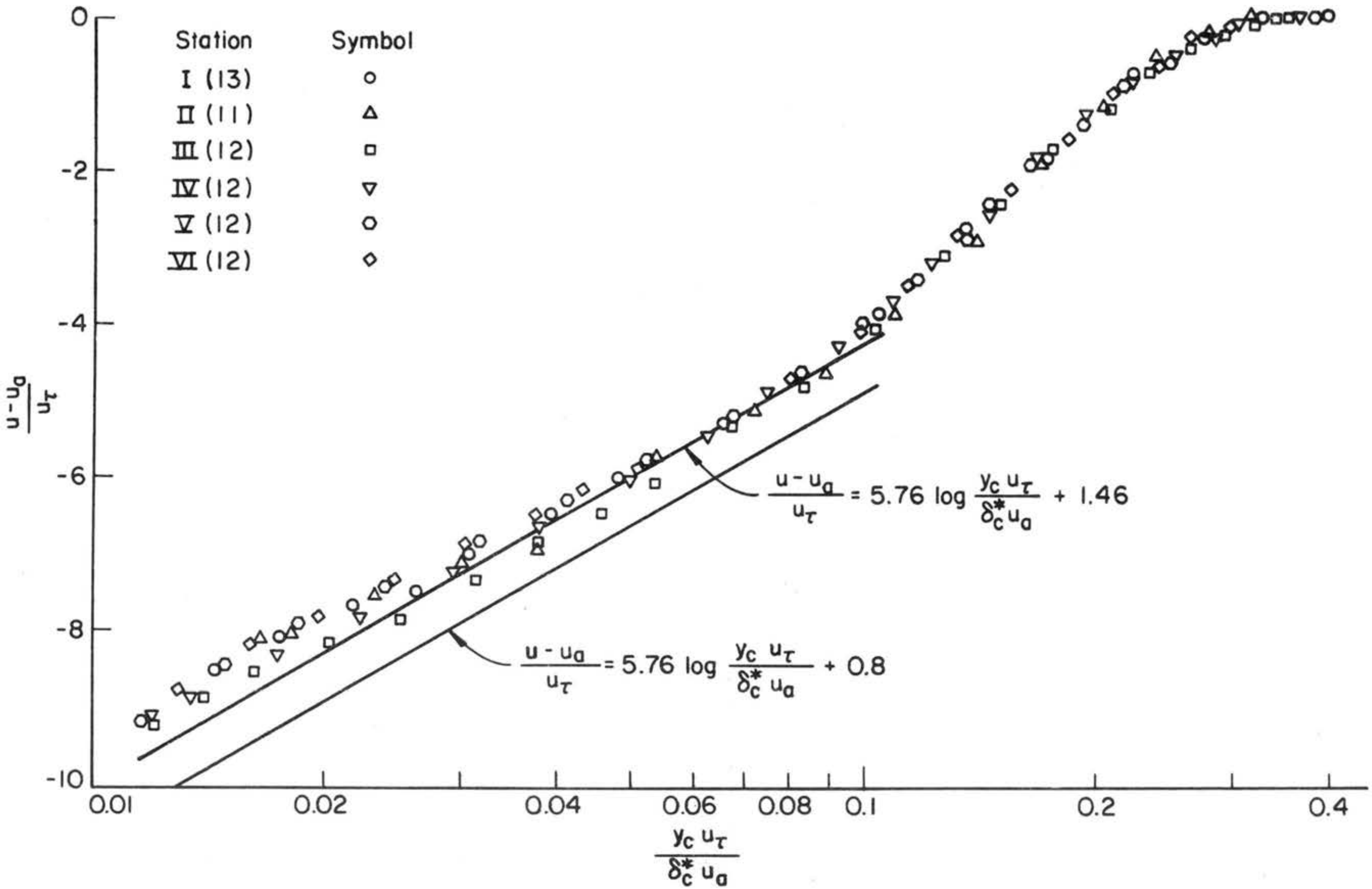

Figure 46a Defect law plots by chosen $\varepsilon = \frac{3}{4}$ h

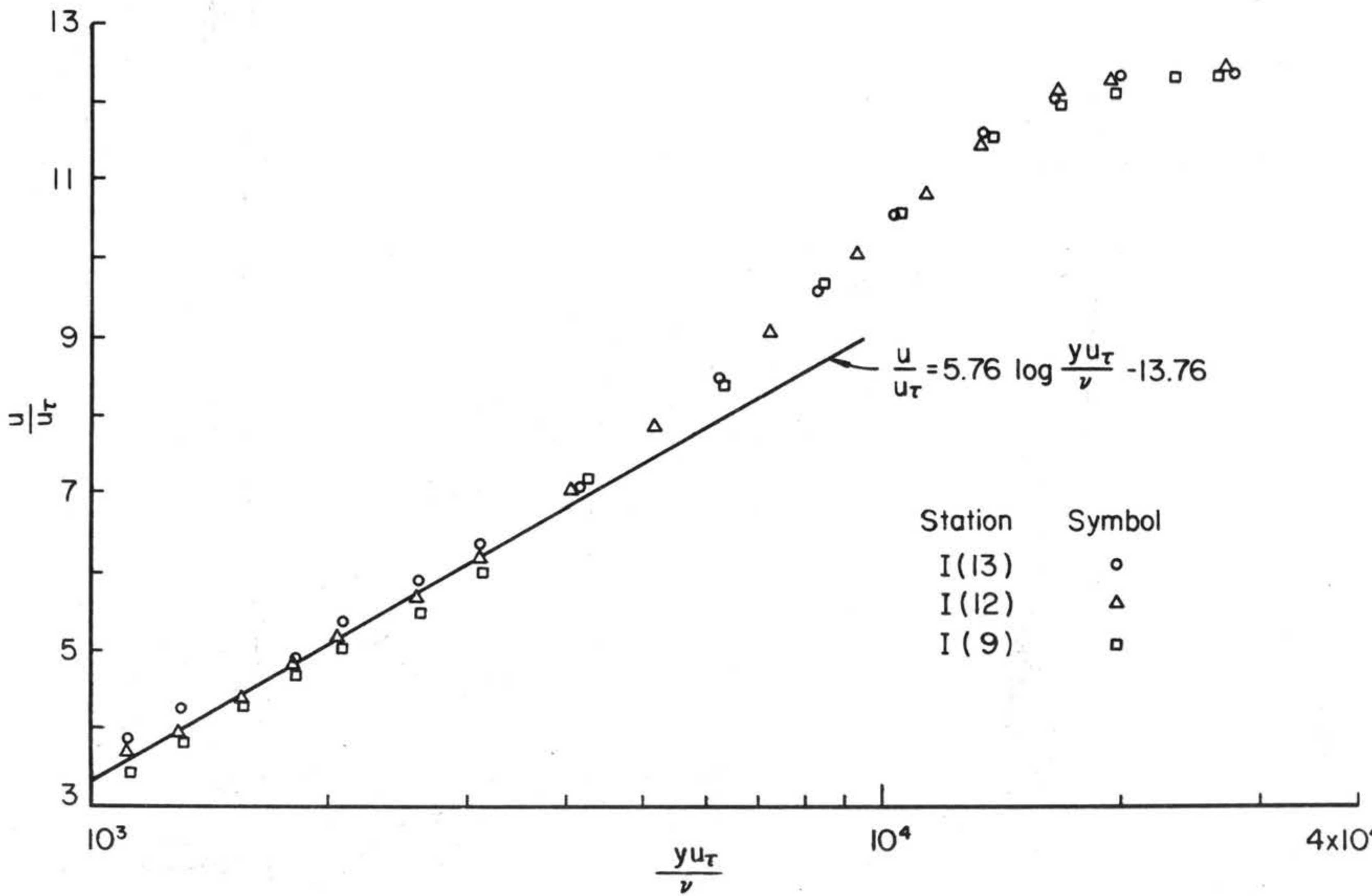

Figure 47 The wall plot of Run I

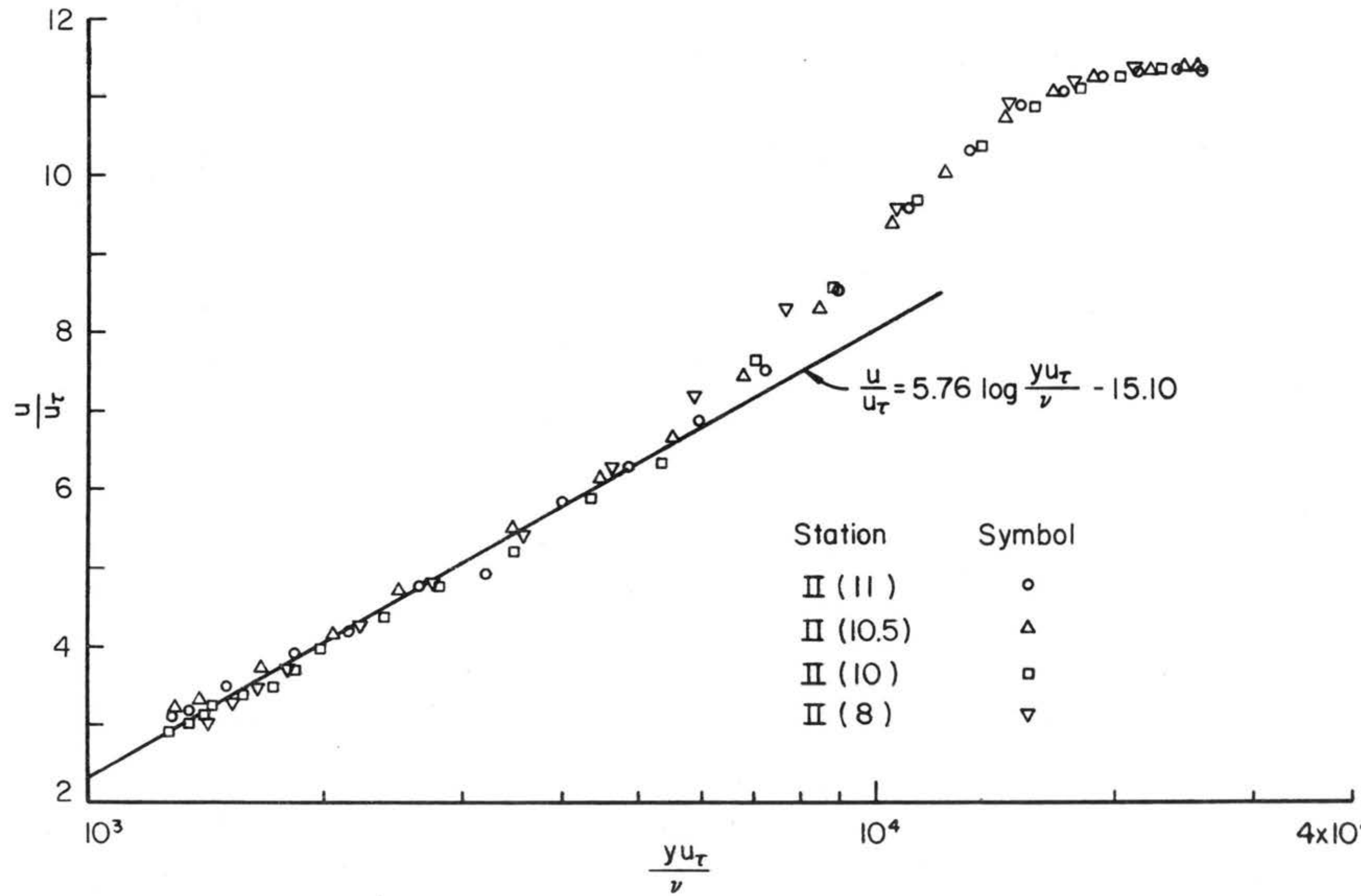

Figure 48 The wall law plot of Run II

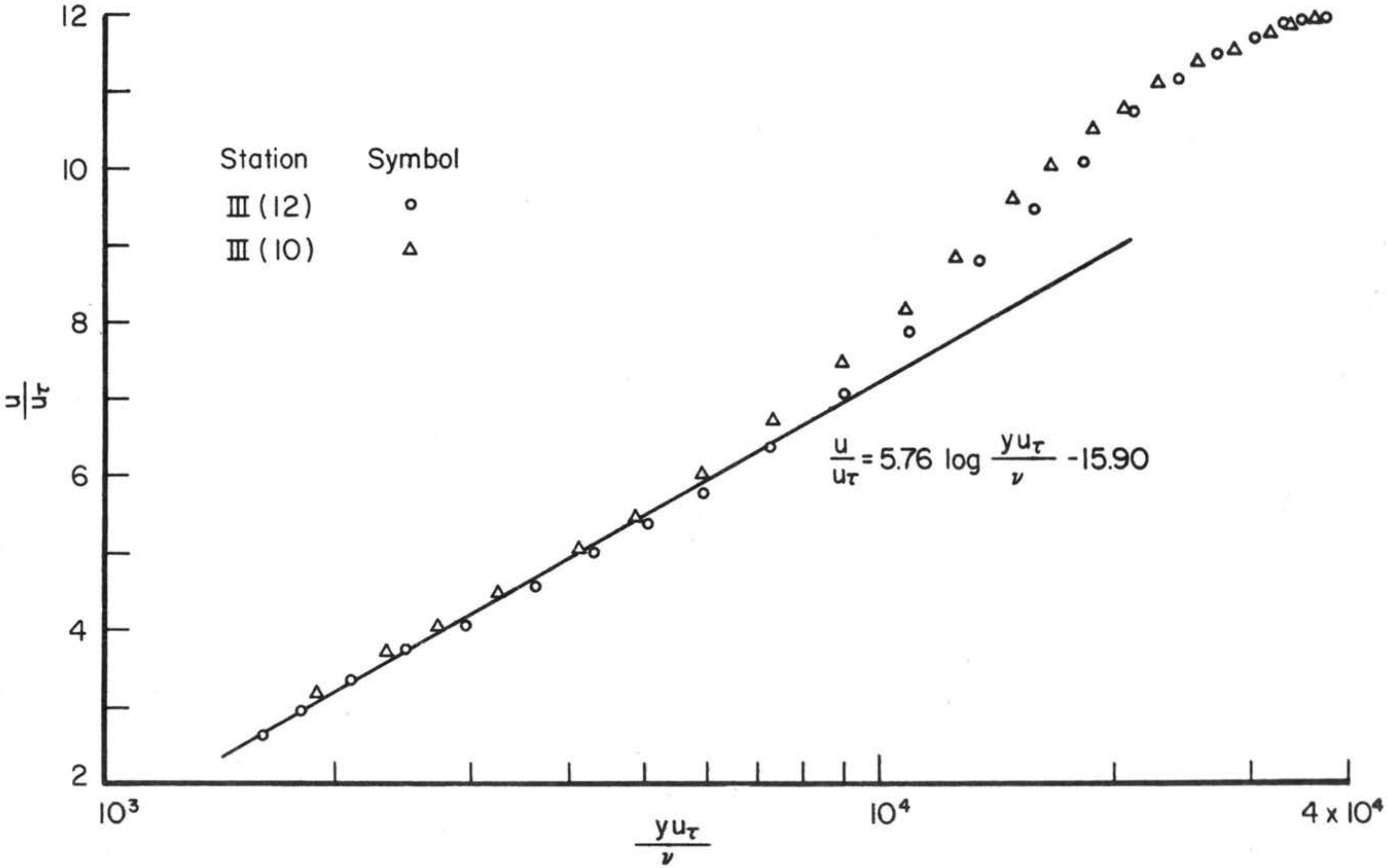

Figure 49 The wall law plot of Run III

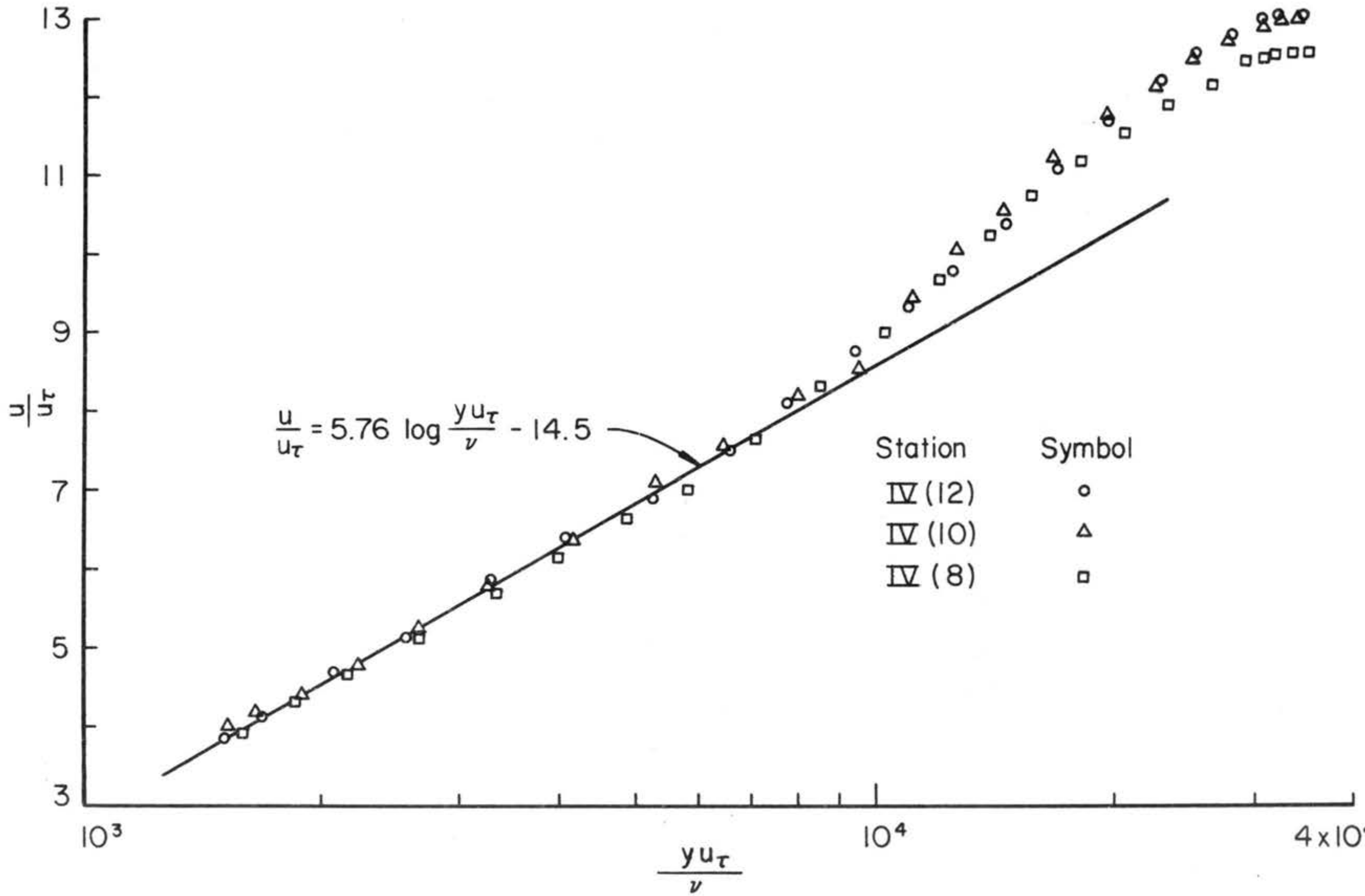

Figure 50 The wall law plot of Run IV

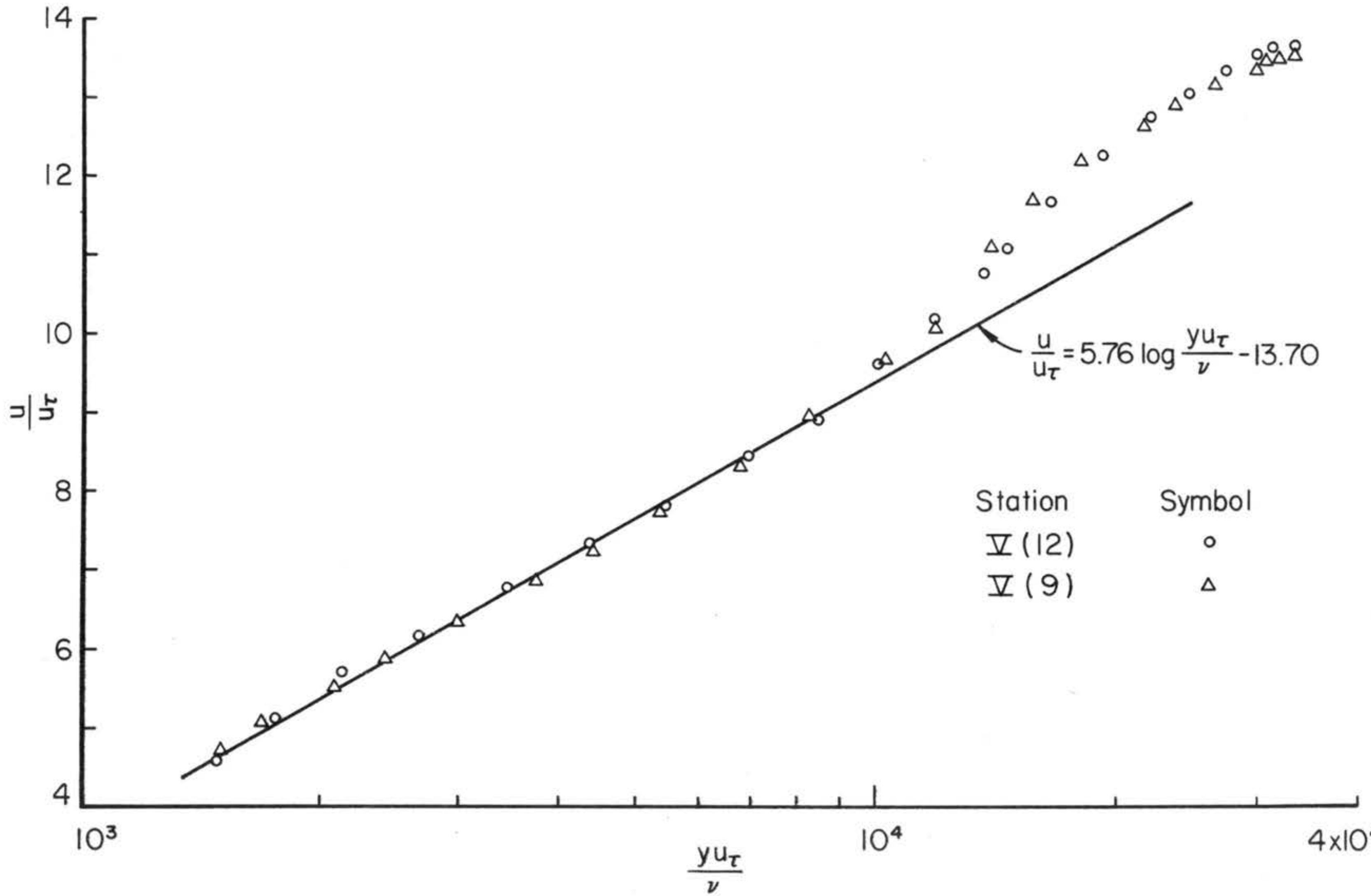

Figure 51 The wall law plot of Run V

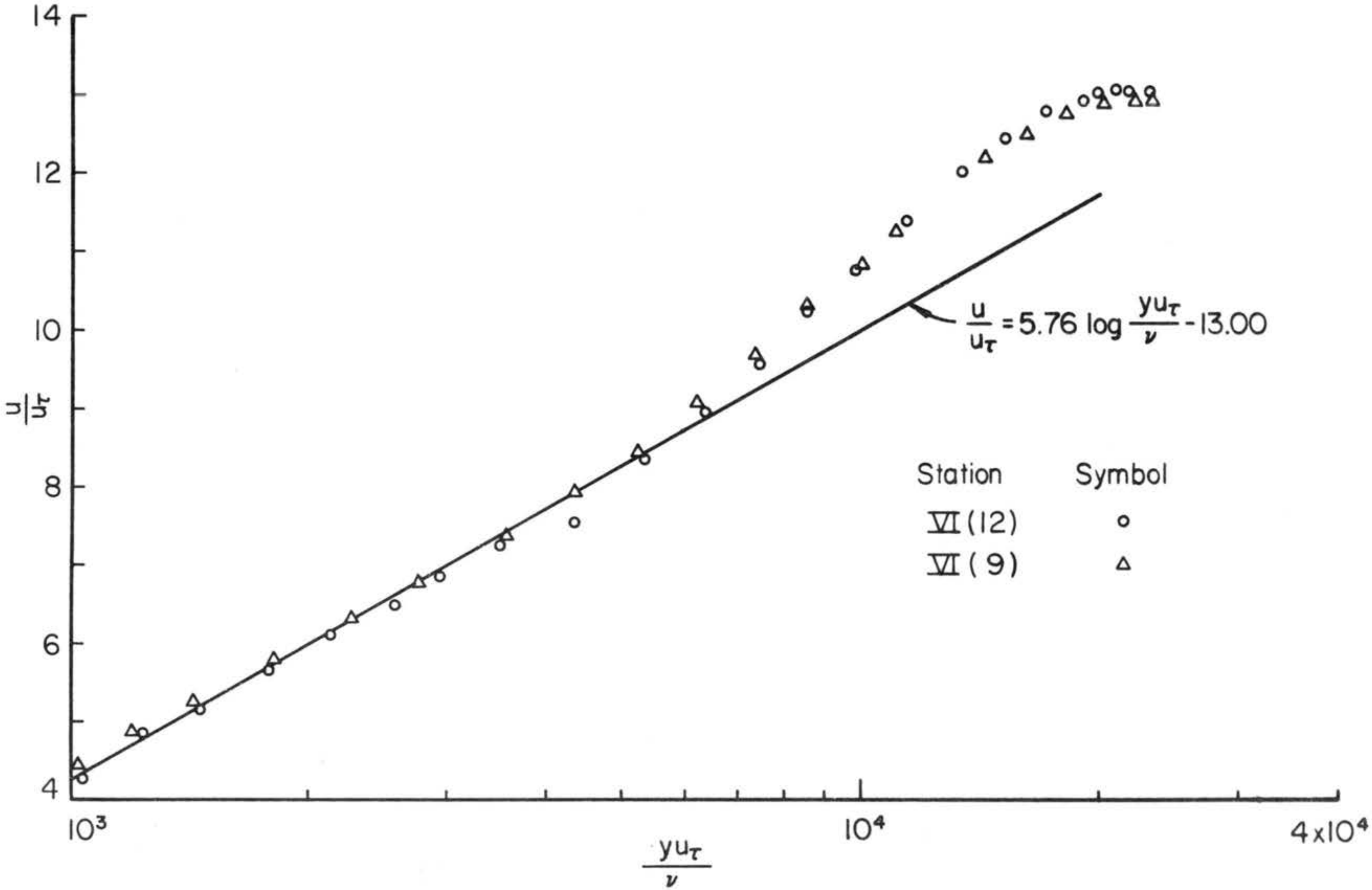

Figure 52 The wall law plot of Run VI

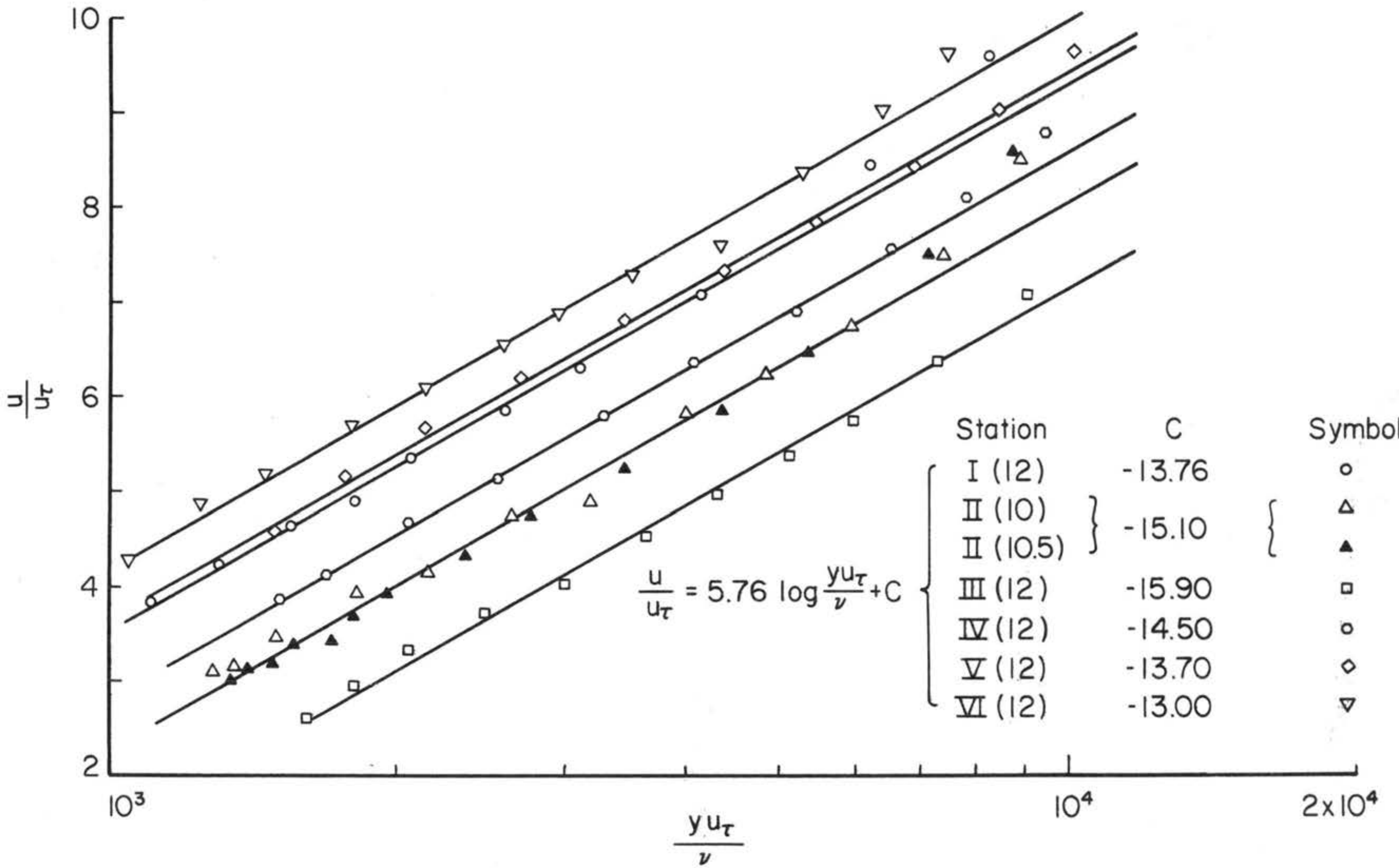

Figure 53 The wall law plot of all six runs

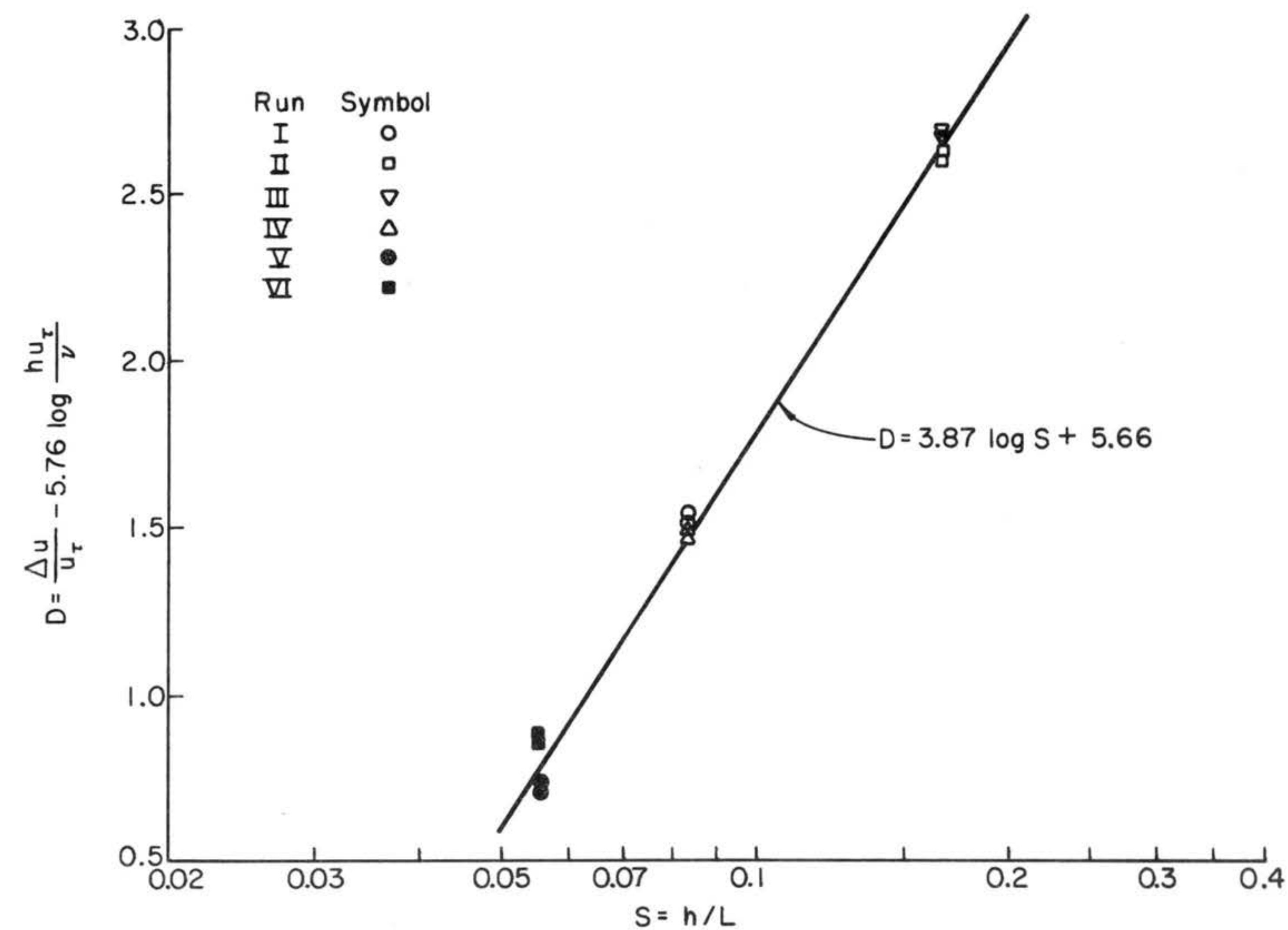

Figure 54 The roughness function as a function of the fence density

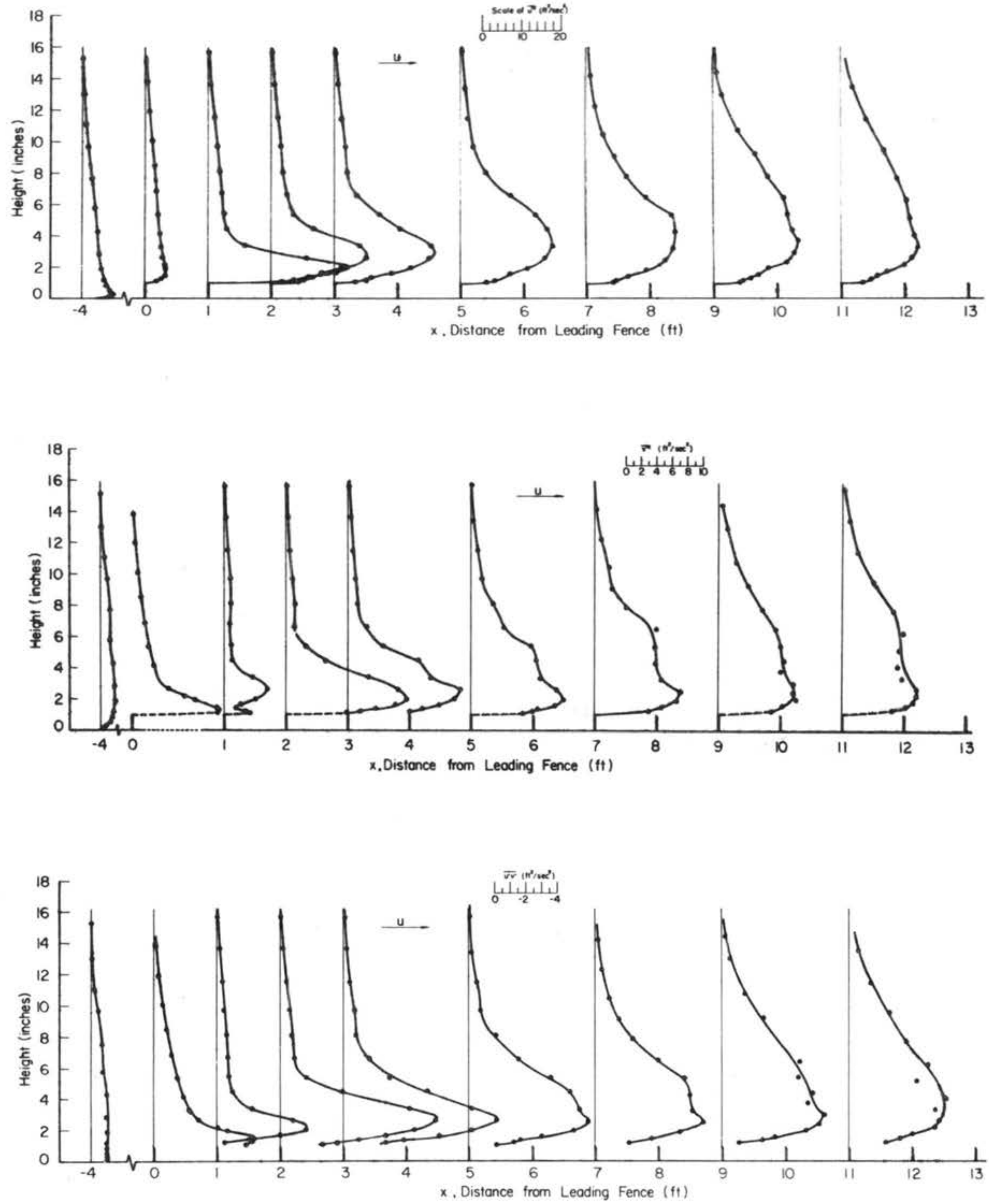

Figure 55 Turbulence distributions of Run I

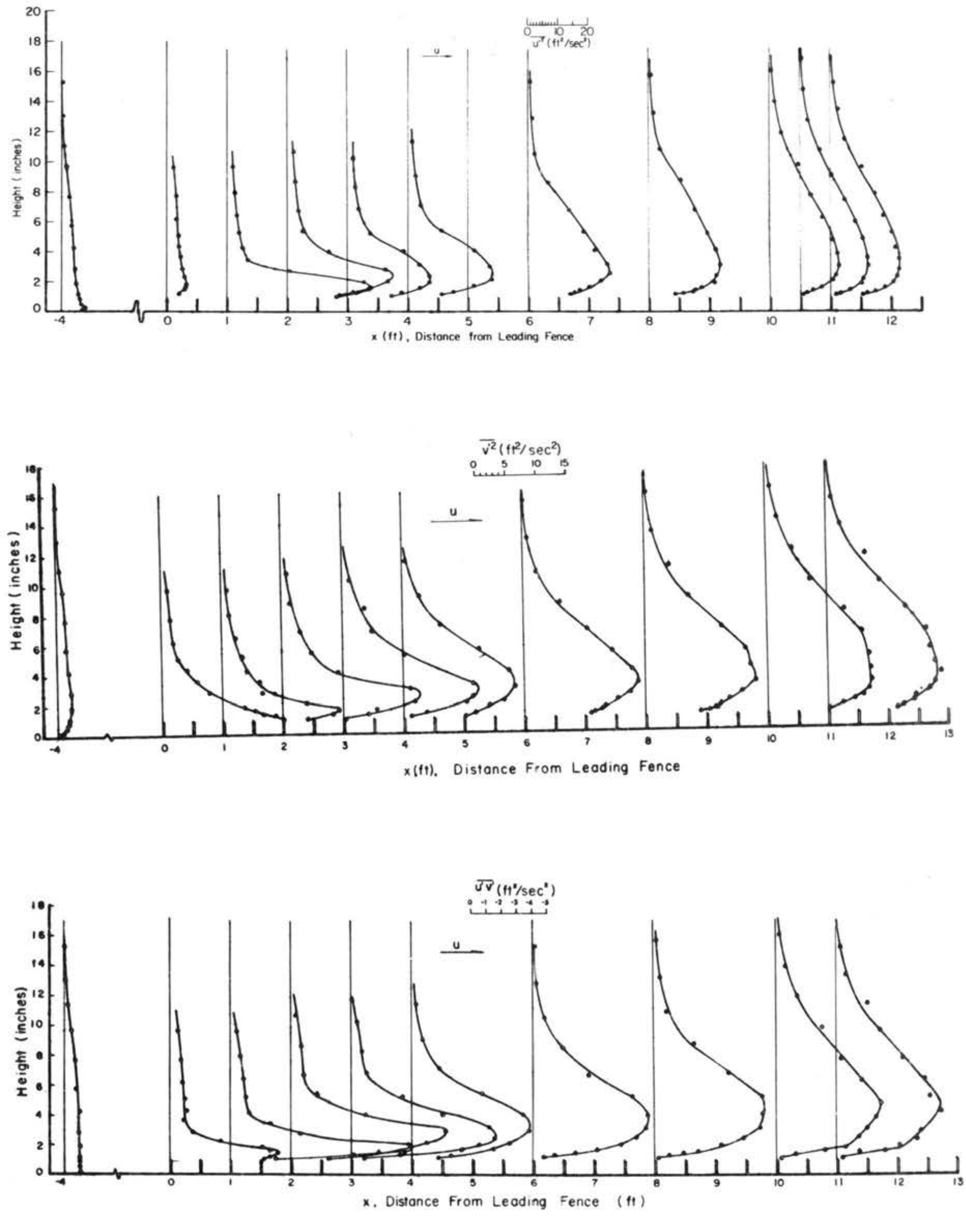

Figure 56 Turbulence distributions of Run II

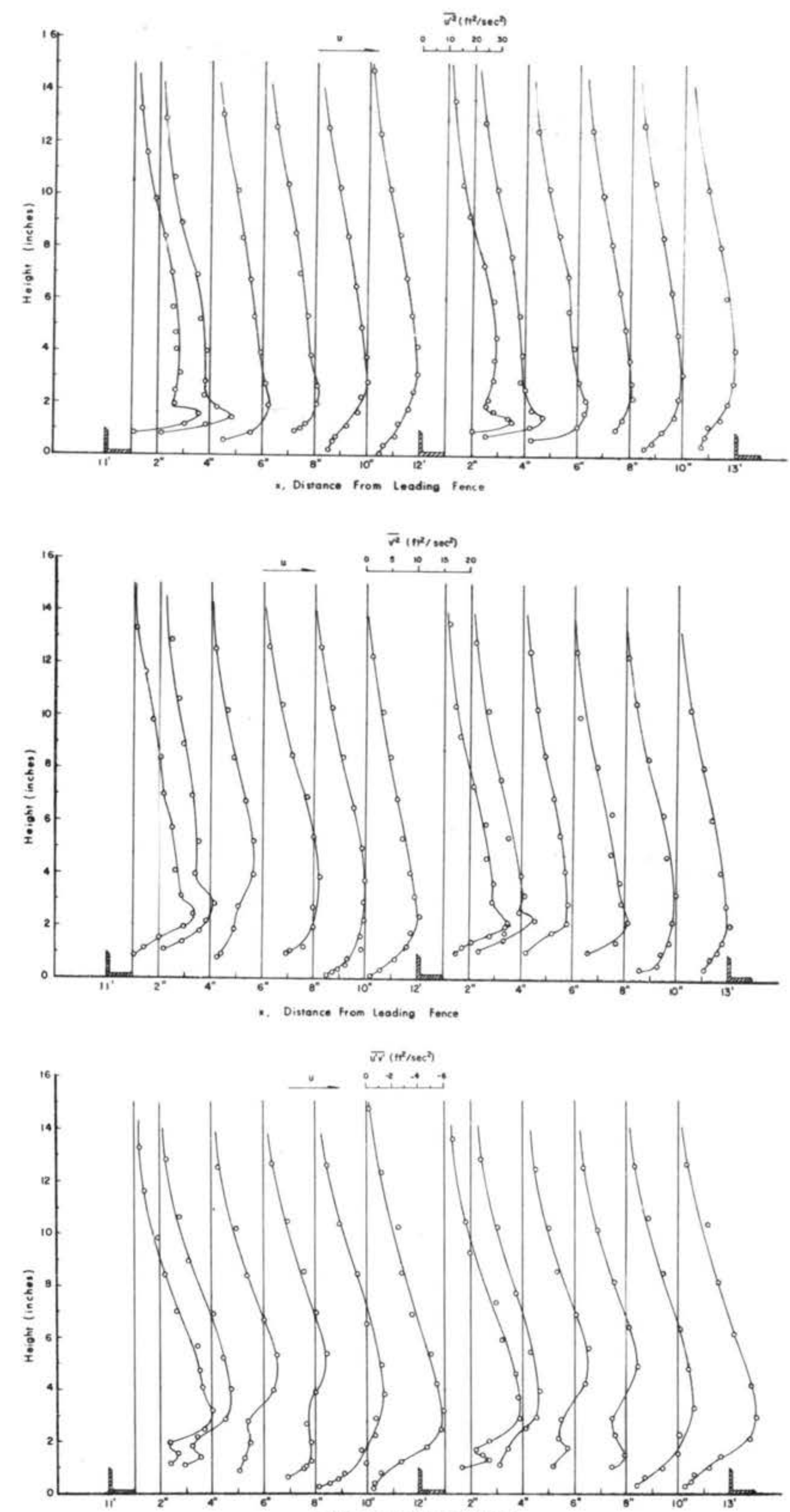

Figure 57 Turbulence distributions of Run Ia

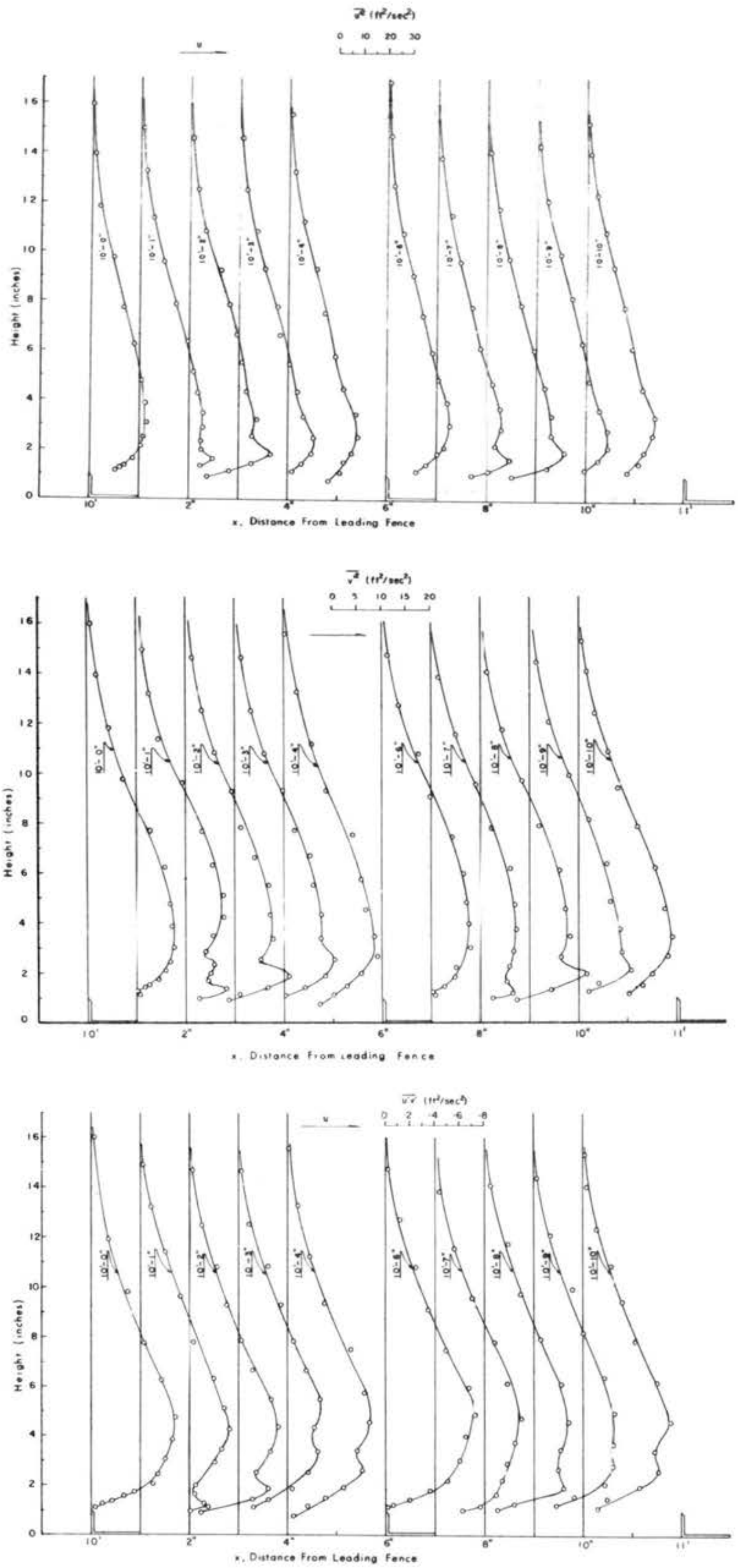

Figure 58 Turbulence distributions of Run IIa

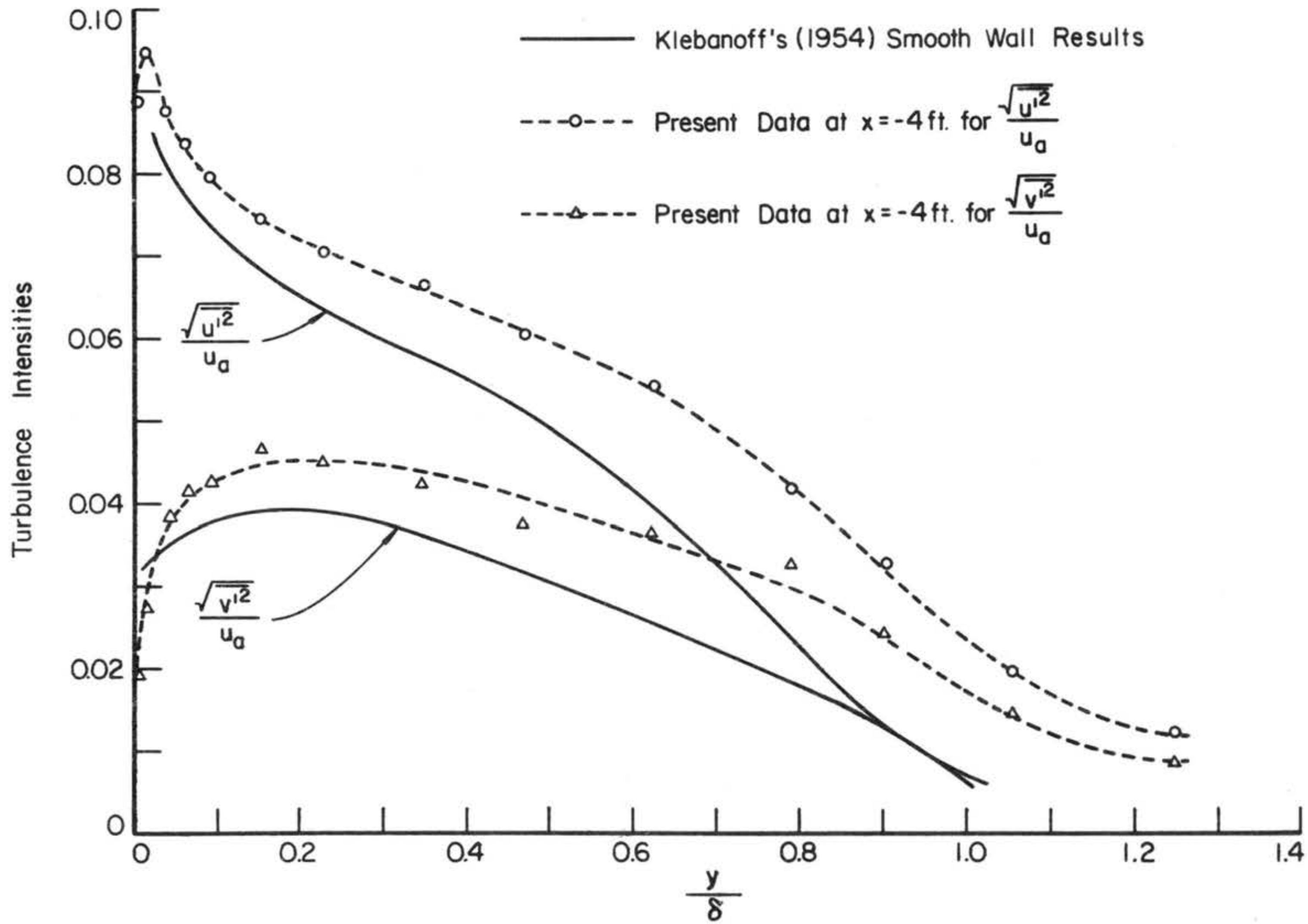

Figure 59 Turbulence distribution at x = - 4 ft

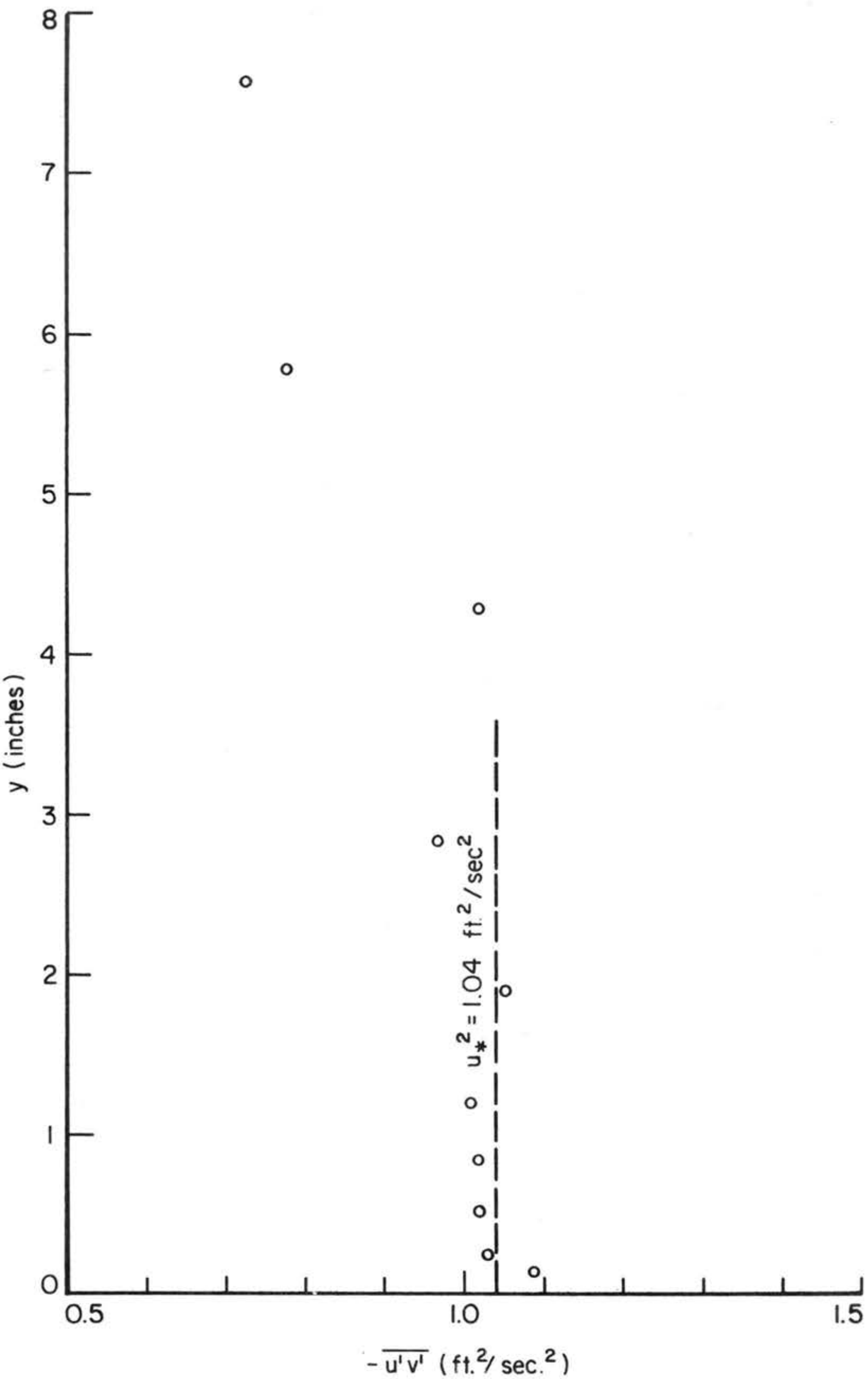

Figure 60 Turbulent shear stress distribution at $x = -4$ ft

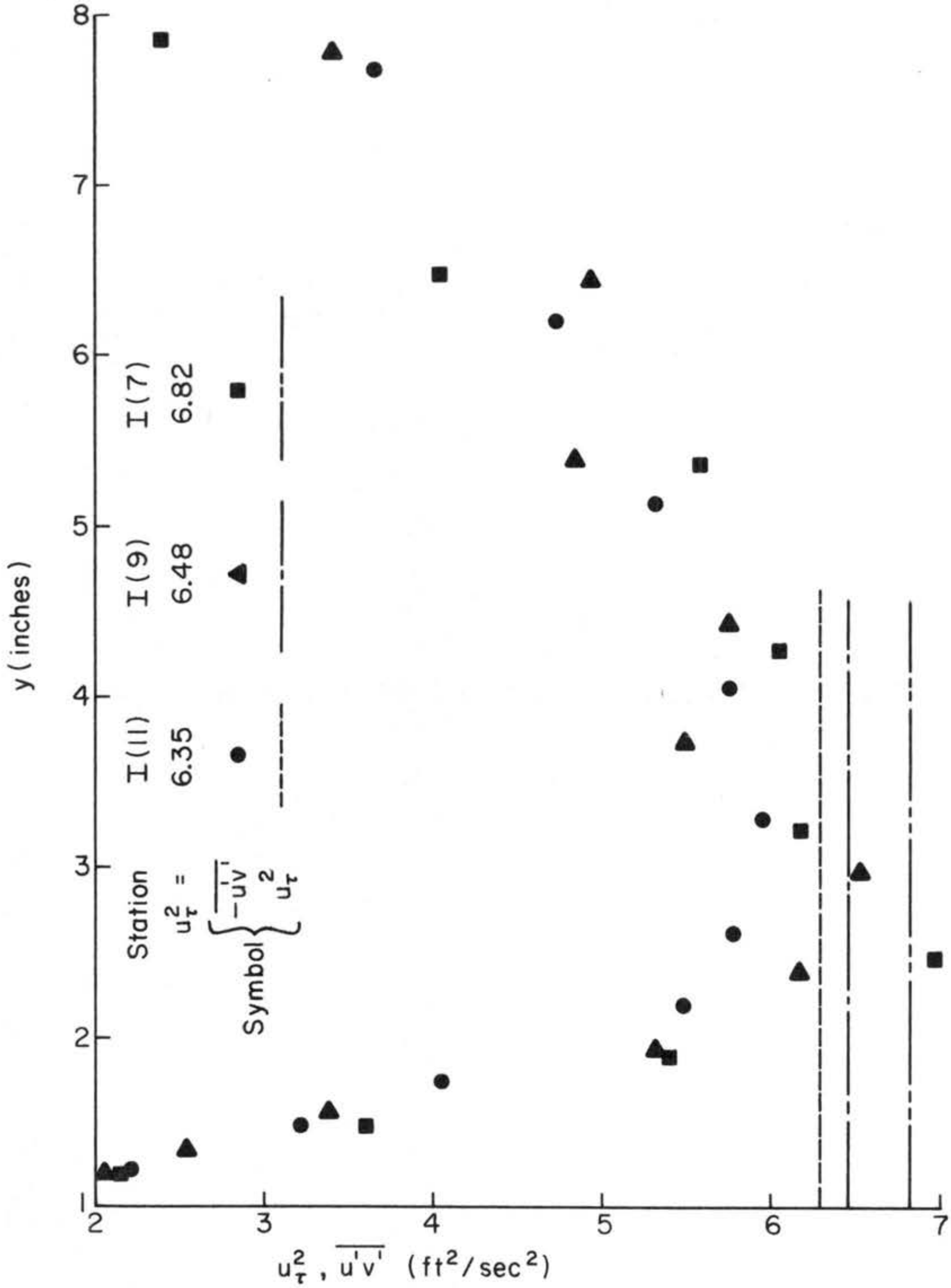

Figure 61 Turbulent shear stress distribution at Stations I(7), I(9) and I(11)

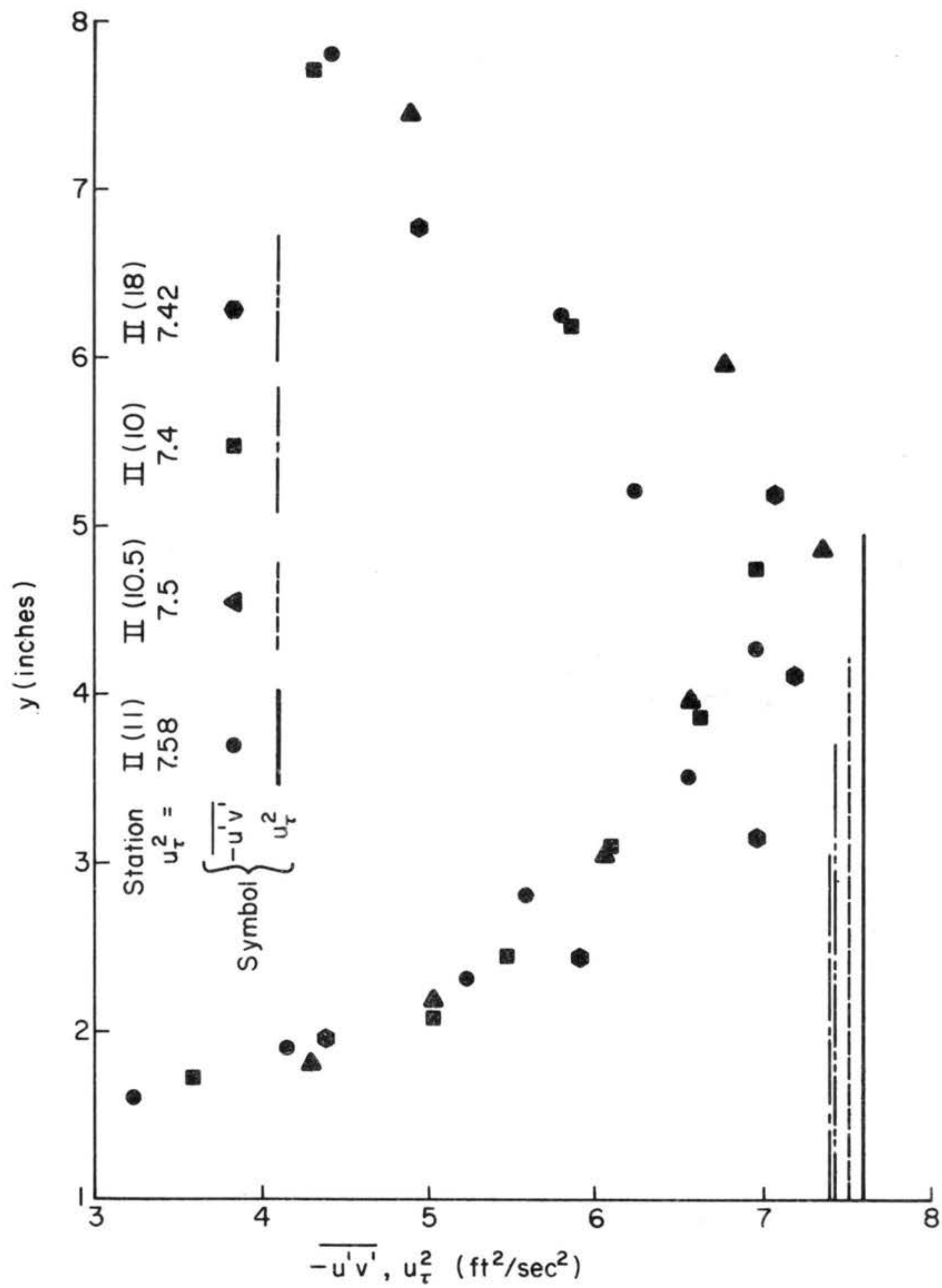

Figure 62 Turbulent shear stress distribution at Stations II(8), II(10), II(10.5) and II(11)

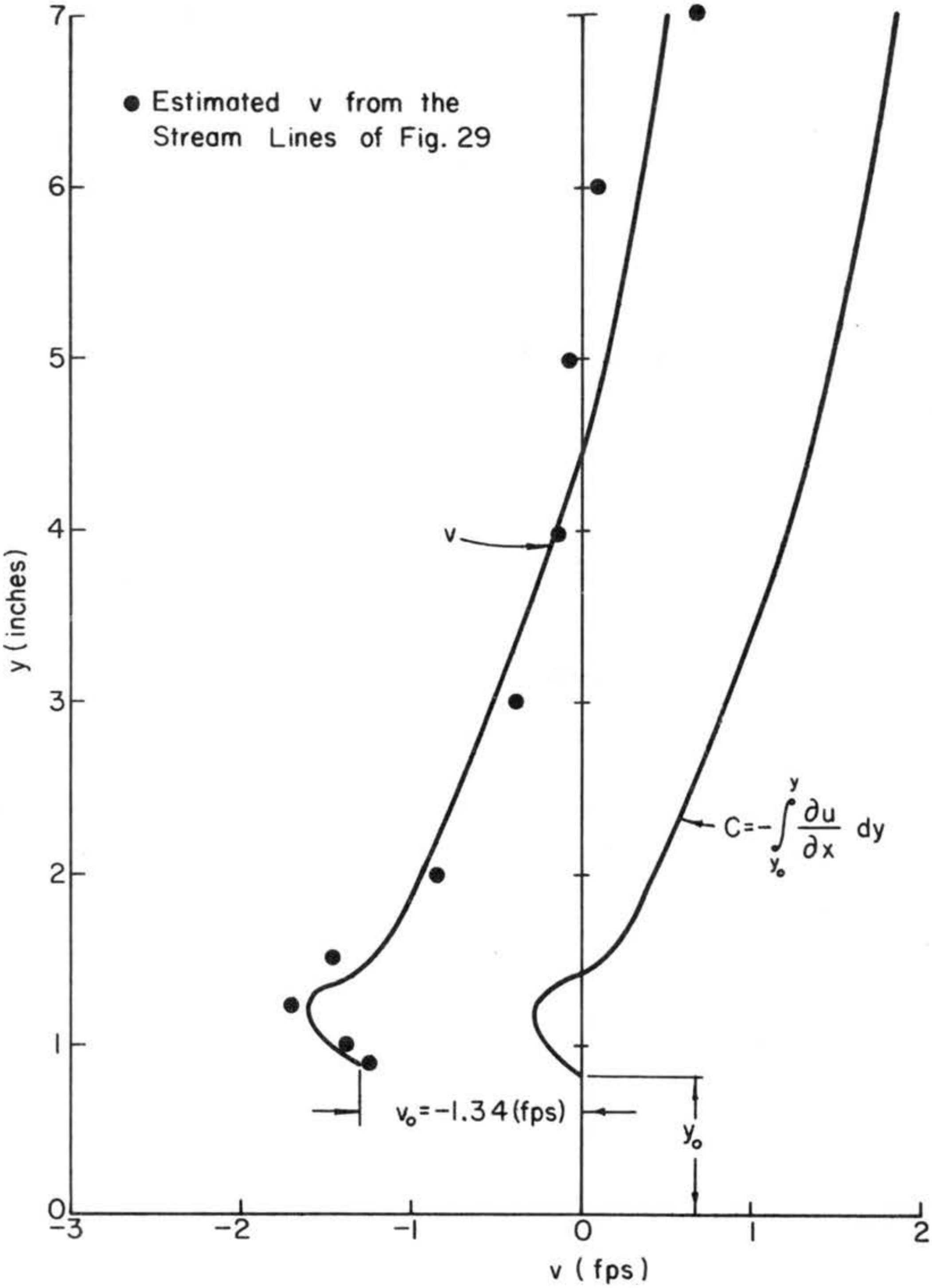

Figure 63 Estimation of v for Station Ia(11,6)

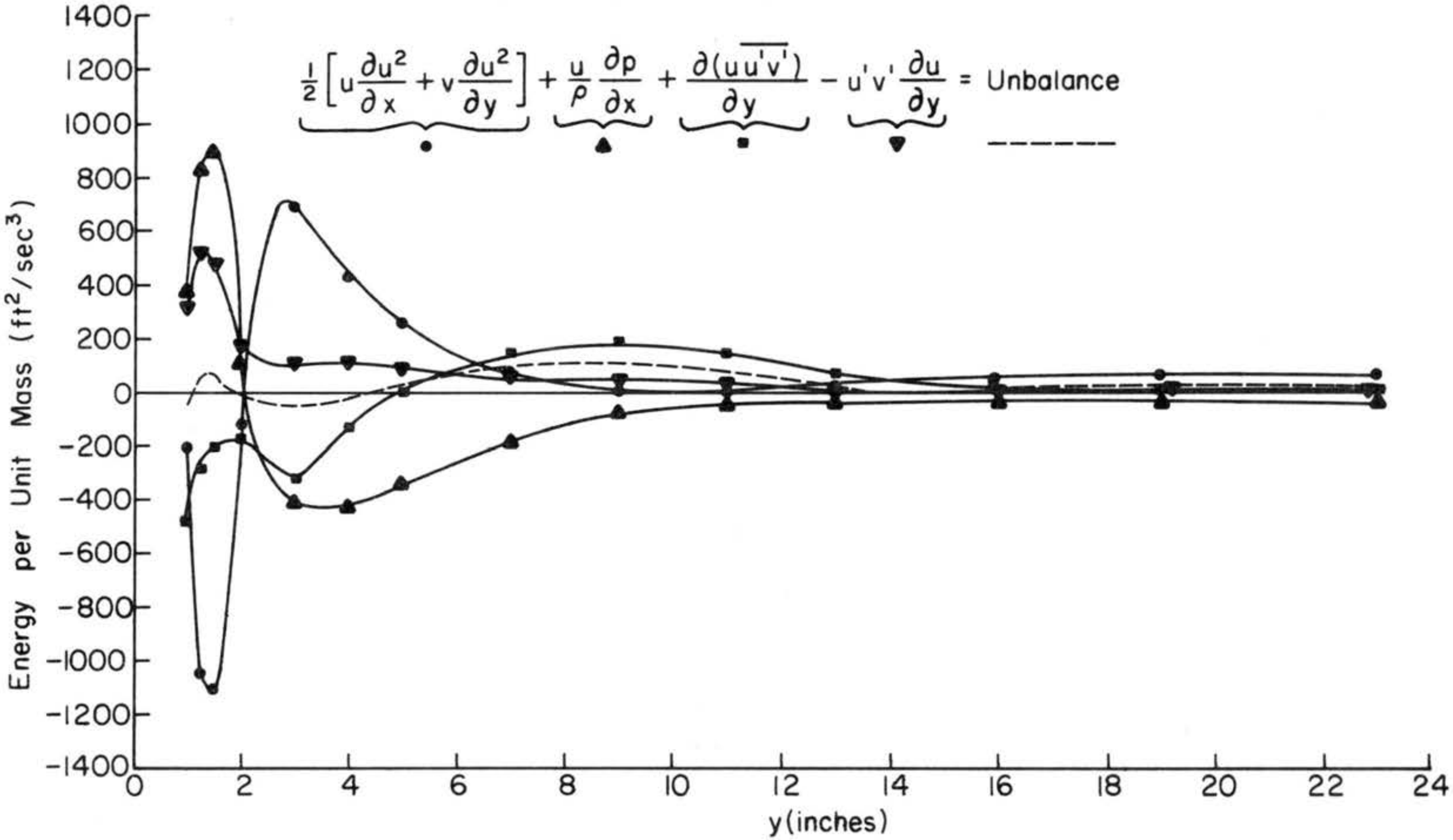

Figure 64 Mean energy balance of Station Ia(11,2)

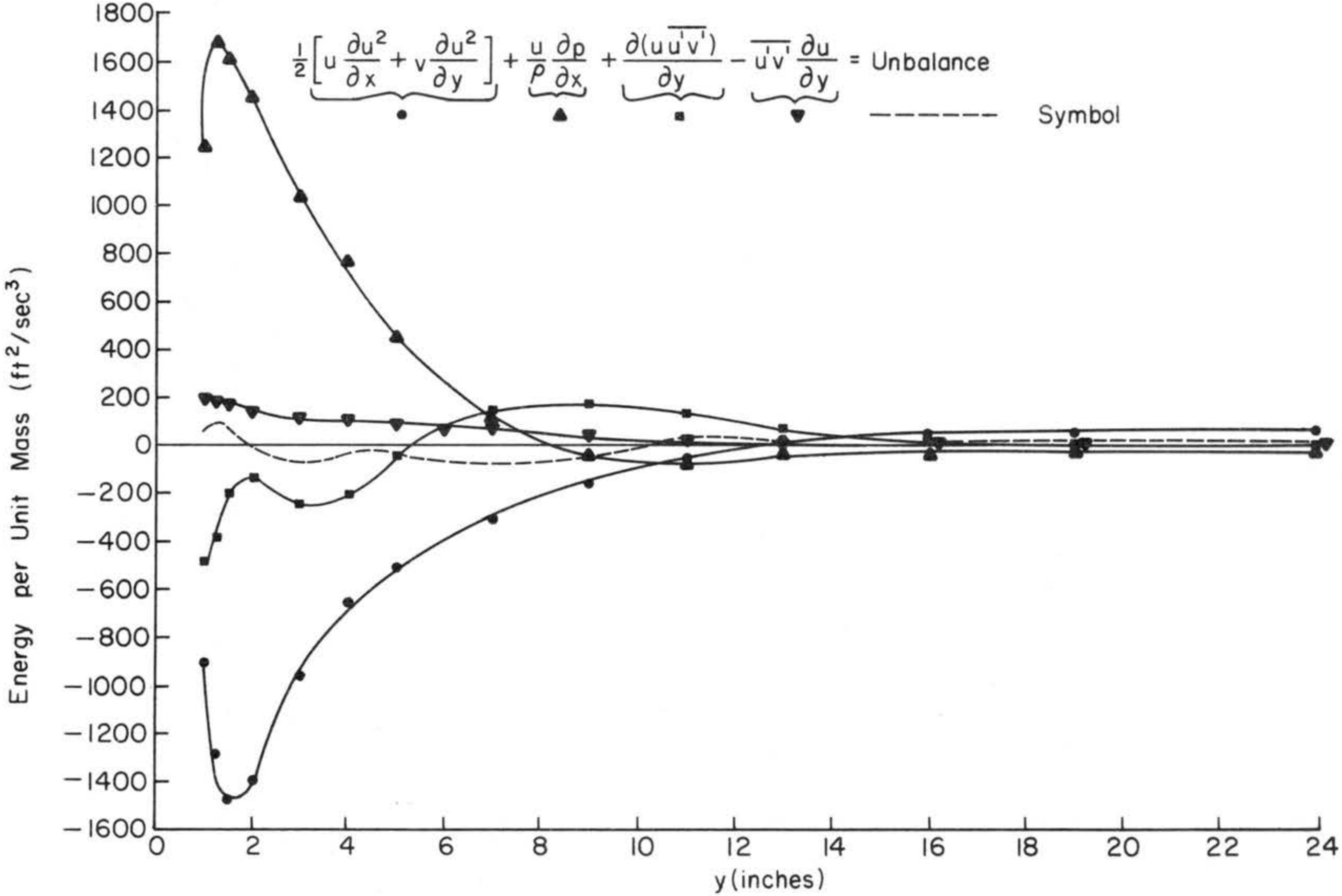

Figure 65 Mean energy balance of Station Ia(11,4)

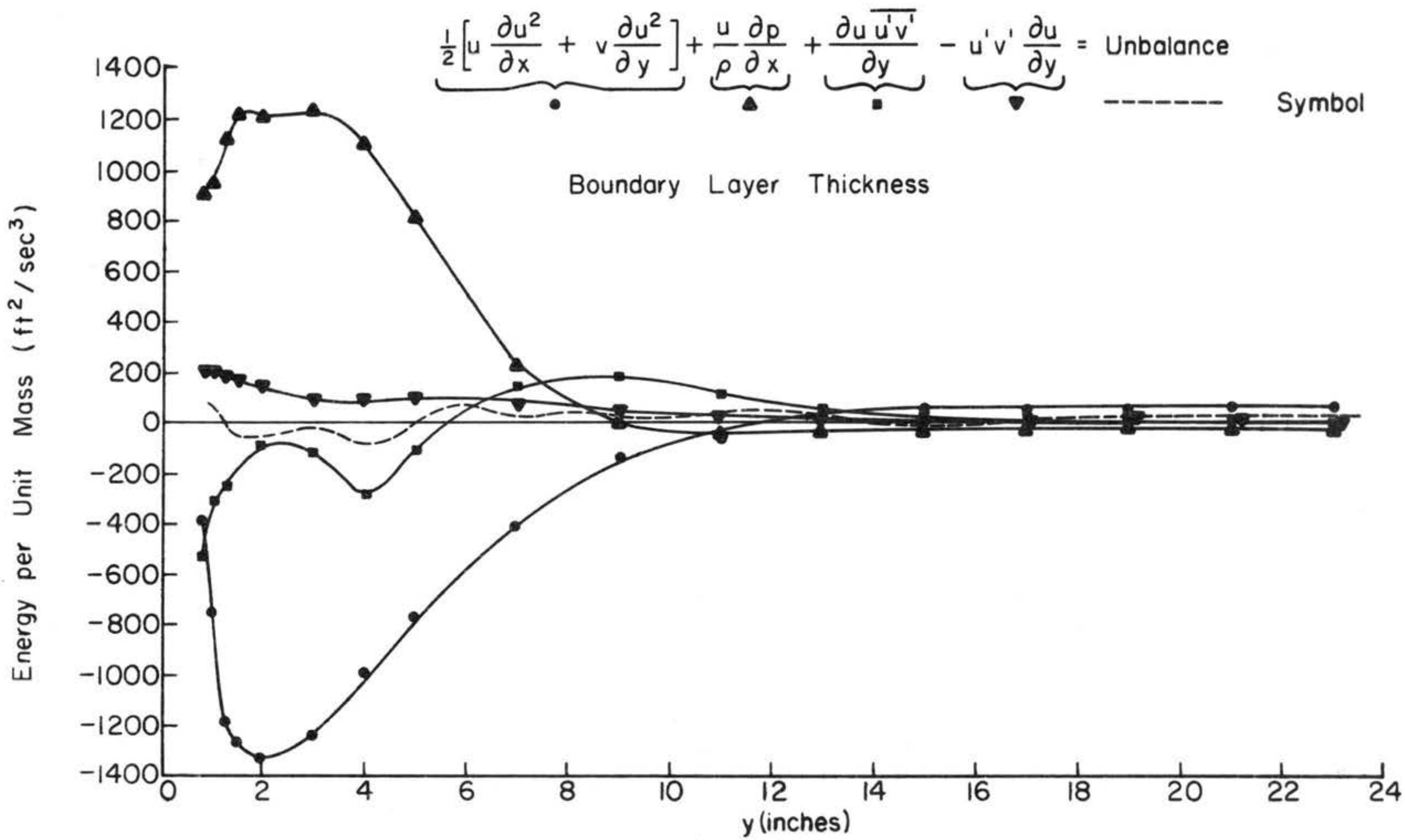

Figure 66 Mean energy balance of Station Ia(11,6)

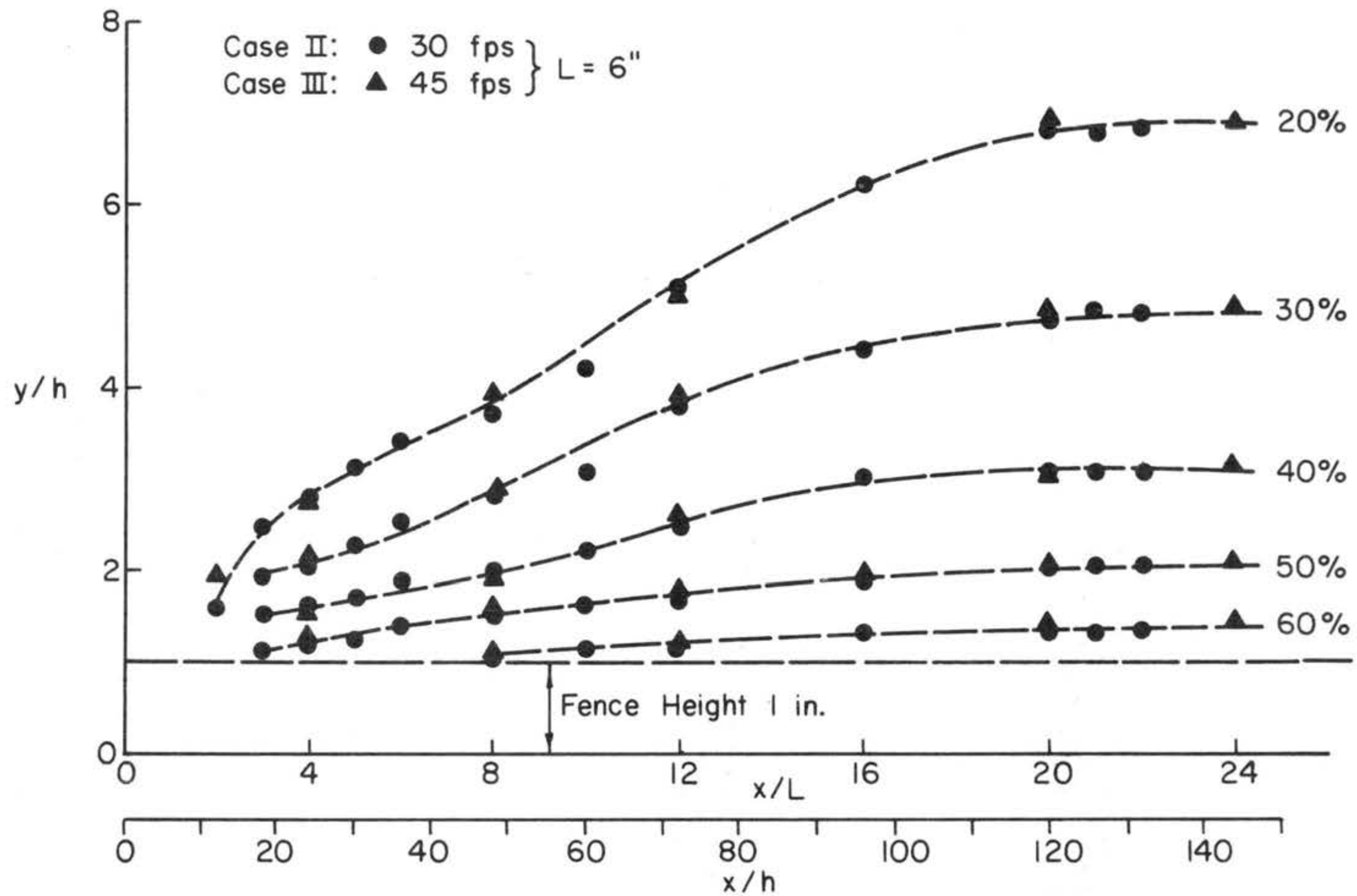

Figure 67 Wind reduction rate of L = 6 in.

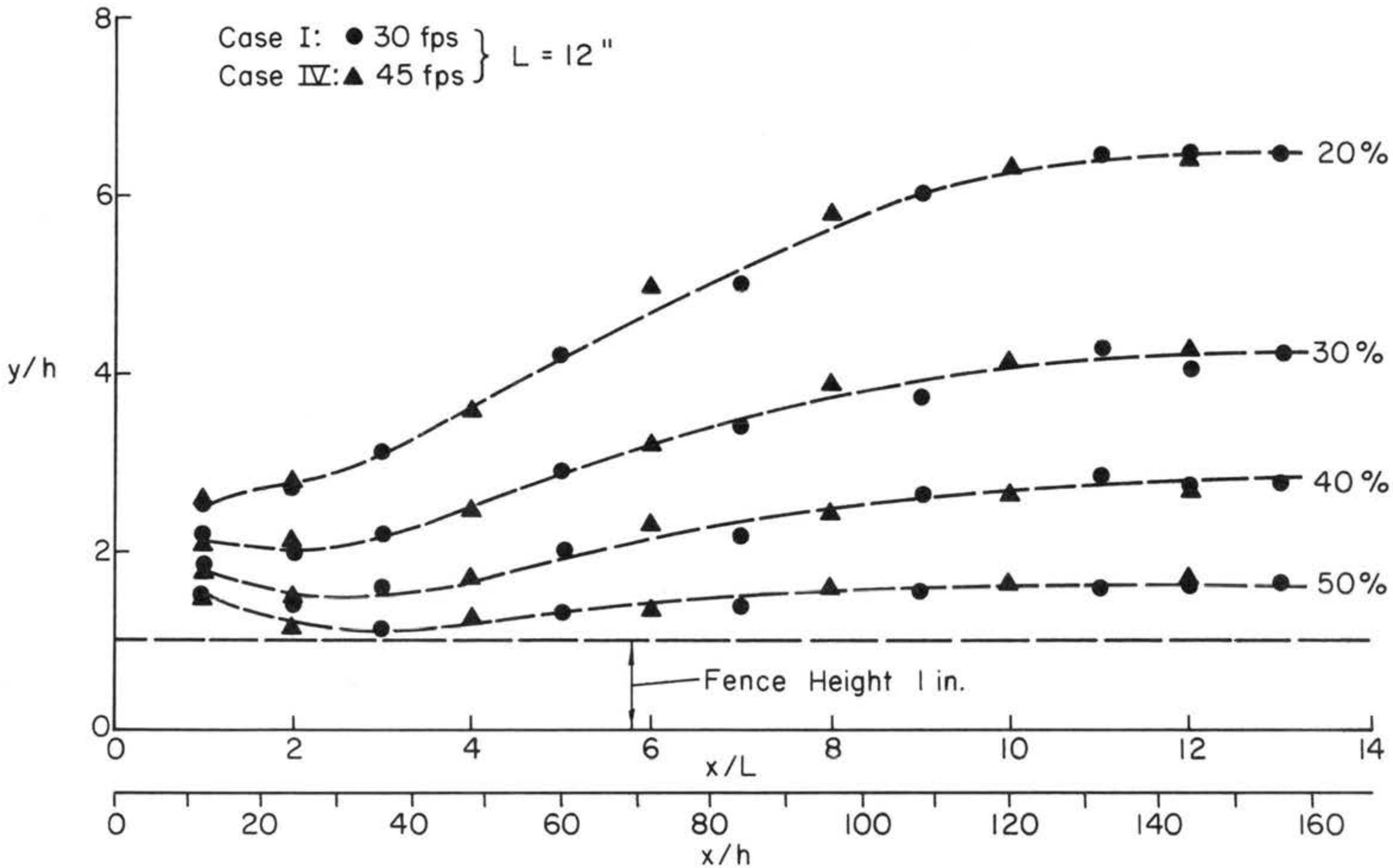

Figure 68 Wind reduction rate of L = 12 in.

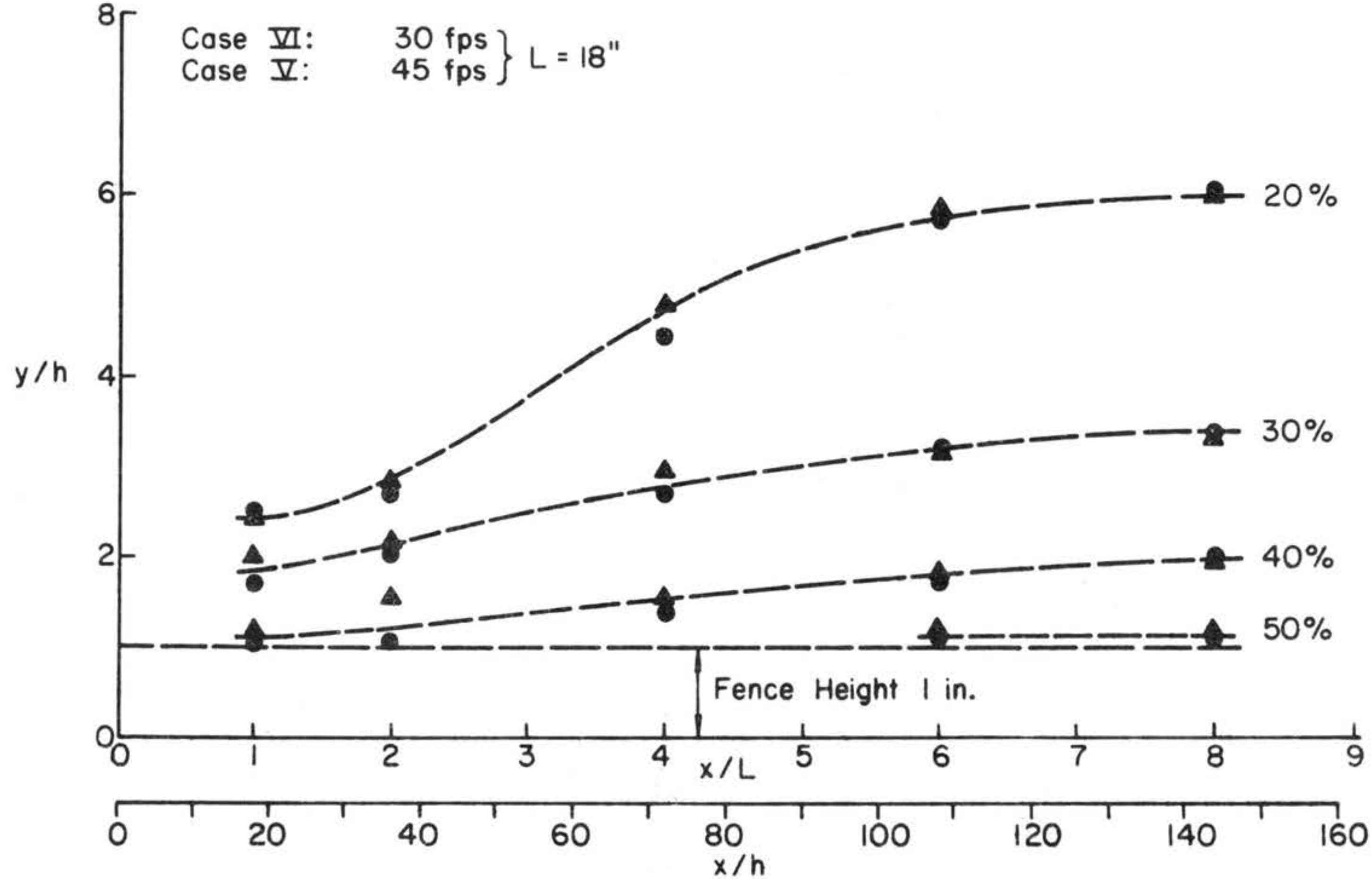

Figure 69 Wind reduction rate of L = 18 in.

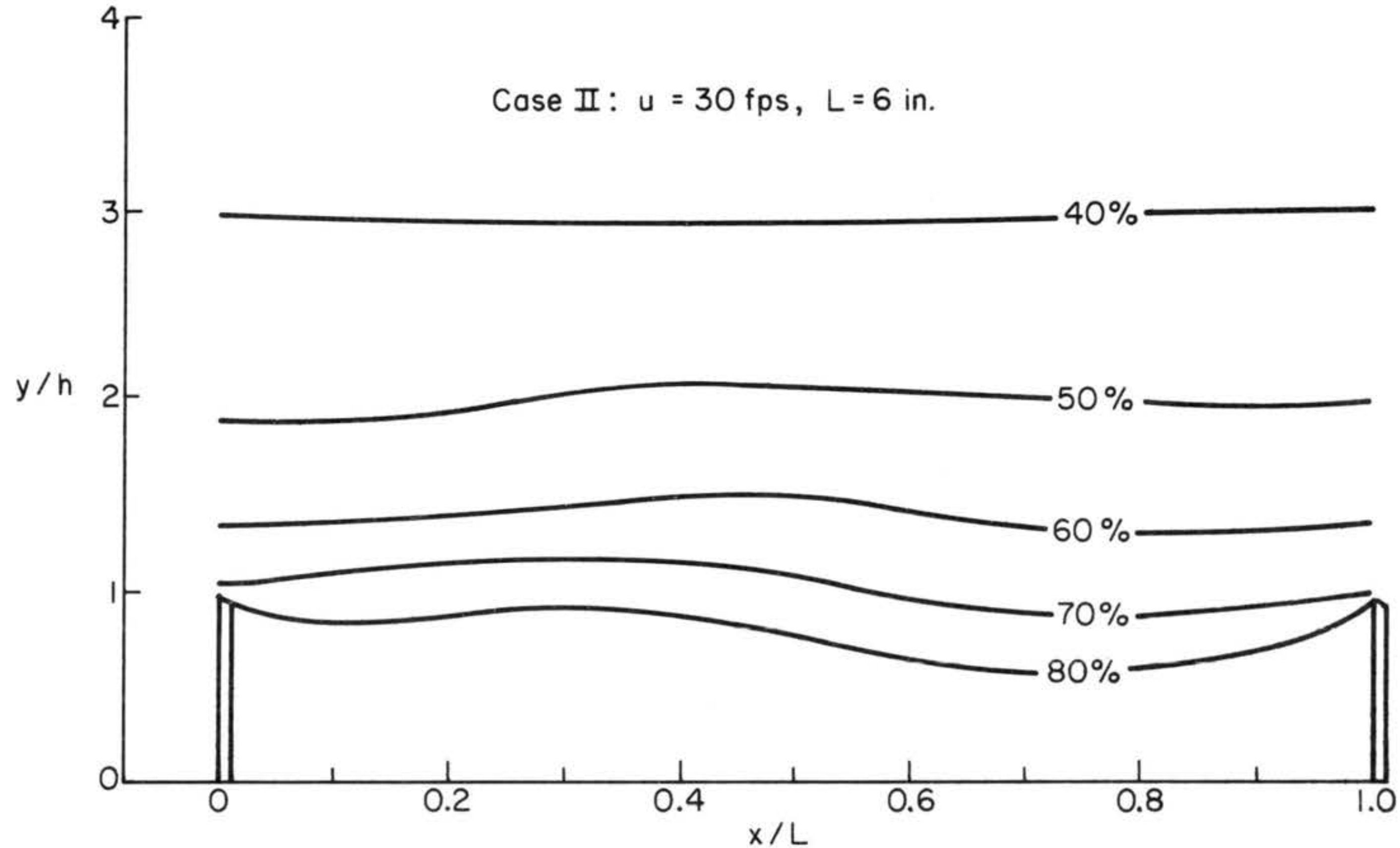

Figure 70 Wind reduction rate between $x = 10$ ft and $x = 10.5$ ft fences and between $x = 10.5$ ft and $x = 11$ ft fences

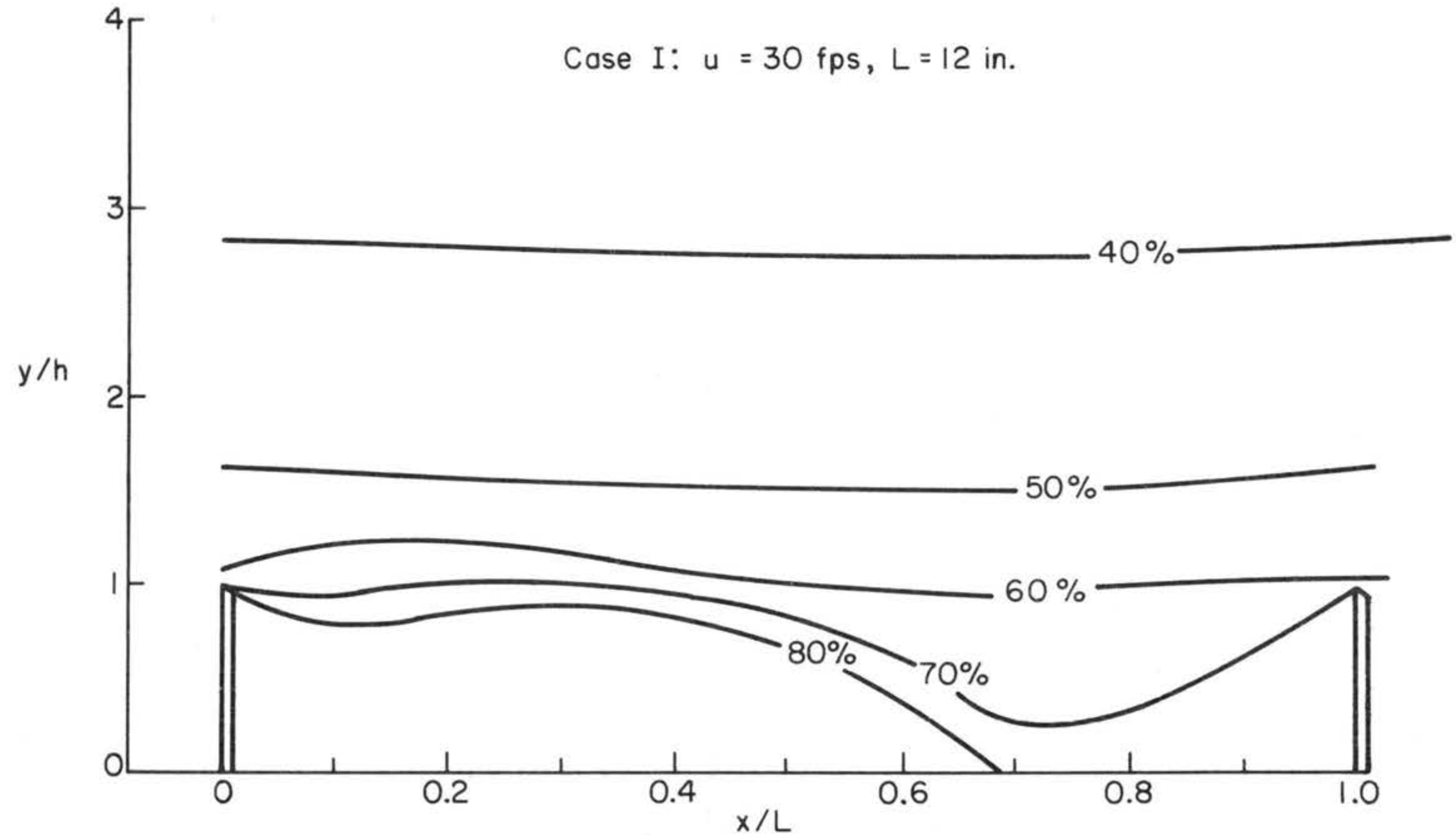

Figure 71 Wind reduction rate between x = 11 ft and x = 12 ft fences and between x = 12 ft and x = 13 ft fences

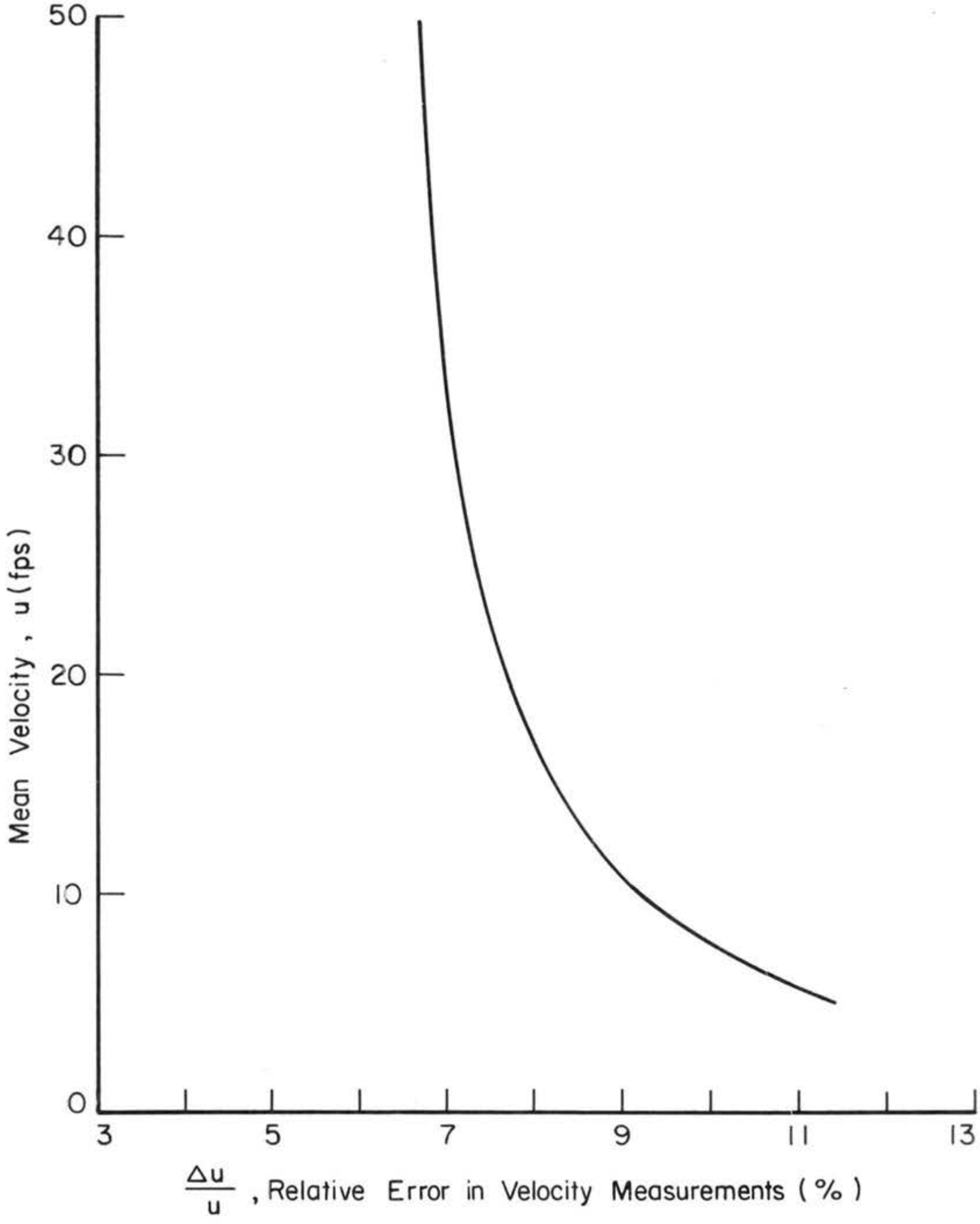

Figure A.1 Relative error on mean velocity measurements by hot wire